Practical Handbook of Endoscopic Ultrasonography

Kazuya Akahoshi
Amol Bapaye *Editors*

Springer

Practical Handbook of Endoscopic Ultrasonography

Kazuya Akahoshi • Amol Bapaye
Editors

Practical Handbook of Endoscopic Ultrasonography

Springer

Editors
Kazuya Akahoshi, M.D., Ph.D.
Department of Gastroenterology
Aso Iizuka Hospital
Yoshiomachi 3-83, Iizuka city
Fukuoka 820-8505, Japan

Amol Bapaye, M.D. (M.S.)
Department of Digestive Diseases
and Endoscopy
Deenanath Mangeshkar Hospital
and Research Center
Erandwane, Pune 411004
Maharashtra, India

ISBN 978-4-431-54013-7 ISBN 978-4-431-54014-4 (eBook)
DOI 10.1007/978-4-431-54014-4
Springer Tokyo Heidelberg New York Dordrecht London

Library of Congress Control Number: 2012931855

© Springer Japan 2012
This work is subject to copyright. All rights are reserved by the Publisher, whether the whole or part of the material is concerned, specifically the rights of translation, reprinting, reuse of illustrations, recitation, broadcasting, reproduction on microfilms or in any other physical way, and transmission or information storage and retrieval, electronic adaptation, computer software, or by similar or dissimilar methodology now known or hereafter developed. Exempted from this legal reservation are brief excerpts in connection with reviews or scholarly analysis or material supplied specifically for the purpose of being entered and executed on a computer system, for exclusive use by the purchaser of the work. Duplication of this publication or parts thereof is permitted only under the provisions of the Copyright Law of the Publisher's location, in its current version, and permission for use must always be obtained from Springer. Permissions for use may be obtained through RightsLink at the Copyright Clearance Center. Violations are liable to prosecution under the respective Copyright Law.
The use of general descriptive names, registered names, trademarks, service marks, etc. in this publication does not imply, even in the absence of a specific statement, that such names are exempt from the relevant protective laws and regulations and therefore free for general use.
While the advice and information in this book are believed to be true and accurate at the date of publication, neither the authors nor the editors nor the publisher can accept any legal responsibility for any errors or omissions that may be made. The publisher makes no warranty, express or implied, with respect to the material contained herein.

Printed on acid-free paper

Springer is part of Springer Science+Business Media (www.springer.com)

Preface

Endoscopic ultrasonography (EUS) has evolved from an obscure investigation with doubtful clinical applications in the 1980s to a distinct endoscopy subspecialty with interventional and therapeutic capabilities. Learning EUS is the current aspiration of every new endoscopist.

Training in EUS has traditionally been considered challenging. Mastering the art of interpreting these black, white, and gray images is no doubt a daunting task. However, it is not as difficult as it appears. Using a step-by-step approach, it is possible for every endoscopist to master this skill. To achieve this feat, one needs a book that is concise, simple to read, and amply illustrated, and that describes the technique in a stepwise manner. EUS appearances of various diseases must be illustrated adequately. Lengthy literature reviews, although important, often deter the novice learner. Radial and linear techniques need separate discussion and illustrations.

It gives us great pleasure therefore to present this unique work, *Practical Handbook of Endoscopic Ultrasonography*. The book is handy enough to be used as a reference handbook in the endoscopy suite, yet contains all relevant information required to perform EUS, interpret images, and reach a diagnosis. It is an optimum combination of technique and literature review. The various sections enable a quick reference to the topic of interest. Each chapter begins with a detailed stepwise description of the technique. This is amply illustrated using line diagrams and high-resolution EUS images obtained on the latest electronic high-resolution SU-7000 and SU-8000 EUS processors (Fujifilm Inc., Japan). Thereafter, important pathological conditions are discussed point by point in a uniform style using representative EUS images, salient differentiating features, and relevant literature reviews. Separate sections on radial and linear EUS provide the reader ample opportunity to learn and interpret both views with ease.

The section on interventional EUS deals with advanced interventional or therapeutic procedures. The technique is described in a simple stepwise manner for ease of understanding and is illustrated with images. Potential complications, methods to avoid them, and a brief review of the relevant literature on the topic are discussed. Specific tips and tricks are highlighted to improve success in these otherwise challenging procedures.

Endosonographers may find different uses for this book. For the novice, the book is designed to teach EUS using a step-by-step approach with ample images, line

diagrams, and descriptions. For the seasoned endosonographer, it represents a practical reference tool while performing EUS and may be used for the differentiation of various pathologies.

Writing and editing this book has been a mammoth task that could not have been completed without the support, guidance, and assistance of many individuals and organizations. Foremost are our contributing authors and co-authors Drs. R P Wadhwa, Vijayshri Pethe-Bhide, Advay Aher, Masaru Kubokawa, and Masafumi Oya, whose knowledge fills many of these pages. This book would not have seen the light of day without the continuous and generous support of Fujifilm® Inc., Japan, and their officials: Katsuya Kikuchi, Kaoru Watanabe, Masaki Yamada, Eko Purwanto, and Toshizumi Tanaka; Fujifilm representatives in India: Mitra Medical Services and their officials-Nitin Mahajan and Jaideep Dutta. We thank the publishing team of Springer Japan for their efforts to present this handbook in its current form. Drs. M.Y. Bapaye and Shirish Bhave provided informative input and editing assistance. The staff at the endoscopy departments of Deenanath Mangeshkar and Iizuka hospitals provided administrative and technical support. Shivangi Dorwat, Pooja Shrivastava, Yukiko Horiuchi, and Shinichi Tamura deserve special mention for their constant and tireless secretarial and research assistance. We thank our wives and children, Dr. Charulata Bapaye, Jay and Harsh, Akiko Akahoshi, Kazuaki, Haruna, and Hikaru, for their constant support and understanding. Lastly, the images and words in this book would not exist without the innumerable patients who underwent EUS. We dedicate this book to all of them and to future patients.

It has been an exciting and informative experience to write this unique handbook. We hope that, as a reader, you will find the book just as enjoyable and useful. We wish our readers all the very best for their endosonographic journey.

Iizuka, Japan — Kazuya Akahoshi
Pune, India — Amol Bapaye

Contents

Part I Instrumentation

1 Instrumentation 3
Kazuya Akahoshi

Part II Ultrasound Catheter Probe

2 Ultrasound Catheter Probe (UCP) 13
Kazuya Akahoshi and Masaru Kubokawa

Part III Radial Endoscopic Ultrasonography (EUS)

3 Basic Scanning Methods of Radial EUS 33
Kazuya Akahoshi

4 Radial EUS of the Esophagus and Mediastinum 37
Kazuya Akahoshi

5 Radial EUS of the Stomach 49
Kazuya Akahoshi

6 Radial EUS of the Anus and Rectum 65
Kazuya Akahoshi

7 Radial EUS of Pancreatico-Biliary System 83
Kazuya Akahoshi

Part IV Linear EUS

8 Basic Scanning Techniques of Linear EUS 119
Amol Bapaye and Advay Aher

9 Linear EUS of the Esophagus and Mediastinum 125
Amol Bapaye and Advay Aher

10 Linear EUS of the Stomach 143
Amol Bapaye and Advay Aher

11 Linear EUS of the Anorectum 155
Amol Bapaye and Advay Aher

12 Linear EUS of the Pancreas, Biliary Tract and Liver 165
Amol Bapaye and Advay Aher

Part V Endoscopic Ultrasonography-Guided Fine Needle Aspiration (EUS-FNA)

13 Techniques of EUS-FNA 209
Amol Bapaye and Advay Aher

14 Cytopathological Aspects of EUS-FNA 217
Vijayshri Pethe-Bhide and Amol Bapaye

15 EUS-FNA of the Esophagus and Mediastinum 223
Amol Bapaye and Advay Aher

16 EUS-FNA of Lesions of the Pancreas, Biliary Tract, and Liver 235
Amol Bapaye and Advay Aher

17 EUS-FNA for Submucosal Tumor 251
Kazuya Akahoshi and Masafumi Oya

Part VI Interventional EUS

18 EUS Guided Drainage of Pancreatic Pseudocysts (PPC's), Abscesses and Fluid Collections (PFC's) 263
Amol Bapaye and Advay Aher

19 EUS Guided Biliary and Pancreatic Duct Interventions 277
Amol Bapaye and Advay Aher

20 EUS Guided Celiac Plexus Interventions 287
Rajkumar Wadhwa and Amol Bapaye

21 EUS Guided Anorectal Interventions 293
Amol Bapaye and Advay Aher

Index 299

Contributors

Advay Aher *(Chapters 8–13, 15, 16, 18, 19, 21)*
Department of Digestive Diseases and Endoscopy, Deenanath Mangeshkar Hospital and Research Center, Erandwane, Pune 411004, Maharashtra, India

Kazuya Akahoshi *(Chapters 1–7, 17)*
Department of Gastroenterology, Aso Iizuka Hospital, Yoshiomachi 3-83, Iizuka city, Fukuoka 820-8505, Japan

Amol Bapaye *(Chapters 8–16, 18, 20, 21)*
Department of Digestive Diseases and Endoscopy, Deenanath Mangeshkar Hospital and Research Center, Erandwane, Pune 411004, Maharashtra, India

Masaru Kubokawa *(Chapter 2)*
Department of Gastroenterology, Aso Iizuka Hospital, Yoshiomachi 3-83, Iizuka city, Fukuoka 820-8505, Japan

Masafumi Oya *(Chapter 17)*
Department of Pathology, Aso Iizuka Hospital, Yoshiomachi 3-83, Iizuka city, Fukuoka 820-8505, Japan

Vijayshri Pethe-Bhide *(Chapter 14)*
Department of Pathology, Deenanath Mangeshkar Hospital and Research Center, Erandwane, Pune 411004, Maharashtra, India

Rajkumar Wadhwa *(Chapter 20)*
Department of Gastroenterology, Vikram Jyoth – Centre for Advanced GI and Hepato-biliary Sciences, 2909 Temple Road, V. V. Moholla, Mysore, Karnataka, India

Part I

Instrumentation

Instrumentation

1

Kazuya Akahoshi

1.1 Dedicated Echoendoscope

Standard EUS is performed with radial ultrasound imaging perpendicular to the endoscope shaft. Radial ultrasound imaging is preferred for some diagnostic and staging purposes because of ease of use as well as the production of a full 360° field of view like a CT scan. The convex array echoendoscope incorporates a transducer placed at the tip of an oblique viewing endoscope and provides ultrasound images in a plane parallel to the direction of the insertion of the echoendoscope [1]. Use of the convex device offers the significant advantage of facilitating intervention. The curved linear array design also makes it possible to direct needle aspiration for biopsy and/or fine needle injection, a useful feature in the diagnosis and treatment of a variety of clinical conditions [1, 2].

The EG-530UR2 electronic radial echoendoscope (FUJIFILM Corporation, Tokyo, Japan) has a 360º radial ultrasound image, forward-viewing optics (view angle 140º) with a digital tip diameter of 11.4 mm, a 2.2 mm forceps channel, and a working length of 1,254 mm, 180º up, 90º down, and 100º left/right tip deflection (Fig. 1.1, Table 1.1). The EG-530UT convex echoendoscope (FUJIFILM) has a 110º convex ultrasound image, oblique-viewing optics (view angle 140º) with a digital tip diameter of 13.9 mm, a 3.8 mm forceps channel, a working length of 1,254 mm, 160º up, 160º down, and 120º left/right tip deflection (Fig. 1.2, Table 1.1). These scopes have a transducer with variable frequency (5.0, 7.5, 10.0, 12.0 MHz) and color and power Doppler flow mapping capabilities. They provide endoscopic and ultrasound images with Fujifilm type 4400 endoscopic and SU-7000 or SU-8000 (Fig. 1.3) ultrasound processors (Table 1.2) in a one cart system (Fig. 1.4). Therefore, this system can optimize the use of limited space. Furthermore, it is useful in

K. Akahoshi
Department of Gastroenterology, Aso Iizuka Hospital,
Yoshiomachi 3-83, Iizuka city, Fukuoka 820-8505, Japan
e-mail: kakahoshi2@aol.com

K. Akahoshi, A. Bapaye (eds.), *Practical Handbook of Endoscopic Ultrasonography*,
DOI 10.1007/978-4-431-54014-4_1, © Springer 2012

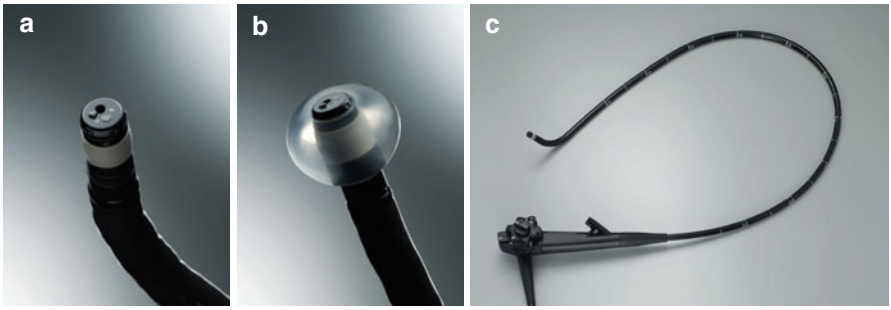

Fig. 1.1 EG-530UR2 electric radial scan ultrasound video endoscope. (**a**) Distal tip of echoendoscope, (**b**) distal tip of echoendoscope with balloon inflation, (**c**) overview

Table 1.1 Echoendoscope EG-530UR2/EG-530UT2 specification

	EG-530UR2	EG-530UT2
Endoscopic function		
Optics		
Field of view	140°	140°
Viewing direction	40°	0°
Observation range	3–100 mm	3–100 mm
Insertion portion		
Dital end diameter	11.4 mm	13.9 mm
Flexible portion diameter	11.5 mm	12.1 mm
Working length	1,250 mm	1,250 mm
Overall length	1,550 mm	1,550 mm
Forceps channel		
Diameter of forceps	2.2 mm	3.8 mm
Raising mechanism	–	Yes
Bending portion		
Up/down/left/right	180°/90°/100°/100°	160°/160°/120°/120°
Ultrasonic function		
Scanning mode	Color Doppler, power Doppler, pulse wave, B mode, M mode	Color Doppler, power Doppler, pulse wave, B mode, M mode
Scanning method	Electronic radial scan	Electronic convex scan
Scanning angle	360°	110° (Combination with SU-7000) 124° (Combination with SU-8000)
Frequency	5/7.5/10/12 MHz	5/7.5/10/12 MHz

performing diagnostic and interventional EUS procedures in different procedure rooms within an endoscopy unit and in other areas of a hospital (radiology, emergency, operating room) [2]. Acoustic coupling is achieved by means of a balloon filled with water attached to the tip and/or luminal water infusion.

Fig. 1.2 EG-530UT2 electric convex scan ultrasound video endoscope. (**a**) Distal tip of echoendoscope, (**b**) distal tip of echoendoscope with balloon inflation, (**c**) overview

Fig. 1.3 Ultrasound processor SU-8000

Table 1.2 Ultrasound processor SU-7000/SU-8000 specifications

	SU-7000	SU-8000
External dimension (W×H×D)	400×260×465 mm	375×215×445 mm
Weight	28 kg	12.5 kg
Applicable probe type	Convex/radial	Convex/radial
Display mode	B mode/THI/power Doppler/color Doppler/PW Doppler/M mode	B mode/THI/power Doppler/color Doppler/PW Doppler/M mode
Display range	2–14 cm	1.5–12 cm
Frequency	5/7.5/10/12 MHz	5/7.5/10/12 MHz

The forward-viewing optics of EG-530UR2 was specifically cited as facilitating intubation and advancement of the electronic instrument as compared with the oblique-viewing conventional type echoendoscope. Furthermore, the tip's small bending radius allows observation of previously inaccessible sites.

Fig. 1.4 Endoscopic system (type 4400) and ultrasound system (SU-8000) are on single unified cart

Therefore, EG-530UR2 could be used for routine esophagogastroduodenoscopy [2] (Fig. 1.5). In other words, endoscopy and ultrasonography can both be performed without changing the endoscope, thus minimizing the number of endoscopic examinations.

Although convex type EUS scope (EG-530UT2) has an oblique view, good direct visualization is obtained since the angle of view is wide (140°) and also the direction of the viewing field is more like a forward view (40°) [2, 3]. Therefore, EG-530UT2 enables us to perform EUS-FNA for the sigmoid colon, because the advancement of the scope into the sigmoid colon is easy and safe (Fig 1.6) [3].

1.2 Ultrasound Catheter Probe

The ultrasound catheter probe (Sonoprobe system SP702, FUJIFILM Corporation, Tokyo, Japan) is passed through the working channel of the standard endoscope (Figs. 1.7 and 1.8). Frequencies of 12, 15, 20, and 25 MHz are used with these

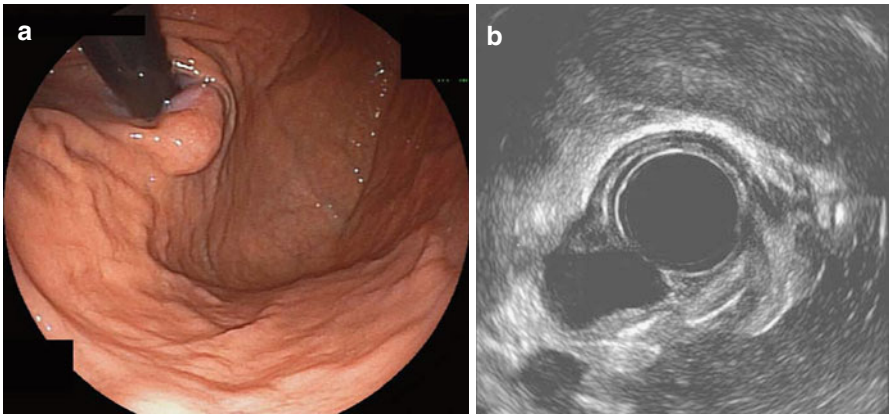

Fig. 1.5 Endoscopic view and SU-8000 EUS image of cardial SMT by EG-530UR2. (**a**) Retroflexion view of cardiac SMT, (**b**) EUS showing hypoechoic solid tumor with continuity to the muscularis propria

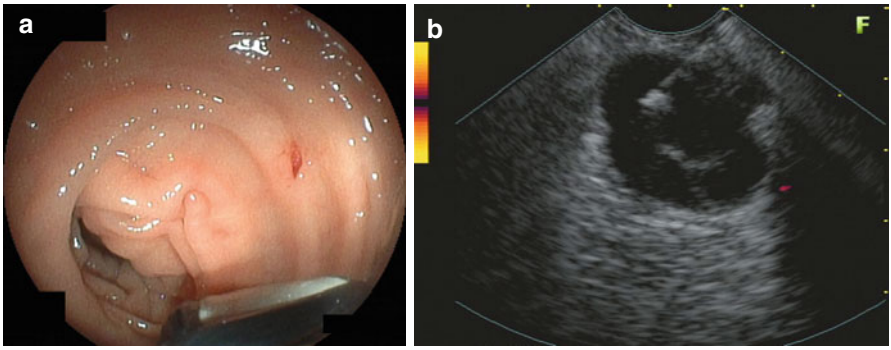

Fig. 1.6 EUS-FNA from the sigmoid colon by EG-530UT2. (**a**) Endoscopic view of the sigmoid colon. (**b**) EUS image of the intraabdominal mass during EUS-FNA

probes, allowing for high resolution of structures within 0.5–2 cm of the transducer. Ultrasound catheter probes are particularly useful for examining the layers of the gastrointestinal wall. In addition, a catheter probe allows the endoscopist to use a standard endoscope, which is easier to use than the dedicated echoendoscopes. The passage of the ultrasound catheter probe through the working channel during conventional endoscopy is convenient for routine use. Endoscopy and ultrasonography can both be performed without changing the endoscope, thus minimizing the number of endoscopic examinations. The ultrasound catheter probe is particularly useful when attempting to traverse luminal strictures that do not permit easy passage of the dedicated echoendoscope [1, 4].

Fig. 1.7 Overview of Fujifilm Sonoprobe System SP702

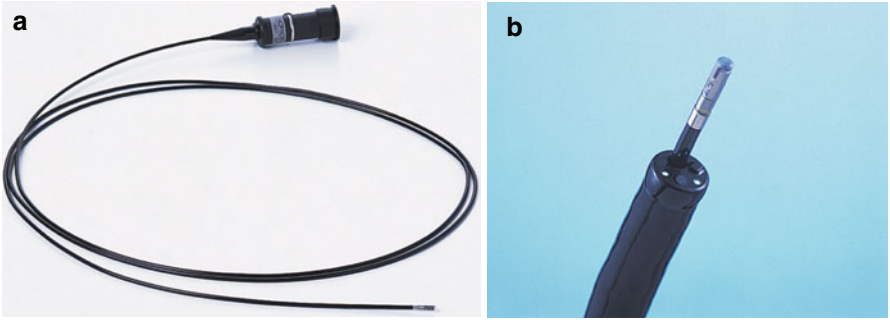

Fig. 1.8 Ultrasound catheter probe (Fuijifilm P2615-M). (**a**) Overview, (**b**) distal tip

1.3 Front Loading Ultrasound Probe

Image quality of high-frequency ultrasound catheter probe is severely limited when the lesion is large or broad-based. To resolve the problems associated with the use of tiny probes, we previously developed a 7.5 MHz front-loading probe

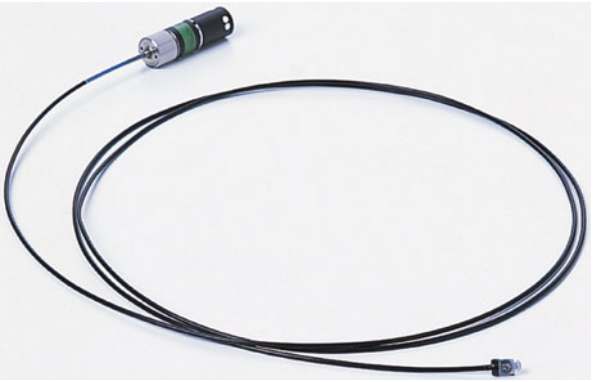

Fig. 1.9 Overview of the front loading ultrasound probe

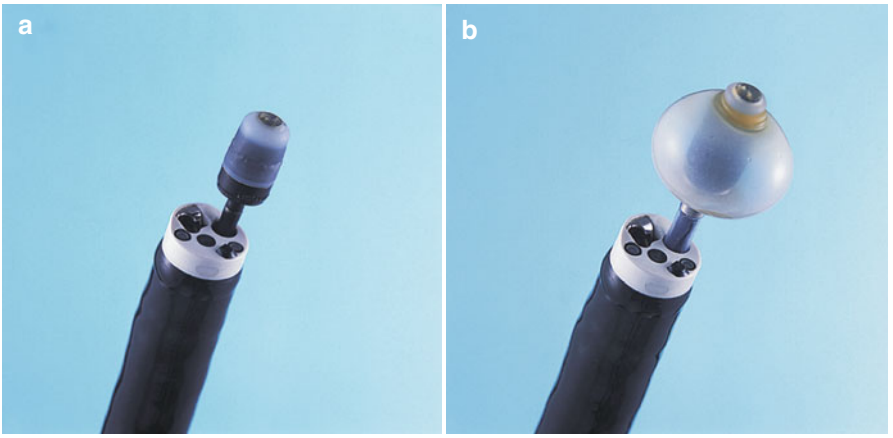

Fig. 1.10 The front loading ultrasound probe inserted in retrograde fashion through the accessory channel of the standard endoscope. (**a**) Without balloon, (**b**) with balloon inflation

(Figs. 1.9 and 1.10) [5]. This device can be inserted through the accessory channel of a standard videoendoscope in a retrograde fashion and is used under direct endoscopic guidance. This 7.5 MHz probe provides good images of small and advanced or broad lesions because its frequency is lower, and the caliber of the transducer is large compared with the catheter probe.

References

1. Akahoshi K, Harada N, Nawata H (2003) The current state of endoscopic ultrasonography. In: Pandalai SG (ed) Recent research developments in radiology. Transworld Research Network, Trivandrum, pp 1–37
2. Akahoshi K, Tanaka T, Matsui N et al (2007) Newly developed all in one EUS system: one cart system, forward-viewing optics type 360º electronic radial array echoendoscope and oblique-viewing type convex array echoendoscope. Fukuoka Acta Med 98:82–89

3. Matsui N, Akahoshi K, Motomura Y et al (2010) Successful EUS-FNA of the pelvic lymph node through the sigmoid colon: report of acase. Dig Endosc 22:337–340
4. Akahoshi K, Chijiiwa Y, Hamada S et al (1998) Pretreatment staging of endoscopically early gastric cancer with a 15 MHz ultrasound catheter probe. Gastrointest Endosc 48:470–476
5. Akahoshi K, Kondoh A, Nagaie T et al (2000) Preoperative staging of rectal cancer using a 7.5 MHz front-loading US probe. Gastrointest Endosc 50:95–98

Part II

Ultrasound Catheter Probe

Ultrasound Catheter Probe (UCP)

2

Kazuya Akahoshi and Masaru Kubokawa

2.1 Indication

The UCP that can be passed through the accessory channel of standard endoscopes, allows easier imaging of small lesions under direct endoscopic guidance. The indication of UCP is shown in the Table 2.1.

2.2 Basic Anatomy and Scanning Technique

The high frequency ultrasound (12, 15, 20, 25 MHz) of UCP provides excellent resolution of the GI tract wall. Usually, a five-layered structure is seen like a conventional echoendoscope (7.5 ~ 12 MHz). However, sometimes a high-frequency UCP (15, 20, 25 MHz) produces a nine-layered structure of the normal gastric wall (Fig. 2.1) in the best scanning conditions. The first three layers represent the mucosa; the fourth, thin, hypoechoic layer represents the muscularis mucosae; the fifth, hyperechoic layer represents the submucosa; the sixth, hypoechoic layer is the inner circular muscle; the seventh, thin hyperechoic layer is the intermuscularis; the eighth, hypoechoic layer represents the outer longitudinal muscle; and the ninth hyperechoic layer represents the subserosa and serosa [1, 2]. For EUS, a special condition is required, i.e. a sonolucent material must be between the UCP and the target lesion, and usually de-aerated water is employed. Three kinds of

K. Akahoshi (✉) • M. Kubokawa
Department of Gastroenterology, Aso Iizuka Hospital,
Yoshiomachi 3-83, Iizuka city, Fukuoka 820-8505, Japan
e-mail: kakahoshi2@aol.com; mkubokawah1@aih-net.com

K. Akahoshi, A. Bapaye (eds.), *Practical Handbook of Endoscopic Ultrasonography*,
DOI 10.1007/978-4-431-54014-4_2, © Springer 2012

Table 2.1 Indication of ultrasound catheter probe

Cancer staging of Early GI tract cancer
Small submucosal tumor (smaller than 2 cm)
Vascular disease (varices, AVM, Dieulafoy's lesion, etc.)
Endosonographic monitoring during endoscopic therapy
Stenotic disease of the GI tract
Intraductal ultrasonography of bilopancreatic tract

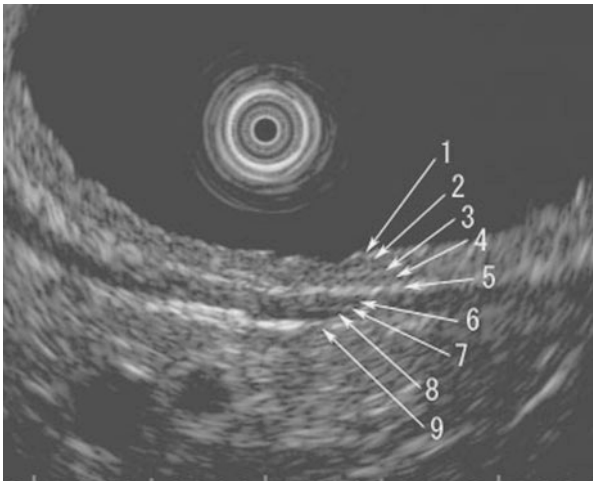

Fig. 2.1 Nine-layer structure of the normal gastric wall imaged by a 15 MHz UCP. *1* mucosal interface echo, *2* remainder of mucosa, *3* interface echo between the mucosa and muscularis mucosae, *4* muscularis mucosae, *5* submucosa, *6* inner circular muscle, *7* intermuscular connective tissue layer, *8* outer longitudinal muscle, *9* subserosa and serosa

scanning techniques are used in EUS using UCP (Fig. 2.2). The water-filling method is the standard one for the all GI tract. If it is difficult to submerge the lesion in de-aerated water (usually in the esophagus), the water-filled condom method [3] or EUS using balloon-sheathed UCP method [4] are effective as alternatives.

2.3 Preparation, Sedation

The premedication for EUS using UCP is the same as for conventional endoscopy (EGD, TCS etc.). EUS was performed on an outpatient basis, with the patient under conscious sedation. In our institute, each patient was sedated with an intravenous injection of flunitrazepam (0.2–0.4 mg) and pethidine hydrochloride (35 mg).

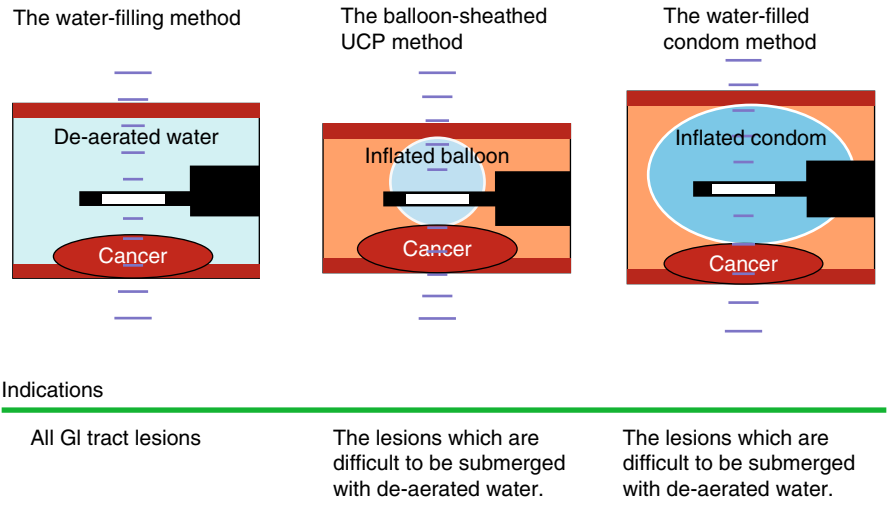

Fig. 2.2 Three kinds of scanning techniques for EUS using UCP

2.4 Complications and Their Prevention

Usually there are no specific complications [1, 2]. The estimated rate of complications is the same as those of EGD, double balloon enteroscopy, and colonoscopy.

2.5 Diagnosis

2.5.1 GI Tract Cancer

EUS using UCP has been reported to be valuable for the staging of GI tract cancers. Furthermore, in stenosing GI tract cancers, EUS staging with UCP appears to be recommendable, as passage is always possible without prior bougienage or balloon dilatation of the stenosis. However, due to the limited depth of penetration, its use should be limited to small GI tract cancers. In other words, it is very useful for the staging of early stage GI tract cancers, i.e. determination for endoscopic mucosal resection (EMR) or endoscopic submucosal dissection (ESD). Reported diagnostic accuracy for each organ with early stage cancers were 64.7–75% for esophagus [5, 6], 67–71% for stomach [2, 7], and 76–88% for colon [8, 9].

2.5.2 How to Diagnose the GI Tract Cancer

GI cancers are usually imaged as hypoechoic tumors. Depth of invasion is determined as the deepest layer of the GI tract of infiltration of the hypoechoic tumor (Fig. 2.3).

Knack-Decrease of Peristalsis

1. Instillation of lukewarm de-aerated water
2. Intravenous injection of anticolinergic agents
3. Infusion of peppermint oil solution [10]

Pitfall-Prevention of Artificial Over-Staging of Early GI Tract Cancer

1. If a biopsy of the tumor is needed, it should be performed after EUS, to prevent overstaging due to artificial imaging (tissue defect, bleeding, edema, etc.)

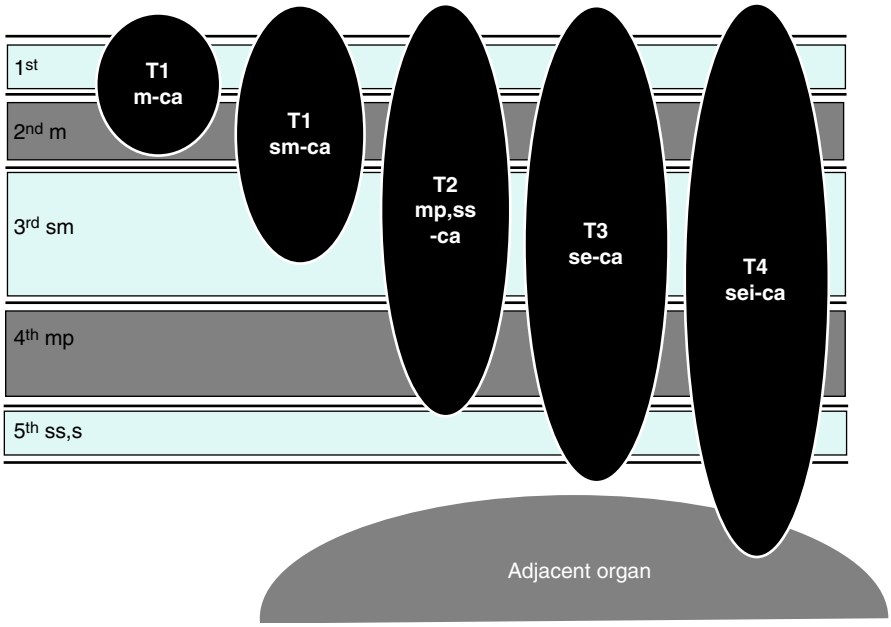

Fig. 2.3 Diagnosis of depth of invasion of GI tract cancer by EUS. *m-ca* intramucosal cancer, *sm-ca* submucosal cancer, *mp,ss-ca* muscularis propria or subserosal cancer, *se-ca* serosal exposed cancer, *sei-ca* serosal exposed cancer infiltrating to the adjacent organ

Fig. 2.5 Esophageal T4 cancer. (**a**) EGD revealing the large advanced esophageal cancer in the middle portion of the esophagus. (**b**, **c**) EUS reveals hypoechoic tumor (*T*) extending into the descending aorta (*DA*). The border-echo is interrupted (*arrow*) by cancer invasion

2.5.3 Esophageal Cancer

2.5.3.1 Intramucosal Cancer (Fig. 2.4)

Typical Findings

1. Irregularity, thinness, or disappearance of the first hyperechoic layer
2. Slight thickness and hypoechoic change of the second hypoechoic layer
3. The third hyperechoic layer intact

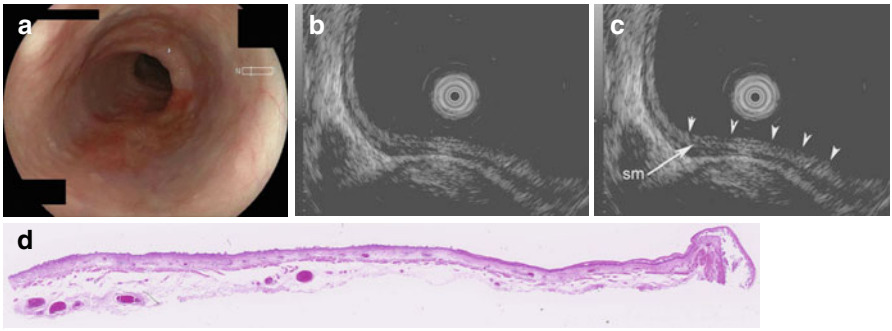

Fig. 2.4 Esophageal intramucosal cancer. (**a**) EGD showing a broad IIc type superficial esophageal cancer in the middle esophagus. (**b**, **c**) EUS revealing thinness of first hyperechoic layer (*arrowheads*) and mild thickness and hypoechoic change of the second hypoechoic layer and normal third hyperechoic layer (*arrow-sm*). (**d**) Cross section of the corresponding histology (ESD specimen) demonstrating intramucosal cancer

2.5.3.2 T4-Cancer (Invasion to the Descending Aorta) (Fig. 2.5)

Typical Findings

1. Irregularity, thinness, or disappearance of the first hyperechoic layer
2. Hypoechoic tumor extends to the descending aorta
3. The border echo between esophagus and the descending aorta is interrupted by tumor echo

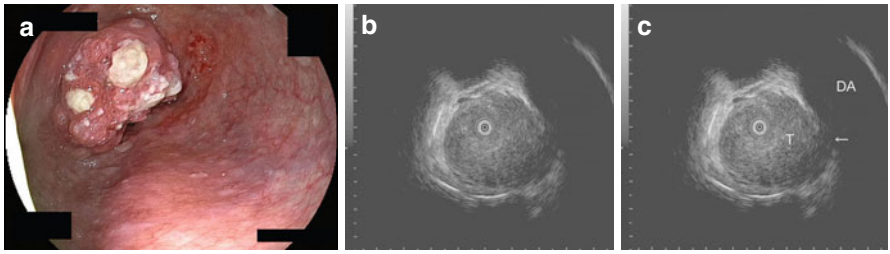

2.5.4 Gastric Cancer

2.5.4.1 Intramucosal Gastric Cancer (Fig. 2.6)

Typical Findings

1. Irregularity, thinness, or disappearance of the first hyperechoic layer
2. Thickness and hypoechoic change of the second hypoechoic layer
3. The third hyperechoic layer intact

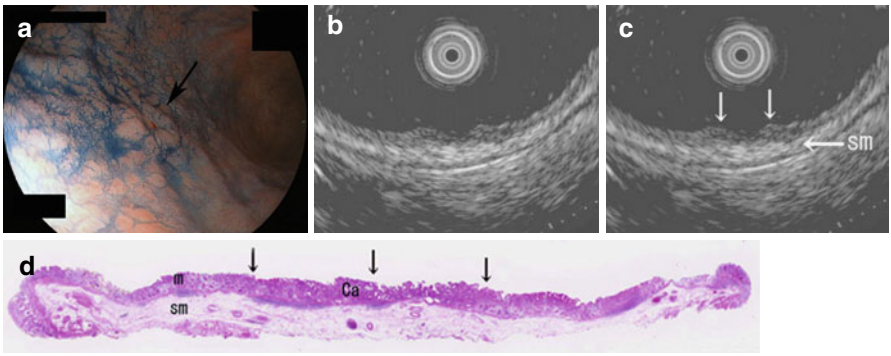

Fig. 2.6 Gastric intramucosal cancer. (**a**) EGD showing a small IIc type early gastric cancer (*arrow*) in the lower gastric body (Chromoendoscopic image using indigocarmine dye). (**b**, **c**) EUS revealing disappearance of first hyperechoic layer (*arrows*) and mild hypoechoic change of the second hypoechoic layer and normal third hyperechoic layer (*arrow-sm*). (**d**) Cross section of the corresponding histology (ESD specimen) demonstrating intramucosal cancer (*arrows*). *m* mucosa, *sm* submucosa, *Ca* cancer

2.5.4.2 Submucosal Cancer (Fig. 2.7)

Typical Findings

1. Irregularity, thinness, or disappearance of the first hyperechoic layer
2. Thickness and hypoechoic change of the second hypoechoic layer
3. Hypoechoic change of the third hyperechoic layer
4. The fourth hypoechoic layer intact

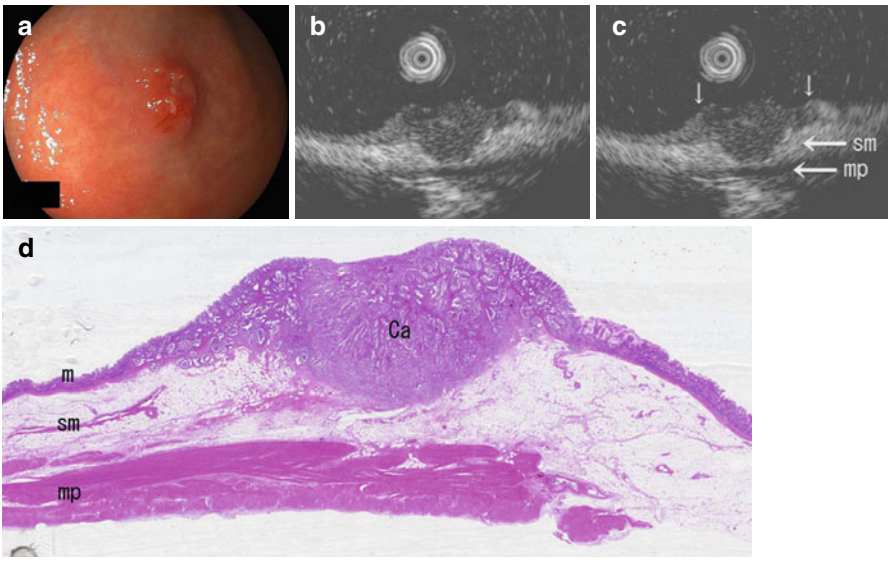

Fig. 2.7 Gastric submucosal cancer. (**a**) EGD showing a small IIa + IIc type early gastric cancer in the gastric body. (**b**, **c**) EUS revealing disappearance of first hyperechoic layer (*arrows*), mild thickness and hypoechoic change of the second hypoechoic layer, hypoechoic change of the third hyperechoic layer, and normal fourth hypoechoic layer. *Arrow-sm* submucosal layer, *arrow-mp* muscularis propria. (**d**) Cross section of the corresponding histology (surgical specimen) demonstrating submucosal cancer. *m* mucosa, *sm* submucosa, *mp* muscularis propria, *Ca* cancer

2.5.5 Colo-Rectal Cancer

2.5.5.1 Intramucosal Cancer (Fig. 2.8)

Typical Findings

1. Irregularity, thinness, or disappearance of the first hyperechoic layer
2. Thickness and hypoechoic change of the second hypoechoic layer
3. The third hyperechoic layer intact

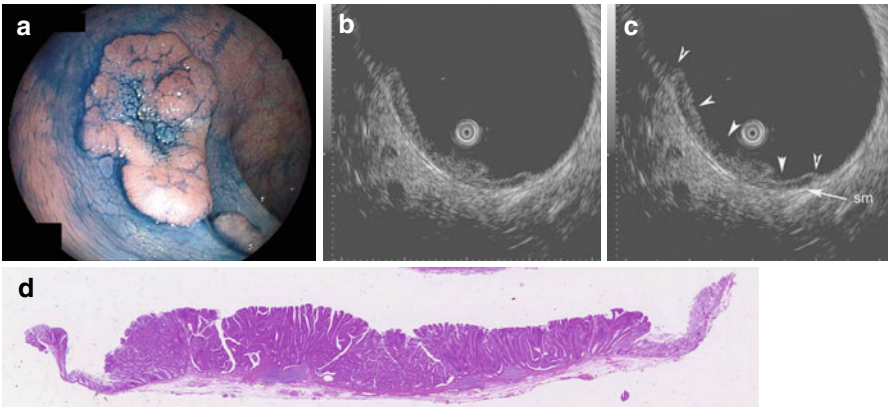

Fig. 2.8 Rectal intramucosal cancer. (**a**) Colonoscopy showing a small IIa+I type early rectal cancer in the rectum (Chromoendoscopic image using indigocarmine dye). (**b**, **c**) EUS revealing irregularity of first hyperechoic layer (*arrowheads*) and mild thickness and hypoechoic change of the second hypoechoic layer and normal third hyperechoic layer. *Arrow-sm* submucosal layer. (**d**) Cross section of the corresponding histology (ESD specimen) demonstrating intramucosal cancer

2.5.5.2 T3 Cancer (Serosa) (Fig. 2.9)

Typical Findings

1. Irregularity, thinness, or disappearance of the first hyperechoic layer
2. Hypoechoic tumor extends to the fifth hyperechoic layer

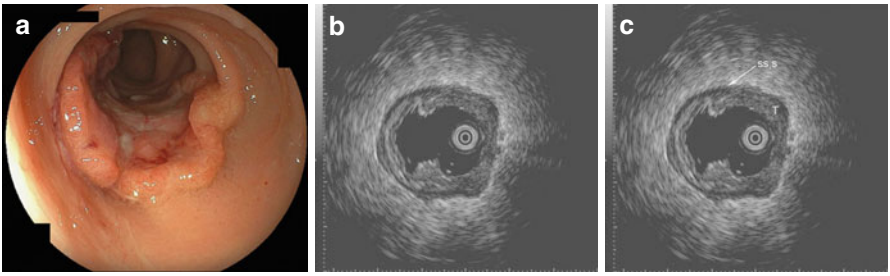

2.5.6 Gastric MALT Lymphoma

2.5.6.1 Superficial Spreading Type Gastric MALT Lymphoma (Submucosal Infiltration) (Fig. 2.10)

Typical Findings

1. Thickness and hypoechoic change of the second hypoechoic layer
2. Superficial hypoechoic change of the third hyperechoic layer
3. The fourth hypoechoic layer intact

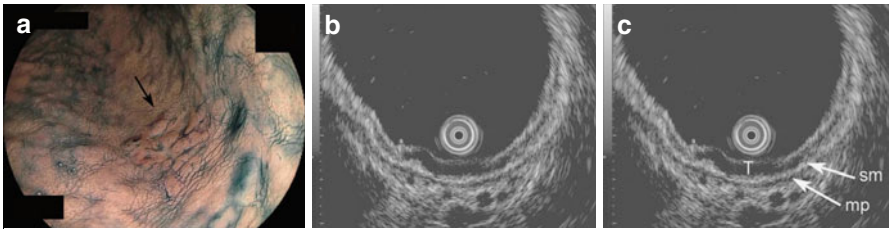

Fig. 2.10 Superficial spreading type gastric MALT lymphoma. (**a**) EGD showing a flat elevated type (superficial spreading type) MALT lymphoma (*arrow*) in the gastric angulus. (**b**, **c**) EUS revealing homogeneous hypoechoic tumor (*T*) extends to the superficial third hyperechoic layer. *Arrow-sm* submucosal layer, *arrow-mp* muscularis propria

Fig. 2.9 Colonic T3 cancer. (**a**) Endoscopic image showing type 2 advanced colonic cancer. (**b**, **c**) EUS reveals hypoechoic tumor (*T*) extending into the fifth hyperechoic layer (*arrow-ss,s*). The fifth hyperechoic layer is interrupted by cancer invasion

2.5.7 GI Tract Submucosal Tumor

EUS using UCP also allows clear imaging of the gastrointestinal wall layers and precise evaluation of the submucosal tumor (Please see Fig. 17.1) [1]. However, UCP has a limited depth of penetration. It enables the evaluation of small subepithelial lesions, but it is often insufficient to allow detailed imaging and diagnosis of external wall impressions. Best indication of UCP for submucosal tumor is one less than 2 cm. We recommend the use of a dedicated echoendoscope for one greater than 2 cm.

Knack-Scanning of Protruded Lesion (Fig. 2.11)

1. It is necessary to scan at the three portions of the protruded lesion to obtain sufficient US information. First (A) is scanning from the top to assess the whole image (Maximum size, shape, etc.), Second (B) and third (C) is scanning from both sides of the base of the lesion to assess the continuity with the muscularis propria (location of the tumor in the GI tract wall)

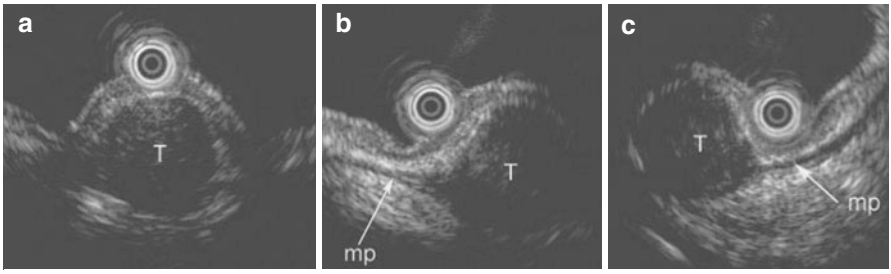

Fig. 2.11 Three important scanning points for protruded lesion. (**a**) Scanning image from the top of the tumor (*T*). (**b**) Scanning image from the left side of the base of the lesion. EUS clearly demonstrates that the tumor continues with the muscularis propria (*arrow-mp*). (**c**) Scanning image from the right side of the base of the lesion. EUS clearly shows that the tumor continues with the muscularis propria (*arrow-mp*)

2.5.8 Typical Case Presentation

2.5.8.1 Gastric Lipoma (Fig. 2.12)

Typical Findings
1. Hyperechoic mass
2. It usually locates within submucosal layer (rarely extends to the serosa)

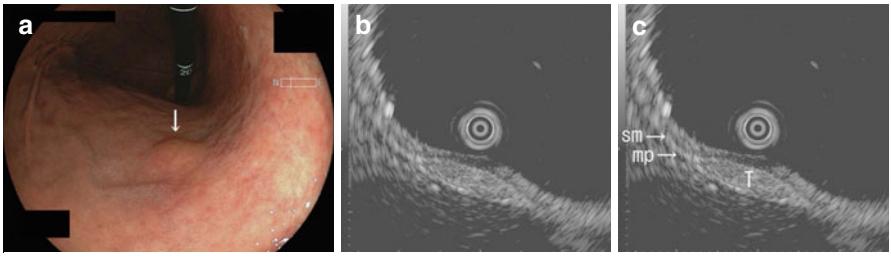

Fig. 2.12 Gastric lipoma. (**a**) EGD showing a small SMT in the gastric body. (**b**, **c**) EUS revealing a submucosal hyperechoic mass (*T*). *Arrow-sm* submucosal layer, *arrow-mp* muscularis propria

2.5.8.2 Cyst (Fig. 2.13)

Typical Findings
1. Anechoic mass
2. It usually locates within submucosal layer

Fig. 2.13 Duodenal cyst. (**a**) EGD showing a small duodenal SMT (6 o'clock side). (**b**, **c**) EUS revealing a submucosal anechoic mass (*Cyst*). *Arrow-sm* submucosal layer, *arrow-mp* muscularis propria

2.5.8.3 Ectopic Pancreas (Fig. 2.14)

Typical Findings

1. Hypoechoic mass with small cystic structures (pancreatic duct)
2. It is usually located within the submucosal layer, but often affects the muscularis propria (thickness of the muscularis propria)

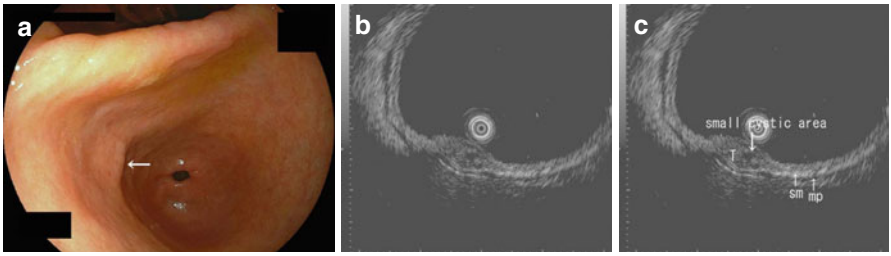

Fig. 2.14 Gastric ectopic pancreas. (**a**) EGD showing a small SMT (*arrow*) in the gastric antrum. (**b**, **c**) EUS revealing a hypoechoic tumor (*T*) in the submucosal layer (*arrow-sm*). This tumor contains small cystic area. *mp* muscularis propria

2.5.8.4 Gastrointestinal Mesenchymal Tumor (GIMT) (Fig. 2.15)

Typical Finding

1. Hypoechoic solid mass with continuity to the muscularis propria

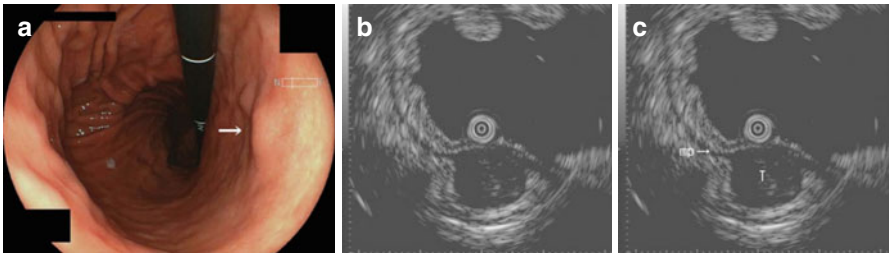

Fig. 2.15 Gastrointestinal mesenchymal tumor of the stomach. (**a**) EGD showing a small SMT (*arrow*) in the gastric body. (**b**, **c**) EUS revealing a hypoechoic solid tumor (*T*) with continuity to the muscularis propria (*arrow-mp*)

2.5.8.5 Esophageal Varices

Masaru Kubokawa

EUS using UCP is relatively noninvasive and provides high-resolution images of the esophageal varices and collateral veins around the esophagus with portal hypertension. Esophageal varices are displayed as echo-free lumina in the third sonographic layer (submucosal). Some investigators supposed that variceal recurrences arise from remnant vessels in the esophagus that could not be visualized by endoscopic images. Previous studies have demonstrated that intramural varices can be assessed with greater accuracy by EUS than with conventional endoscopy. Therefore, EUS is useful for evaluating the effectiveness of endoscopic therapy for esophageal varices.

Schematic representation of esophageal variceal EUS findngs are shown at Fig. 2.16.

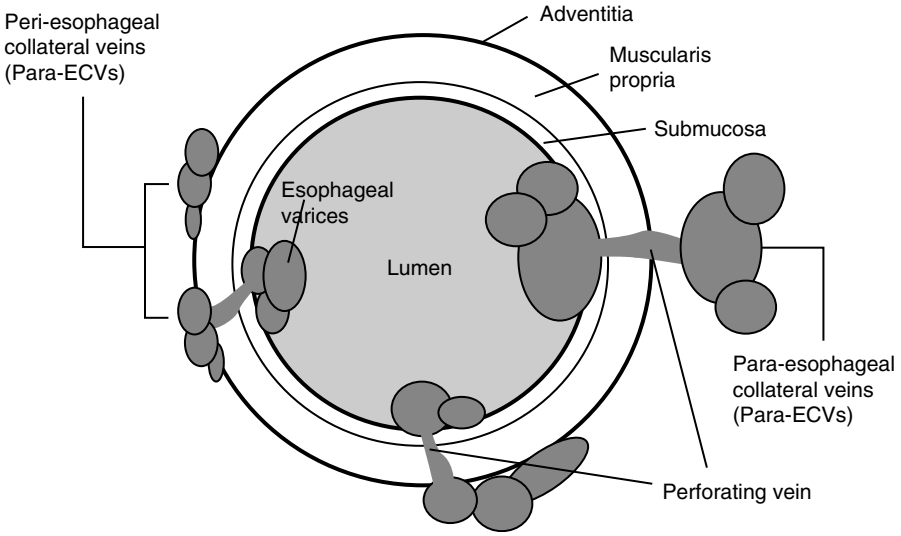

Fig. 2.16 Schematic representation of esophageal variceal findings by EUS. The EUS and EVIS (Endoscopic Varicealography during injection sclerotherapy) findings of the representative case are shown at Figs. 2.17, 2.18, 2.19, and 2.20

Two types of collateral esophageal veins are observed by EUS according to location: periesophageal collateral veins (peri-ECVs) and paraesophageal collateral veins (para-ECVs) (Figs. 2.16, 2.17, and 2.18). Peri-ECVs are smaller vessels lateral to the muscularis propria or veins within the adventitia, and para-ECVs are larger vessels lateral to and separate from the muscularis propria of the esophagus.

In addition, perforating veins connecting the extramural collateral veins to the submucosal varices have been identified (Figs. 2.16, 2.19, and 2.20). Because peri-ECVs and perforating veins are associated with the development of esophageal varices and variceal recurrence after endoscopic treatment, these structures have clinical significance [11–13].

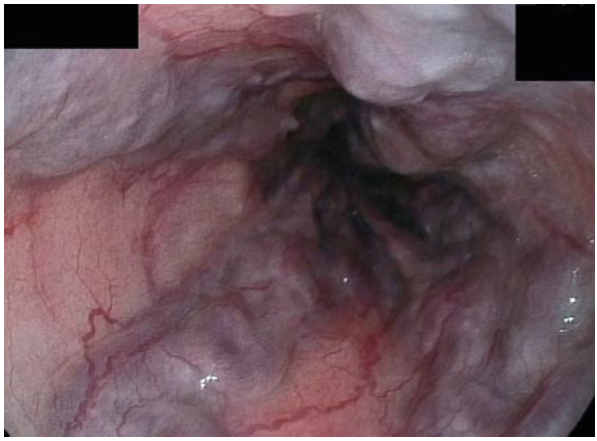

Fig. 2.17 EGD showing esophageal varices with red color signs

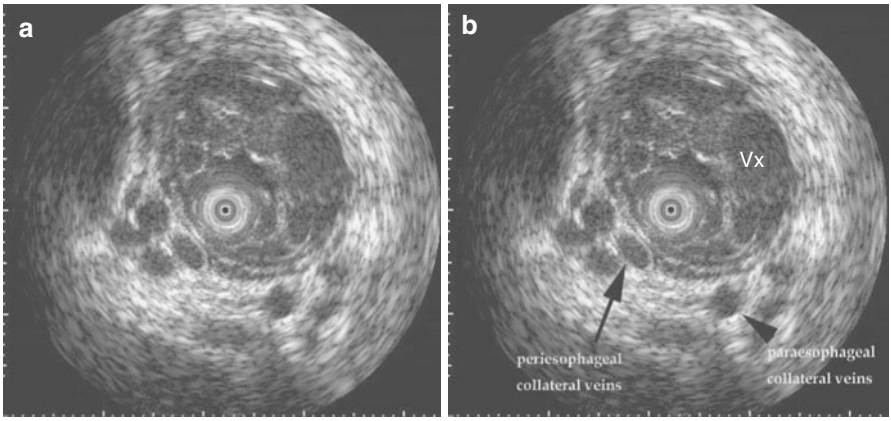

Fig. 2.18 (**a**, **b**) EUS showing esophageal varice as echo-free lumina in the submucosa (*Vx*) and periesophageal collateral veins (*arrow*) and paraesophageal collateral veins (*arrowhead*)

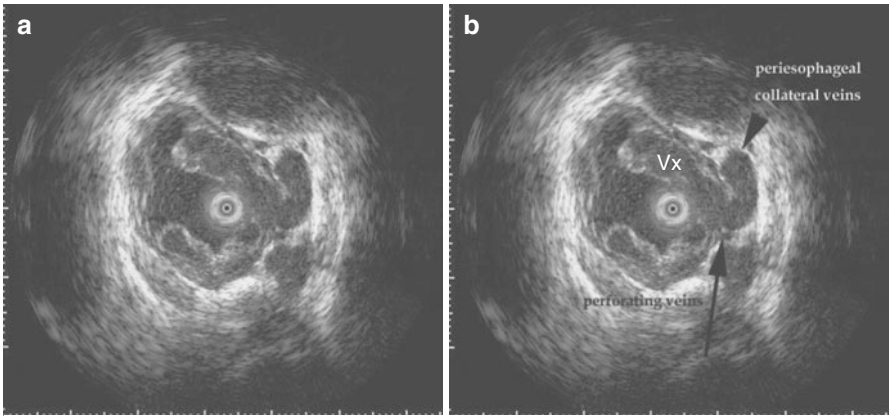

Fig. 2.19 (**a**, **b**) EUS showing perforating vein (*arrow*) connecting the periesophageal collateral veins (*arrowhead*) to the submucosal varices (*Vx*)

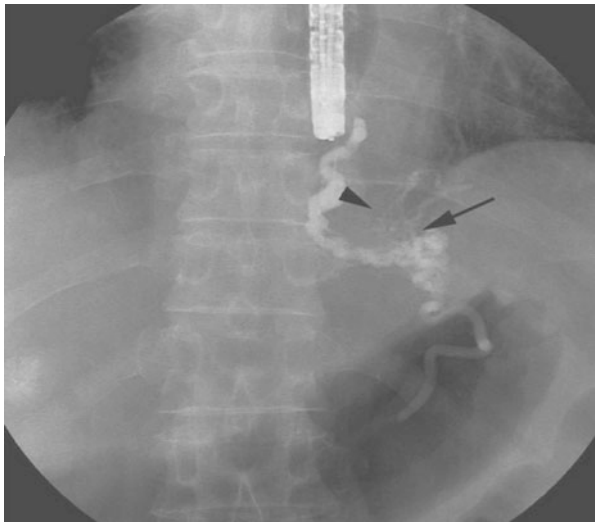

Fig. 2.20 EVIS showing esophageal varices and perforating veins (*arrow*) connecting the periesophageal collateral veins (*arrowhead*)

Various information from EUS may be clinically useful in determining appropriate follow-up intervals or, potentially, in selecting the most suitable endoscopic treatment for esophageal varices.

2.6 Intramural Evaluation for Endoscopic Resection

The increasing acceptance of endoscopic resection as definitive treatment for early stage GI tract cancer has been made possible by technologic advances in endoscopy, improved devices, and the development of EUS staging. The incidence of severe complications related to endoscopic resection has variously been reported as 1–14% [14, 15]. Severe

Table 2.2 Usefullness of EUS for endoscopic resection (excluding staging)

1. Evaluation of underlying blood vessel
Location (which layer; i.e. shallow or deep submucosal layer)
Diameter
2. Evaluation of coexisting ulcer scarring
Measurement of space of fibrosis
Depth of ulcer scarring (i.e. sm, mp, mp< etc.)
3. Evaluation of the intramural changes after submucosal injection
Distribution of injected solution
Measurement of submucosal dissociation by injected solution

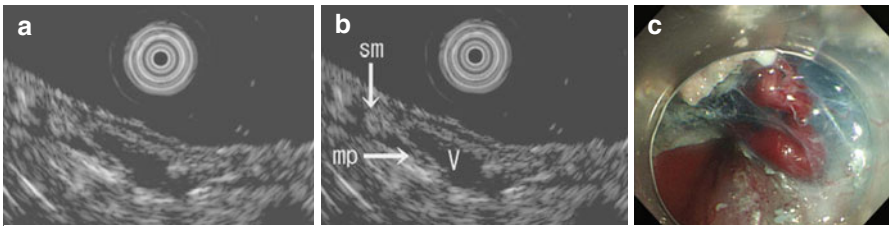

Fig. 2.21 Intramural evaluation for endoscopic resection (blood vessel). (**a**, **b**) Pretreatment EUS showing a large submucosal blood vessel (*V*). *Arrow-sm* submucosal layer, *arrow-mp* muscularis propria. (**c**) Endoscopic image during ESD revealing a large submucosal blood vessel. This vessel was sufficiently coagulated before cutting

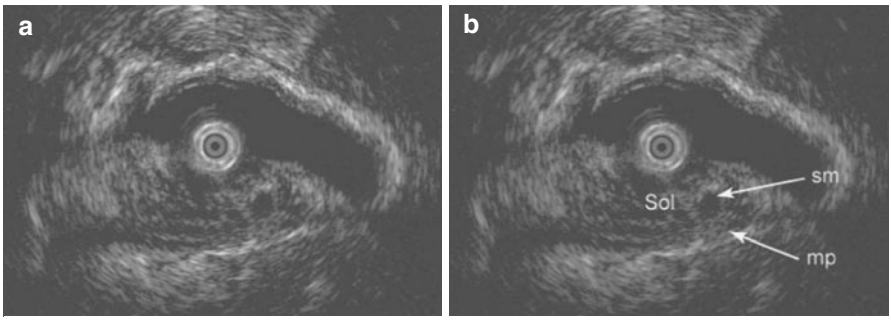

Fig. 2.22 Intramural evaluation for endoscopic resection (submucosal thickness after injection). (**a**, **b**) EUS image of the lesion after the injection of a glycerin solution (Sol) into the submucosal layer during endoscopic mucosal resection. EUS image shows the third layer to be markedly thickened, with low echogenecity, while the other layers are intact. *Arrow-sm* submucosal layer, *arrow-mp* muscularis propria

complications, such as perforation and profuse bleeding, are attributed to cutting of the muscularis propria due to insufficient submucosal injection and large intramural vessels [14, 15]. It is impossible to predict the existence of such dangerous intramural conditions by routine endoscopy alone. Table 2.2 shows useful information for endoscopic resection using UCP (Figs 2.21 and 2.22). Previous studies [15–17] demonstrated that EUS permits excellent visualization of the intramural architecture, including whether or

not large submucosal vessels (Fig. 2.21) are present below the lesion and whether adequate submucosal space has been created by liquid solution injection (Fig. 2.22) [1]. Furthermore, scanning the target lesion with the UCP is simple and repeatable during endoscopic resection. Aggressive use of EUS using the UCP before resection provides us useful information for reducing complications of endoscopic resection.

References

1. Akahoshi K, Harada N, Nawata H (2003) The current state of endoscopic ultrasonography. In: Pandalai SG (ed) Recent research developments in radiology. Trivandrum, Transworld Research Network, pp 1–37
2. Akahoshi K, Chijiiwa Y, Hamada S et al (1998) Pretreatment staging of endoscopically early gastric cancer with a 15 MHz ultrasound catheter probe. Gastrointest Endosc 48:470–476
3. Wallace MB, Hoffman BJ, Sahai AS et al (2000) Imaging of esophageal tumors with a water-filled condom and a catheter US probe. Gastrointest Endosc 51:597–600
4. Schembre D, Chak A, Stevens P et al (2001) Prospective evaluation of balloon-sheathed catheter US system. Gastrointest Endosc 53:758–763
5. Yanai H, Yoshida T, Harada T et al (1996) Endoscopic ultrasonography of superficial esophageal cancers using a thin ultrasound probe system equipped with switchable radial and linear scanning modes. Gastrointest Endosc 44:578–582
6. Murata Y, Suzuki S, Ohta M et al (1996) Small ultrasonic probe for determination of the depth of superficial esophageal cancer. Gastrointest Endosc 44:23–28
7. Yanai H, Noguchi T, Mizumachi S et al (1999) A blind comparison of the effectiveness of endoscopic ultrasonography and endoscopy in staging early gastric cancer. Gut 44:361–365
8. Yoshida M, Tsukamoto Y, Niwa Y et al (1995) Endoscopic assessment of invasion of colorectal tumors with a new high-frequency ultrasound probe. Gastrointest Endosc 41:587–592
9. Saitoh Y, Obara T, Einami K et al (1996) Efficacy of high-frequency ultrasound probes for the preoperative staging of invasion depth in flat and depressed colorectal tumors. Gastrointest Endosc 44:34–39
10. Hiki N, Kurosaka H, Tatsutomi Y et al (2003) Peppermint oil reduces gastric spasm during upper endoscopy: a randomized double-blind, double-dummy controlled trial. Gastrointest Endosc 57:475–482
11. Kishimoto H, Sasaki M, Kajiyama T et al (1995) Miniture ultrasonic probe evaluation of esophageal varices after endoscopic variceal ligation. Gastrointest Endosc 42:256–260
12. Irisawa A, Obara K, Sato Y et al (1990) EUS analysis of collateral veins inside and outside the esophageal wall in portal hypertension. Gastrointest Endosc 50:374–380
13. Irisawa A, Saito A, Obara K et al (2001) Endoscopic reccurence of esophageal varices is associated with the specific EUS abnormalities; severe periesophageal collateral veins and large perforating veins. Gastrointest Endosc 53:77–84
14. Akahoshi K, Akahane H (2010) A new breakthrough: endoscopic submucosal dissection using a newly developed grasping type scissors forceps for early gastrointestinal tract neoplasms. World J Gastrointest Endosc 2:90–96
15. Akahoshi K, Chijiiwa Y, Tanaka M et al (1995) Endosonography probe-guided endoscopic mucosal resection of gastric neoplasms. Gastrointest Endosc 42:248–252
16. Ochiai T, Akahoshi K, Chijiiwa Y et al (1998) Endosonography-probe guided endoscopic resection of colonic lipoma: report of a case. Endoscopy 30:65–66
17. Akahoshi K, Fujimaru T, Nakanishi K et al (2001) Endosonography probe-guided endoscopic resection of small flat rectal carcinoid tumor using band ligation technique. Endoscopy 33:471

Part III

Radial Endoscopic Ultrasonography (EUS)

Basic Scanning Methods of Radial EUS

3

Kazuya Akahoshi

3.1 Preparation, Sedation, and Insertion

Essentially the premedication for EUS is the same as for conventional endoscopy (EGD, TCS etc.). Standard EUS was performed on an outpatient basis, with the patient under conscious sedation. In our institute, each patient was sedated with an intravenous injection of flunitrazepam (0.2–0.4 mg) and pethidine (35 mg). The insertion of the echoendoscope is in the same way as conventional endoscopy, i.e. under forward-viewing endoscopic image guidance (Fig. 3.1) [1].

3.2 Basic Scanning Technique

For EUS, a special condition is required, i.e. a sonolucent material must be between the scanner and the target lesion, and usually de-aerated water is employed.

Three kinds of scanning techniques are used in EUS [2] (Fig. 3.2).

3.2.1 The Balloon-Contact Method

This method is performed by filling the balloon at the tip of the echoendoscope with de-aerated water and contacting the balloon against the GI tract wall to examine the esophagus and pancreaticobiliary system. The balloon is usually inflated by about 1–7 mL de-aerated water.

K. Akahoshi
Department of Gastroenterology, Aso Iizuka Hospital,
Yoshiomachi 3-83, Iizuka city, Fukuoka 820-8505, Japan
e-mail: kakahoshi2@aol.com

K. Akahoshi, A. Bapaye (eds.), *Practical Handbook of Endoscopic Ultrasonography*,
DOI 10.1007/978-4-431-54014-4_3, © Springer 2012

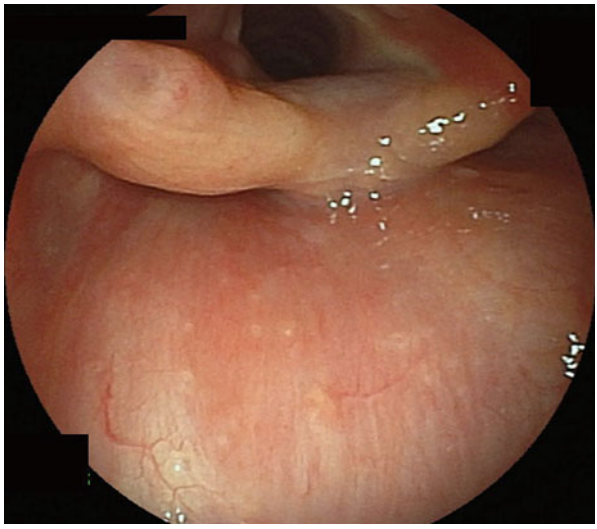

Fig. 3.1 Endoscopic image at the time of esophageal intubation by EG-530UR2

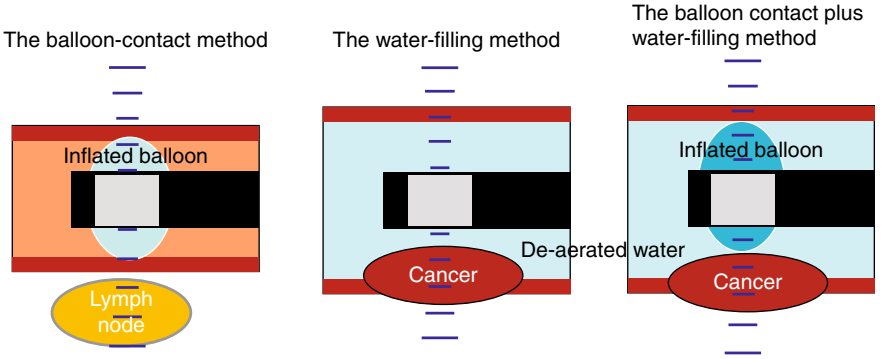

Indications		
Pancreatico-biliary lesions Extra GI tract lesions Esophageal lesions	GI tract lesions	GI tract lesions The lesion of the papilla of vater

Fig. 3.2 EUS scanning techniques

3.2.2 The Water-Filling Method

This method used for GI tract lesions is the water-filling method in which the de-aerated water is infused into the GI tract through the working channel of the echoendoscope until the GI tract lumen is filled and extended by de-aerated water. The volume of de-aerated water infused depends on each organ, usually about 100–500 mL. This method is useful to evaluate the layered structure of the GI tract wall, and is usually used for GI tract cancer T staging and diagnosis of submucosal tumor, etc.

3.2.3 The Balloon Contact Plus Water-Filling Method

This method is a combination of the balloon contact and water filling methods, and is useful for GI tract lesions and lesions of the papilla of Vater.

Knack (For Obtaining Good Images)

1. As the scanner has its own focal distance according to the frequency of the ultrasound, usually 20–30 mm, the target area should be placed at the correct distance
2. A vertical scan of the target lesion is recommended for GI tract diseases
3. Continuous EUS scanning is recommended to prevent making a blind spot

References

1. Akahoshi K, Tanaka T, Matsui N et al (2007) Newly developed all in one EUS system: one cart system, forward-viewing optics type 360º electronic radial array echoendoscope and oblique-viewing type convex array echoendoscope. Fukuoka Acta Med 98:82–89
2. Yasuda K (2000) The handbook of endoscopic ultrasonography in digestive tract, 1st edn. Blackwell Science, Tokyo

Radial EUS of the Esophagus and Mediastinum

4

Kazuya Akahoshi

4.1 Indication

EUS is indicated for the intra-esophageal or extra-esophageal (within about 3–4 cm from the esophagus) lesion (Table 4.1).

4.2 Scanning Technique

The water filling method is not recommended in the esophagus, due to the risk of aspiration.

Therefore, the balloon contact method (Fig. 3.2) is usually used. Starting EUS in the distal part of the esophagus, filling the balloon with 1–7 mL de-aerated water allows us to remove the intervening air.

4.3 Basic Anatomy

4.3.1 Normal Esophageal Wall

Using the balloon contact method, the normal esophageal wall can be delineated as a five layered structure (Fig. 4.1) that corresponds well to the histological layers. The first, echogenic layer and the second, hypoechoic layer correspond to the mucosal layer. The third hyperechoic layer is the submucosa and the fourth

K. Akahoshi
Department of Gastroenterology, Aso Iizuka Hospital,
Yoshiomachi 3-83, Iizuka city, Fukuoka 820-8505, Japan
e-mail: kakahoshi2@aol.com

K. Akahoshi, A. Bapaye (eds.), *Practical Handbook of Endoscopic Ultrasonography*,
DOI 10.1007/978-4-431-54014-4_4, © Springer 2012

Table 4.1 Indication of Radial EUS for the esophagus and mediastinum

Staging of esophageal cancer
Evaluation of submucosal tumor or extra-esophageal compression
Restaging of malignant tumor after chemo and/or radiotherapy
Pre and post treatment hemodynamic assessment for esophageal varices
Evaluation of detectable mediastinal disease

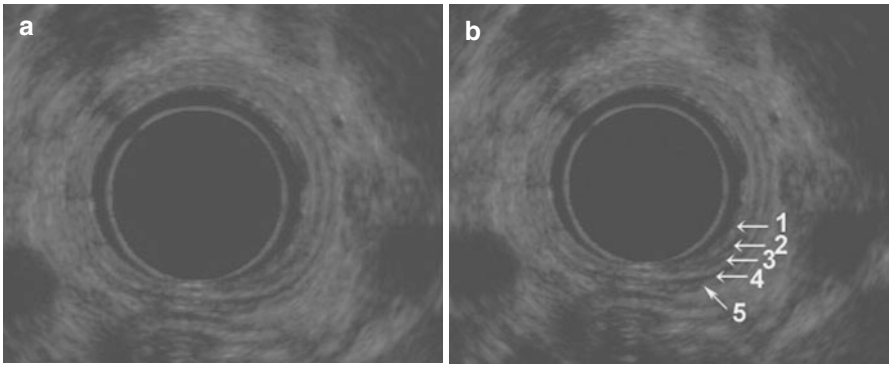

Fig. 4.1 EUS image of normal esophageal wall with a five-layered structure. (**a**, **b**) *Arrow-1* first hyperechoic layer (balloon echo and mucosal surface), *Arrow-2* second hypoechoic layer (mucosa), *Arrow-3* third hyperechoic layer (submucosa), *Arrow-4* fourth hypoechoic layer (muscularis propria), *Arrow-5* fifth hyperechoic layer (adventitia)

hypoechoic layer corresponds to the muscularis propria. The fifth, hyperechoic layer corresponds to the adventitia [1, 2].

4.3.2 Transesophageal Scanning (Esophago-gastric Junction ~ Cervix)

At the level of the near esophago-gastric junction (Fig. 4.2), usually the inferior vena cava, descending aorta and spine (6 o' clock side) are imaged as land marks on the monitor.

At the level of the lower mediastinum (Fig. 4.3), usually the left atrium and pulmonary veins are visualized as land marks.

At the level of middle mediastinum (Fig. 4.4), usually the right and left bronchus and right pulmonary artery are visualized as land marks.

At the level of the upper mediastinum (Fig. 4.5), usually the aortic arch is visualized as land mark.

At the level of the cervix (Fig. 4.6), usually the trachea and lower lobes of the thyroid gland are visualized as land marks.

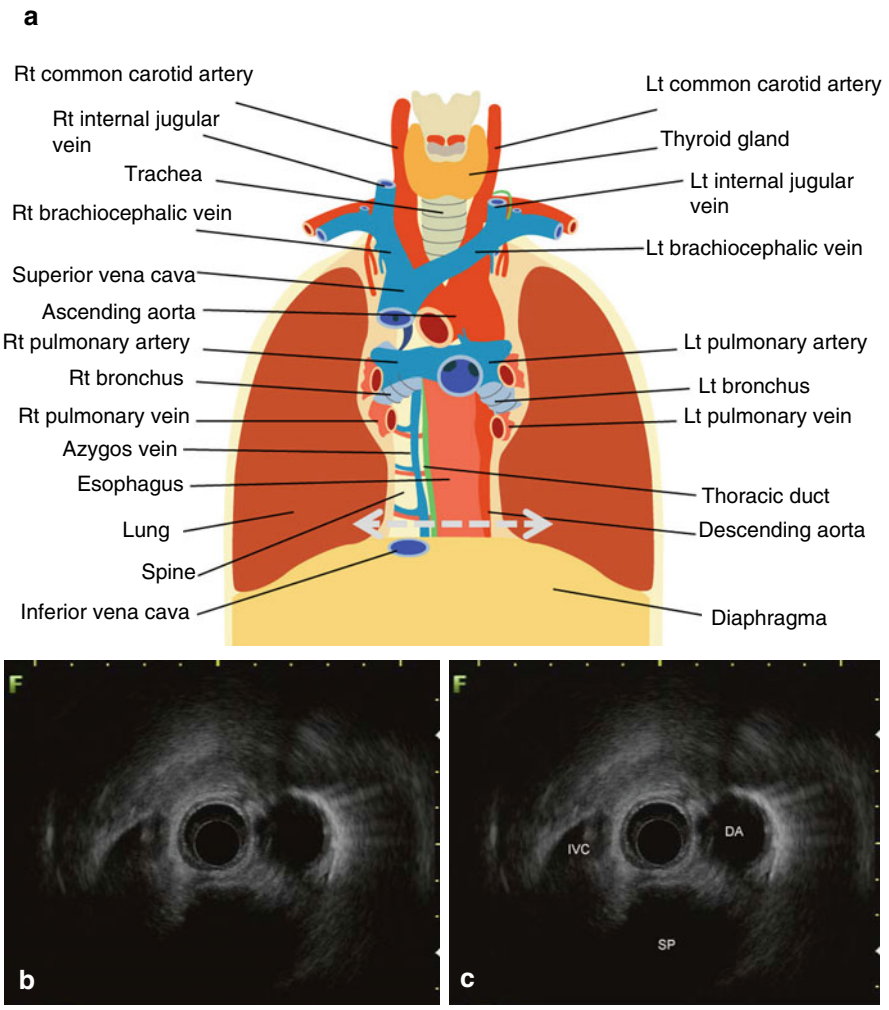

Fig. 4.2 EUS image of trans-esophageal scanning (above EGJ portion). (**a**) Scanning portion, (**b**) EUS image, (**c**) EUS image with abbreviations. *DA* descending aorta, *IVC* inferior vena cava, *SP* spine

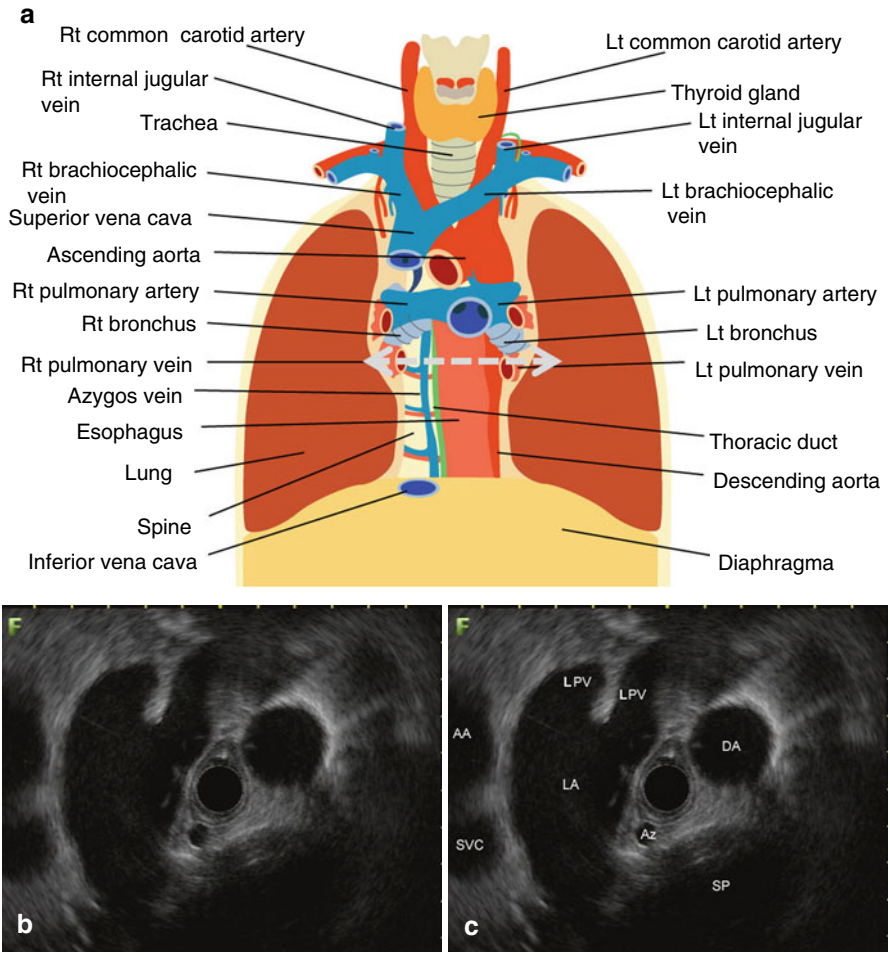

Fig. 4.3 EUS image of trans-esophageal scanning (lower mediastinum portion). (**a**) Scanning portion, (**b**) EUS image, (**c**) EUS image with abbreviations. *AA* ascending aorta, *SVC* superior vena cava, *LA* left atrium, *LPV* left pulmonary vein, *Az* azygos vein, *DA* descending aorta, *SP* spine

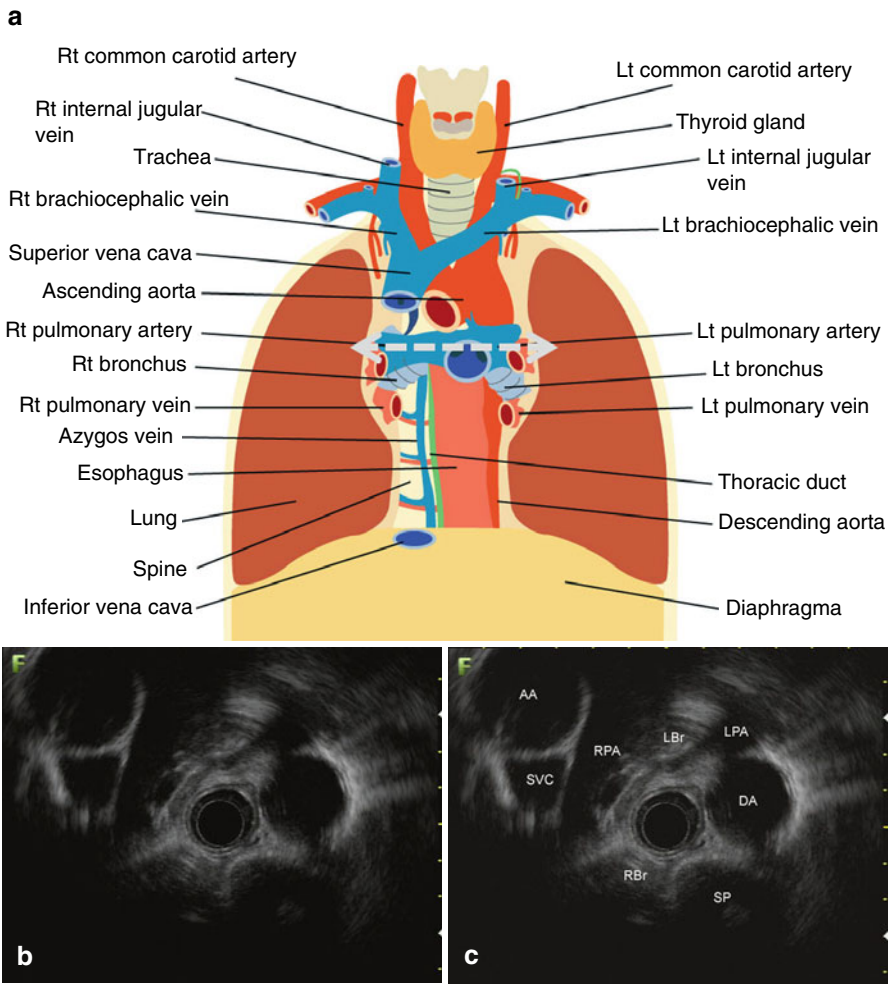

Fig. 4.4 EUS image of trans-esophageal scanning (middle mediastinum portion). (**a**) Scanning portion, (**b**) EUS image, (**c**) EUS image with abbreviations. *AA* ascending aorta, *SVC* superior vena cava, *RPA* right pulmonary artery, *RBr* right bronchus, *LBr* left bronchus, *LPA* left pulmonary artery, *DA* descending aorta, *SP* spine

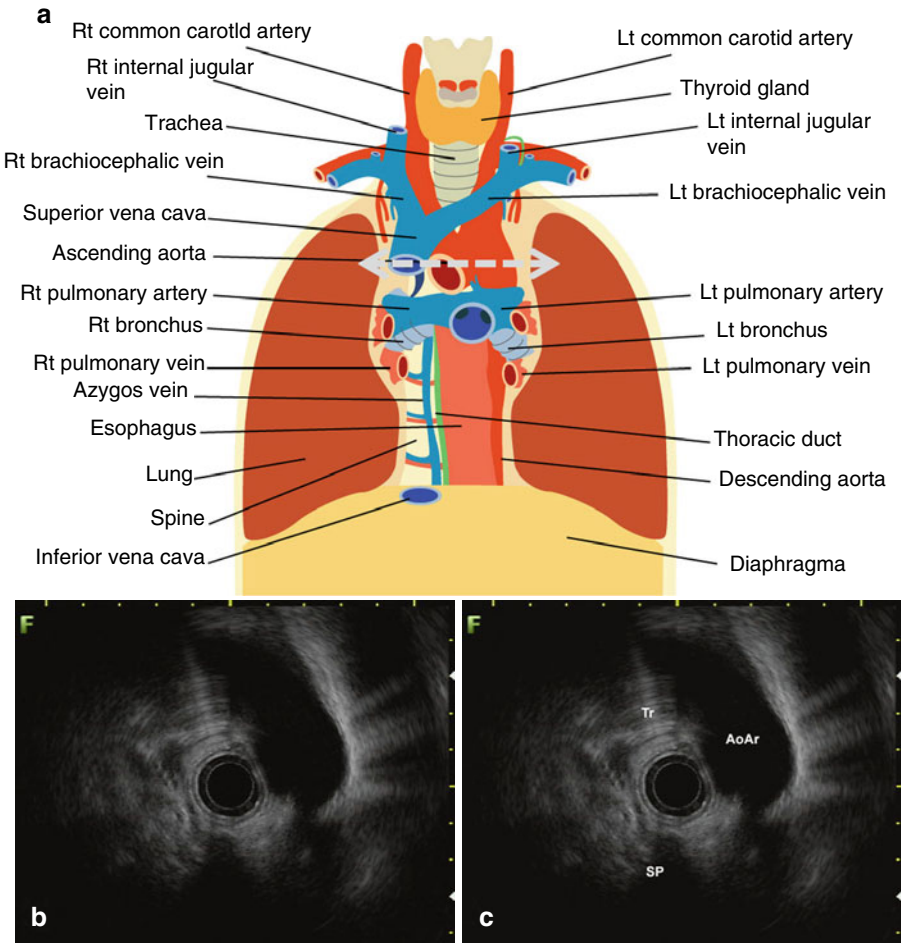

Fig. 4.5 EUS image of trans-esophageal scanning (upper mediastinum portion). (**a**) Scanning portion, (**b**) EUS image, (**c**) EUS image with abbreviations. *Tr* trachea, *SP* spine, *AoAr* aortic arch

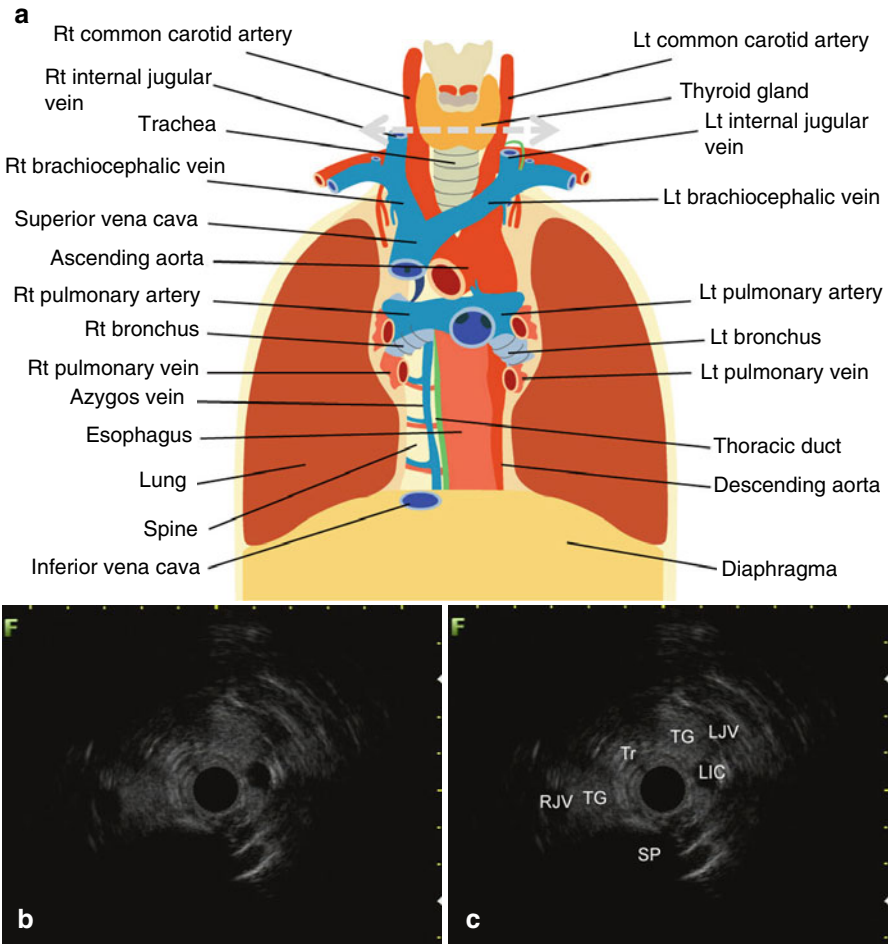

Fig. 4.6 EUS image of trans-esophageal scanning (cervix). (**a**) Scanning portion, (**b**) EUS image, (**c**) EUS image with abbreviations. *RJV* right internal jugular vein, *TG* thyroid gland, *Tr* trachea, *SP* spine, *LIC* left internal carotid artery, *LJV* left internal jugular vein

4.4 Diagnosis

4.4.1 Esophageal Cancer

The main purpose of EUS for this disease is TN staging. Esophageal cancer is usually imaged as hypoechoic tumor. Depth of invasion is determined by the deepest layer of the esophagus infiltration of the hypoechoic tumor (Please see Fig. 2.3). The accuracy of EUS ranges from 69% to 89% and 69% to 81% for T and N staging, respectively [2–5]. At present, EUS is significantly more accurate than CT in TN staging.

4.4.1.1 T1-Submucosal Cancer (Fig. 4.7)

Typical Findings

1. Thickness and hypoechoic change of the second hypoechoic layer
2. Partial hypoechoic change of the third hyperechoic layer
3. Intact fourth hypoechoic layer

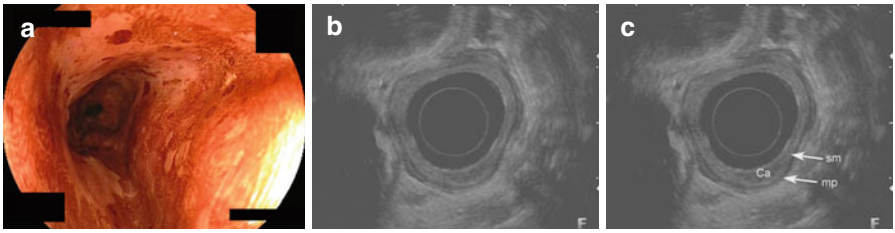

Fig. 4.7 EUS image of esophageal T1 submucosal cancer. (**a**) EGD showing a broad IIc type superficial esophageal cancer in the middle esophagus (Lugor staining). (**b**, **c**) EUS revealing mild thickness and hypoechoic change of the second hypoechoic layer and hypoechoic change of the upper part of the third hyperechoic layer, but the fourth hypoechoic layer is intact. *Ca* cancer, *arrow-sm* submucosal layer, *arrow-mp* muscularis propria

4.4.1.2 T3 Cancer (Fig. 4.8)

Typical Finding

1. Hypoechoic tumor extends from the second to the fifth layer

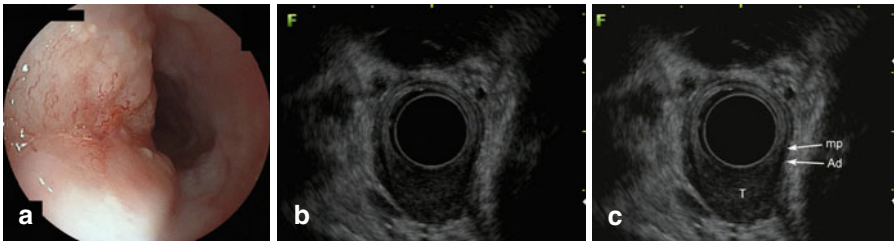

Fig. 4.8 EUS image of T3 cancer. (**a**) Endoscopic image showing type 2-like advanced esophageal cancer. (**b**, **c**) EUS reveals hypoechoic tumor (*T*) extending into the fifth hyperechoic layer. The fifth hyperechoic layer is interrupted by cancer invasion. *T* tumor, *arrow-mp* muscularis propria, *arrow-Ad* adventitia

4.4.1.3 Periesophageal Lymph Node Metastasis (Fig. 4.9)

Typical Finding

1. Well-defined round or elliptical structures adjacent to the esophageal wall that have a more hypoechoic pattern than the surrounding tissues

Knack and Pitfall 1 (Differential Diagnosis Between Benign and Malignant Lymph Node)

1. Lymph node characteristics on EUS can be helpful in classifying benign from malignant lymph nodes. However, no established EUS criteria exists at present
2. Reported EUS criteria [6] for malignant lymph node are (1) hypoechoic pattern, (2) clearly delineated boundaries, and (3) direct extension of the primary tumor into adjacent lymph nodes

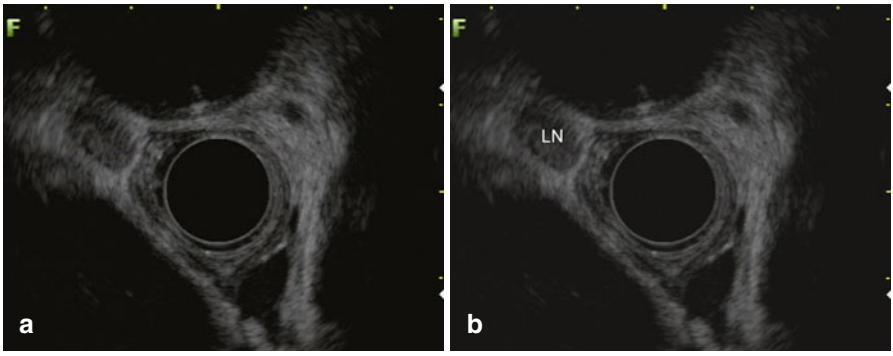

Fig. 4.9 EUS image of peri-esophageal lymph node metastasis. (**a**, **b**) EUS revealing peri-esophageal well-defined elliptical hypoechoic mass. *LN* lymph node

4.4.2 Esophageal Submucosal Tumor

The main purpose of EUS for this disease is the evaluation of the submucosal tumor or extra-esophageal compression. EUS also allows clear imaging of the esophageal wall layers and precise evaluation of the submucosal tumor such as layer of origin, histological nature, real size of the tumor, etc. [7, 8].

4.4.2.1 Gastrointestinal Mesenchymal Tumor of the Esophagus (Fig. 4.10)

Typical Findings

1. Hypoechoic solid tumor
2. Continuity with the muscularis propria

Pitfall

1. EUS can't replace histologic diagnosis, i.e. GIST, leiomyoma, neurinoma, etc. EUS-FNA is the only way to obtain histologic diagnosis

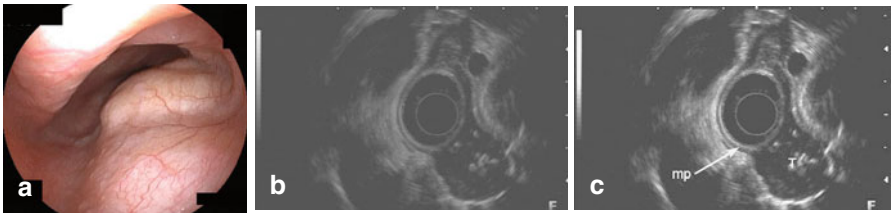

Fig. 4.10 Esophageal leiomyoma (diagnosed by EUS-FNA). (**a**) EGD showing a submucosal tumor in the middle esophagus. (**b**, **c**) EUS reveals a hypoechoic solid tumor (*T*) with continuity to the fourth hypoechoic layer (muscularis propria, *arrow-mp*). This tumor has several strong echos with acoustic shadow (calcification)

4.4.2.2 Extraesophageal Compression Due to Spine (Fig. 4.11)

Typical Findings

1. Compression of normal esophageal wall by the spine
2. There is no mass in the esophageal wall

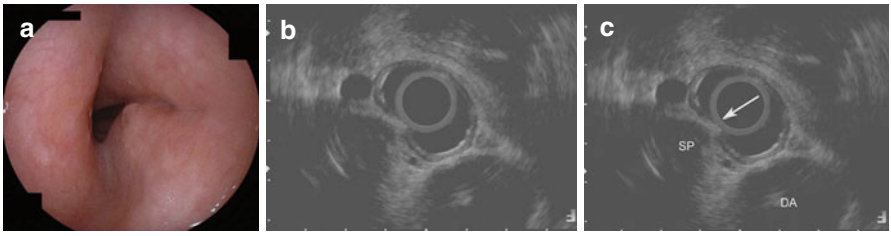

Fig. 4.11 Extraesophageal compression by spine. (**a**) EGD showing a submucosal bulging in the upper esophagus. (**b**, **c**) EUS revealing extra-esophageal compression (*arrow*) by spine (*SP*). *DA* descending aorta

References

1. Aibe T, Takemoto T (1986) A fundamental study of normal layer structure of the gastrointestinal wall visualized by endoscopic ultrasonography. Scand J Gastroenterol Suppl 123:6–15
2. Fuijishima H, Chijiiwa Y, Maruoka A et al (1994) Endoscopic US and dynamic CT in preoperative TN staging of esophageal squamous cell carcinoma. Dig Endosc 6:224–231
3. Ziegler K, Sanft C, Zeitz M et al (1991) Evaluation of endosonography in TN staging of oesophageal cancer. Gut 32:16–20
4. Kienle P, Buhl K, Kuntz C et al (2002) Prospective comparison of endoscopy, endosonography and computed tomography for staging of tumours of the oesophagus and gastric cardia. Digestion 66:230–236
5. Weaver SR, Blackshaw GR, Lewis WG et al (2004) Comparison of special interest computed tomography, endosonography and histopathological stage of oesophageal cancer. Clin Radiol 59:499–504
6. Tio TL, Coene PPLO, Luiken GJHM et al (1990) Endosonography in the clinical staging of esophagogastric carcinoma. Gastrointest Endosc 36:S2–S10
7. Akahoshi K, Harada N, Nawata H (2003) The current state of endoscopic ultrasonography. In: Pandalai SG (ed) Recent research developments in radiology. Transworld Research Network, Trivandrum, pp 1–37
8. Akahoshi K, Oya M (2010) Gastrointestinal stromal tumor of the stomach: how to manage? World J Gastrointest Endosc 2:271–277

Radial EUS of the Stomach

5

Kazuya Akahoshi

5.1 Indication

EUS is indicated for as intra-gastric or extra-gastric (within about 3–4 cm from the stomach) lesion (Table 5.1).

5.2 Scanning Technique

The water filling method (Fig. 3.2, please see Chap. 3) is usually indicated in the stomach. First, sufficient suction of air and gastric juice is necessary. Second, the echoendoscope is positioned at the prepylorus. Third, 300–500 mL de-aerated water is introduced into the gastric lumen via the biopsy channel. EUS is then performed to evaluate the lesion.

5.3 Basic Anatomy

5.3.1 Gastric Wall

Using the water filling method, the normal gastric wall can be delineated as a five layered structure (Fig. 5.1) that corresponds well to the histological layers. The first, echogenic layer and the second, hypoechoic layer correspond to the mucosal layer. The third hyperechoic layer is the submucosa and the fourth hypoechoic layer

K. Akahoshi
Department of Gastroenterology, Aso Iizuka Hospital,
Yoshiomachi 3-83, Iizuka city, Fukuoka 820-8505, Japan
e-mail: kakahoshi2@aol.com

K. Akahoshi, A. Bapaye (eds.), *Practical Handbook of Endoscopic Ultrasonography*,
DOI 10.1007/978-4-431-54014-4_5, © Springer 2012

Table 5.1 Indication of Radial EUS for the gastric lesion

Staging of gastric cancer
Evaluation of submucosal tumor or extragastric compression
Restaging of malignant tumor after chemo and/or radiotherapy
Evaluation of vascular disease (Dieulafoy's lesion, gastric varices, etc.)
Evaluation of peptic ulcer
Differential diagnosis of wall thickness of the stomach

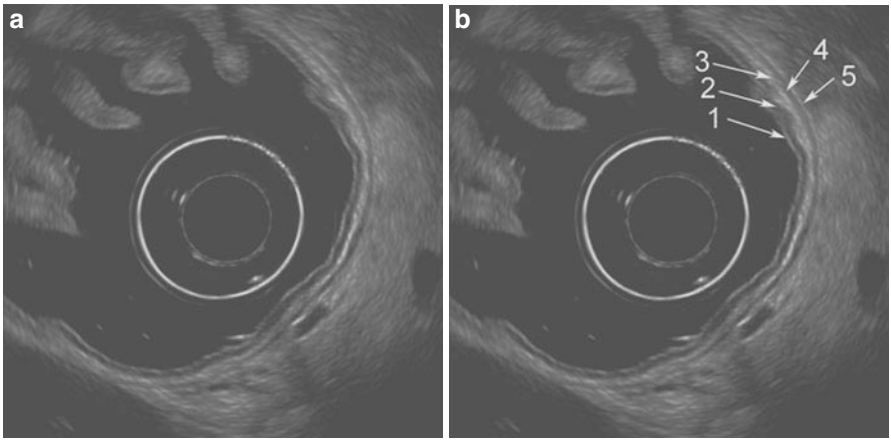

Fig. 5.1 EUS image of normal gastric wall with a five-layered structure by SU-8000 system. (**a**, **b**) *Arrow-1* first hyperechoic layer, *Arrow-2* second hypoechoic layer (mucosa), *Arrow-3* third hyperechoic layer (submucosa), *Arrow-4* fourth hypoechoic layer (muscularis propria), *Arrow-5* fifth hyperechoic layer (subserosa and serosa)

corresponds to the muscularis propria. The fifth, hyperechoic layer corresponds to the subserosa and serosa [1, 2].

5.3.1.1 Transgastric Scanning

At the level of the gastric antrum (Fig. 5.2), usually EUS probes are contacted on the greater curvature.

At the level of the gastric body (Fig. 5.3), usually liver (anterior wall side), pancreas (posterior wall side) and folds (great curvature side) are visualized as land marks.

5.4 Diagnosis

5.4.1 Gastric Cancer

The main purpose of EUS for gastric cancer is pretherapeutic TN staging [1, 3, 4]. Gastric cancer is usually imaged as a hypoechoic tumor. Depth of invasion is determined as the deepest layer of the stomach infiltrated by the hypoechoic tumor

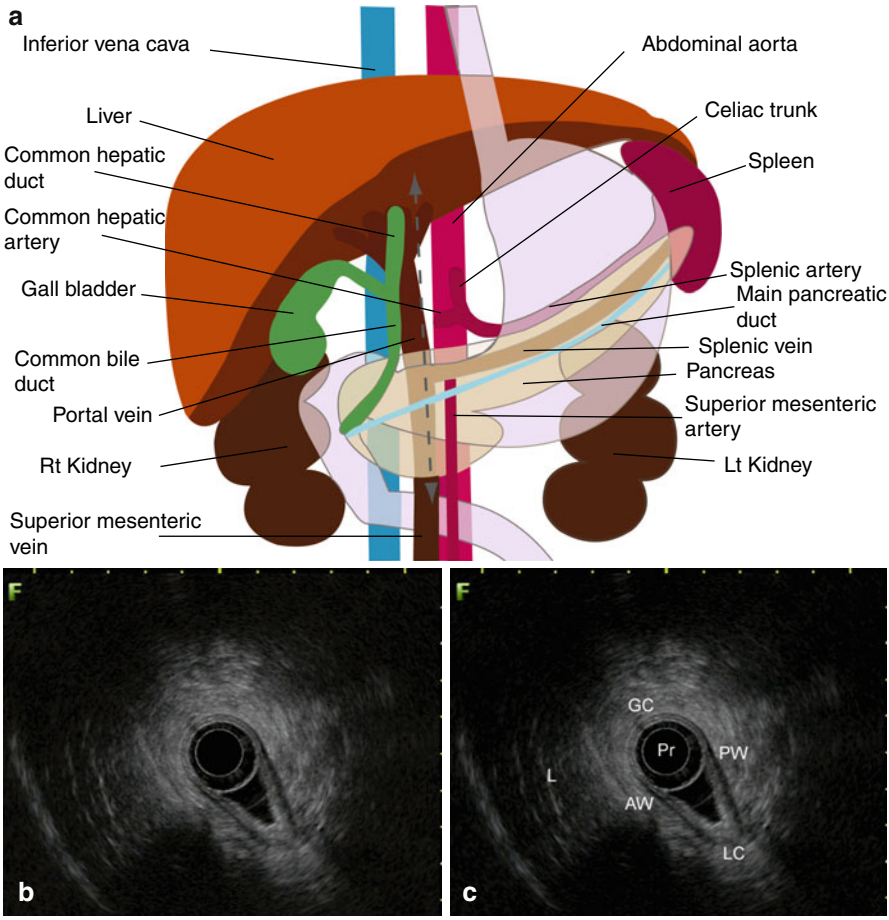

Fig. 5.2 EUS image at gastric antrum. (**a**) Scanning portion, (**b**) EUS image, (**c**) EUS image with abbreviations. *L* liver, *AW* anterior wall, *PW* posterior wall, *Pr* probe, *GC* greater curvature, *LC* lesser curvature

(Fig. 2.3, please see Chap. 2) [1]. Many studies have demonstrated the superior accuracy of EUS over CT, ranging from 80% to 92% (T-stage) and 50% to 90% (N-stage) [1, 4, 5]. Understaging due to microscopic infiltration and overstaging due to peritumoral inflammation or accompanying ulcerative changes, such as edema, inflammation, and fibrosis, can occur [1, 4–6].

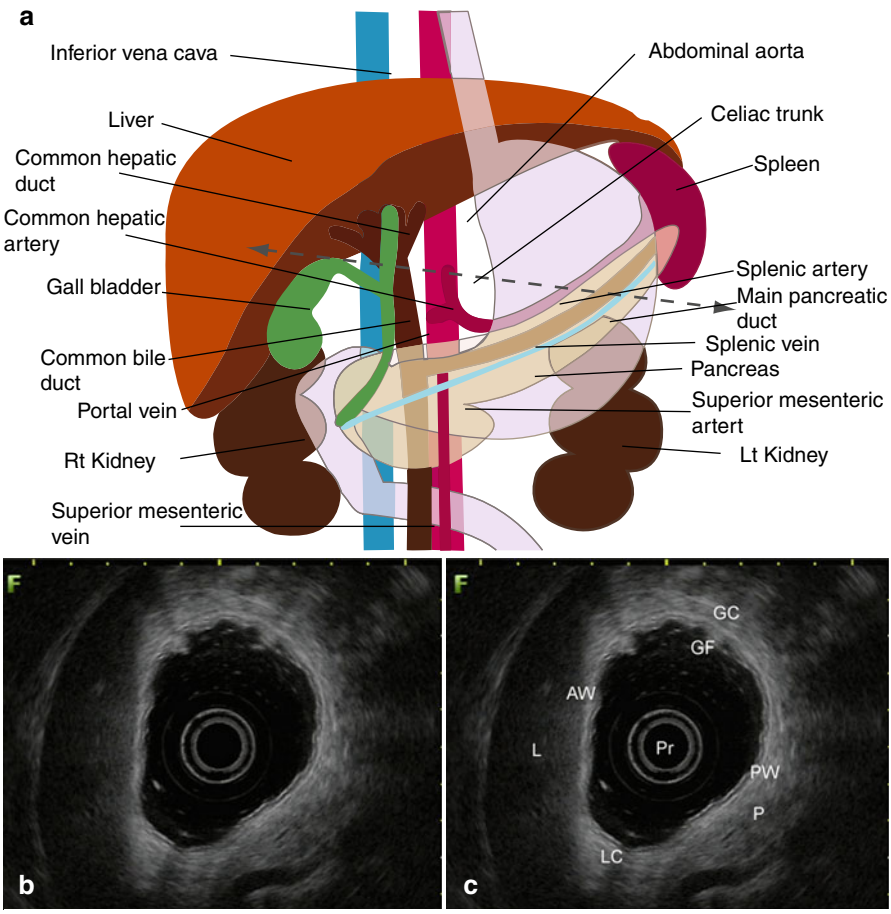

Fig. 5.3 EUS image at gastric body. (**a**) Scanning portion, (**b**) EUS image, (**c**) EUS image with abbreviations. *L* liver, *GF* gastric fold, *AW* anterior wall, *PW* posterior wall, *Pr* probe, *GC* greater curvature, *LC* lesser curvature, *P* pancreas

5.4.1.1 T1-Intramucosal Cancer (Fig. 5.4)

Typical Findings

1. Irregularity, thinness, or disappearance of the first hyperechoic layer
2. Thickness and hypoechoic change of the second hypoechoic layer
3. The third hyperechoic layer intact

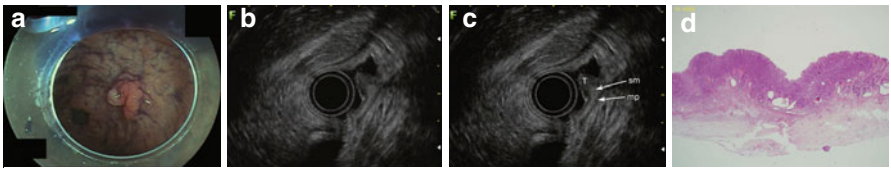

Fig. 5.4 Gastric T1 intramucosal cancer. (**a**) EGD showing a small 0-I type (protruded type) early gastric cancer in the gastric antrum. (**b**, **c**) EUS revealing irregularity of the first hyperechoic layer and mild thickness and hypoechoic change of the second hypoechoic layer (*T*) and normal third hyperechoic layer. *Arrow-sm* submucosal layer, *arrow-mp* muscularis propria. (**d**) Cross section of the corresponding histology (ESD specimen) demonstrating intramucosal cancer

5.4.1.2 T1-Submucosal Cancer (Fig. 5.5)

Typical Findings

1. Irregularity, thinness, or disappearance of the first hyperechoic layer
2. Thickness and hypoechoic change of the second hypoechoic layer
3. Hypoechoic change of the third hyperechoic layer
4. The fourth hypoechoic layer intact

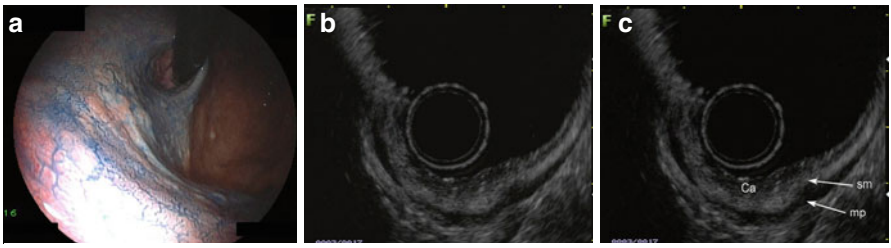

Fig. 5.5 Gastric T1 submucosal cancer. (**a**) EGD showing a IIc type early gastric cancer in the gastric cardia (Indigocarmine dye spreading method). (**b**, **c**) EUS revealing irregularity of first hyperechoic layer, mild thickness and hypoechoic change of the second hypoechoic layer, hypoechoic change of the superficial part of the third hyperechoic layer, and normal fourth hypoechoic layer. *Arrow-sm* submucosal layer, *arrow-mp* muscularis propria, *Ca* cancer

5.4.1.3 T2-Cancer (Muscularis Propria or Subserosa) (Fig. 5.6)

Typical Findings

1. Irregularity, thinness, or disappearance of the first hyperechoic layer
2. Hypoechoic tumor extends to the fourth hypoechoic layer
3. The fifth hyperechoic layer intact

Fig. 5.6 Gastric T2 cancer. (**a**) Endoscopic image showing type 3 (ulcerated type) advanced gastric cancer. (**b**, **c**) EUS reveals hypoechoic tumor extending into the fourth hypoechoic layer (*arrow-mp*). The fifth hyperechoic layer is intact (*arrow-ss,s*). *Ca* cancer

5.4.1.4 T3 Cancer (Serosa) (Fig. 5.7)

Typical Findings

1. Irregularity, thinness, or disappearance of the first hyperechoic layer
2. Hypoechoic tumor extends to the fifth hyperechoic layer

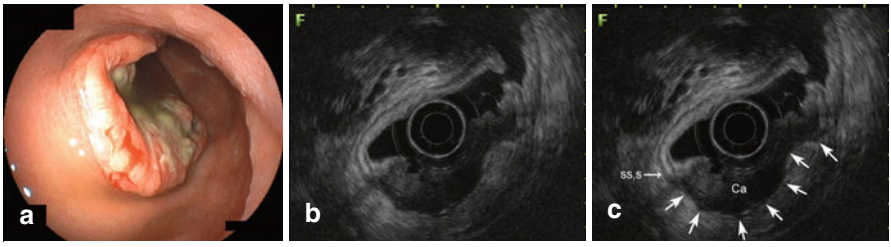

Fig. 5.7 Gastric T3 cancer. (**a**) Endoscopic image showing type 2 advanced gastric cancer. (**b**, **c**) EUS reveals hypoechoic tumor extending into the fifth hyperechoic layer (*arrow-ss,s*). The fifth hyperechoic layer is interrupted (*arrows*) by cancer invasion. *Ca* cancer invasion

5.4.1.5 T4-Cancer (Invasion to Pancreas) (Fig. 5.8)

Typical Findings

1. Irregularity, thinness, or disappearance of the first hyperechoic layer
2. Hypoechoic tumor extends to the pancreas
3. The border echo between stomach and pancreas is interrupted by tumor echo

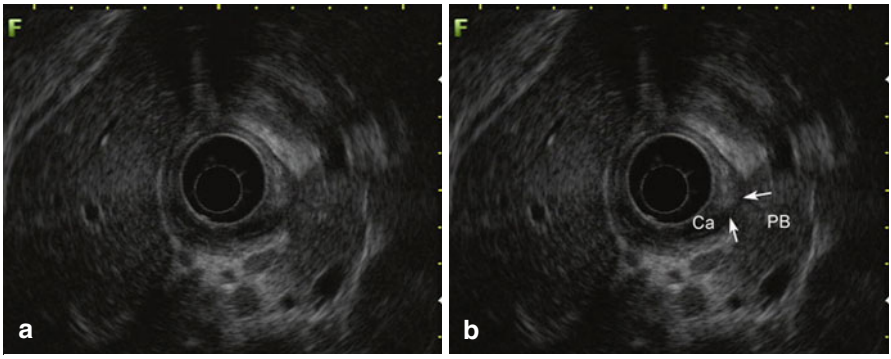

Fig. 5.8 Gastric T4 cancer. (**a**, **b**) EUS reveals hypoechoic tumor (*Ca*) extending into the pancreas (*PB*). The border-echo is interrupted (*arrows*) by cancer invasion

5.4.1.6 Lymph Node Metastasis (Gastric Cancer) (Figs. 5.9 and 5.10)

Typical Finding

1. Well-defined round or elliptical structures adjacent to the gastric wall that has a more hypoechoic pattern than the surrounding tissues

Knack 1 (Differential Diagnosis Between Lymph Node and Blood Vessel)

1. The differentiation of lymph nodes from vessels is best accomplished with the same slow, back-and-forth motion used when round structures are visualized until we can decide whether the structure is a continuation of the vessel [7]
2. Check the blood flow using color Doppler flow mapping. If hypoechoic mass has no blood flow, it is a lymph node. If whole area of hypoechoic mass has blood flow, it is a blood vessel [1]

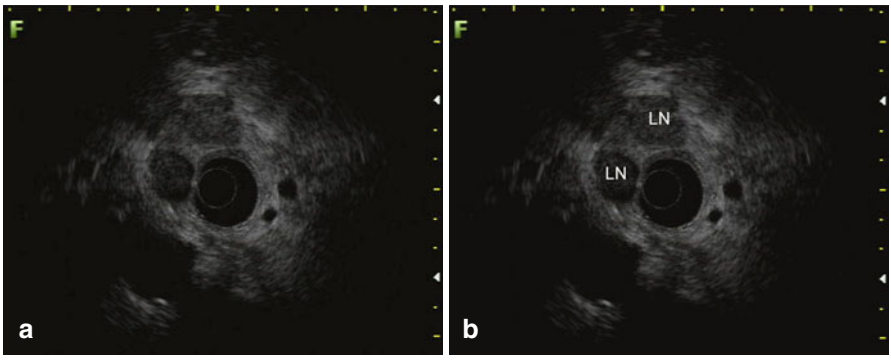

Fig. 5.9 Peri-gastric lymph node metastasis of lesser curvature group. (**a**, **b**) EUS revealing peri-gastri well-defined elliptical hypoechoic mass. *LN* lymph node

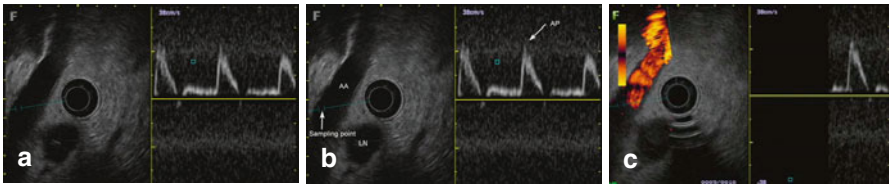

Fig. 5.10 Para-aortic lymph node metastasis of gastric cancer. (**a**, **b**) EUS revealing para-aortic well-defined elliptical hypoechoic mass (*LN* lymph node). Pulse-wave mode image showing arterial pulsation (*AP*). *AA* abdominal aorta. (**c**) Color Doppler flow mapping image showing no blood flow in para-aortic well-defined elliptical hypoechoic mass (lymph node)

5.4.1.7 Scirrhous Type Cancer (Fig. 5.11)

Scirrhous type cancer is a subtype of gastric cancer. Usually hypoechoic tumors cannot be seen by EUS. A characteristic feature of scirrhous carcinoma is an irregular hypoechoic enlargement of the third (submucosa) and fourth (muscularis propria) layers [8].

Typical Findings

1. Thickness of gastric wall (mainly third and fourth layer)
2. There is no hypoechoic tumor
3. Preserving the five echogenic layers
4. Mild hypoechoic change of the thickened third hyperechoic layer
5. Heterogenic change of the thickened fourth hypoechoic layer

Pitfall

It is difficult to differentiate between scirrhous type cancer and diffuse infiltrating type diseases (malignant lymphoma, eosinophilic gastroenteritis, etc.) by EUS image only. Endoscopic bite biopsy is vital to confirm it

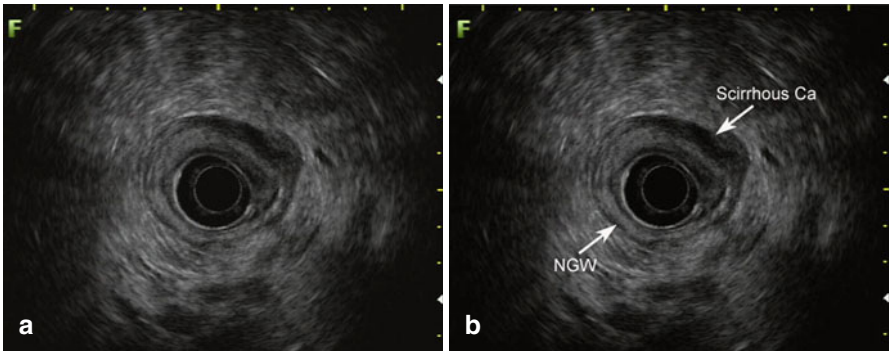

Fig. 5.11 Scirrhous cancer. (**a**, **b**) EUS revealing the thickness of gastric wall, and an irregular hypoechoic enlargement of the third (submucosa) and fourth (muscularis propria) layers (*arrow-Scirrhous Ca*). *NGW* normal gastric wall

5.4.2 Gastric Ulcer (Peptic Ulcer)

Endosonographically, gastric ulcer is usually imaged as a defect of the partial gastric wall and hypoechoic change due to edema and fibrosis. The depth of ulcerative change is determined as the deepest layer of stomach infiltration of the hypoechoic changes [9]. EUS can evaluate not only the depth of ulcerative change, but also the vessel beneath the ulcer base [10].

5.4.2.1 Gastric Peptic Ulcer (Ulcerative Change Affects over Muscularis Propria) (Fig. 5.12)

Typical Findings

1. Defect of the first to third layers
2. Thickness of gastric wall
3. Hypoechoic area (ulcerative change) extends over the fourth hypoechoic layer

Pitfall

It is difficult to differentiate between peptic ulcer and cancer by EUS image only. Endoscopic bite biopsy is vital to confirm it

Fig. 5.12 Deep gastric ulcer (over the muscularis propria). (**a**) Endoscopic image showing gastric ulcer in the anglus. (**b**, **c**) EUS revealing defect of the first to third layers (*arrow*), thickness of gastric wall, and ulcerative hypo-echoic area (*ULE*) extending over the fourth hypo-echoic layer (*arrow-mp*)

5.4.3 Gastric Malignant Lymphoma

The main purpose of EUS for this disease is pretreatment staging (depth of invasion and lymph node involvement) [11, 12]. Malignant lymphoma is usually visualized as relatively homogeneous hypo-echoic tumor. However, it sometimes expresses diffuse infiltrating growth (diffuse infiltrating type). This type mimics scirrhous type gastric cancer. EUS-FNA or bite biopsy is needed to obtain conclusive histologic diagnosis for such cases.

5.4.3.1 Superficial Spreading Type Gastric Malignant Lymphoma (Submucosal Infiltration) (Fig. 5.13)

Typical Findings

1. Smooth surface of first hyperechoic layer
2. Thickness and hypoechoic change of the second hypoechoic layer
3. Superficial hypoechoic change of the third hyperechoic layer
4. The fourth hypoechoic layer intact

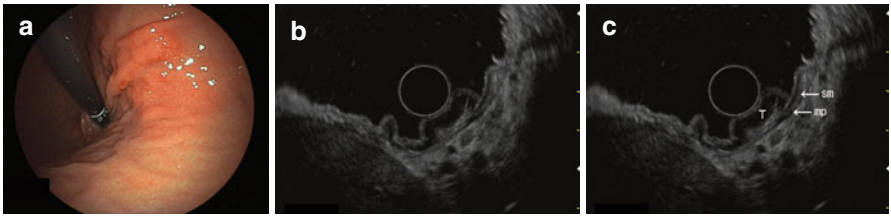

Fig. 5.13 Superficial spreading type gastric malignant lymphoma (submucosal infiltration). (**a**) EGD showing a flat elevated type (superficial spreading type) malignant lymphoma in the gastric cardia. (**b**, **c**) EUS revealing smooth surface of first hyperechoic layer, mild thickness and hypoechoic change of the second hypoechoic layer, hypoechoic change of the superficial third hyperechoic layer, and normal fourth hypoechoic layer. *Arrow-sm* submucosal layer, *arrow-mp* muscularis propria, *T* tumor

5.4.3.2 Mass Forming Type Malignant Lymphoma (Serosal Infiltration) (Fig. 5.14)

Typical Findings

1. Irregularity, thinness, or disappearance of the first hyperechoic layer
2. Hypoechoic tumor extends to the fifth hyperechoic layer

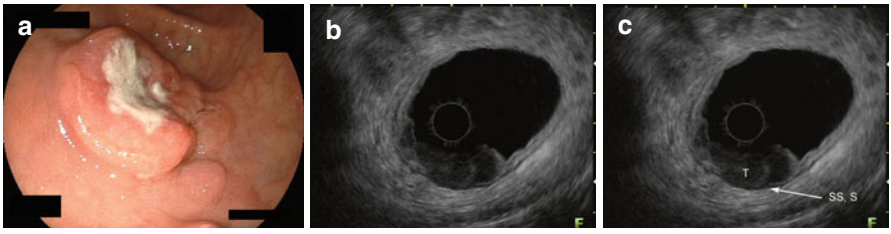

Fig. 5.14 Mass–forming type gastric malignant lymphoma. (**a**) Endoscopic image showing ulcerated type gastric malignant lymphoma. (**b**, **c**) EUS reveals hypoechoic tumor extending into the fifth hyperechoic layer (*arrow-ss,s*). The fifth hyperechoic layer is interrupted by lymphoma infiltration. *T* tumor infiltration

5.4.4 Gastric Submucosal Tumor

The main purpose of EUS for this disease is evaluation of submucosal tumor or extra-gastric compression. EUS can provide much useful information (such as layer of origin, histological nature, and real size, etc.), but cannot provide us conclusive histologic diagnosis (Table 5.2) [7, 12]. Therefore, aggressive use of EUS-FNA is helpful for overcoming this limitation.

Table 5.2 Usefulness and limitation of EUS for submucosal tumor

***Usefulness**: EUS can evaluate the following aspects of the SMT.*
1. Differentiation of intra- or extra-wall lesions.
2. Location or originating layer.
3. Presumption of its histological nature. (cyst, lipoma, vessel, or solid tumor)
4. Measurement of the real size of the lesion.
5. Evaluation of the blood flow of the lesion.
Limitation
1. Diagnosis on the basis of EUS is presumptive and cannot replace a histological diagnosis of SMT.

5.4.4.1 Gastrointestinal Mesenchymal Tumor of the Stomach (Fig. 5.15)

Typical Findings

1. Hypoechoic solid tumor
2. Continuity with muscularis propria

Pitfall

1. EUS can't replace histologic diagnosis, i.e. GIST, leiomyoma, neurinoma, etc. EUS-FNA is the only way to obtain histologic diagnosis

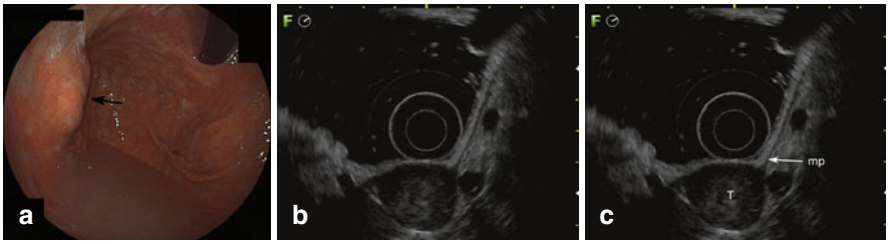

Fig. 5.15 Gastric GIST (diagnosed by EUS-FNA). (**a**) EGD showing a submucosal tumor (*black arrow*) in the upper gastric body. (**b**, **c**) EUS revealing hypoechoic solid tumor (*T*) with continuity with fourth hypoechoic layer (muscularis propria, *arrow-mp*)

5.4.4.2 Gastric Lipoma (Fig. 5.16)

Typical Findings

1. This tumor is usually located in the third hyperechoic layer (submucosa)
2. Hyper-echoic tumor

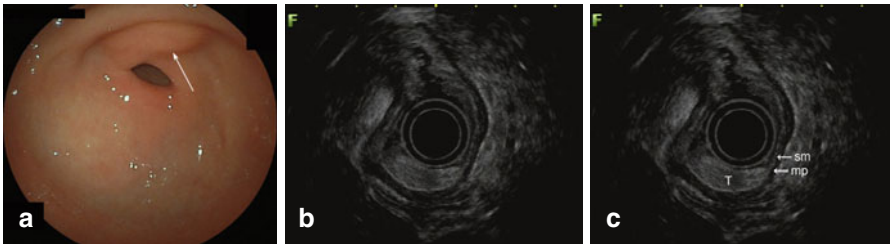

Fig. 5.16 Gastric lipoma. (**a**) EGD showing a submucosal tumor (*arrow*) in the prepylorus. (**b**, **c**) EUS revealing hyperechoic solid tumor (*T*) in the third hyperechoic layer. *Arrow-sm* submucosa, *arrow-mp* muscularis propria

5.4.4.3 Gastric Ectopic Pancreas (Fig. 5.17)

Typical Findings

1. This tumor usually locates in the third hyperechoic layer (submucosa)
2. Hypo-echoic tumor with small cystic component (dilated duct)
3. Sometimes the focal thickness of the muscularis propria is observed

Fig. 5.17 Gastric ectopic pancreas. (**a**) EGD showing a submucosal tumor (*black arrow*) in the antrum. (**b**, **c**) EUS revealing hypo-echoic solid tumor (*large arrow*) with small cystic components (*small arrows*) in the third hyperechoic layer. *Arrow-sm* submucosa, *arrow-mp* muscularis propria

5.4.4.4 Gastric Cyst (Fig. 5.18)

Typical Findings

1. This tumor is usually located in the third hyperechoic layer (submucosa)
2. An-echoic mass

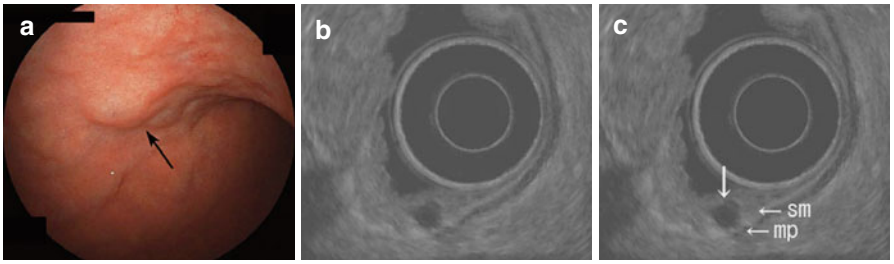

Fig. 5.18 Gastric cyst. (**a**) EGD showing a submucosal tumor (*black arrow*) in the lower gastric body. (**b**, **c**) EUS revealing an-echoic mass (*arrow*) in the third hyperechoic layer. *Arrow-sm* submucosa, *arrow-mp* muscularis propria

5.4.4.5 Extra-gastric Compression due to Splenic Artery Aneurysm (Fig. 5.19)

Typical Findings

1. Compression of normal gastric wall by focally dilated splenic artery [13]
2. Pulse wave EUS shows arterial flow

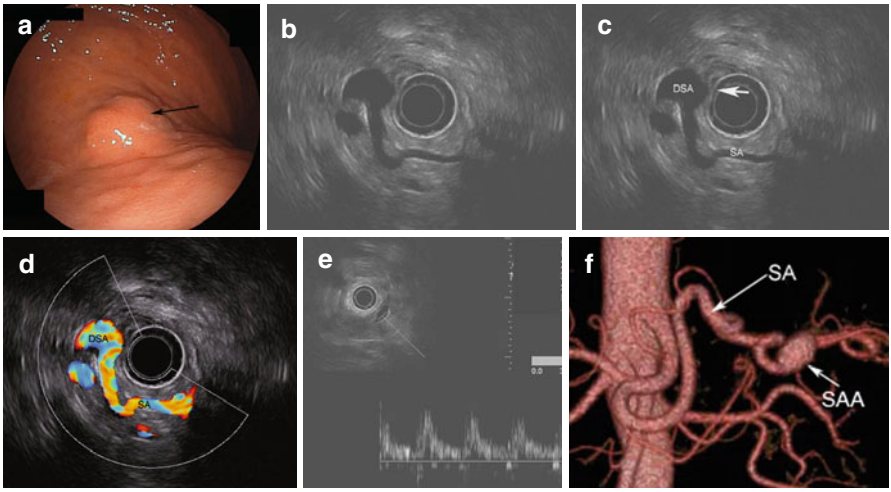

Fig. 5.19 Extra-gastric compression due to splenic artery aneurysm. (**a**) EGD showing a submucosal bulging (*arrow*) in the upper gastric body. (**b**, **c**) EUS revealing extra-gastric compression (*arrow*) by focally dilated splenic artery (splenic artery aneurysm). *DSA* dilated splenic artery, *SA* splenic artery. (**d**) Color Doppler EUS image showing blood flow in focally dilated splenic artery. *DSA* dilated splenic artery, *SA* splenic artery. (**e**) Pulse-wave EUS demonstrating arterial flow in the dilated splenic artery. (**f**) 3D-CT revealing splenic artery aneurysm (*arrow-SAA*). *Arrow-SA* splenic artery

References

1. Akahoshi K, Misawa T, Fujishima H et al (1991) Preoperative evaluation of gastric cancer by endoscopic ultrasound. Gut 32:479–482
2. Aibe T, Takemoto T (1986) A fundamental study of normal layer structure of the gastrointestinal wall visualized by endoscopic ultrasonography. Scand J Gastroenterol Suppl 123:6–15
3. Akahoshi K, Misawa T, Fujishima H et al (1992) Regional lymph node metastasis in gastric cancer: evaluation with endoscopic US. Radiology 182:559–564
4. Ziegler K, Sanft C, Zimmer T et al (1993) Comparison of computed tomography, endosonography, and intraoperative assessment in TN staging of gastric carcinoma. Gut 34: 604–610
5. Habermann CR, Weiss F, Riecken R et al (2004) Preoperative staging of gastric adenocarcinoma: comparison of helical CT and endoscopic US. Radiology 230:465–471
6. Caletti G, Ferrari A, Brocchi E et al (1993) Accuracy of endoscopic ultrasonography in diagnosis and staging of gastric cancer and lymphoma. Surgery 113:14–27
7. Akahoshi K, Oya M (2010) Gastrointestinal stromal tumor of the stomach: how to manage? World J Gastrointest Endosc 2:271–277
8. Fujishima H, Misawa T, Chijiiwa Y et al (1991) Scirrhous carcinoma of the stomach versus hypertrophic gastritis: finding at endoscopic US. Radiology 181:197–200
9. Maruoka A, Fujishima H, Misawa T et al (1993) Evaluation of acetic acid-induced gastric ulcers in dogs by endoscopic ultrasonography. Scand J Gastroenterol 28:1055–1061

10. Akahoshi K, Chijiiwa Y, Misawa T et al (1993) Confirmation of Dieulafoy's vascular lesion by endoscopic ultrasonography in three cases. Dig Endosc 5:383–390
11. Fujishima H, Misawa T, Maruoka A et al (1991) Staging and follow-up of primary gastric lymphoma by endoscopic ultrasonography. Am J Gastroenterol 86:719–724
12. Brugge WR (1998) Endoscopic ultrasonography: the current status. Gastroenterology 115:1577–1583
13. Higuchi N, Akahoshi K, Honda K et al (2010) Diagnosis of a small splenic artery aneurysm mimicking a gastric submucosal tumor on endoscopic ultrasound. Endoscopy 42(suppl 2): E107–E108, Epub 2010

Radial EUS of the Anus and Rectum

6

Kazuya Akahoshi

6.1 Indication

Anal and rectal EUS have been shown to be useful imaging modalities in evaluating colorectal, and pelvic disorder due to its high resolution [1–4]. EUS is indicated for the intra-rectal or extra-rectal (within about 3–4 cm from the rectum) lesion (Table 6.1).

6.2 Scanning Technique

The water filling method with or without balloon inflation (Fig. 3.2. Please see Chap. 3) is usually indicated in the rectum and anus. First, sufficient suction of air and rectal juice is necessary. Second, the echoendoscope is positioned at the oral side of the target lesion. Third, 200–300 mL de-aerated water is introduced into the rectal lumen via the biopsy channel.

6.3 Basic Anatomy

6.3.1 Rectal Wall

Using the water filling method, the normal rectal wall can be delineated as a five-layered structure (Fig. 6.1) that correspond well to the histological layers. The first echogenic layer and the second hypoechoic layer correspond to the mucosal layer.

K. Akahoshi
Department of Gastroenterology, Aso Iizuka Hospital,
Yoshiomachi 3-83, Iizuka city, Fukuoka 820-8505, Japan
e-mail: kakahoshi2@aol.com

K. Akahoshi, A. Bapaye (eds.), *Practical Handbook of Endoscopic Ultrasonography*,
DOI 10.1007/978-4-431-54014-4_6, © Springer 2012

Table 6.1 Indication of Radial EUS for the ano-rectal lesion

Staging of ano-rectal cancer
Evaluation of submucosal tumor or extrarectal compression
Restaging of malignant tumor after chemo and/or radiotherapy
Evaluation of vascular disease (rectal varices, etc.)
Evaluation of sphincter morphology
Assessment of extra-rectal disease (abscess, fistula, etc.)

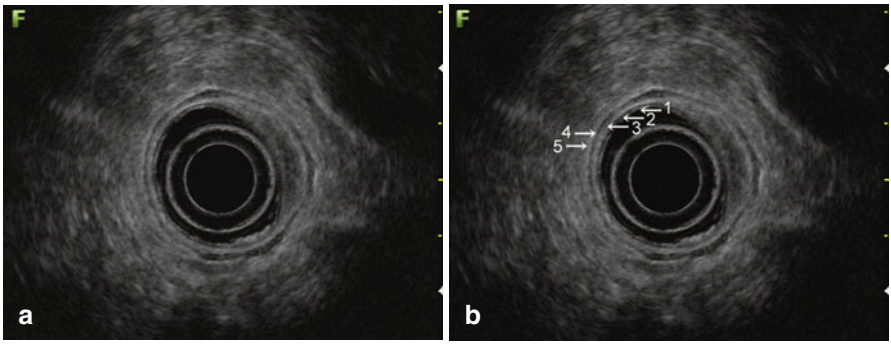

Fig. 6.1 EUS image of normal rectal wall with a five-layered structure. (**a**, **b**) *Arrow-1* first hyperechoic layer, *Arrow-2* second hypoechoic layer (mucosa), *Arrow-3* third hyperechoic layer (submucosa), *Arrow-4* fourth hypoechoic layer (muscularis propria), *Arrow-5* fifth hyperechoic layer (subserosa and serosa or adventitia)

The third hyperechoic layer is the submucosa and the fourth hypoechoic layer corresponds to the muscularis propria. The fifth, hyperechoic layer corresponds to the adventitia (or subserosa and serosa).

6.3.2 Transrectal (Anal) Scanning

When EUS is performed via the rectum, obviously male and female anatomy differs.

6.3.2.1 Male

At the level of the middle portion of the rectum (Fig. 6.2), usually urinary bladder and seminal vesicle are imaged as land marks on the monitor.

At the level of the lower portion of the rectum (Fig. 6.3), the prostate is usually imaged as a land mark on the monitor.

At the level of the pelvic floor (Fig. 6.4), usually levator ani muscles such as the puborectalis (PR), pubococcygeus (PC), sphincter urethrae muscle (SUM), and bulbourethral gland (BUG) are imaged as land marks on the monitor.

At the level of the anus (Fig. 6.5), the internal anal sphincter muscle (IASM) and external anal sphincter muscle (EASM) are usually imaged as land marks on the monitor.

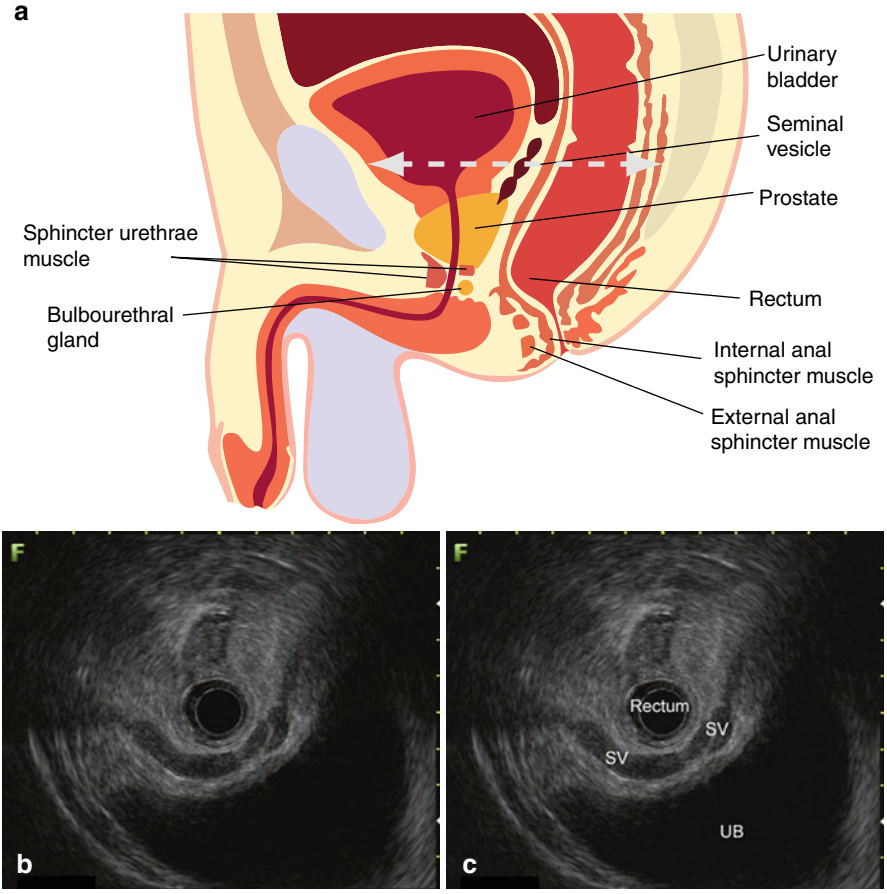

Fig. 6.2 EUS image of trans-rectal scanning (*middle portion*). (**a**) Scanning portion, (**b**) EUS image, (**c**) EUS image with abbreviations. *SV* seminal vesicle, *UB* urinary bladder

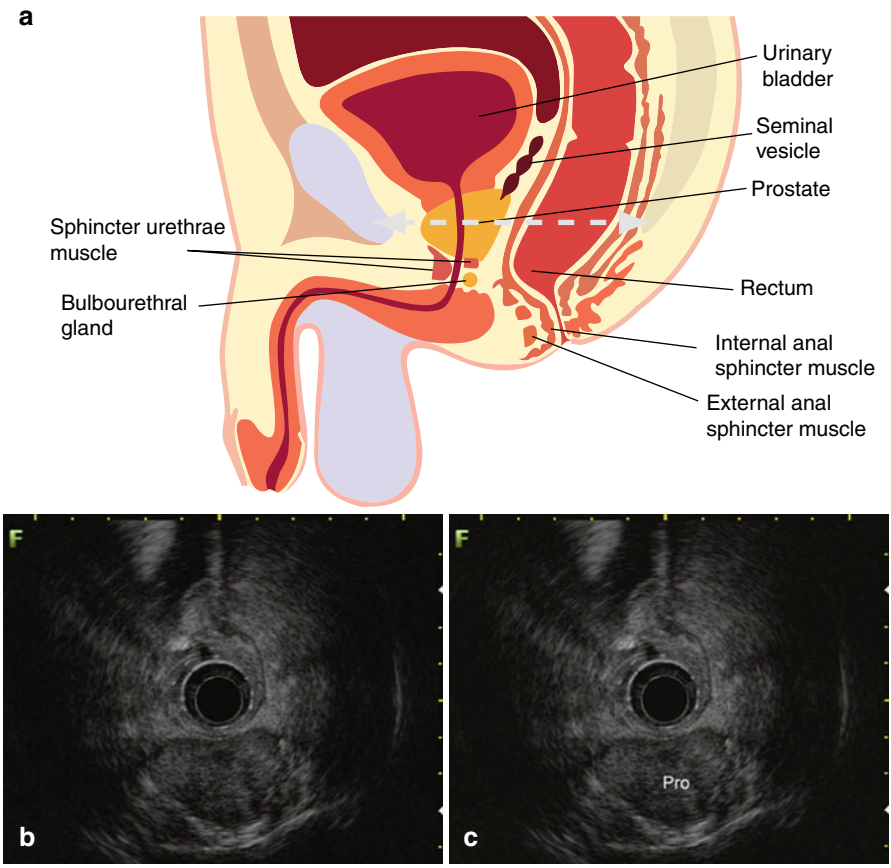

Fig. 6.3 EUS image of trans-rectal scanning (*lower portion*). (**a**) Scanning portion, (**b**) EUS image, (**c**) EUS image with abbreviation. *Pro* prostate

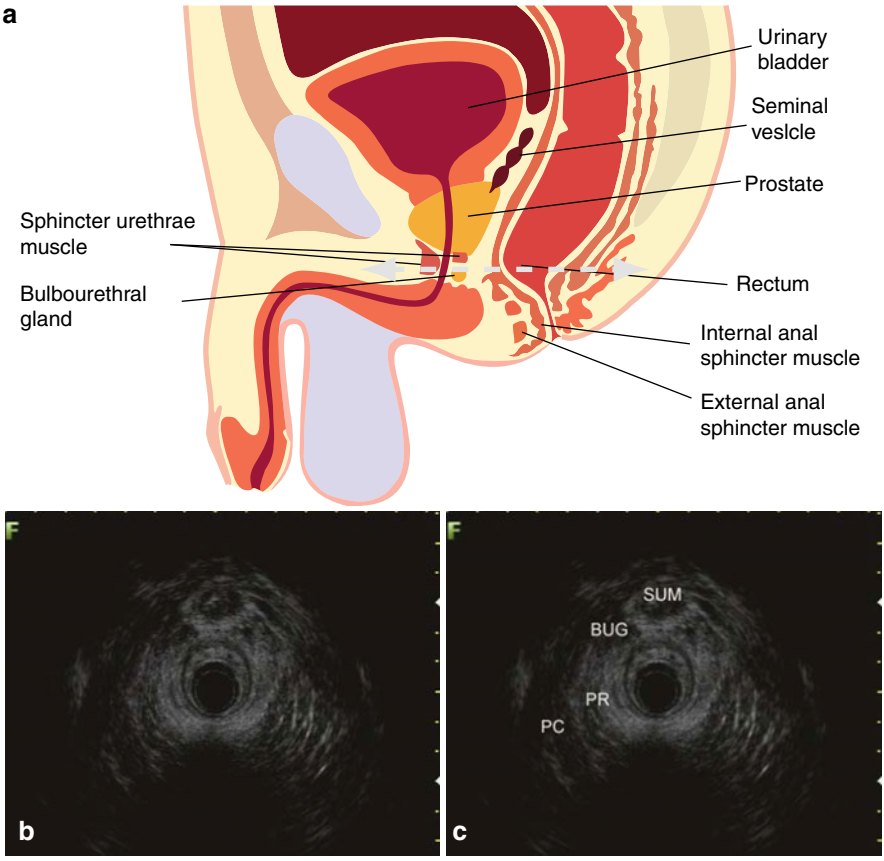

Fig. 6.4 EUS image of trans-rectal scanning (pelvic floor level). (**a**) Scanning portion, (**b**) EUS image, (**c**) EUS image with abbreviation. *PR* puborectalis, *PC* pubococcygeus, *SUM* sphincter urethrae muscle, *BUG* bulbourethral gland

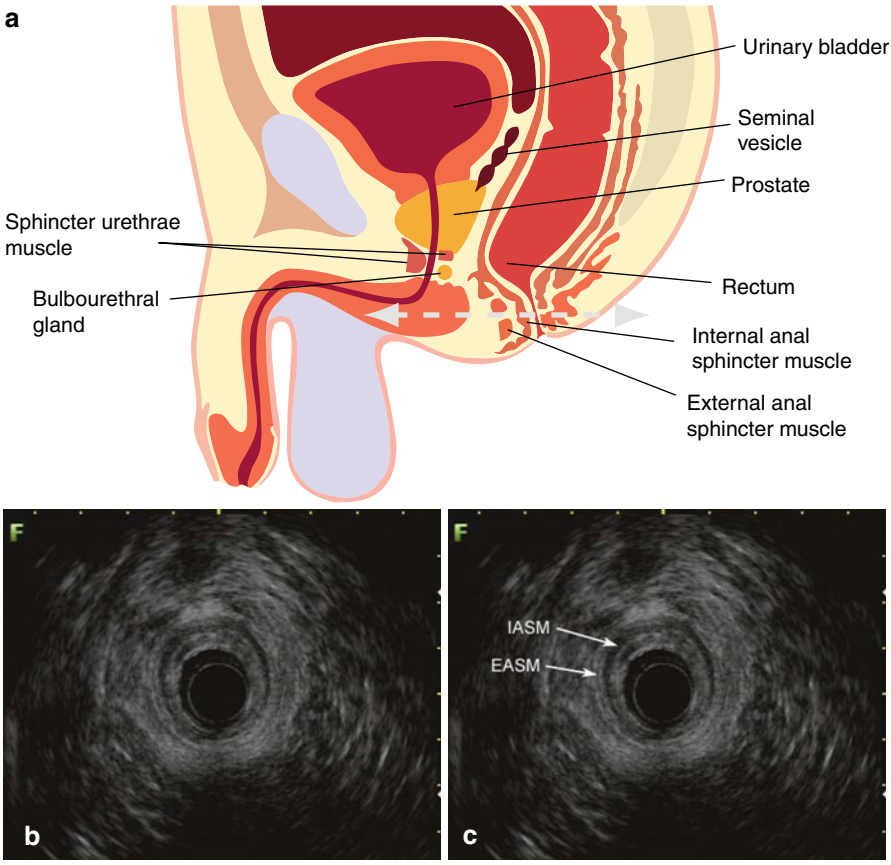

Fig. 6.5 EUS image of trans-anal scanning (anus level). (**a**) Scanning portion, (**b**) EUS image, (**c**) EUS image with abbreviation. *IASM* internal anal sphincter muscle, *EASM* external anal sphincter muscle

6.3.2.2 Female

At the level of the middle portion of the rectum (Fig. 6.6), the urinary bladder and uterus are usually imaged as land marks on the monitor.

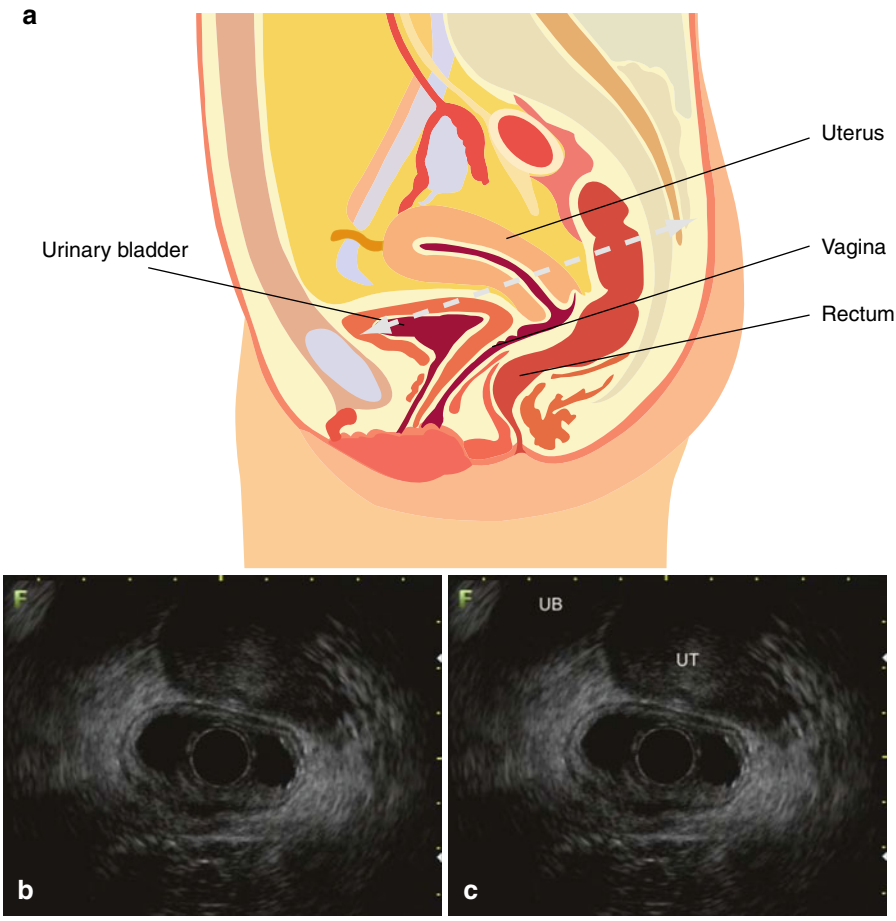

Fig. 6.6 EUS image of trans-rectal scanning (*middle portion*). (**a**) Scanning portion, (**b**) EUS image, (**c**) EUS image with abbreviations. *UT* uterus, *UB* urinary bladder

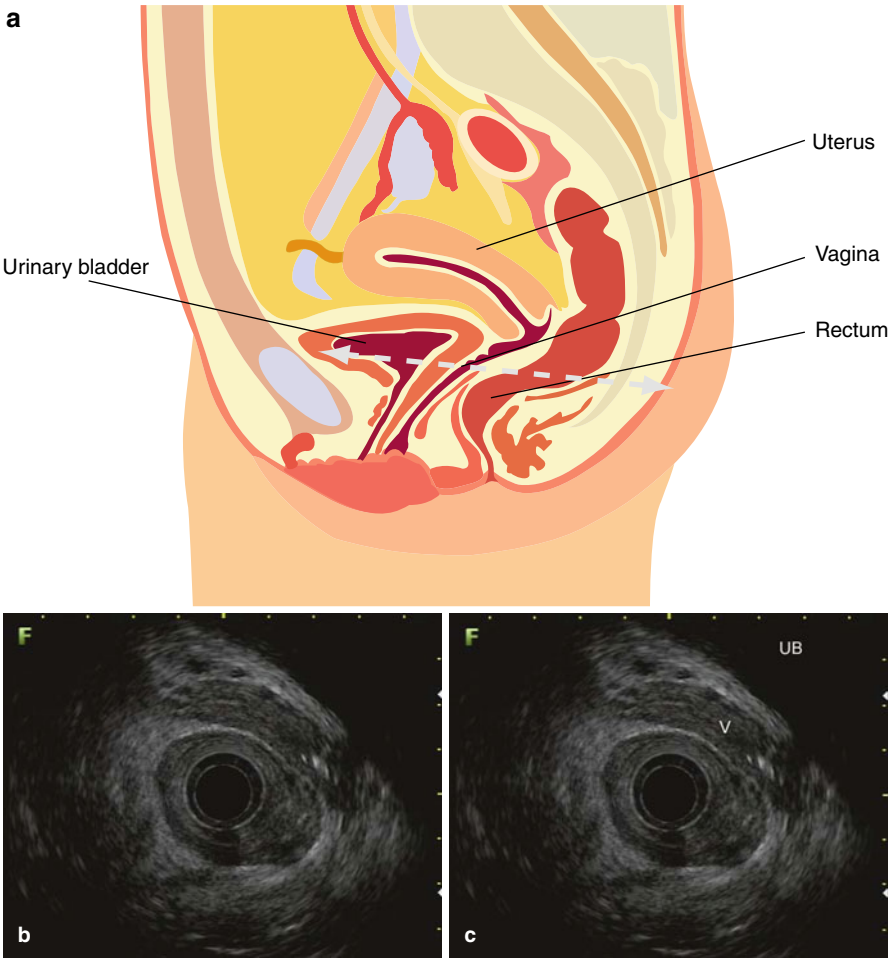

Fig. 6.7 EUS image of trans-rectal scanning (*lower portion*). (**a**) Scanning portion, (**b**) EUS image, (**c**) EUS image with abbreviation. *V* vagina, *UB* urinary bladder

At the level of the lower portion of the rectum (Fig. 6.7), the vagina and urinary bladder are usually imaged as land mark on the monitor.

6.4 Diagnosis

6.4.1 Rectal Cancer

Rectal cancer is usually imaged as hypoechoic tumor. Depth of invasion is determined as the deepest layer of the rectum infiltrated by the hypoechoic tumor (Fig. 2.3, please see Chap. 2). The reported accuracy of EUS ranges from 69% to 89% and 64% to 76% for T and N staging, respectively [2–4].

6.4.1.1 T1-Intramucosal Cancer (Fig. 6.8)

Typical Findings

1. Irregularity, thinness, or disappearance of the first hyperechoic layer
2. Thickness and hypoechoic change of the second hypoechoic layer
3. The third hyperechoic layer intact

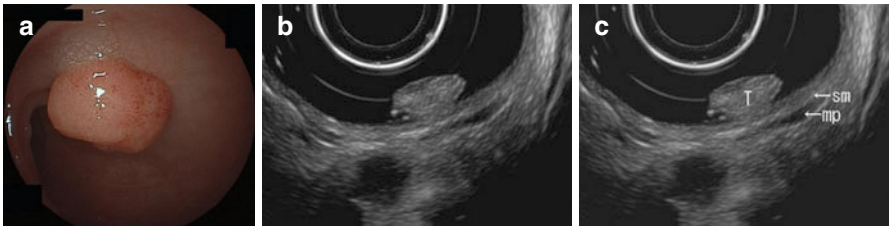

Fig. 6.8 Rectal T1 intramucosal cancer. (**a**) Colonoscopy showing a small 0-Isp type (semipedunculated type) early rectal cancer in the rectosigmoid junction. (**b**, **c**) EUS revealing irregularity of first hyperechoic layer and mild thickness and hypoechoic change of the second hypoechoic layer (*T*) and normal third hyperechoic layer. *Arrow-sm* submucosal layer, *arrow-mp* muscularis propria

6.4.1.2 T2-Cancer (Muscularis Propria) (Fig. 6.9)

Typical Findings

1. Irregularity, thinness, or disappearance of the first hyperechoic layer
2. Hypoechoic tumor extends to the fourth hyperechoic layer
3. The fifth hyperechoic layer intact

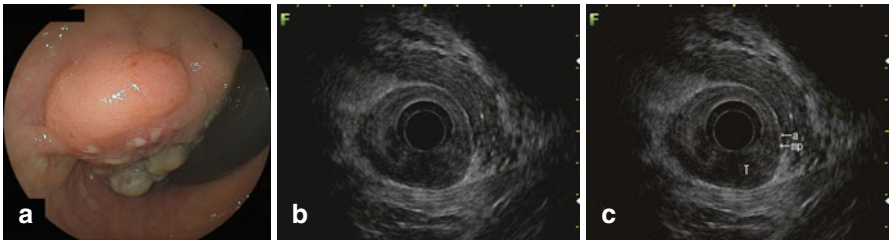

Fig. 6.9 Rectal T2 cancer. (**a**) Endoscopic image showing protruded type advanced rectal cancer. (**b**, **c**) EUS reveals hypoechoic tumor (*T*) extending into the fourth hyperechoic layer (*arrow-mp*). The fifth hyperechoic layer is intact (*arrow-a*). *mp* muscularis propria, *a* adventitia

6.4.1.3 T3 Cancer (Serosa) (Fig. 6.10)

Typical Findings

1. Irregularity, thinness, or disappearance of the first hyperechoic layer
2. Hypoechoic tumor extends to the fifth hyperechoic layer

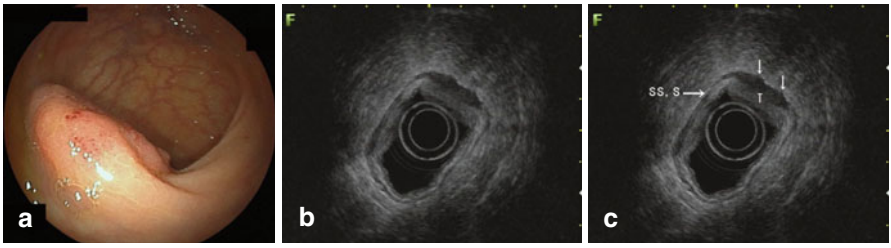

Fig. 6.10 T3 rectal cancer. (**a**) Endoscopic image showing type 1 advanced rectal cancer. (**b**, **c**) EUS reveals hypoechoic tumor (*T*) extending into the fifth hyperechoic layer (*arrow-ss,s*). The fifth hyperechoic layer is interrupted (*arrows*) by cancer invasion

6.4.1.4 T4-Cancer (Invasion to the Prostate) (Fig. 6.11)

Typical Findings

1. Irregularity, thinness, or disappearance of the first hyperechoic layer
2. Hypoechoic tumor extends to the prostate
3. The borderecho between rectum and prostate is interrupted by tumor echo

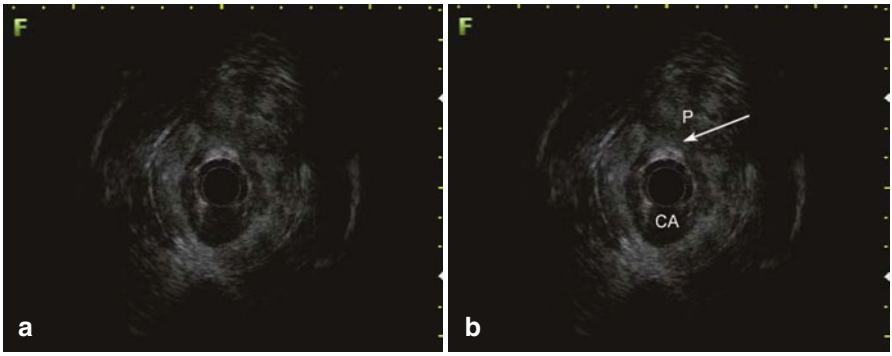

Fig. 6.11 T4 rectal cancer. (**a**, **b**) EUS reveals hypoechoic tumor (*CA*) extending into the prostate gland (*P*). The border-echo is interrupted (*arrow*) by cancer invasion

6.4.1.5 Lymph Node Metastasis (Rectal Cancer) (Fig. 6.12)

Typical Finding

1. Well-defined round or elliptical structures adjacent to the rectal wall that has a more hypoechoic pattern than the surrounding tissues

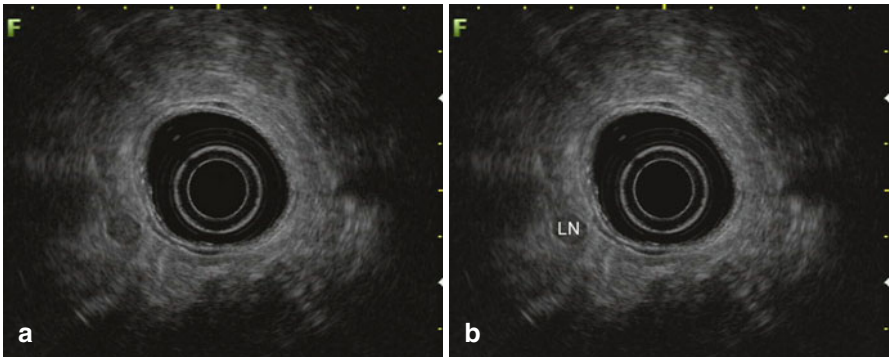

Fig. 6.12 Peri-rectal lymph node metastasis of advanced rectal cancer. (**a**, **b**) EUS revealing peri-rectal well-defined elliptical hypoechoic mass. *LN* lymph node

6.4.2 Rectal Submucosal Tumor

6.4.2.1 Gastrointestinal Mesenchymal Tumor of the Rectum (Fig. 6.13)

Typical Findings

1. Hypoechoic solid tumor
2. Continuity with muscularis propria

Pitfall

1. EUS can't replace histologic diagnosis, i.e. GIST, leiomyoma, neurinoma, endometriosis etc. EUS-FNA is the only way to obtain histologic diagnosis

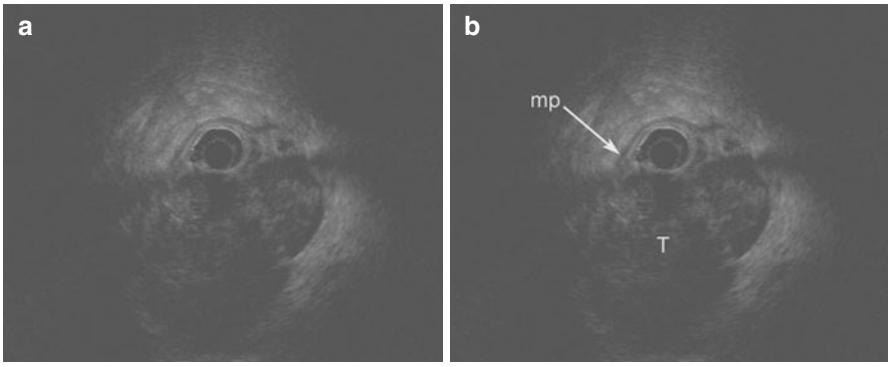

Fig. 6.13 Rectal GIST (Diagnosed by EUS-FNA). (**a**, **b**) EUS revealing hypoechoic solid tumor (*T*) with continuity to the fourth hypoechoic layer (muscularis propria, *arrow-mp*)

6.4.2.2 Rectal Abscess (Fig. 6.14)

Typical Finding

1. Hypoechoic mass in the submucosa, musculari propria, or perirectal area

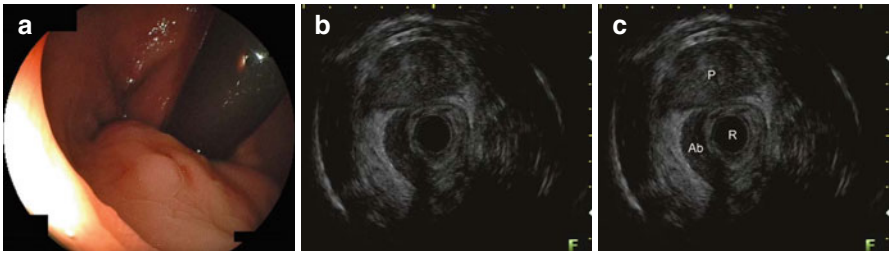

Fig. 6.14 Rectal abscess. (**a**) Endoscopic image showing rectal submucosal tumor like lesion. (**b**, **c**) EUS revealing perirectal hypoechoic mass (*Ab*). *P* prostate, *R* rectum

6.4.2.3 Rectal Carcinoid Tumor

The rectum is one of the most frequent primary sites of carcinoid tumors. Rectal carcinoid tumor is usually imaged as hypoechoic tumor. Depth of invasion is determined as the deepest layer of the rectum infiltrated by the hypoechoic tumor (Fig. 2.3, please see Chap. 2). When the tumor is smaller than 1 cm and the depth of invasion is limited within the submucosa, the risk of metastatic disease is extremely low, and endoscopic resection including endoscopic submucosal dissection is considered curative [5].

Submucosal Rectal Carcinoid Tumor Treated by Endoscopic Submucosal Dissection (Fig. 6.15)

Typical Findings

1. Intact of the first hyperechoic layer
2. Hypoechoic mass locates from the second hypoechoic layer to the third hyperechoic layer
3. The fourth hypoechoic layer intact

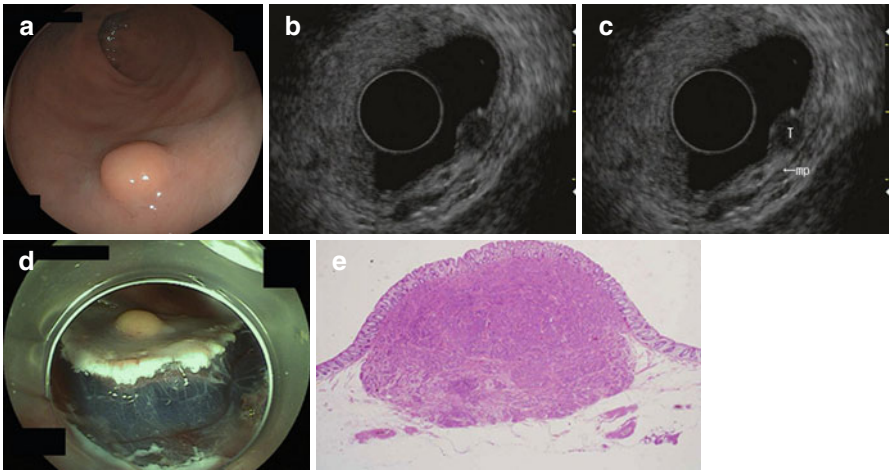

Fig. 6.15 Small submucosal rectal carcinoid tumor. (**a**) Colonoscopy showing a small 0-I type (protruded type) rectal carcinoid tumor in the lower rectum. (**b**, **c**) EUS revealing small hypoechoic mass (*T*) in the second hypoechoic layer and third hyperechoic layer. The fourth hypoechoic layer (*arrow-mp*, muscularis propria) is intact. (**d**) Colonoscopic image during ESD for this lesion. The lesion is sufficiently elevated after submucosal injection. (**e**) The resected specimen showing curative en bloc resection of the lesion

Rectal Carcinoid Tumor (Invasion to the Muscularis Propria) (Fig. 6.16)

Typical Findings

1. The first hyperechoic layer intact
2. Hypoechoic mass locates from the second hypochoic layer to the fourth hypoechoic layer
3. The fifth hyperechoic layer intact

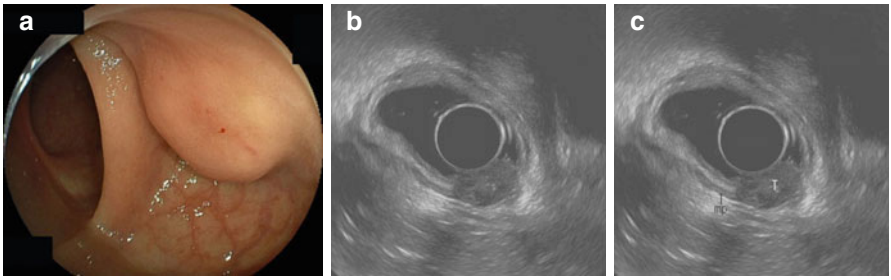

Fig. 6.16 Rectal carcinoid tumor invading into the muscularis propria. (**a**) Colonoscopy showing a rectal submucosal bulging in the lower rectum. (**b**, **c**) EUS revealing a hypoechoic mass (*T*) locating from the second hypoechoic layer to the fourth hypoechoic layer (*arrow-mp*, muscularis propria). The fifth hyperechoic layer is intact

6.4.2.4 Rectal Endometriosis

The main area of the GI tract affected by deep pelvic endometriosis is the rectosigmoid colon in 3–37% of cases. Due to the risk of infiltration and the clinical symptoms of endometriosis, with pain and infertility, the condition may require medical or surgical treatment. Pretherapeutic imaging diagnosis of the rectosigmoid is therefore important [6]. EUS is a noninvasive, sensitive technique for the diagnosis of endometriotic implants in the rectosigmoid wall. Rectal endometriosis usually appears as a hypoechoic, heterogeneous triangular mass developed into the muscularis propria of the anterior side of the mid rectum and between the rectum and the uterus and/or the vagina [7]. The addition of EUS-FNA can confirm the diagnosis when it shows characteristic cytopathologic elements of endometrial glands and stroma [8].

Rectal Endometriosis Treated by Hormonal Therapy (Fig. 6.17)

Typical Findings

1. Hypoechoic mass in the third hyperechoic layer and the fourth hypoechoic layer
2. Hypoechoic mass sometimes extends into the recto-vaginal septum

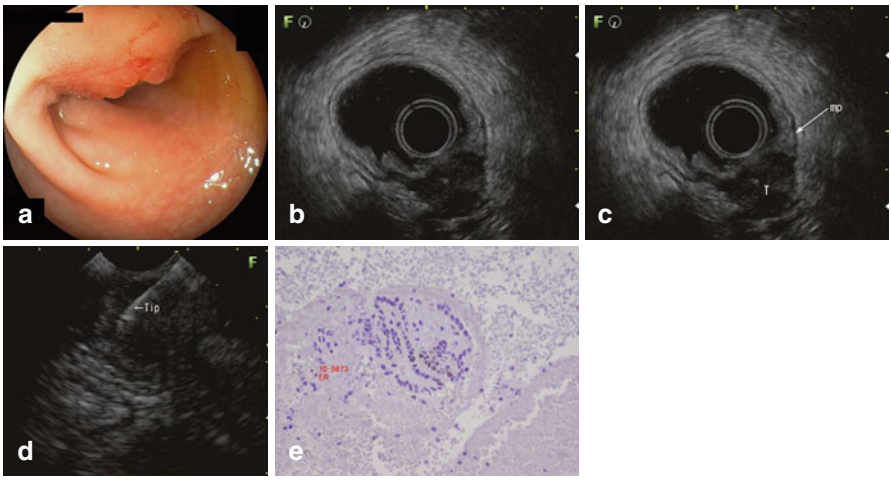

Fig. 6.17 **Rectal endometriosis** (diagnosed by EUS-FNA). (**a**) Endoscopic image showing rectal SMT-like protruded lesion. (**b**, **c**) EUS revealing hypoechoic mass (*T*) in the fourth hypoechoic layer (*arrow-mp*, muscularis propria). This mass extends to the pelvic space. (**d**) EUS image during EUS-FNA for the lesion. (**e**) EUS-FNA specimen showing endometrial gland and stroma. The endometrial gland cells is mildly positive for estrogen receptor

References

1. Brugge WR (1998) Endoscopic ultrasonography: the current status. Gastroenterology 115:1577–1583
2. Akahoshi K, Kondoh A, Nagaie T et al (2000) Preoperative staging of rectal cancer using a 7.5 MHz front-loading US probe. Gastrointest Endosc 52:529–534
3. Akasu T, Sugihara K, Moriyama Y et al (1997) Limitations and pitfalls of transrectal ultrasonography for staging of rectal cancer. Dis Colon Rectum 40(10 Suppl 10):S10–S15
4. Garcia-Agguilar J, Pollack J, Lee SH et al (2002) Accuracy of endorectal ultrasonography in preoperative staging of rectal tumors. Dis Colon Rectum 45:10–15
5. Akahoshi K, Motomura Y, Kubokawa M et al (2009) Endoscopic submucosal dissection of rectal carcinoid tumor using a grasping type scissors forceps. World J Gastroenterol 15:2162–2165
6. Chapron C, Dumontier I, Dousset B et al (1998) Results and role of rectal endoscopic ultrasonography for patients with deep pelvic endometriosis. Hum Reprod 13:2266–2270
7. Roseau G, Dumontier I, Palazzo L et al (2000) Rectosigmoid endometriosis: endoscopic ultrasound features and clinical implications. Endoscopy 32:525–530
8. Pishvaian AC, Ahlawat SK, Garvin D et al (2006) Role of EUS and EUS-guided FNA in the diagnosis of symptomatic rectosigmoid endometriosis. Gastrointest Endosc 63:331–335

Radial EUS of Pancreatico-Biliary System

7

Kazuya Akahoshi

7.1 Indication

EUS can evaluate the entire pancreas including the pancreatic duct, the neighboring organs including blood vessels, gall bladder, and the common bile duct from the stomach and duodenum. Therefore, indications of EUS are all conditions of pancreatico-biliary disease (Table 7.1).

7.2 Basic Scanning Technique

Basically, the balloon contact method is used for the pancreatico-biliary system. There are three steps (Fig. 7.1) below for scanning the whole of them.

7.3 Basic Anatomy

7.3.1 Transgastric Scanning

To demonstrate the pancreatic body and tail, the scope is advanced to the gastric body and the balloon is inflated by infusing 1-7 mL de-aerated water. In addition, sufficient suction should be applied until the gastric lumen is completely collapsed. EUS scanning is started by pushing and withdrawing the scope to detect the splenic vein or artery. This image is easy to interpret, as it is similar to the transabdominal ultrasound one. Figures 7.2, 7.3, 7.4, 7.5, and 7.6. shows the transgastric EUS images. The EUS images of the pancreatic body and tail with the pancreatic duct

K. Akahoshi
Department of Gastroenterology, Aso Iizuka Hospital,
Yoshiomachi 3-83, Iizuka city, Fukuoka 820-8505, Japan
e-mail: kakahoshi2@aol.com

K. Akahoshi, A. Bapaye (eds.), *Practical Handbook of Endoscopic Ultrasonography*,
DOI 10.1007/978-4-431-54014-4_7, © Springer 2012

Table 7.1 Indication of Radial EUS for the pancreatico-biliary lesion

Staging of pancreatico-biliary cancer
Differential diagnosis of pancreatic solid mass
Differential diagnosis of pancreatic cystic mass
Diagnosis and staging of chronic pancreatitis
Diagnosis of the gall bladder and common bile duct stone
Differential diagnosis of the gall bladder polypoid lesions

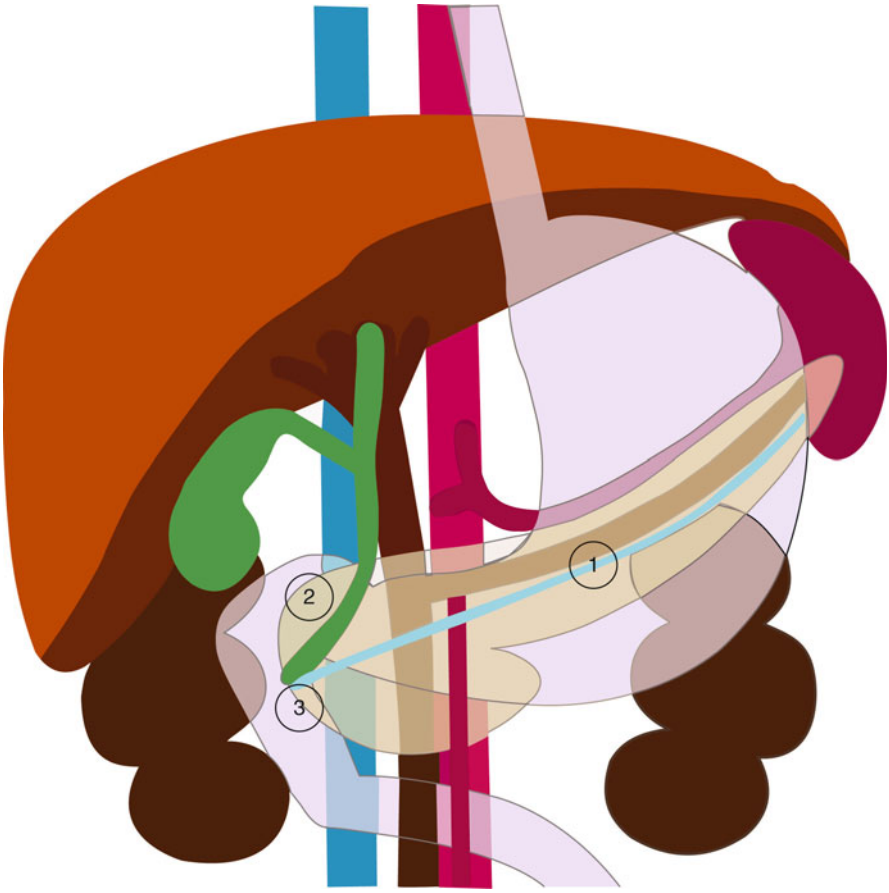

Fig. 7.1 Three steps for scanning the whole of the pancreatico-biliary system. (1): Transgastric scanning for pancreatic body and tail. (2): Transbulbar scanning for pancreatic head, gall bladder, and common bile duct. (3): Scanning from second portion of the duodenum for pancreatic head, papilla of Vater, and common bile duct

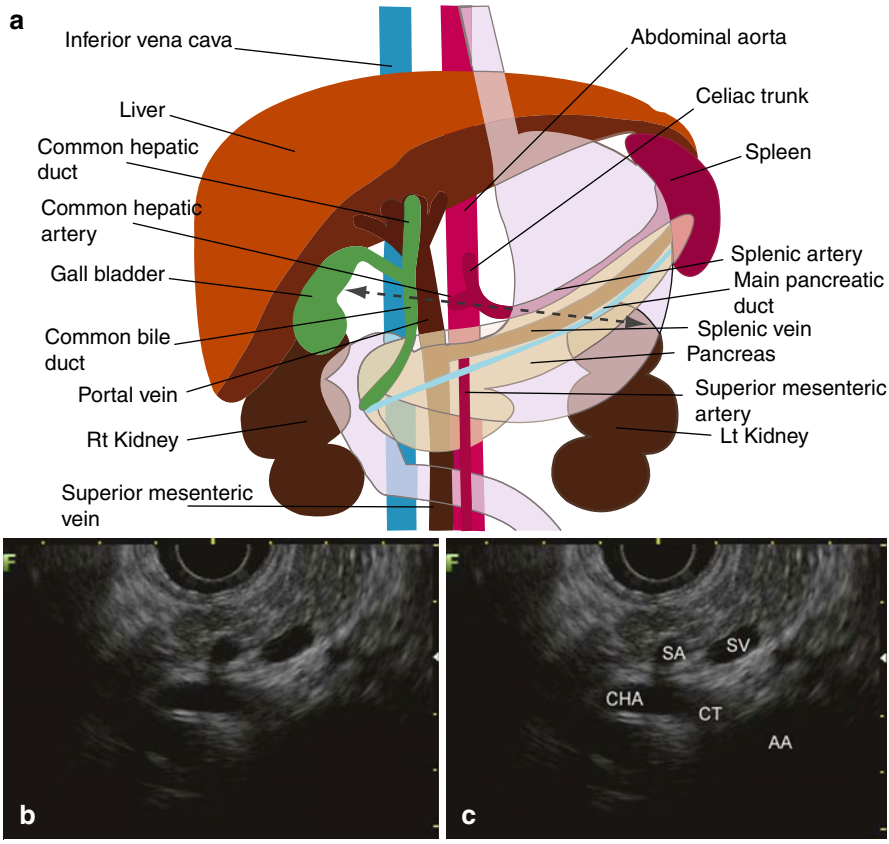

Fig. 7.2 EUS image of trans-gastric scanning (at the level of celiac axis). (**a**) Scanning portion, (**b**) EUS image, (**c**) EUS image with abbreviations. *AA* abdominal aorta, *CT* celiac trunk, *CHA* common hepatic artery, *SA* splenic artery, *SV* splenic vein

and the adjacent organs and blood vessels, such as, the liver, left kidney, adrenal gland, spleen, the splenic artery and vein, as well as cross-sections of the superior mesenteric artery and celiac trunk, and common hepatic artery, are obtained through the wall of the gastric body. Sufficient scope manipulation using to and fro motion, and clockwise and counterclockwise rotation is vital to makes it possible to see the entire body and tail of the pancreas. The counterclockwise rotation and pushing of the scope provides the movement of EUS images to the pancreatic head side. The clockwise rotation and pulling of the scope provides the movement of EUS images to the pancreatic tail side.

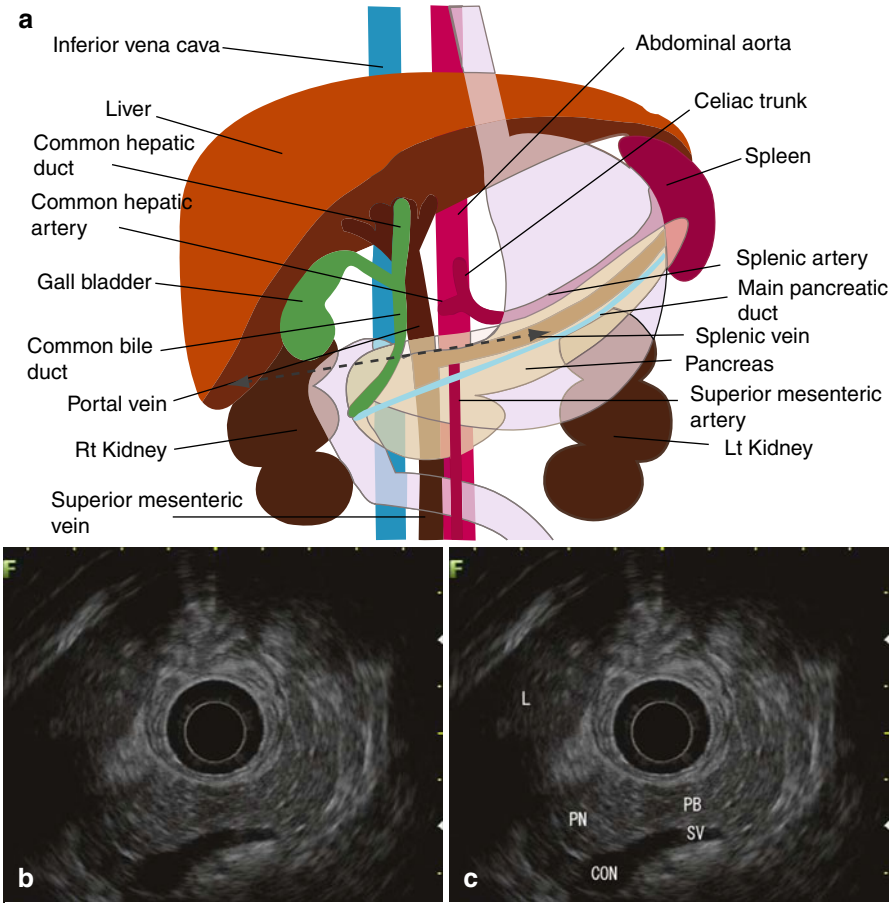

Fig. 7.3 EUS image of trans-gastric scanning (at the level of pancreatic neck). (**a**) Scanning portion, (**b**) EUS image, (**c**) EUS image with abbreviations. *L* liver, *PN* pancreatic neck, *CON* confluence of the superior mesenteric vein with the portal vein and splenic vein, *PB* pancreatic body, *SV* splenic vein

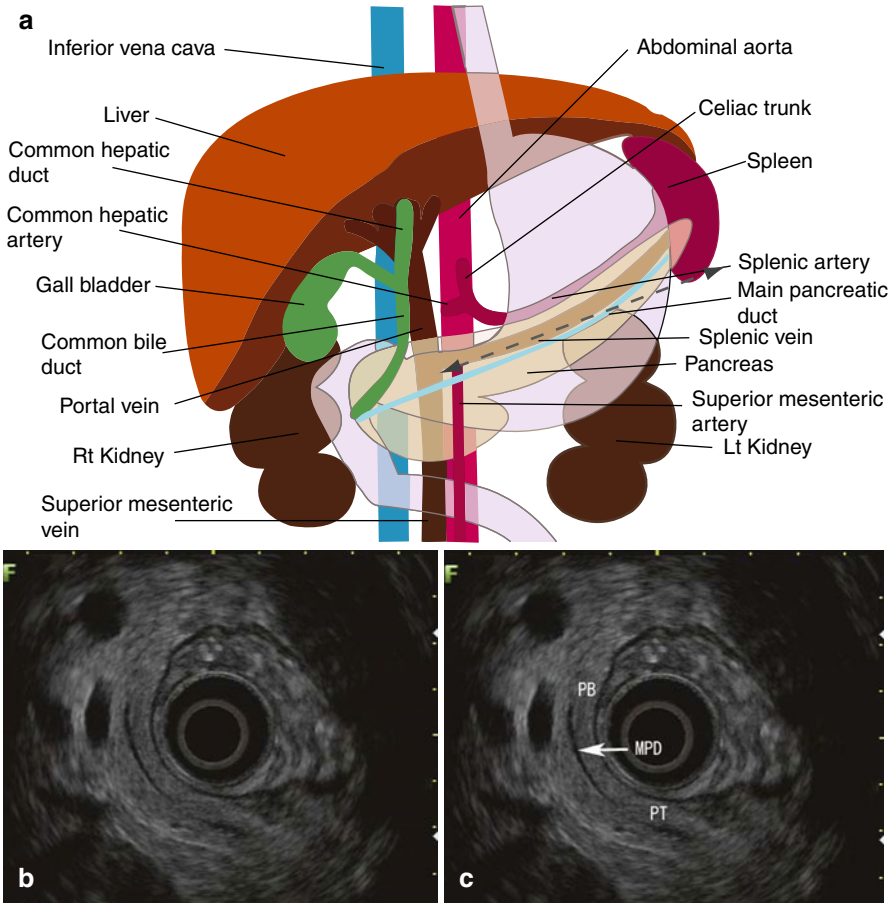

Fig. 7.4 EUS image of trans-gastric scanning (at the level of pancreatic body and tail). (**a**) Scanning portion, (**b**) EUS image, (**c**) EUS image with abbreviations. *PB* pancreatic body, *MPD* main pancreatic duct, *PT* pancreatic tail

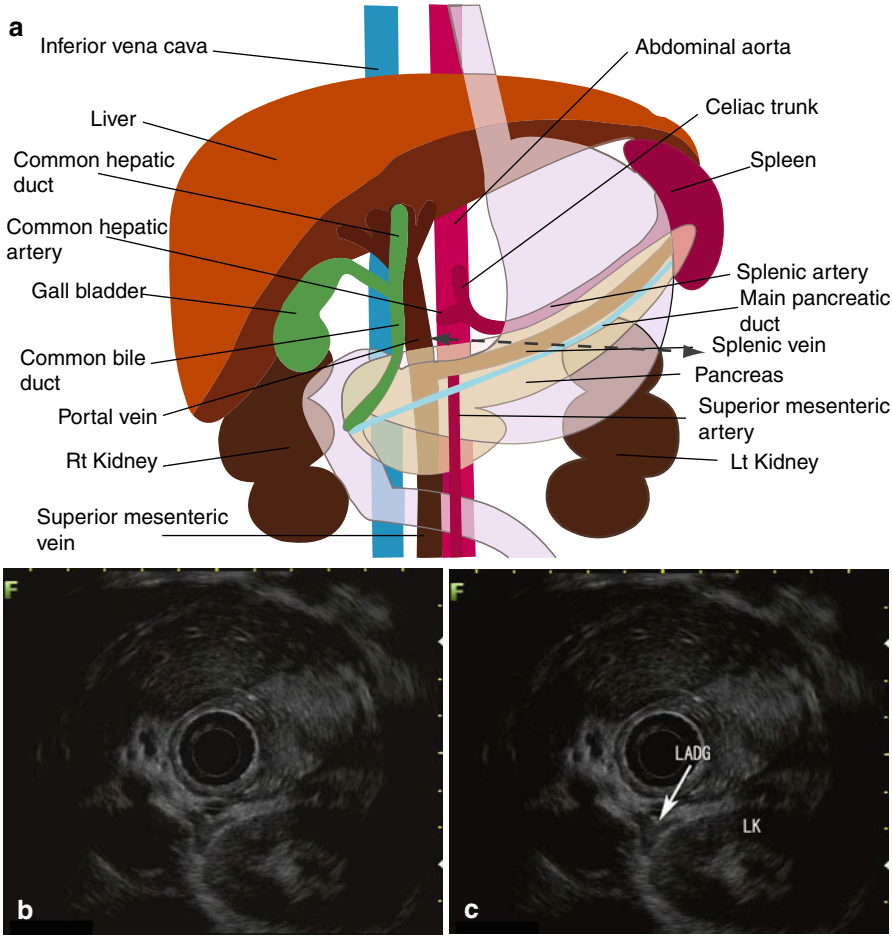

Fig. 7.5 EUS image of trans-gastric scanning (at the level of the left adrenal gland). (**a**) Scanning portion, (**b**) EUS image, (**c**) EUS image with abbreviations. *LADG* left adrenal gland, *LK* left kidney

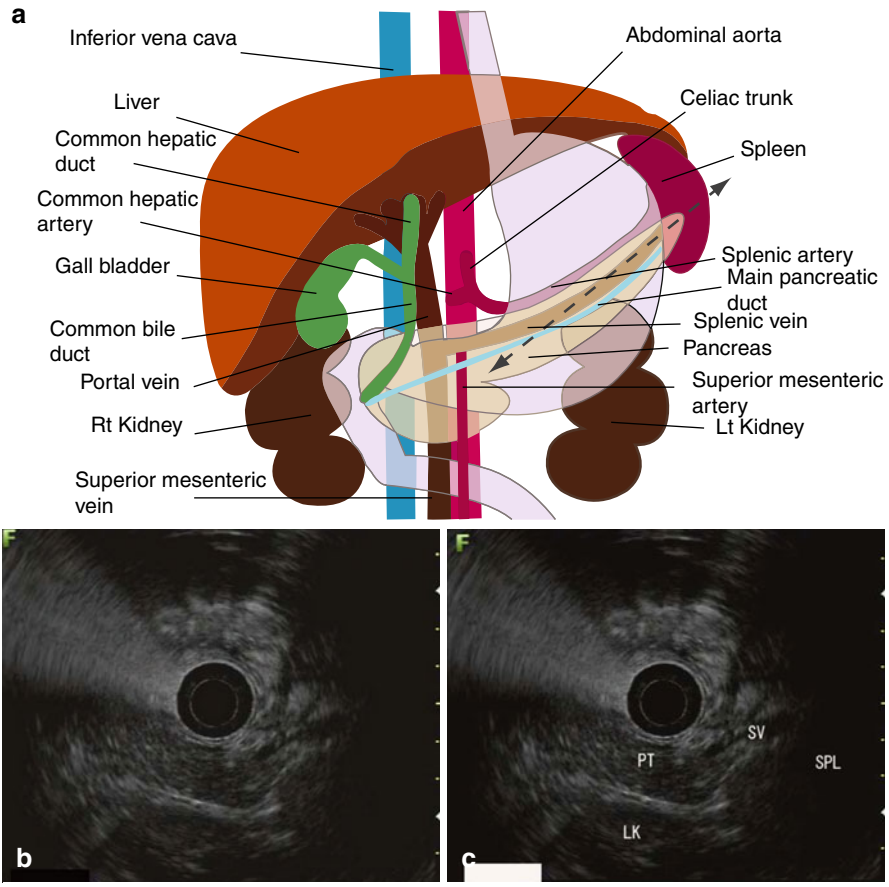

Fig. 7.6 EUS image of trans-gastric scanning (at the level of pancreatic tail). (**a**) Scanning portion, (**b**) EUS image, (**c**) EUS image with abbreviations. *PT* pancreatic tail, *LK* left kidney, *SV* splenic vein, *SPL* spleen

7.3.2 Trans-bulbar Scanning

After trans-gastric scanning, the balloon is deflated, and then the scope is advanced to the duodenal bulb under forward endoscopic view. To demonstrate the gall bladder, the common bile duct, and pancreatic head, the balloon is inflated by infusing 2-4 mL de-aerated water. In addition, sufficient suction should be applied until the duodenal lumen is completely collapsed. EUS scanning is started by pushing and withdrawing the scope to detect the gall bladder, common bile duct, portal vein or pancreatic head. Figures 7.7 and 7.8 shows the trans-bulbar EUS images. Sufficient scope manipulation using to and fro motion, and clockwise and counterclockwise rotation is vital to makes it possible to see the entire gall bladder and common bile duct.

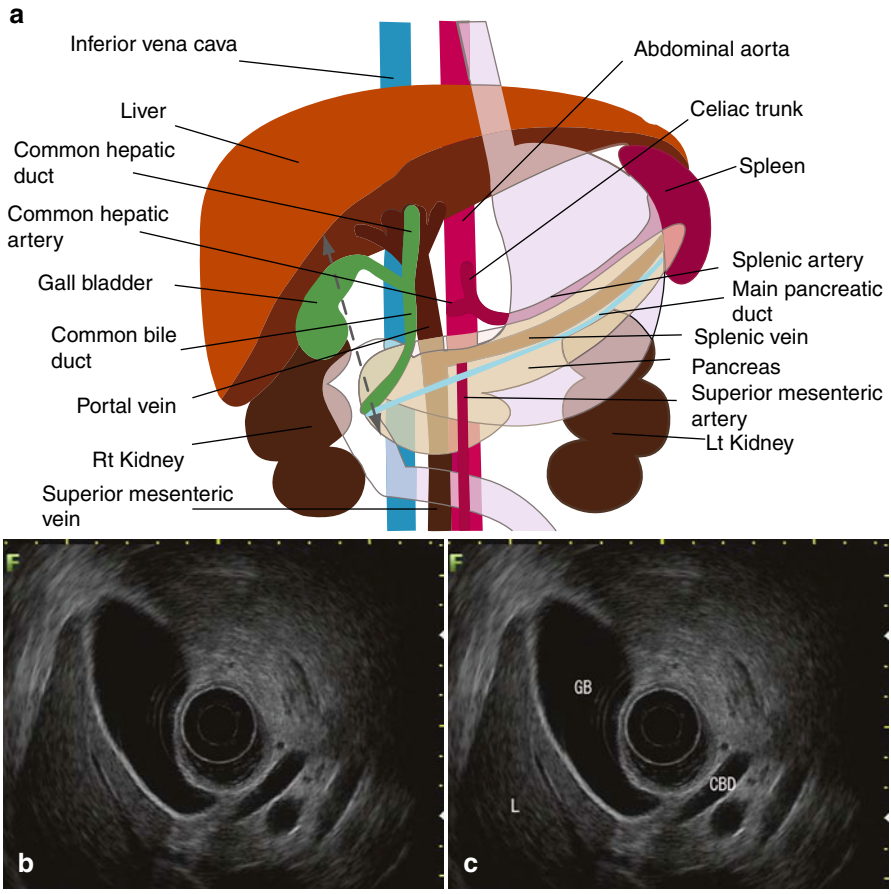

Fig. 7.7 EUS image of trans-bulbar scanning (at the level of the gall bladder). (**a**) Scanning portion, (**b**) EUS image, (**c**) EUS image with abbreviations. *L* liver, *GB* gall bladder, *CBD* common bile duct

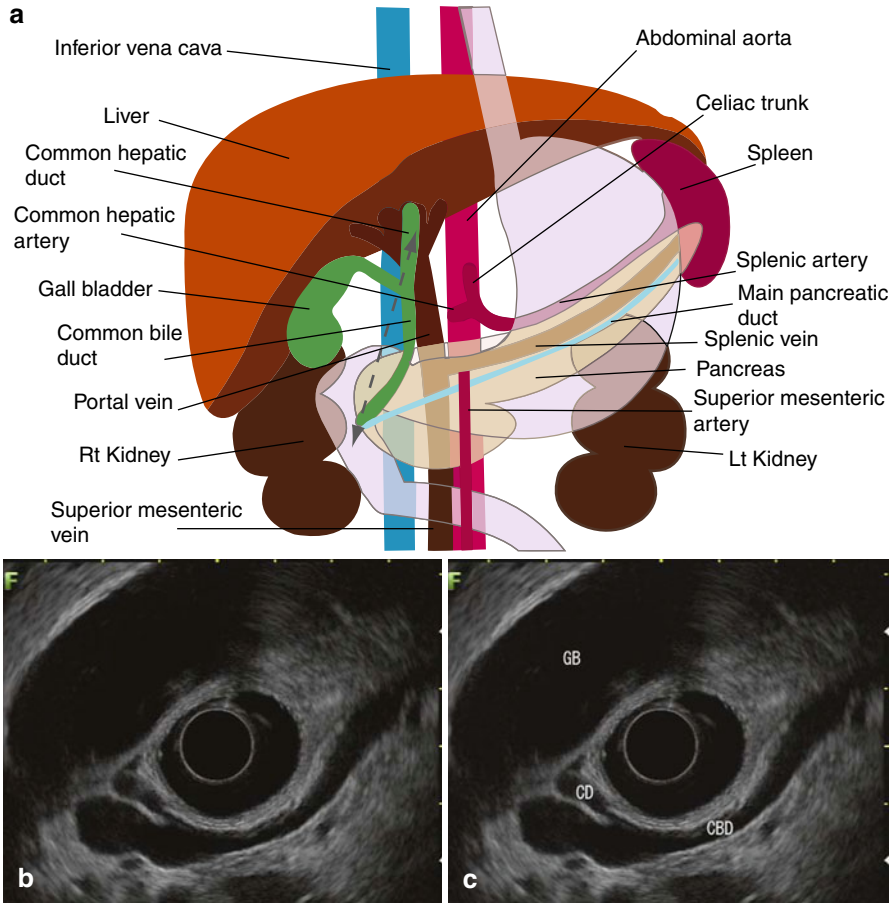

Fig. 7.8 EUS image of trans-bulbar scanning (at the level of the common bile duct). (**a**) Scanning portion, (**b**) EUS image, (**c**) EUS image with abbreviations. *GB* gall bladder, *CD* cystic duct, *CBD* common bile duct

7.3.3 Trans-duodenal Scanning (Second Portion)

After trans-bulbar scanning, the scope is advanced to the second portion of the duodenum. To demonstrate the common bile duct, pancreatic head, and uncinate process, sufficient suction should be applied until duodenal lumen is completely collapsed. EUS scanning is started by pushing and withdrawing the scope to advance a scope to the deep duodenum. Figures 7.9, 7.10, and 7.11 shows the trans-2nd duodenal EUS images. Sufficient scope manipulation using to and fro motion, and clockwise and counterclockwise rotation is vital to makes it possible to see the entire pancreatic head , uncinate process, and common bile duct.

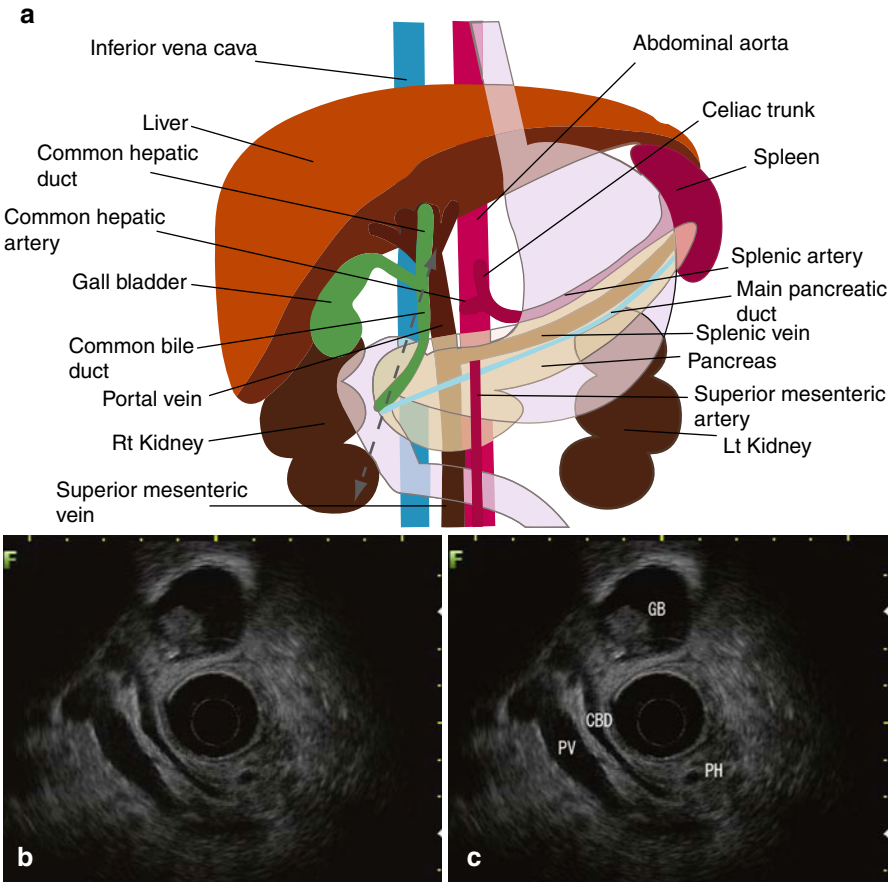

Fig. 7.9 EUS image of trans-2nd duodenal scanning (at the level of middle portion of the 2nd duodenum). (**a**) Scanning portion, (**b**) EUS image, (**c**) EUS image with abbreviations. *GB* gall bladder, *PV* portal vein, *CBD* common bile duct, *PH* pancreatic head

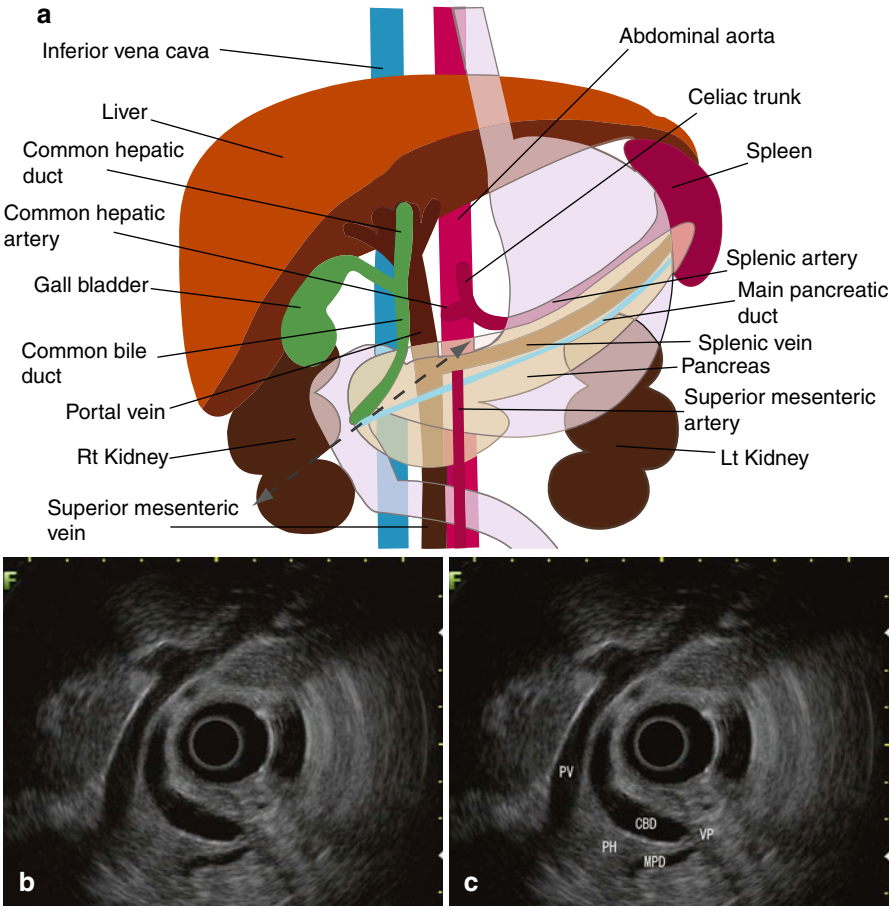

Fig. 7.10 EUS image of trans-2nd duodenal scanning (at the level of the vicinity of the papilla of Vater). (**a**) Scanning portion, (**b**) EUS image, (**c**) EUS image with abbreviations. *PV* portal vein, *CBD* common bile duct, *PH* pancreatic head, *MPD* main pancreatic duct, *VP* papilla of Vater

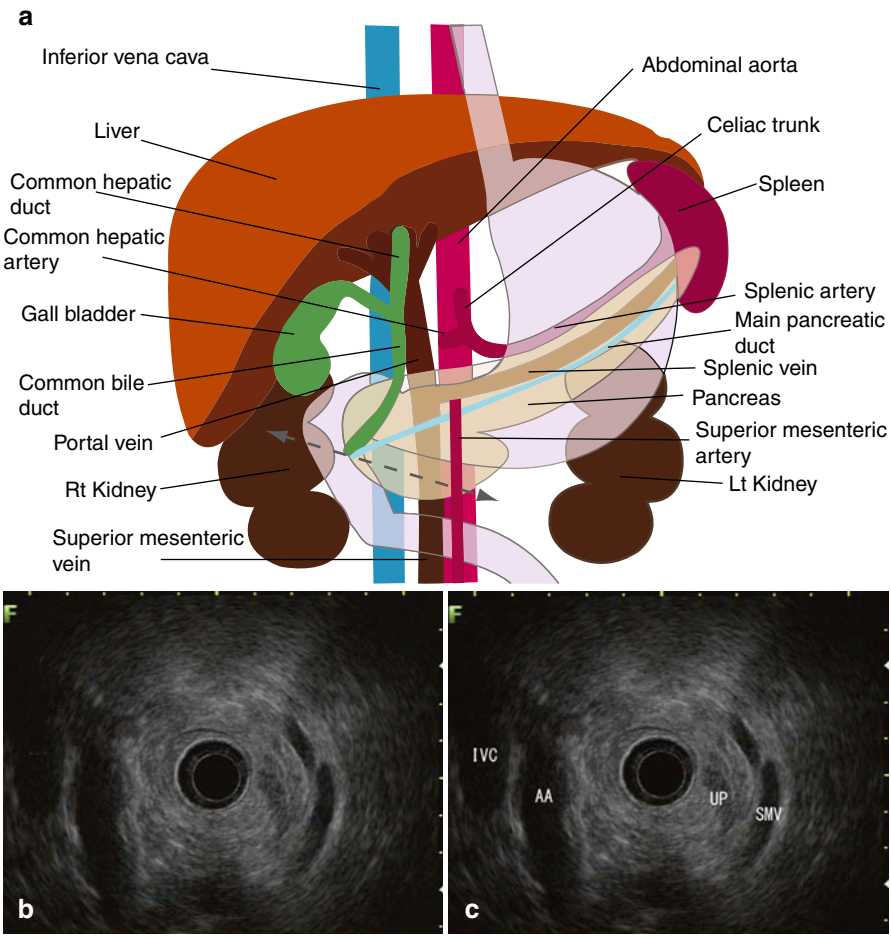

Fig. 7.11 EUS image of trans-duodenal scanning (at the level of second to third portion of the duodenum). (**a**) Scanning portion, (**b**) EUS image, (**c**) EUS image with abbreviations. *IVC* inferior vena cava, *AA* abdominal aorta, *UP* uncinate process, *SMV* superior mesenteric vein

7.4 Diagnosis

7.4.1 Pancreatic Cancer

Pancreatic cancer is usually detected at an advanced stage. Early diagnosis and accurate preoperative staging are vital to improve the prognosis of this disease. The pancreas lies in close proximity to the stomach and duodenum and is well within the range of EUS. The head, body, and tail of the pancreas can all be imaged in detail [1]. The main pancreatic duct can be seen clearly and its diameter measured.

The echo-texture of the pancreatic parenchyma also can be evaluated in detail. Therefore, EUS is more accurate than other imaging modalities for tumor localization, lymph node involvement and vascular invasion. Reported accuracy of tumor staging (TNM system, Table 7.2) [2] ranges from 64% to 84% for T staging, and from 50% to 74% for N staging [3–6]. EUS had excellent sensitivity regardless of tumor size and location. EUS was accurate (90%) in determining tumor size in pancreatic cancers smaller than 3 cm in maximum diameter, but not for tumors larger than 3 cm (30%) [3]. The difficulty in estimating the size of a large pancreatic tumor by EUS was due to the limited depth of penetration by high frequency transducers. CT, or magnetic resonance imaging (MRI) should therefore be used to estimate size when the tumor diameter exceeds 3 cm [3]. EUS can exclude the presence of cancer because its resolution is excellent. However, the presence of inflammatory masses such as chronic and autoimmune pancreatitis, etc. can lead to a false-positive diagnosis of pancreatic cancer. It is difficult to distinguish tumorous pancreatitis from pancreatic cancer on the basis of imaging alone. EUS-guided fine-needle aspiration (EUS-FNA) is useful to solve such a problem by providing us with histological diagnosis [7].

Table 7.2 TNM staging for pancreatic cancer

Tumor (T)	
Tx	Primary tumor cannot be assessed
T0	No evidence of primary tumor
Tis	Carcinoma in situ
T1	Tumor limited to the pancreas, 2 cm or smaller in largest diameter
T2	Tumor limited to the pancreas, larger than 2 cm in larger diameter
T3	Tumor extension beyond the pancreas (i.e., duodenum, bile duct, portal or superior mesenteric vein) but not involving the celiac axis or superior mesenteric artery
T4	Tumor involving the celiac axis or superior mesenteric arteries
Regional lymph nodes (N)	
Nx	Regional lymph nodes cannot be assessed
N0	No regional lymph node metastasis
N1	Regional lymph node metastasis
Diatant metastasis (M)	
Mx	Distant metastasis cannot be assessed
M0	No distant metastasis
M1	Distant metastasis

Quoted and modified from [2]

7.4.1.1 T1 Pancreatic Cancer (Fig. 7.12)

Typical Findings

1. Small (less than 2 cm) localized hypoechoic nodule within the pancreas
2. Heterogeneous internal echo
3. Irregular margin

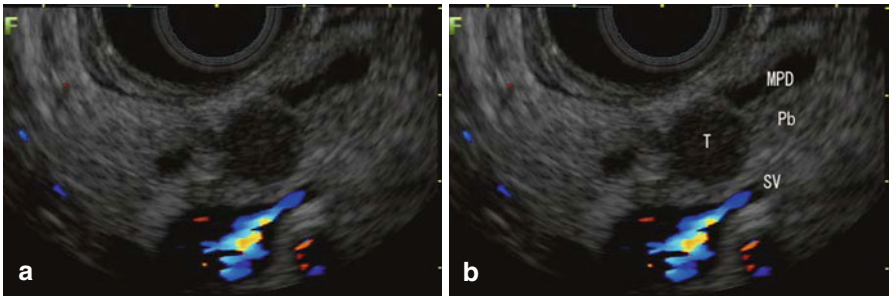

Fig. 7.12 T1 pancreatic cancer. (**a**, **b**) EUS showing a 10 mm hypoechoic tumor (*T*) in the pancreatic body (*Pb*). Splenic vein (*SV*) is intact. The main pancreatic duct (*MPD*) of the tail side is dilated

7.4.1.2 T2 Pancreatic Cancer (Fig. 7.13)

Typical Findings

1. Large (greater than 2 cm) localized hypoechoic nodule within the pancreas
2. Heterogeneous internal echo
3. Irregular margin

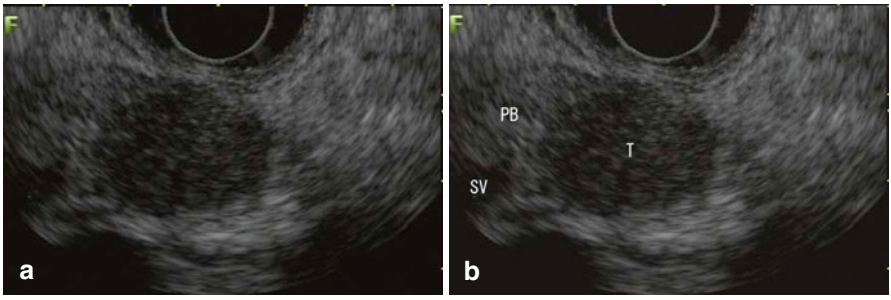

Fig. 7.13 T2 pancreatic cancer. (**a**, **b**) EUS showing a 29 mm hypoechoic tumor (*T*) in the pancreatic body (*PB*). Splenic vein (*SV*) is intact

7.4.1.3 T3 Pancreatic Cancer (Infiltration to the Portal Vein) (Fig. 7.14)

Each of the related blood vessels which may be affected by pancreatic cancer may be readily assessed by EUS. In the absence of invasion, there should be an intact hyperechoic tissue border echo separating the cancer and blood vessel in all scanning images. A loss of this interface echo is suggestive of infiltration. The reported specific findings [8–10] of vascular invasion by the tumor is shown in Table 7.3.

Typical Findings

1. Localized hypoechoic nodule in the pancreas
2. Heterogeneous internal echo
3. Irregular margin
4. Loss of interface echo between cancer and portal vein

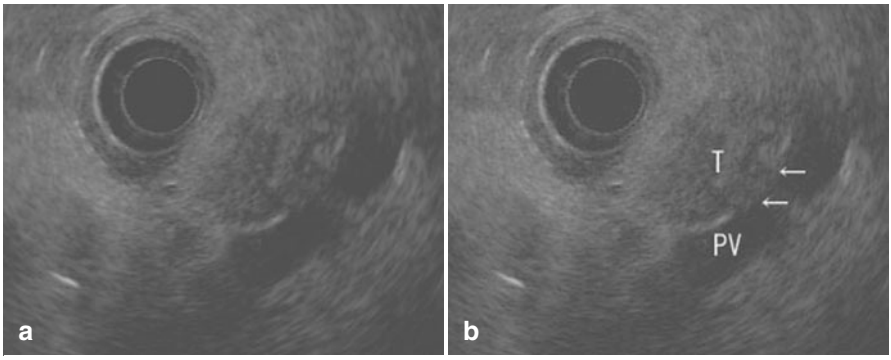

Fig. 7.14 T3 pancreatic cancer (portal invasion). (**a**, **b**) EUS showing a hypoechoic tumor (*T*) in the pancreatic head. The interface echo between tumor and portal vein (*PV*) is partially interrupted (*arrows*)

Table 7.3 Specific EUS findings for vascular invasion by the tumor

1. Loss of interface
2. Irregular vascular wall
3. Cross-sectional vascular encasement
4. Luminal narrowing
5. Presence of intravascular filling defects
6. Vascular occlusion
7. Venous collaterals

Quoted and modified from [8–10]

7.4.1.4 T3 Pancreatic Cancer (Tumor Penetration to the Portal Vein) (Fig. 7.15)

Typical Findings

1. Localized hypoechoic nodule in the pancreatic head
2. Heterogeneous internal echo
3. Irregular margin
4. Intravascular filling defect of the portal vein

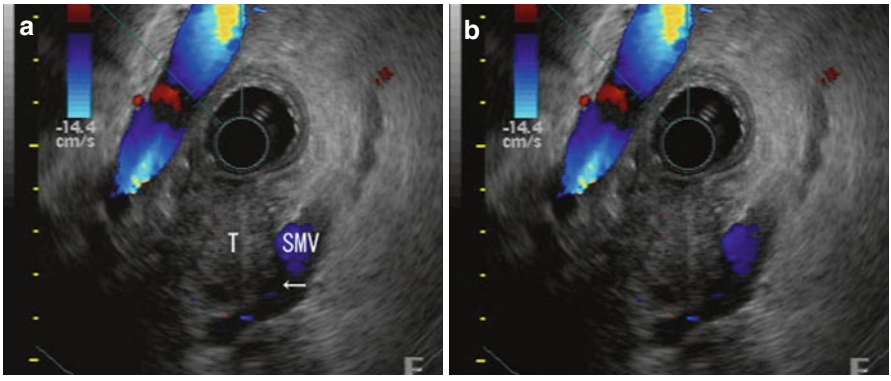

Fig. 7.15 T3 pancreatic cancer (portal invasion). (**a**, **b**) Color Doppler EUS image showing a hypoechoic tumor (*T*) in the pancreatic head. The tumor focally penetrating (*arrow*) into the superior mesenteric vein (*SMV*)

7.4.1.5 Collateral Veins of T3 Pancreatic Cancer (Case of Occlusion of Splenic Vein by Cancer) (Fig. 7.16)

Typical Finding

1. Multiple dilated veins in the gastric submucosal layer

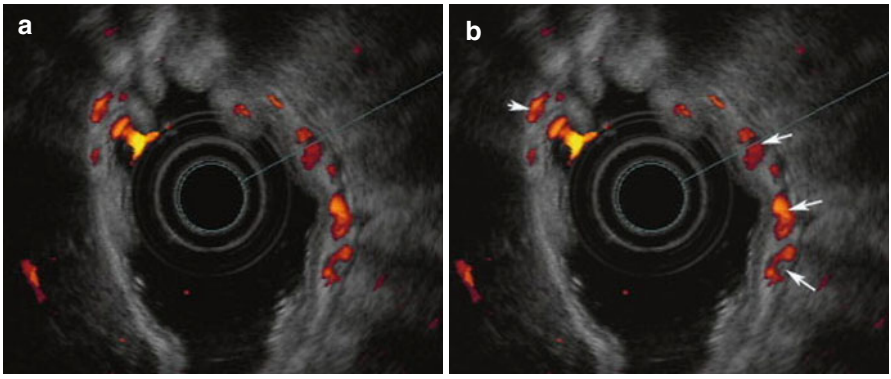

Fig. 7.16 Gastric varices in T3 pancreatic cancer (splenic vein occlusion). (**a**, **b**) Color Doppler image of EUS showing multiple gastric varices (*arrows*) in the submucosal layer of the stomach

7.4.1.6 T3 Pancreatic Cancer (Direct Invasion to the Stomach) (Fig. 7.17)

Typical Findings

1. Localized hypoechoic nodule in the pancreas
2. Heterogeneous internal echo
3. Irregular margin
4. Loss of interface echo between cancer and muscularis propria of the stomach

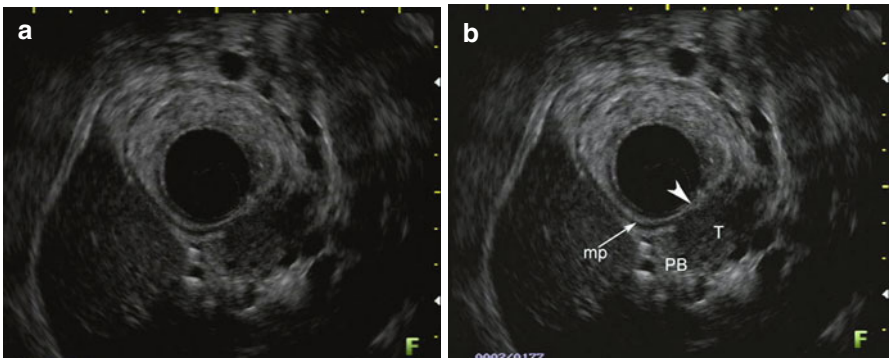

Fig. 7.17 T3 pancreatic cancer (direct infiltration to the gastric wall). (**a**, **b**) EUS shows hypoechoic tumor (*T*) of the pancreatic body (*PB*) invading (*arrow head*) the muscularis propria (*arrow-mp*) of the stomach

7.4.1.7 T4 Pancreatic Cancer (Invasion to the Superior Mesenteric Artery) (Fig. 7.18)

Typical Findings

1. Huge hypoechoic mass in the pancreatic head
2. Encasement of superior mesenteric artery

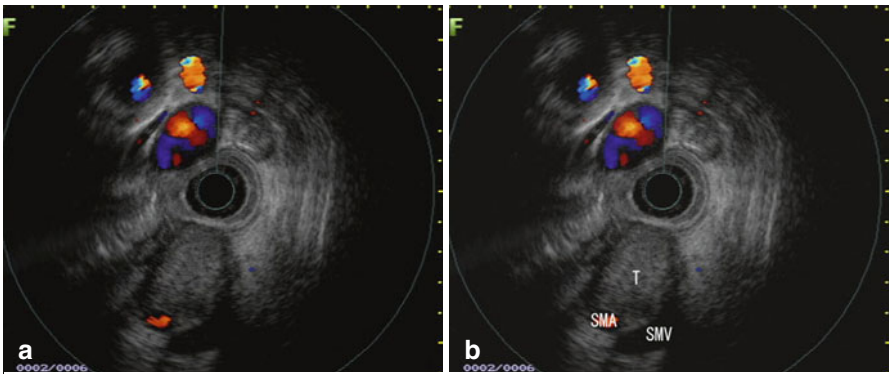

Fig. 7.18 T4 pancreatic cancer (tumor involvement of superior mesenteric artery). (**a**, **b**) Color Doppler EUS imaging showing an encasement of superior mesenteric artery (*SMA*) by tumor (*T*). *SMV* superior mesenteric vein

7.4.2 Cystic Lesions of the Pancreas

Cystic lesions of the pancreas consist of pseudocysts, congenital cysts and cystic neoplasms including serous cystadenomas, mucinous cystadenomas and cystadenocarcinomas, and intraductal papillary mucinous neoplasm (IPMN) [11]. Other pancreatic tumors may contain cystic regions of cystic degeneration, such as solid-pseudopapillary neoplasms, cystic endocrine tumors, and even ductal adenocarcinomas [12]. Certain pancreatic cystic lesions have some characteristic features. The finding of multiple small (<3 mm) compartments within a cystic lesion, also called a microcystic lesion, is suggestive of a serous cystadenoma, with an accuracy of 92–96%, and is not seen in mucinous cystadenomas[13,14]. A cystic lesion without septations or solid components and seen within a pancreas having parenchymal abnormal findings suggests a pseudocyst with a sensitivity of 94% and a specificity of 85% [15]. However, the EUS diagnosis is not accurate enough to diagnose the type of cystic lesion of the pancreas definitively, or to determine its malignant potential in all cases.

7.4.2.1 Serous Cystic Tumor of the Pancreas (Fig. 7.19)

Serous cystadenoma is cystic neoplasm without significant malignant potential. This cystic tumor is most commonly seen in woman [13,14]. This condition does not require surgical resection unless the patient has symptoms.

Typical Finding

1. This tumor contains multiple small cystic spaces (<3 mm) with fibrous septation (Honey comb or Sponge-like appearance)

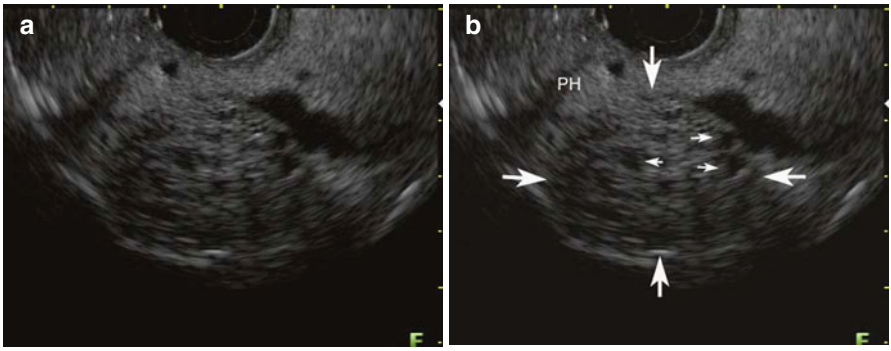

Fig. 7.19 EUS image of serous cystic tumor of the pancreas. (**a**, **b**) EUS showing a multicystic tumor (*large arrows*) of the pancreatic head. This tumor has multiple small cystic spaces (*small arrows*) with fibrous septation, a sponge-like appearance

7.4.2.2 Intraductal Papillary Mucinous Neoplasia (IPMN) of the Pancreas

IPMN is characterized by cystic dilatation of the main pancreatic duct or its branches due to intraductal growth of mucin-producing neoplastic epithelium, thus disease types include main duct, branch duct and mixed types [16]. The cystic dilatations of the branch ducts mimic true pancreatic cysts, however communication of the cyst with the pancreatic duct helps to distinguish IPMN from mucinous cystic neoplasm (MCN), which do not typically communicate with the duct [16]. The main duct type and mixed-type IPMN are potentially highly malignant. Therefore, they should be resected. On the other hand, small incidental branch duct type IPMN appears benign with a low risk of malignant potential in the short term. As the natural history of branch duct type IPMN is still unknown, in those without international consensus-guideline indications for surgical resection (symptoms, size > 3 cm, mural nodules, or cytology causing suspicion of malignancy), conservative follow-up with periodical examination is an acceptable choice [17].

Low Risk Group of Branch Duct Type IPMN (Fig. 7.20)

Typical Findings

1. Dilated side branches (multilocular cystic mass) locates in the pancreas
2. Cystic mass is smaller than 3 cm
3. There is no solid component (mural nodule)

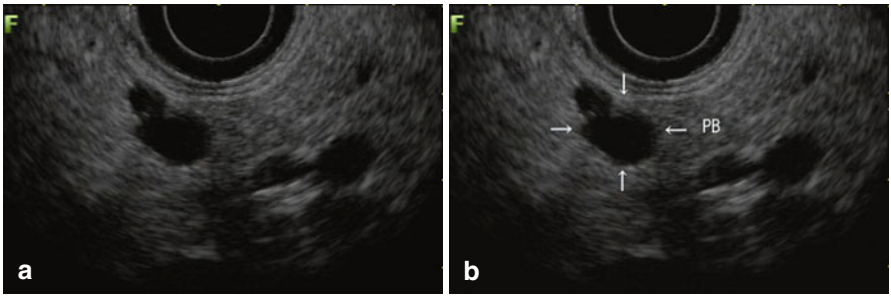

Fig. 7.20 EUS image of low risk group of branch duct type IPMN. (**a**, **b**) EUS showing a 2.5 cm multilocular cystic tumor (*arrows*) of the pancreatic body. No solid component is seen in the cystic mass

High Risk Group of Branch Duct Type IPMN (Fig. 7.21)

Typical Findings

1. Dilated side branches (multilocular cystic mass) locates in the pancreas
2. The size of cystic mass is larger than 3 cm
3. There is a solid component (mural nodule)

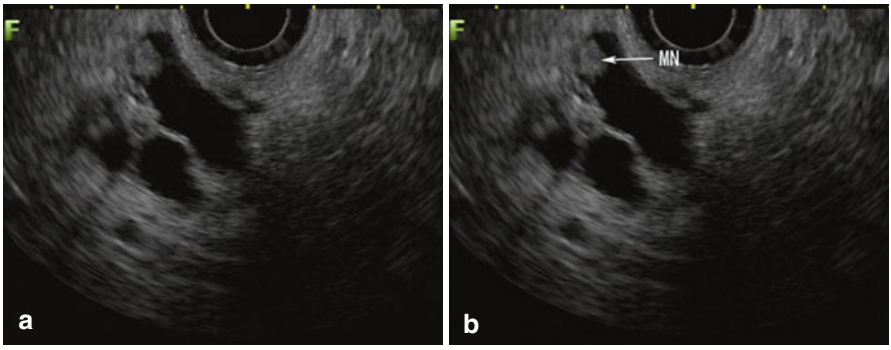

Fig. 7.21 EUS image of High risk group of branch duct type IPMN. (**a**, **b**) EUS showing a 3.5 cm multilocular cystic tumor of the pancreatic body. Solid component (*arrow-MN*, 8 mm mural nodule) is seen in the cystic mass

7.4.2.3 Lymphoepithelial Cyst of the Pancreas (Fig. 7.22)

Lymphoepithelial cyst of the pancreas is an extremely rare condition. It is a benign and non-neoplastic cyst that can mimic solid tumor or cystic neoplasm radiographically. By EUS, it can appear predominantly solid, multilocular or microcystic [16]. Histologically, this lesion is lined by mature stratified squamous epithelium surrounded by dense lymphoid tissue with prominent follicle [16, 18]. It should only be resected if symptomatic, because it has a benign nature.

Typical Finding

1. Hypoechoic solid mass arising from the pancreas

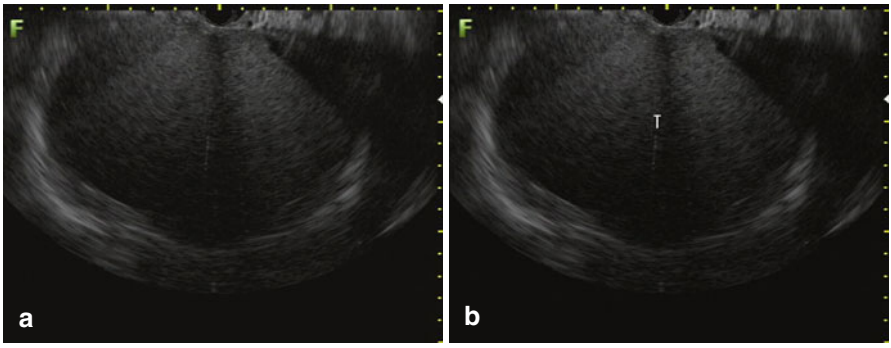

Fig. 7.22 EUS image of lymphoepithelial cyst of the pancreas. (**a**, **b**) EUS showing a 14 cm well demarcated hypoechoic solid tumor (*T*) arising from the pancreatic body

7.4.2.4 Pseudocyst of the Pancreas (Fig. 7.23)

Pseudocyst is the result of acute or chronic pancreatitis, or pancreatic trauma. EUS image of pseudocyst usually lacks septations and mural nodules, although internal debris is frequently observed [11,16].

Typical Findings

1. Monolocular cyst of the the pancreas
2. No septations and mural nodules
3. Internal debris is frequently seen

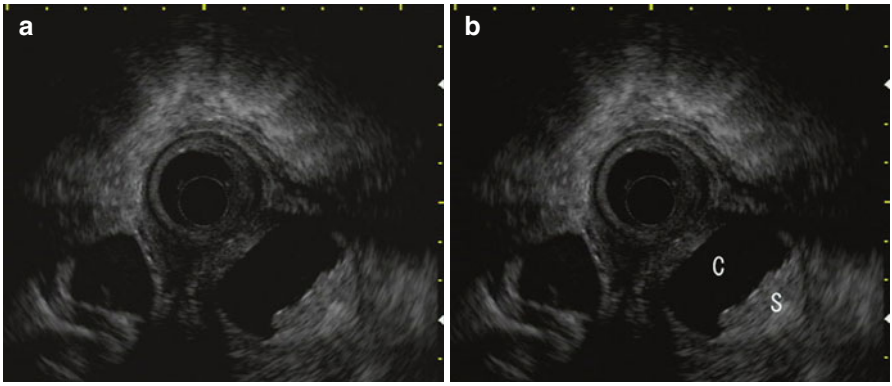

Fig. 7.23 EUS image of pseudocyst of the pancreas. (**a**, **b**) EUS showing a 4 cm monolocular cyst (*C*) with sludge (*S*). There are no septations and mural nodules in this lesion

7.4.3 Chronic Pancreatitis

Chronic pancreatitis is defined as irreversible pancreatic parenchymal damage with development of inflammation and fibrosis that may lead to various degrees of exocrine and endocrine dysfunction [19]. At present, EUS has become a most sensitive diagnostic imaging test because of the capability to visualize subtle alterations in pancreatic structure before traditional imaging (transabdominal US, CT, etc.) and functional tests show any abnormality [20]. The EUS diagnosis of chronic pancreatitis is based on morphologic criteria of the ductal and parenchyma described by the International Working Group using minimum standard terminology (Table 7.4) [20,21]. The more abnormal findings of the above criteria visualized, the more likely the diagnosis of chronic pancreatitis. EUS may be most reliable when it is clearly positive (>5 criteria) or negative (<2 criteria) [22].

Table 7.4 EUS criteria for chronic pancreatitis and corresponding histology

EUS criteria	Corresponding histology
Parenchymal abnormalities	
Hyperechoic foci	Focal fibrosis
Hyperechoic strands	Bridging fibrosis
Lobular contour	Interlobular fibrosis
Cysts	Cyst/ pseudocyst
Ductal abnormalities	
Main duct dilatation	>3 mm (head), >2 mm (body), >1 mm (tail)
Duct irregularity	Focal dilatation/narrowing
Hyperechoic margins	Periductal fibrosis
Visible side branches	Side branch dilatation
Stones	Calcified stones

Quoted and modified from [20,21]

Pitfall (Differential Diagnosis Between Chronic Pancreatitis and Other Conditions)

1. In early stage of chronic pancreatitis, histologic, morphological, and functional abnormalities may be absent or patchy, and other non-inflammatory reasons of fibrosis (e.g. High age and smoking) may cause diagnostic confusion [23]

7.4.3.1 Chronic Pancreatitis (Hyperechoic Foci) (Fig. 7.24)

Typical Finding

1. Small distinct reflectors in the pancreatic parenchyma

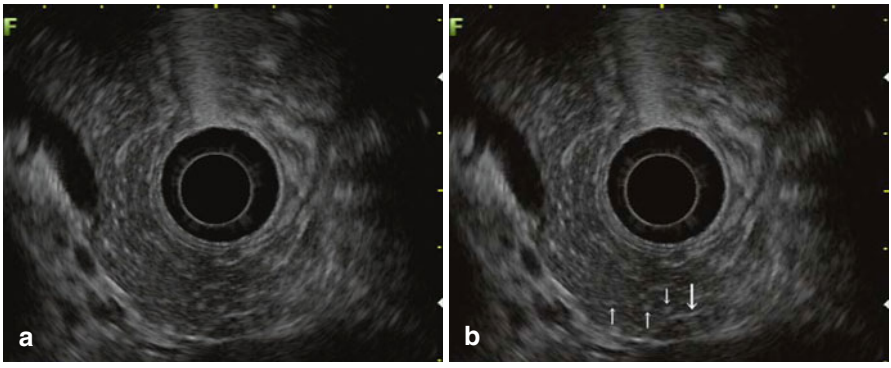

Fig. 7.24 EUS image of chronic pancreatitis (hyperechoic foci and echogenic strain). (**a**, **b**) EUS revealing hyperechoic foci (*small arrows*) and echogenic strain (*large arrow*) in the pancreatic body

7.4.3.2 Chronic Pancreatitis (Hyperechoic Strands) (Fig. 7.25)

Typical Finding

1. Small string-like hyperechoic structures in the pancreatic parenchyma

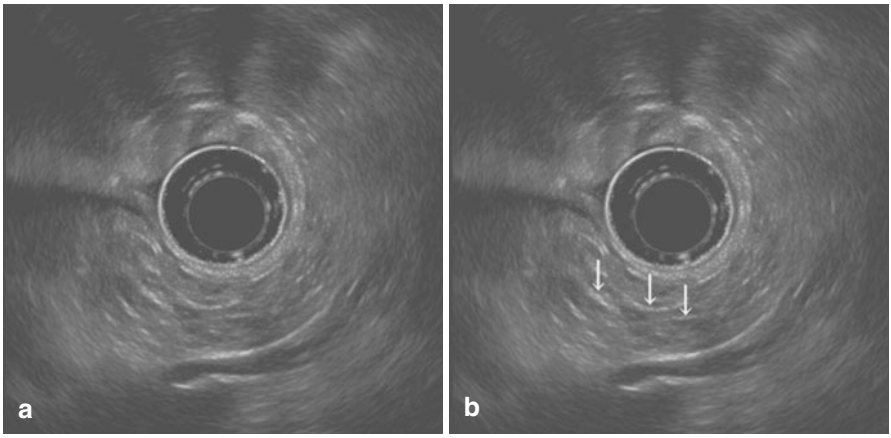

Fig. 7.25 EUS image of Chronic pancreatitis (Hyperechoic strands). (**a**, **b**) EUS revealing echogenic string like structures (*arrows*) in the pancreatic body

7.4.3.3 Chronic Pancreatitis (Lobular Contour) (Fig. 7.26)

Typical Finding

1. Containing lobules-rounded homogeneous areas separated by strands of another echogenecity in the pancreatic parenchyma

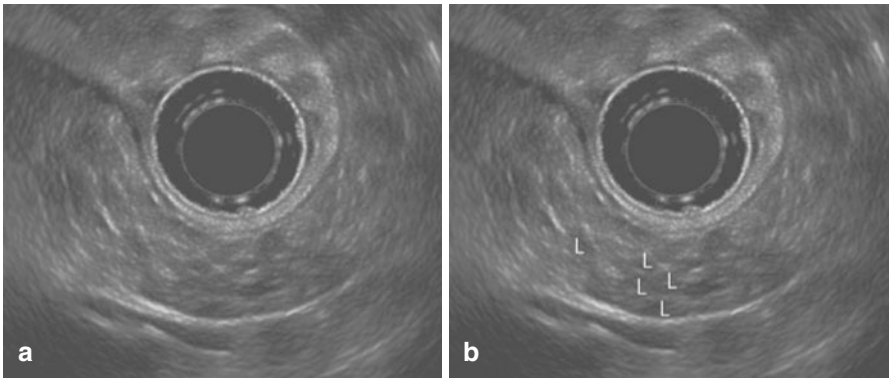

Fig. 7.26 EUS image of Chronic pancreatitis (Lobular contour). (**a**, **b**) EUS of pancreatic body. Hyperechoic strains forming lobules (*L*)

7.4.3.4 Chronic Pancreatitis (Calcified Stone) (Fig. 7.27)

Typical Finding

1. Hyperechoic lesion with acoustic shadow within the pancreatic duct

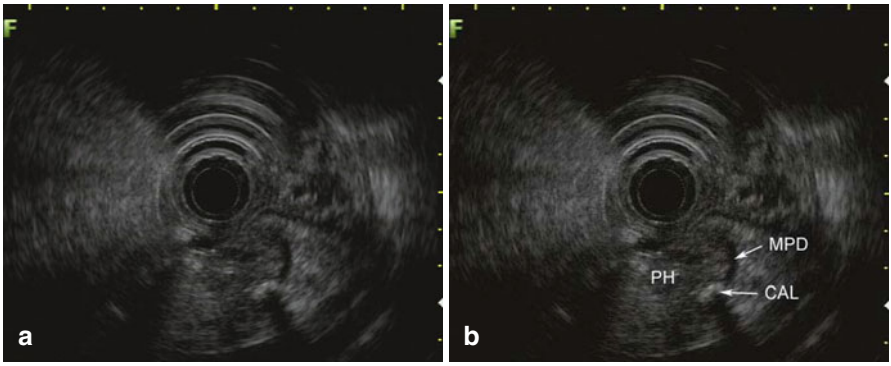

Fig. 7.27 EUS image of chronic pancreatitis (calcified stone). (**a**, **b**) EUS revealing a strong echo with acoustic shadow in the pancreatic head (*PH*). *Arrow-MPD* main pancreatic duct, *arrow-CAL* calcified stone

7.4.3.5 Chronic Pancreatitis (Hyperechoic Duct Margins) (Fig. 7.28)

Typical Finding

1. Both wall of the main pancreatic duct are hyperechoic

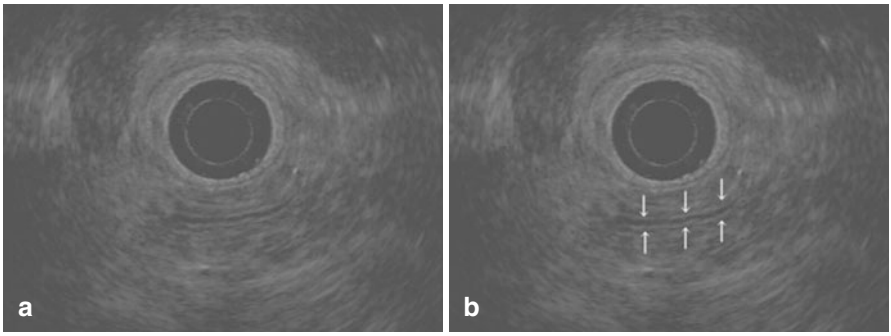

Fig. 7.28 EUS image of chronic pancreatitis (hyperechoic duct margins). (**a**, **b**) EUS revealing a hyperechoic duct margin (*arrows*) of main pancreatic duct in the pancreatic body

7.4.3.6 Chronic Pancreatitis (Main Duct Dilatation) (Fig. 7.29)

Typical Finding

1. Dilatation of main pancreatic duct (>3 mm head, >2 mm body, >1 mm tail)

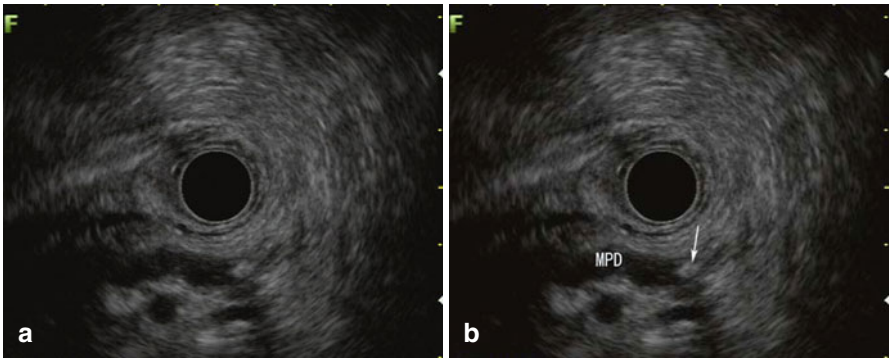

Fig. 7.29 EUS image of chronic pancreatitis (main duct dilatation). (**a**, **b**) EUS revealing an irregular dilatation (6 mm) of main pancreatic duct (*MPD*) and strong echo (*arrow*) with acoustic shadow in the pancreatic body

7.4.4 Biliary Diseases

7.4.4.1 Choledocholithiasis (Fig. 7.30)

Common bile duct stones are usually detected by EUS, irrespective of size or bile duct dilatation. The sensitivity of EUS (84–100%) is superior to transabdominal ultrasound (20–25%) and CT (20–75%) for diagnosing bile duct stones [24,25]. Numerous reported studies have shown that EUS and ERCP have similar accuracy rates for detecting common bile duct stones, over 90% for both techniques [26]. Previous study [25] also showed that EUS is comparably accurate but safer and less costly than ERCP for evaluating patients with having suspected choledocholithiasis.

Typical Finding

1. Strong echo with acoustic shadow in the common bile duct

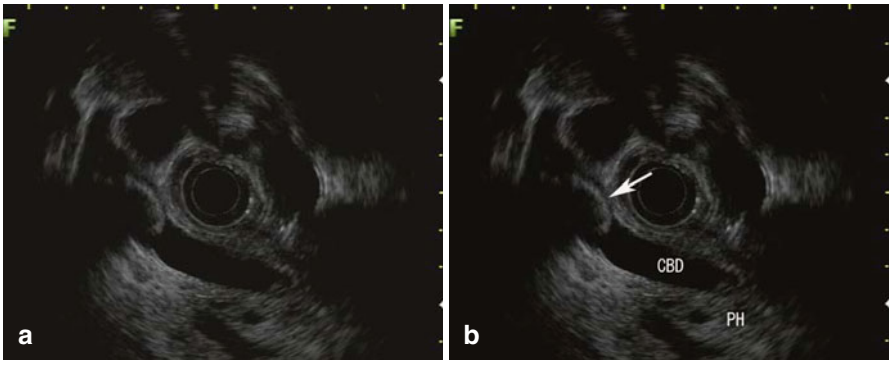

Fig. 7.30 EUS image of choledocholithiasis. (**a**, **b**) EUS showing a strong echo (*arrow*) with acoustic shadow in the common bile duct (*CBD*). *PH* pancreatic head

7.4.4.2 Cancer of the CBD

The typical EUS image of a bile duct cancer shows a hypoechoic mass arising from the bile duct. EUS staging of bile duct tumors is based on the TNM system (Table 7.5)[1]. Diagnostic accuracy has been reported as 72–81% for T staging, and 61–81% for N staging, respectively [27,28].

T3 cancer of the common bile duct (invasion to the pancreas) (Fig. 7.31)

Typical Findings

1. Localized hypoechoic mass in the common bile duct
2. Heterogeneous internal echo
3. Irregular margin

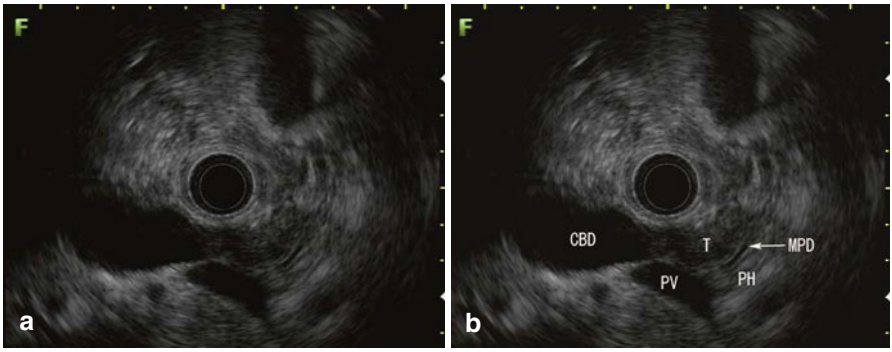

Fig. 7.31 EUS image of T3 cancer of the common bile duct. (**a**, **b**) EUS showing a hypoechoic tumor (*T*) in the lower common bile duct (*CBD*). Upper part of the CBD is dilated. Portal vein (*PV*) is intact. Tumor invades the pancreatic head. The main pancreatic duct (*MPD*) of the pancreatic head (*PH*) is not dilated

Table 7.5 TN staging for bile duct cancer

Tumor (T)	
Tx	Primary tumor cannot be assessed
T0	No evidence of primary tumor
Tis	Carcinoma in situ
T1	Tumor confined to the bile duct histologically
T2	Tumor invades beyond the wall of the bile duct
T3	Tumor invades the liver, gall bladder, pancreas, and/or unilateral branches of the portal vein (right or left) or hepatic artery (right or left)
T4	tumor invades any of the following : main portal vein or its branches bilaterally, common hepatic artery, or other adjacent structures such as colon, stomach, duodenum, or abdominal wall
Regional lymph nodes (N)	
Nx	Regional lymph nodes cannot be assessed
N0	No regional lymph node metastasis
N1	Regional lymph node metastasis

Quoted and modified from [2]

7.4.4.3 GB Cancer

EUS is more accurate than US for visualizing the gall bladder because EUS uses a higher frequency (7.5–12 MHz) than transabdominal ultrasound (3.5 MHz), and the transluminal approach of EUS is not limited by the presence of gas in the bowel. In the differential diagnosis of polypoid lesions of the gall bladder, previous study showed that EUS (sensitivity 92%, specificity 88%) is better than transabdominal US (sensitivity 54%, specificity 54%) for diagnosis of gall bladder cancer [29]. EUS is also useful for UICC TNM staging of gall bladder cancer (Table 7.6) [2]. The gall bladder wall can be imaged as a three-layered structure; that is, the first, hyperechoic layer of the border echo and mucosa, the second, hypoechoic layer of muscle, and the third, hyperechoic layer of serosa. The depth of cancer invasion can be diagnosed based on the layered structure of the wall by EUS. Reported accuracy of TN staging was 76.9% and 89.7%, respectively [30].

Table 7.6 TN staging for gall bladder cancer

Tumor (T)	
Tx	Primary tumor cannot be assessed
T0	No evidence of primary tumor
Tis	Carcinoma in situ
T1	Tumor invades lamina propria or muscle layer
T1a	Tumor invades lamina propria
T1b	Tumor invades muscle layer
T2	Tumor invades perimuscular connective tissue, no extension beyond serosa or into liver
T3	Tumor perforates serosa (visceral peritoneum) and/or directly invades the liver and/or one other adjacent organ or structure, e.g., stomach, duodenum, colon, pancreas, omentum, extrahepatic bile ducts
T4	Tumor invades main portal vein or hepatic artery, or invades two or more extrahepatic organs or structures
Regional lymph nodes (N)	
Nx	Regional lymph nodes cannot be assessed
N0	No regional lymph node metastasis
N1	Regional lymph node metastasis

Quoted and modified from [2]

T1b Cancer (Muscle Layer) of the Gall Bladder (Fig. 7.32)

Typical Findings

1. Irregularity of the first hyperechoic layer
2. Thickness of the second hypoechoic layer
3. Intact third hyperechoic layer
4. Heterogeneous internal echo

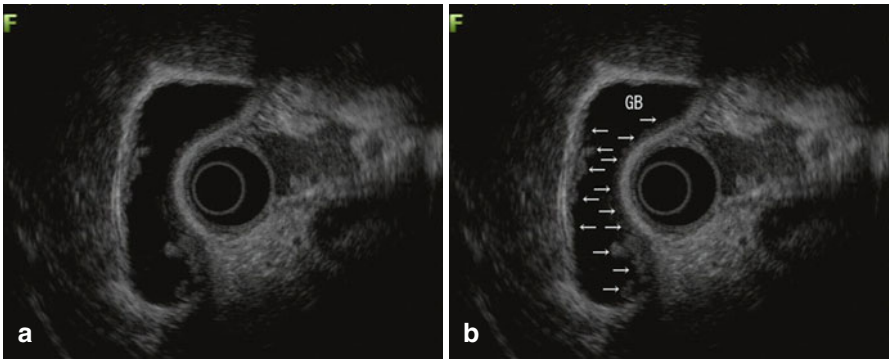

Fig. 7.32 EUS image of T1b gallbladder cancer. (**a**, **b**) EUS showing a broad and flat heterogeneous hypoechoic tumor (*arrows*) in the gall bladder (*GB*). Irregularity of the first hyperechoic layer, thickness of the second hypoechoic layer, and intact third hyperechoic layer is seen

T3 Cancer (Direct Invasion to the Liver) of the Gall Bladder (Fig. 7.33)

Typical Findings

1. Localized hypoechoic mass in the gall bladder
2. Heterogeneous internal echo
3. Irregular margin
4. Border echo is interrupted by hypoechoic tumor

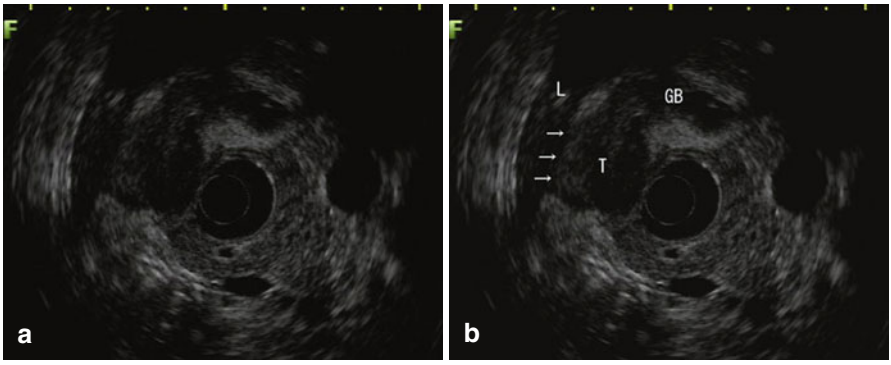

Fig. 7.33 EUS image of T3 gallbladder cancer (direct infiltration to the liver). (**a**, **b**) EUS showing a hypoechoic tumor (*T*) in the gall bladder(*GB*). Loss of the interface (*arrows*) between gall bladder tumor (*T*) and liver (*L*) is seen (direct liver infiltration)

T3 Cancer (Direct Invasion to the Duodenum) of the Gall Bladder (Fig. 7.34)

Typical Findings

1. Localized hypoechoic mass in the gall bladder
2. Heterogeneous internal echo
3. Irregular margin
4. Border echo between gall bladder and duodenum is interrupted by hypoechoic tumor

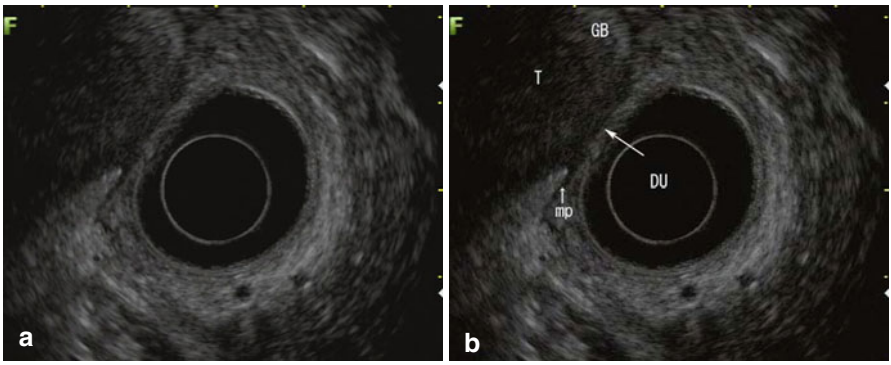

Fig. 7.34 EUS image of T3 gallbladder cancer (direct infiltration to the duodenum). (**a**, **b**) EUS showing a hypoechoic tumor (*T*) in the gall bladder (*GB*). Loss of the interface (*arrow*) between gall bladder tumor and duodenum (*DU*) is seen (direct infiltration to the duodenum). *Arrow-mp* muscularis propria

Lymph Node Metastasis of the T3 Gall Bladder Cancer (Fig. 7.35)

Typical Finding

1. Well-defined round or elliptical structures adjacent to the splenic artery that has a more hypoechoic pattern than the surrounding tissues

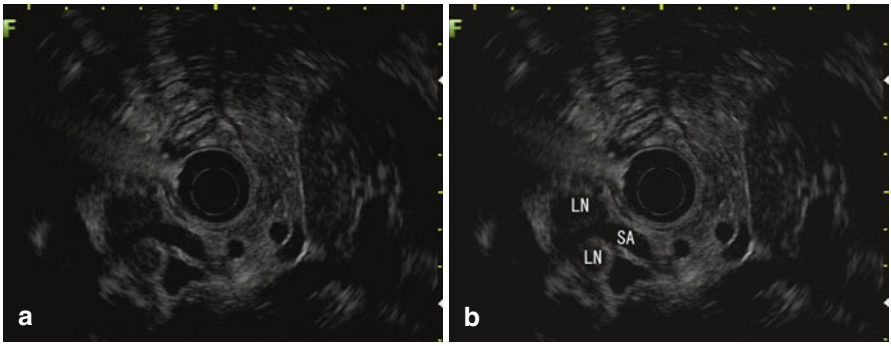

Fig. 7.35 EUS image of peri-splenic artery lymph node metastasis. (**a**, **b**) EUS revealing peri-splenic artery (*SA*) well-defined elliptical hypoechoic mass. *LN* lymph node

7.4.4.4 Cholelithiasis (Fig. 7.36)

Typical Finding

1. Strong echo with acoustic shadow in the GB

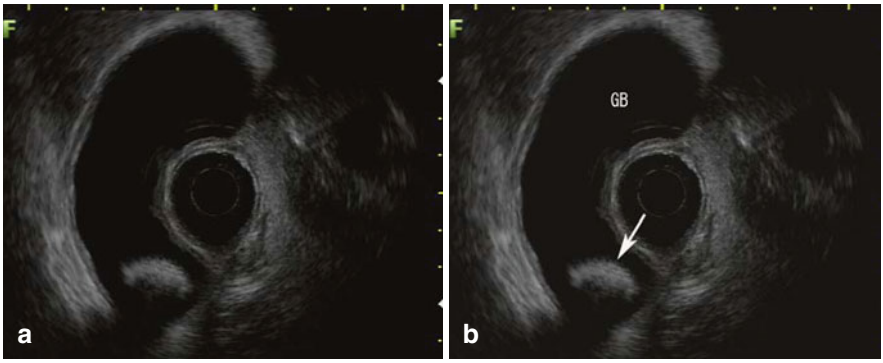

Fig. 7.36 EUS image of cholelithiasis. (**a**, **b**) EUS showing strong echo (*arrow*) with acoustic shadow in the gall bladder (*GB*)

7.4.4.5 Adenomyomatosis of the GB (Fig. 7.37)

Typical Findings

1. Localized wall thickness of the GB
2. Intramural cystic changes (corresponding to the dilated Rokitansky-Aschoff sinus)
3. Sometimes Comet sign positive

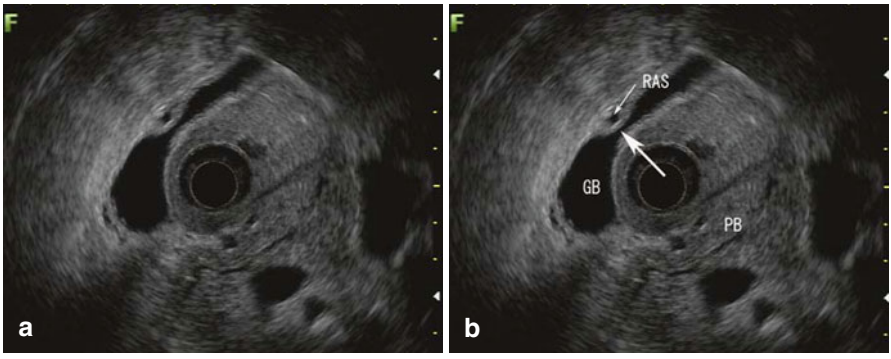

Fig. 7.37 EUS image of adenomyomatosis of the GB. (**a**, **b**) EUS showing a localized wall thickness (*Large arrow*) of the gall bladder (*GB*). This lesion contains a small cystic component (*arrow-RAS*) (corresponding to the dilated Rokitansky-Aschoff sinus). *PB* pancreatic body

7.4.4.6 Cholesterol Polyp of the GB (Fig. 7.38)

Typical Findings

1. Hyperechoic polyp of the GB
2. Pedunculated or semipedunculated polyp
3. The size of polyp usually smaller than 1 cm
4. Multiple polyps

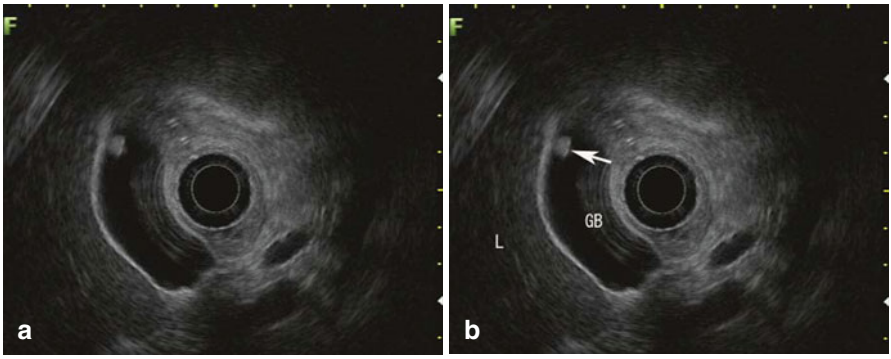

Fig. 7.38 EUS image of cholesterol polyp of the GB. (**a**, **b**) EUS showing a semipedunculated hyperechoic polyp (*Large arrow*) of the gall bladder (*GB*). The size of this polyp is 7 mm (less than 1 cm). *L* liver

References

1. Akahoshi K, Harada N, Nawata H (2003) The current state of endoscopic ultrasonography. In: Pandalai SG (ed) Recent research developments in radiology. Transworld Research Network, Trivandrum, pp 1–37
2. Greene F, Page D, Fleming I, et al. (eds) (2002) In: AJCC cancer staging manual, 6th edn. Springer, New York
3. Akahoshi K, Chijiiwa Y, Nakano I et al (1998) Diagnosis and staging of pancreatic cancer by endoscopic ultrasonography. Br J Radiol 71:492–496
4. Müller MF, MeyenbergerC BP et al (1994) Pancreatic tumors: evaluation with endoscopic US, CT, and MR imaging. Radiology 190:745–751
5. Tio TL, Tytgut GNJ, Cikot RJLM et al (1990) Ampullopancreatic carcinoma: preoperative TNM classification with endosonography. Radiology 175:455–461
6. Tio TL, Sie LH, Kallimanis G et al (1996) Staging of ampullary and pancreatic carcinoma: comparison between endosonography and surgery. Gastrointest Endosc 44:706–713
7. Wittmann J, Kocjan G, Sqouros SN et al (2006) Endoscopic ultrasound-guided tissue sampling by combined fine needle aspiration and trucut needle biopsy: a prospective study. Cytopathology 17:27–33
8. Mallery S, Gupta K (2009) Diagnosis and staging of solid pancreatic neoplasms. In: Gress F, Savides T (eds) Endoscopic ultrasonography. Wiley, West Sussex
9. Brugge WR (1995) Pancreatic cancer staging. Endoscopic ultrasonography criteria for vascular invasion. Gastrointest Endosc Clin N Am 5:742–753

10. Rösch T, Dittler HJ, Strobel K et al (2000) Endoscopic ultrasound criteria for vascular invasion in the staging of cancer of the head of the pancreas: a blind reevaluation of videotapes. Gastrointest Endosc 52:469–477
11. Jacobson BC, Baron TH, Adler DG et al (2005) The role of endoscopy in the diagnosis and the management of cystic lesions and inflammatory fluid collections of the pancreas. Gastrointest Endosc 61:363–370
12. Hamilton SR, Aaltonen LA (2000) Pathology and genetics of tumours of the digestive system. In: Kleihues P, Sobin LH (eds) World Health Organization classification of tumours. IARC, Lyon
13. Koito K, Namieno T, Nagakawa T et al (1997) Solitary cystic tumor of the pancreas: EUS-pathologic correlation. Gastrointest Endosc 45:268–276
14. O'Toole D, Palazzo L, Hammel P et al (2004) Macrocystic pancreatic cystadenoma: the role of EUS and cyst fluid analysis in distinguishing mucinous and serous lesions. Gastrointest Endosc 59:823–829
15. Song MH, Lee SK, Kim MH et al (2003) EUS in the evaluation of pancreatic cystic lesions. Gastrointest Endosc 57:891–896
16. McGrath K (2009) EUS for pancreatic cysts. In: Gress F, Savides T (eds) Endoscopic ultrasonography. Wiley, West Sussex
17. Tanaka M, Chari S, Adsay V et al (2006) International consensus guide-lines for management of intraductal papillary mucinous neoplasms and mucinous cystic neoplasms of the pancreas. Pancreatology 6:17–32
18. Adsay NV, Hasteh F, Cheng JD et al (2002) Lymphoepithelial cysts of the pancreas: a report of 12 case and a review of the literature. Mod Pathol 15:492–501
19. Steer ML, Waxman I, Freedman S (1995) Chronic pancreatitis. N Eng J Med 332:1482–1490
20. Raimondo M, Wallace MB (2004) Diagnosis of early chronic pancreatitis by endoscopic ultrasound. Are we there yet? JOP 5:1–7
21. Gardner TB, Levy MJ (2010) EUS diagnosis of chronic pancreatitis. Gastrointest Endosc 71: 1280–1289
22. Sahai AV (2002) EUS and chronic pancreatitis. Gastrointest Endosc 56:S76–S81
23. Adler DG, Baron TH, Davila RE et al (2005) ASGE guideline: the role of ERCP in diseases of the biliary tract and the pancreas. Gastrointest Endosc 62:1–8
24. Amouyal P, Amouyal G, Levy P et al (1994) Diagnosis of choledocholithiasis by endoscopic ultrasonography. Gastroenterology 106:1062–1067
25. Canto MI, Chak A, Stellato T et al (1998) Endoscopic ultrasonography versus cholangiography for the diagnosis of choledocholithiasis. Gastrointest Endosc 47:439–448
26. de Ledinghen V, Lecesne R, Raymond JM et al (1999) Diagnosis of choledocholithiasis: EUS or magnetic resonance cholangiography? A prospective controlled study. Gastrointest Endosc 49:26–71
27. Qilian ZWN, Lando Z, Jinyu L (1996) Endoscopic ultrasonography assessment in preoperative staging for carcinoma of ampulla of Vater and extrahepatic bile duct. Chin Med J 109: 622–625
28. Mukai H, Nakajima M, Yasuda K et al (1992) Evaluation of endoscopic ultrasonography in the pre-operative staging of carcinoma of the ampulla of Vater and common bile duct. Gastrointest Endosc 38:676–683
29. Azuma T, Yoshikawa T, Araida T et al (2001) Differential diagnosis of polypoid lesions of the gallbladder by endoscopic ultrasonography. Am J Surg 181:65–70
30. Mitake M, Nakazawa S, Naitoh Y et al (1990) Endoscopic ultrasonography in diagnosis of the extent of gallbladder carcinoma. Gastrointest Endosc 36:562–566

Part IV

Linear EUS

Basic Scanning Techniques of Linear EUS

8

Amol Bapaye and Advay Aher

8.1 The Linear Echoendoscope

The linear echoendoscope (EG-530UT) has a curved transducer facing on one side. This provides a 120° sector scanning ultrasound view. The working channel opens just above the transducer and the instruments (commonly needle) can be seen on the ultrasound view. This permits EUS guided biopsies and interventions to be performed. The channel is wide (3.8 mm) and allows passage of instruments up to 10 Fr. diameter through the endoscope.

8.2 Technique

8.2.1 Equipment and Endoscopy Room Setup

1. Load the balloon on the echoendoscope tip, fill with de-aerated water and remove trapped air. Linear EUS can also be performed without the balloon.
2. Ultrasound keyboard must be positioned conveniently near the right hand of the endoscopist.
3. A separate monitor adjacent to the endoscopy monitor for the ultrasound image is recommended.

A. Bapaye, M.D. (M.S.) (✉)
Department of Digestive Diseases and Endoscopy,
Deenanath Mangeshkar Hospital and Research Center,
Erandwane, Pune 411004, Maharashtra, India
e-mail: amolbapaye@gmail.com

A. Aher
Clinical Research Fellow, Department of Digestive Diseases and Endoscopy,
Deenanath Mangeshkar Hospital and Research Center,
Erandwane, Pune 411004, Maharashtra, India

K. Akahoshi, A. Bapaye (eds.), *Practical Handbook of Endoscopic Ultrasonography*,
DOI 10.1007/978-4-431-54014-4_8, © Springer 2012

8.2.2 Patient Preparation

1. Same as standard gastroscopy.
2. Obtain informed consent.
3. Six hours fast.
4. Conscious sedation is used – at our center we use intravenous Midazolam and Butrenorphine. Alternatively, Propofol may also be used. Agents to reduce intestinal peristalsis are helpful.
5. Continuous monitoring during procedure using a pulse oximeter.
6. Prior to EUS examination, patients of esophageal cancer and/or those with symptoms of dysphagia must undergo screening gastroscopy to evaluate the luminal diameter. If necessary, dilate the stricture (up to 15 mm) to facilitate passage of the echoendoscope.
7. Patients scheduled for interventional procedures should have a pre-procedure normalized coagulation profile.
8. Other preparations specific to particular procedures are discussed in the respective chapters.

8.2.3 Basic Principles of Performing a Linear EUS Examination

1. Linear EUS permits one side sector view. Torque must therefore be applied in clockwise (CW) or counter-clockwise (CCW) direction in small incremental steps to obtain complete 360° views.
2. Inflation of the balloon is optional, use balloon only if additional acoustic coupling is required. Minimal inflation of the balloon prevents pressure on adjacent structures and provides better views.
3. Decompress the bowel by suction prior to scanning.
4. Usual scanning frequency is 7.5 MHz. Use lower (5 MHz) to increase depth of scanning and higher (10/ 12 MHz) for examination of wall layers.
5. Orientation of EUS image on screen – monitor's right side corresponds to the cranial and left to the caudal end of the patient. This standard convention is used for description of all linear EUS images in this book.
6. When in doubt, apply Doppler to differentiate vascular structures from ducts.
7. EUS anatomy may be variable. For purpose of demonstration in this book, standard locations and standard appearances of structures have been described. During practice, variations in normal anatomy or appearance may be found which must be differentiated from pathological findings.
8. Performing EUS involves three aspects of learning – (a) identifying anatomical landmarks and various structures, (b) differentiating normal from abnormal structures and (c) establishing a diagnosis based upon the endoscopic and EUS appearance and clinical impression.
9. As a general rule, vascular structures provide a guide to solid organs.
10. Follow tubular structures in their maximally visible length.

11. For mediastinal EUS, the descending aorta (DA) is the chief landmark to be followed to maintain orientation.
12. For abdominal EUS, the abdominal aorta (AA) and portal vein (PV) in the vertical and the pancreas in the transverse axis are the main landmarks.

8.2.4 Standard EUS Appearances and Terminology

The EUS image is an echo signal from the organ being examined. Different organs provide different signal intensities depending upon the tissue resistance to passage of the ultrasound signal. In general, the firmer or harder the tissue, the signal is hyper intense and hence the image is brighter. Similarly, softer tissues or fluid are darker or black. Depending upon these characteristics, EUS appearances are classified as isoechoic (same as surrounding tissue, e.g. normal liver, Fig. 8.1), hypoechoic (darker than surrounding tissue, e.g. malignant tumor, Fig. 8.2), hyperechoic (brighter than surrounding tissue, e.g. calculi, calcification or fat, Fig. 8.3) and anechoic (no signal with a black image, e.g. fluid filled structures like cysts, gall bladder, vascular structures, Fig. 8.4). Vascular structures emit a Doppler signal depending upon the blood flow in the vessel. Calculi reflect the entire signal without permitting it to be transmitted beyond – creating a shadow in the area beyond the calculus.

Fig. 8.1 EUS showing normal isoechoic appearance of liver parenchyma

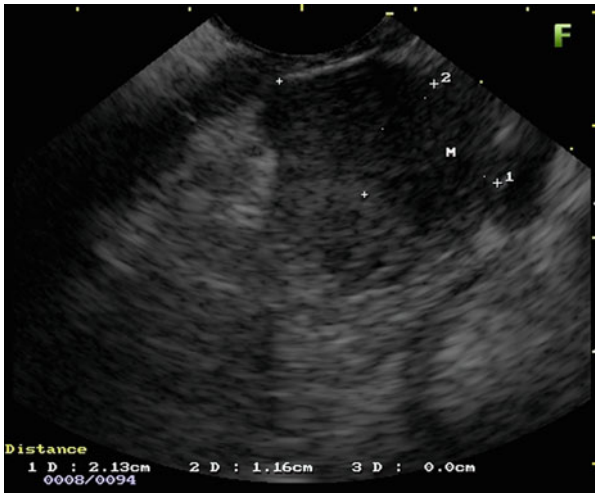

Fig. 8.2 Linear EUS appearance of a hypoechoic pancreatic tumor

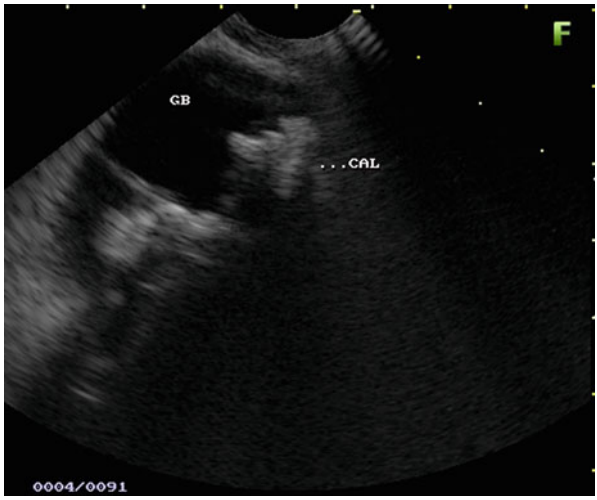

Fig. 8.3 Hyperechoic gall bladder calculi with posterior acoustic shadow on EUS

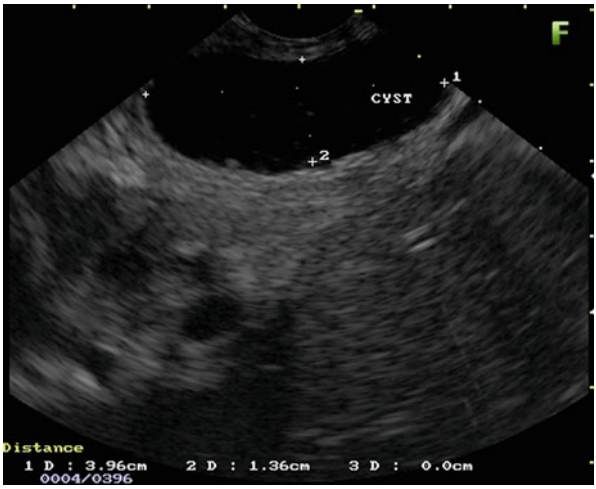

Fig. 8.4 Anechoic appearance of a simple pancreatic cyst on EUS

Linear EUS of the Esophagus and Mediastinum

9

Amol Bapaye and Advay Aher

The esophagus is a tubular organ and is often scanned using the radial echoendoscope. Linear EUS is equally effective in scanning the esophagus and mediastinum, and must be used whenever interventions are planned.

9.1 Indications

- Staging of esophageal cancer
- Staging of lung cancer
- Submucosal tumors of the esophagus
- Enlarged lymph nodes in the posterior mediastinum
- Mass and cystic lesions in the posterior mediastinum

9.2 Technique

Pass the echoendoscope to the gastro-esophageal (GE) junction (approx. 40 cm from incisor teeth) and commence scanning from below upwards. Beginners may find it helpful to identify the Z-line on endoscopic view. Decompress the stomach by suction. The balloon may be slightly inflated for good acoustic coupling with the

A. Bapaye, M.D. (M.S.) (✉)
Department of Digestive Diseases and Endoscopy, Deenanath Mangeshkar Hospital and Research Center,
Erandwane, Pune 411004, Maharashtra, India
e-mail: amolbapaye@gmail.com

A. Aher
Clinical Research Fellow, Department of Digestive Diseases and Endoscopy, Deenanath Mangeshkar Hospital and Research Center,
Erandwane, Pune 411004, Maharashtra, India

K. Akahoshi, A. Bapaye (eds.), *Practical Handbook of Endoscopic Ultrasonography*,
DOI 10.1007/978-4-431-54014-4_9, © Springer 2012

mucosa. Mediastinal or esophageal diseases often extend beyond the diaphragm into the abdomen; examination of these areas is therefore mandatory.

Systematic EUS examination starts with the echoendoscope in the neutral position facing anteriorly. In this position, the left lobe of liver is the first structure seen close to the transducer. Familiarize yourself with the characteristic appearance of the liver parenchyma.

1. Descending thoracic aorta (DA) – In the neutral position, the left lobe of liver is seen. Rotate the endoscope 180° CW to visualize the descending aorta (DA) (Fig. 9.1). To scan the mediastinum, trace the DA cranially. Minor deflections of the tip may be necessary to maintain the DA in longitudinal axis.

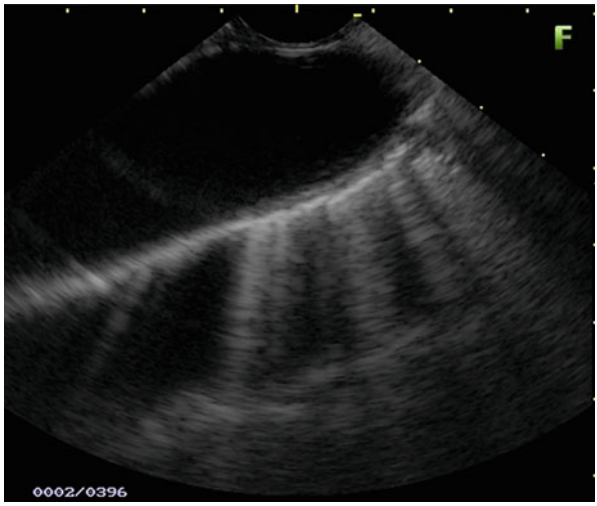

Fig. 9.1 Descending aorta seen on linear EUS. Reverberations from the spine are seen on the posterior aortic wall. The wall is hyperechoic

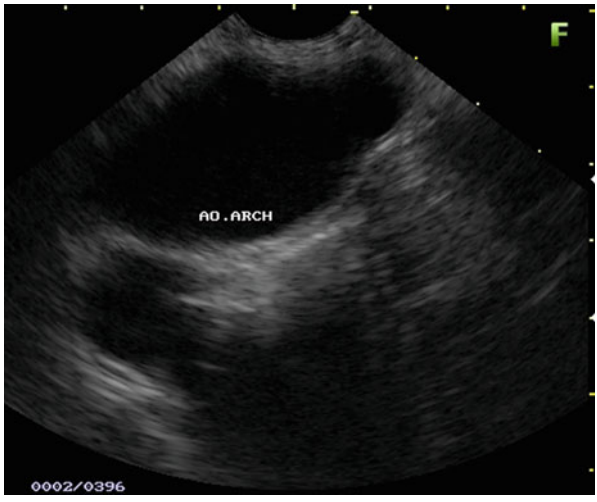

Fig. 9.2 Arch of aorta seen in cross section on linear EUS at 24 cm

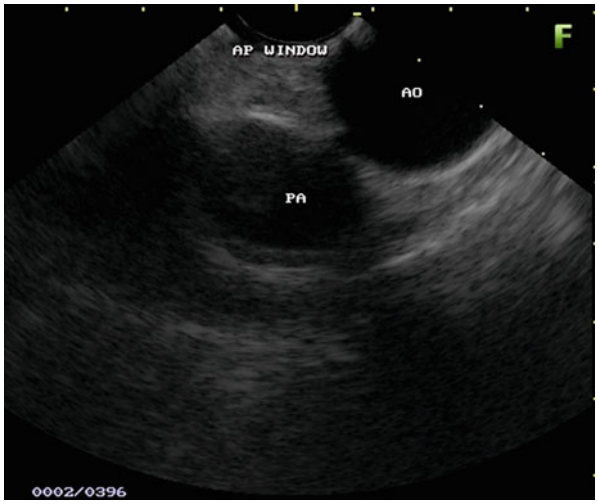

Fig. 9.3 Aorto-pulmonary window on linear EUS. The two vessels in cross section exhibit a characteristic appearance (Mickey Mouse ears sign)

2. Arch of aorta – Withdraw the endoscope gradually keeping the DA in longitudinal plane. At approximately 23–24 cm from incisors, the longitudinal DA becomes circular and is seen in cross section. This is the aortic arch (Fig. 9.2).

1. Branches from the arch – (a) The left subclavian artery (SCA) is seen by rotating the endoscope CCW at the level of the arch; (b) further CCW rotation allows visualization of the left common carotid artery (CCA).
2. Aorto-pulmonary window (A-P window) – At the level of the aortic arch, rotate the endoscope CW and deflect the tip slightly upwards. The aorta becomes further circular and another vascular structure appears in cross section on the left – the pulmonary artery (PA). The space between the two is the A-P window (ATS level 5 lymph nodes) (Fig. 9.3).
3. Heart, cardiac chambers and valves – From the neutral position with the left liver lobe in view, gradually withdraw the endoscope. The left ventricle (LV) is seen as a pulsatile thick walled anechoic structure. On further withdrawal, the left atrium (LA) is seen, with the mitral valve between the two chambers (Fig. 9.4). Center the image over the LA and withdraw the endoscope further. The aortic root with the aortic valve comes into view with the PA in cross section just proximal to it (Fig. 9.5).
4. Sub carinal space (SCS) – On further withdrawal, the LA disappears (towards left of screen) and ring artifacts appear proximal to the PA and aortic root (towards right of screen). These artifacts are caused by the air in the trachea. This is the carina. The space between the carina and LA is the SCS. (ATS level 7 lymph nodes) (Fig. 9.6).
5. Right paraesophageal area – Tracing the DA from the GE junction proximally and rotating CCW, locate the azygos vein adjacent to the distal esophagus. Follow it cranially to its insertion into the superior vena cava (SVC) (Fig. 9.7). Pulsations are seen in the Azygos vein. Visualize the right lung and right pleura, the latter as a bright reflective surface with air reverberations in the underlying lung. Proximal to the aortic arch, look for the right lower paratracheal area (ATS station 4 lymph nodes).

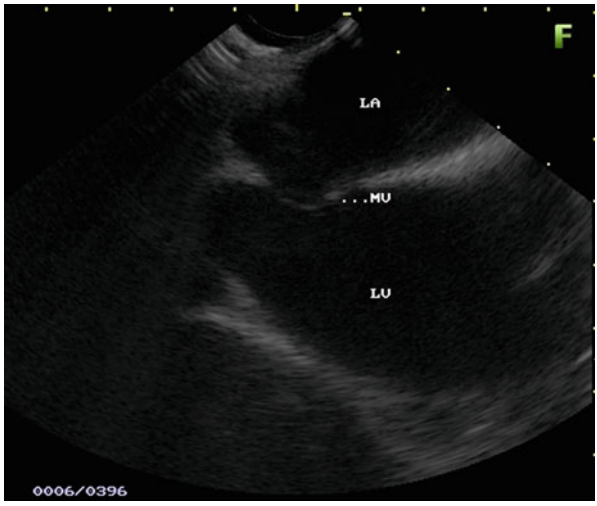

Fig. 9.4 Linear EUS of the heart – the LA, LV and Mitral valve are clearly seen

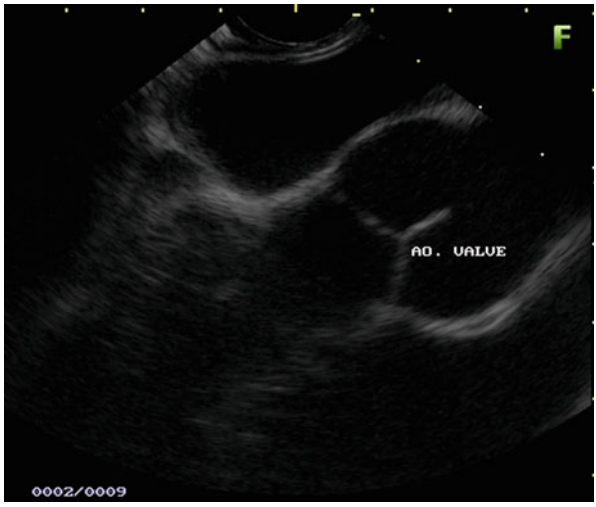

Fig. 9.5 Linear EUS of the heart – note the tricuspid aortic valve in the aortic root

6. Left paraesophageal area – Tracing the DA proximally from the GE junction and rotating CW, locate the left paraesophageal area and the left lung with the bright left pleura. Proximal to the aortic arch, look for the left lower paratracheal area (ATS station 4 lymph nodes).
7. Right and left paratracheal areas – Follow the air shadow of the carina cranially to locate the trachea. Scan on either sides of the trachea by CW or CCW rotation to see the paratracheal regions.

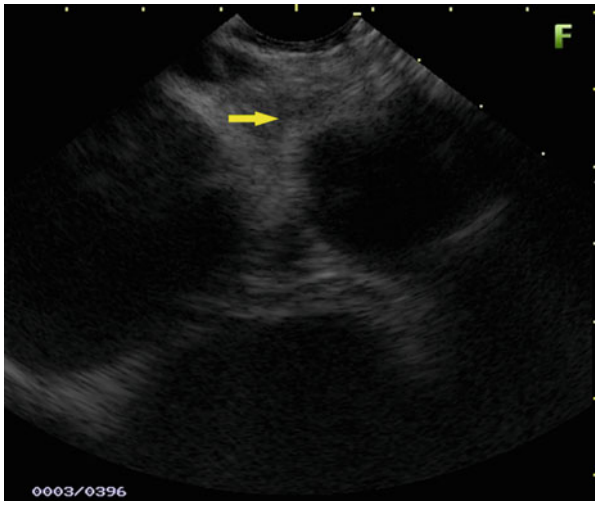

Fig. 9.6 Linear EUS showing sub-carinal space (*arrow*) between the LA and the carina

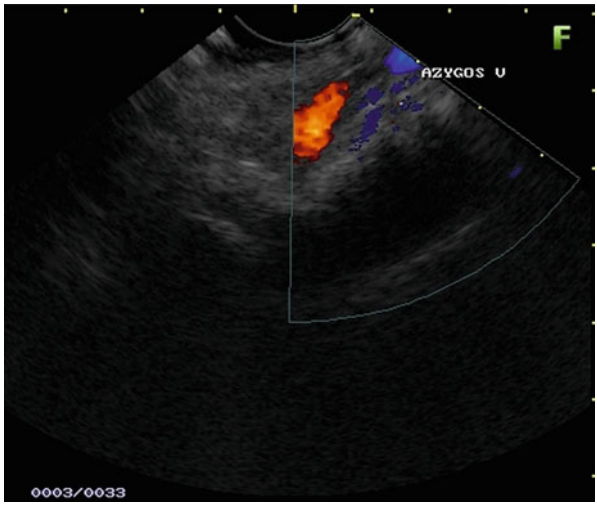

Fig. 9.7 The azygos vein is situated close to the esophageal wall – seen on linear EUS

8. Combination of the above mentioned steps with CW or CCW rotations is necessary for complete examination. During linear EUS, it is important to orient oneself to the direction of examination – dorsal, ventral or lateral. The DA is an important landmark for reorientation if one loses his way in the mediastinum.
9. Esophageal wall layers – The esophageal wall is seen as a five layered structure (Fig. 9.8). Proper orientation in the long axis is necessary to get optimum perpendicular scanning views.

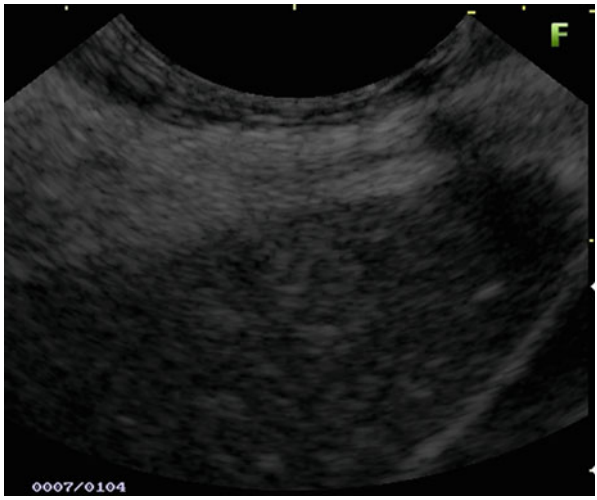

Fig. 9.8 Linear EUS showing five layered wall structure of esophagus

9.3 Mediastinal Lymphadenopathy

Enlarged mediastinal lymph nodes may be found in a variety of diseases – reactive lymphadenopathy, granulomatous inflammations like tuberculosis, histoplasmosis, sarcoidosis or malignancy like lymphoma or metastatic disease. EUS can reliably differentiate between benign and malignant lymphadenopathy [1–4].

9.3.1 Typical EUS Appearances of Various Types of Lymphadenopathy – (Table 9.1; Figs. 9.9, 9.10, 9.11, and 9.12)

EUS has a sensitivity, specificity, positive and negative predictive value of 78%, 71%, 75% and 79% respectively for evaluation of malignant lymphadenopathy [5]. This accuracy can be further enhanced by EUS-FNA (Discussed in detail in Chap. 15).

Table 9.1 EUS appearances of reactive, granulomatous and malignant lymphadenopathy

Characteristic feature	Reactive lymphadenopathy	Granulomatous lymphadenopathy	Malignant lymphadenopathy
Size	Small, short diameter <10 mm	Usually large	Usually large, short diameter >10 mm
Shape	Oval or bean shaped	Matted appearance commonly seen	Usually discreet, rounded appearance, well demarcated border
EUS appearance	Isoechoic	Usually hypoechoic, anechoic when necrosis or caseation	Uniformly hypoechoic, anechoic when necrosis
Hilar architecture	Preserved, seen as hyperechoic center	Not preserved	Not seen, uniformly hypoechoic node
Matted appearance	Never	Common	Less common, usually discreet enlarged nodes

Fig. 9.9 Linear EUS showing an oval isoechoic lymph node. The hilar architecture is preserved suggestive of reactive lymphadenopathy

Fig. 9.10 Hypoechoic matted mediastinal lymph nodes are usually seen in tuberculosis

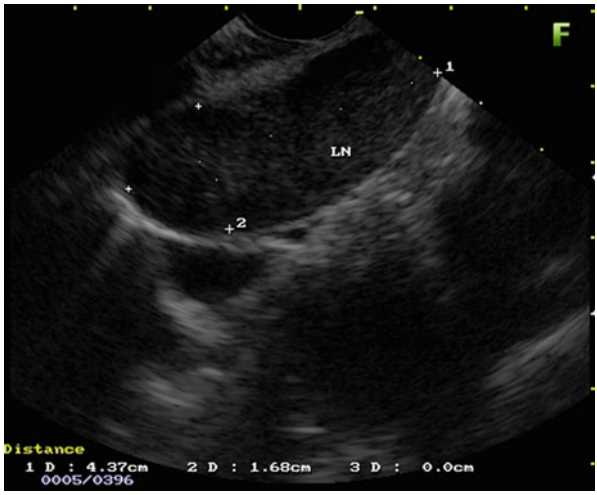

Fig. 9.11 Enlarged lymph nodes without caseation are characteristic of sarcoidosis

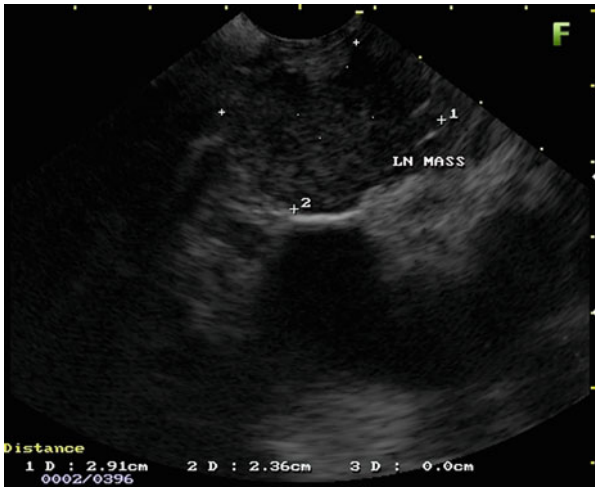

Fig. 9.12 Malignant lymphadenopathy has a rounded, hypoechoic appearance. Central necrosis may be evident (Linear EUS showing lymph node metastasis from lung cancer)

9.4 Esophageal Submucosal Lesions

Submucosal lesions in the esophagus may be leiomyoma, gastrointestinal stromal tumor (GIST), lipoma, varices, or others. It is important to identify the layer of origin of the lesion. Following the esophageal layers at the proximal and distal margins of the lesion will help to identify the layer of origin and infiltration.

9.4.1 Gastrointestinal Stromal Tumor (GIST)

Typical EUS Findings (Fig. 9.13)
1. Hypoechoic mass lesion in layers 2 or 4
2. Heterogeneous appearance with hyper and hypoechoic areas
3. Calcification may be seen
4. Layer structure may be disturbed in case of infiltration

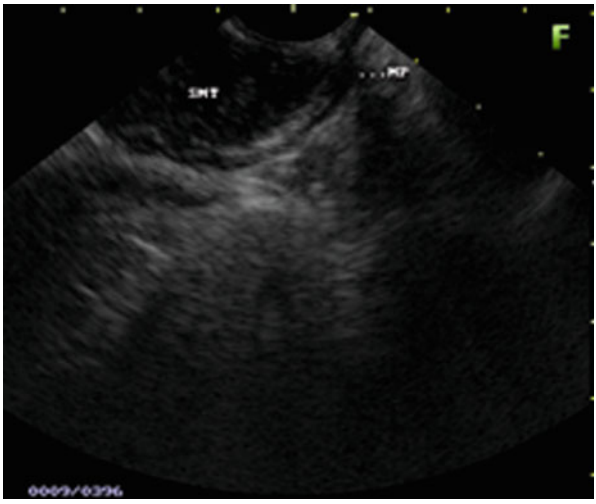

Fig. 9.13 Hypoechoic mass in the esophageal wall arising in layer 2 seen on linear EUS. The layer structure is preserved

9.4.2 Leiomyoma

Typical EUS Findings (Fig. 9.14)
1. Well circumscribed hypoechoic mass in layers 2 or 4
2. Layer structure is well preserved

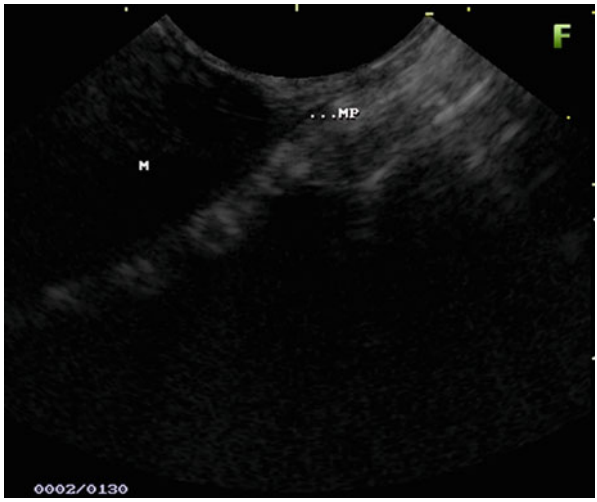

Fig. 9.14 Esophageal leiomyoma arising from the deep muscle layer seen on linear EUS

9.5 Cysts in the Mediastinum

The commonest cystic mediastinal lesions are congenital foregut cysts. They may be esophageal duplication cysts or bronchogenic cysts, depending upon their location near or away from the esophageal wall respectively.

9.5.1 Congenital Duplication Cysts

Typical EUS Appearance (Figs. 9.15 and 9.16)

1. Round, oval or tubular anechoic structure with acoustic enhancement and without color flow on Doppler
2. Layered structure of the cyst wall may sometimes be apparent
3. Contents may be thick gelatinous material causing a hypoechoic rather than anechoic appearance. This sometimes can be mistaken for a mass lesion

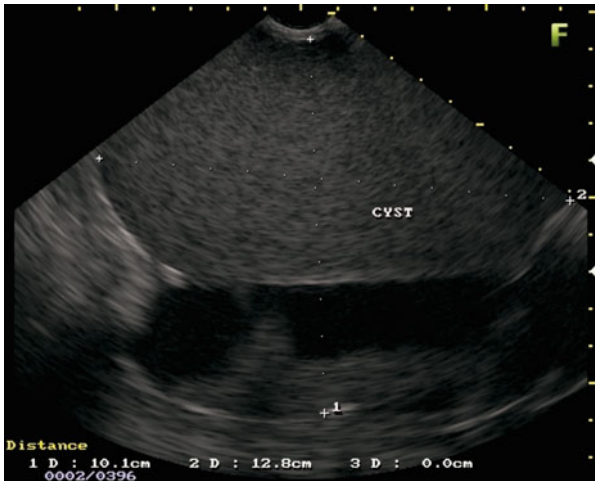

Fig. 9.15 Esophageal duplication cyst seen on linear EUS. Note the layered appearance and turbid contents

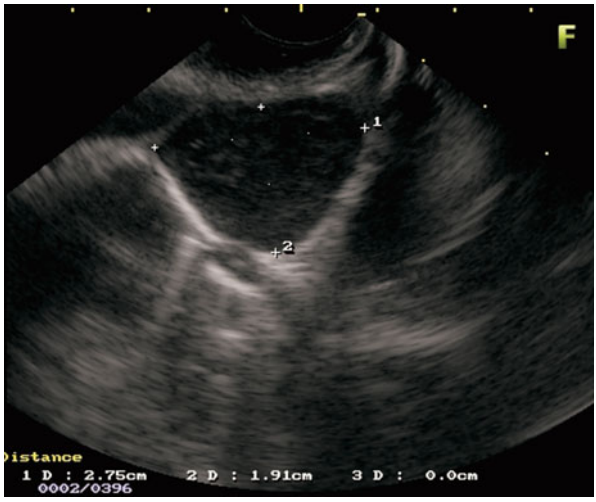

Fig. 9.16 A bronchogenic cyst is situated further away from the esophageal wall

9.5.2 Other Cystic Lesions

Other cystic lesions include pseudocysts extending across the diaphragm (Fig. 9.17), mediastinal abscess or cystic teratoma.

9.6 Solid Mediastinal Masses

Solid mediastinal masses are most often pulmonary tumors infiltrating the mediastinum or metastases from extra thoracic malignancies. EUS-FNA can be performed for tumors adjacent to the esophagus [6].

Neurogenic tumors are the commonest primary posterior mediastinal tumors and account for 75% of all primary posterior mediastinal tumors [7] (Fig. 9.18). They

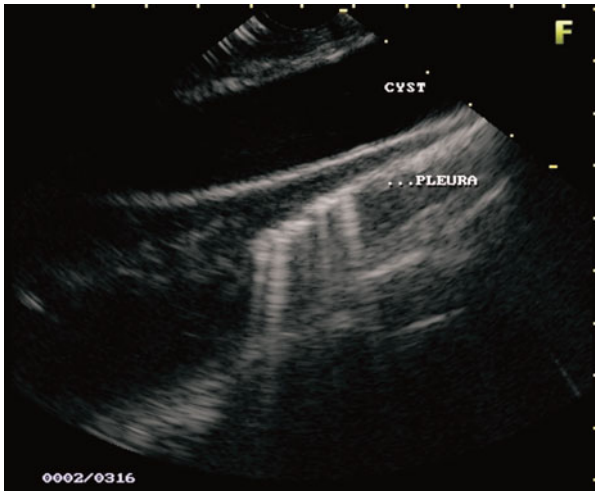

Fig. 9.17 Pancreatic pseudocyst extension into mediastinum in a post acute pancreatitis patient

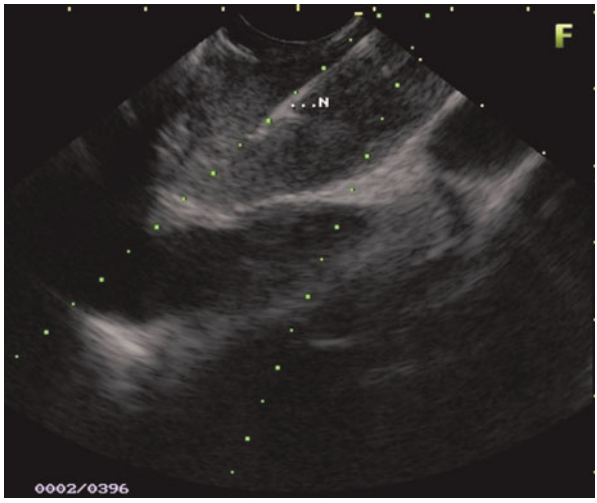

Fig. 9.18 Linear EUS showing a hypoechoic posterior mediastinal mass. FNA showed spindle cells indicating a neurogenic origin

are of various types – schwannoma, neurilemoma, neurofibroma, ganglioneuroma, ganglioneuroblastoma, neuroblastoma or paraganglionoma. Malignancy may be seen in 10–20% tumors. Diagnosis is by FNA [8].

9.7 Lung Cancer Staging

EUS plays an important role in the management algorithm of small cell (SCLC) and non small cell lung cancer (NSCLC) and is useful for T and N staging.

EUS can evaluate centrally situated tumors adjacent to the esophagus, and FNA can be performed for establishing diagnosis [6, 9]. Left upper lobe tumors are visualized from the proximal esophagus adjacent to the aorta. EUS is accurate in assessment of T_4 disease – invasion into mediastinum, great vessels or vertebrae [10].

Regional lymph nodes in NSCLC are classified according to the station approach proposed by Mountain and Dressler [11]. EUS can evaluate lymph node stations adjacent to the esophagus or centrally located vessels, namely – left lower paratracheal (station 4L), AP window (station 5), para aortic (station 6), SCN (station 7), lower para esophageal (station 8) and pulmonary ligament (station 9) (Figs. 9.19 and 9.20). EUS confirmation of contralateral lymph node involvement can avoid unnecessary thoracotomy in patients of NSCLC.

Evaluation of the left liver lobe and left adrenal gland (LAG) is mandatory to assess metastases from lung cancer (Fig. 9.21). EUS can detect occult disease when other modalities have failed to demonstrate pathology [12, 13]. Small interlobar pleural effusions may be detected on EUS.

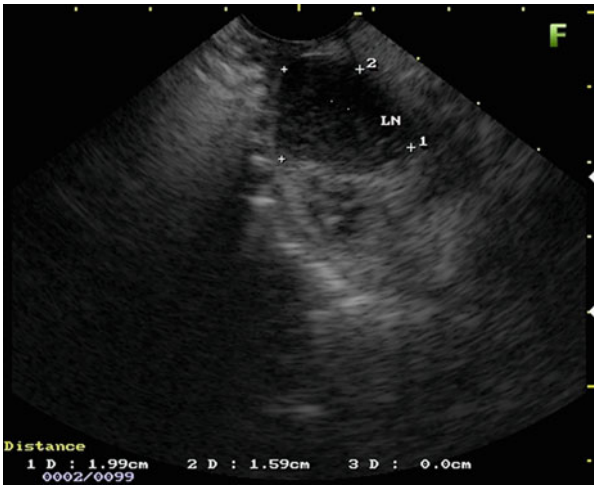

Fig. 9.19 An enlarged homogenous hypoechoic lymph node with sharp borders indicating malignant involvement

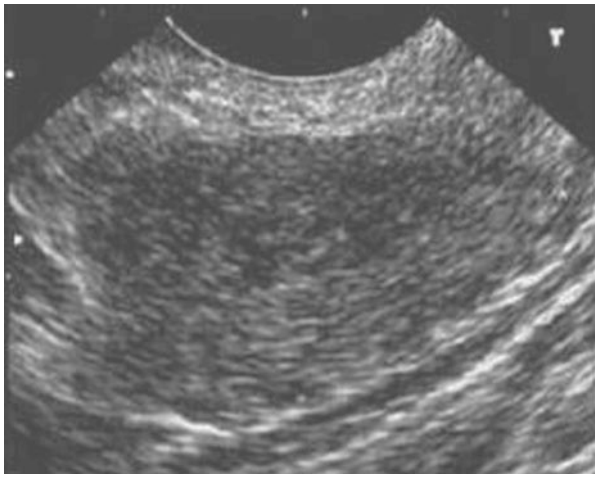

Fig. 9.20 Centrally situated mediastinal nodal mass on linear EUS. FNA revealed NSCLC

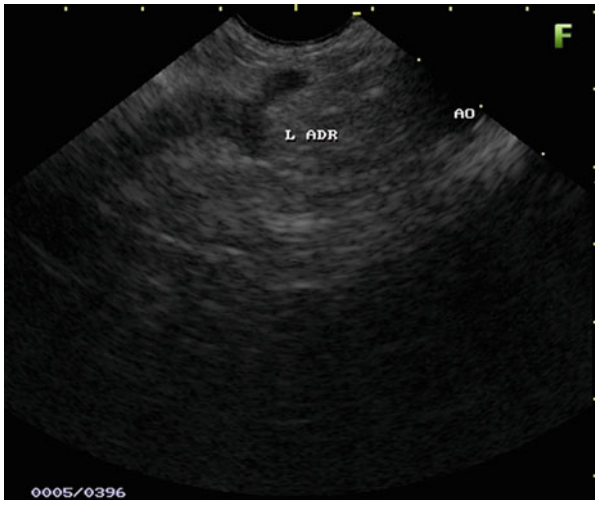

Fig. 9.21 Examination of the left adrenal gland (*LAG*) is mandatory for lung cancer staging

9.8 Esophageal Cancer Staging

EUS is useful in T and N staging of esophageal cancer. Although the radial echoendoscope is often favored over the linear for esophageal cancer staging, linear endosonography has been found to be equally effective, especially for staging of T3 and T4 disease [14]. The linear endoscope also permits an FNA to be performed at the same time if required. Using linear EUS, it is possible to image beyond a stricture without passing the endoscope across. By wedging the EUS probe in the stricture, longitudinal views of the stricture can be obtained. Avoid tangential imaging to prevent overstaging the tumor. Use higher frequencies (10/12 MHz) for accurate

assessment of layer invasion. EUS can detect tumor extension into the mediastinum, aorta, pleura or pericardium. This is seen as breach in the adventitia and loss of fat planes between the tumor and the aorta, pleura or pericardium.

EUS detects enlarged paraesophageal, SC or AP window lymph nodes in patients with esophageal cancer, thus accurately assessing N stage (Fig. 9.22). Celiac lymph node involvement in esophageal cancer signifies M1a disease. Linear EUS is accurate for assessment of celiac lymph nodes (Fig. 9.23). EUS can pick up small liver metastases that were missed by other imaging techniques [15, 16]. Metastases appear as discreet hypoechoic nodules in the liver.

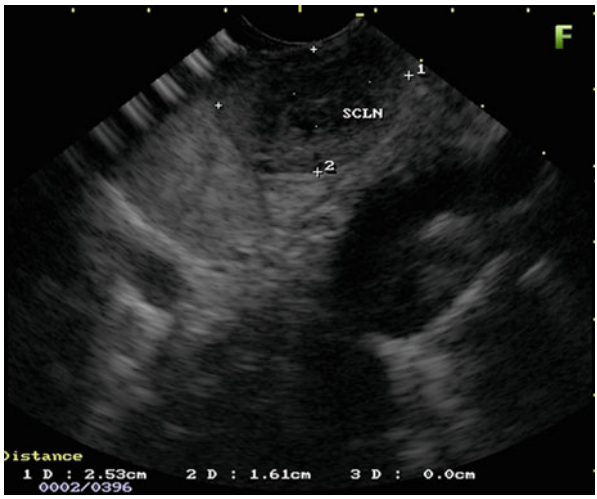

Fig. 9.22 An enlarged sub carinal lymph node seen in a patient with Ca esophagus

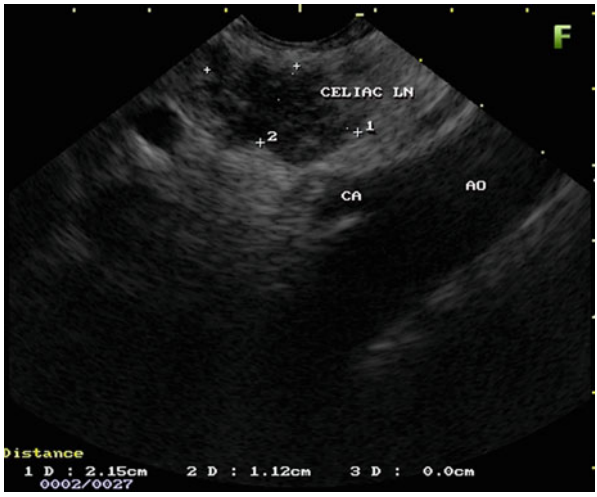

Fig. 9.23 An enlarged celiac node in Ca esophagus signifies M1a stage of disease

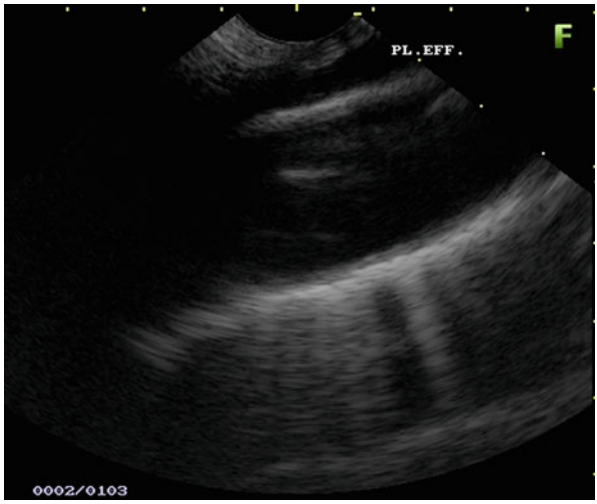

Fig. 9.24 Small pleural effusion seen on linear EUS in a patient with lung cancer

Up to 30% patients with esophageal cancer have obstructing tumors which do not permit passage of the endoscope thus precluding complete evaluation [17]. Strictures can be dilated to permit passage of the large diameter echoendoscope. Although perforation is a potential risk [18], serial dilatation is safe if performed meticulously using the 'rule of three' [17, 19].

Tumor reassessment after neoadjuvant chemotherapy and external beam radiation is necessary to confirm down-staging of disease. EUS has poor accuracy (25–29% for T stage, 48–52% for N stage) in this situation. Residual tumor and post radiation necrosis/fibrosis cannot be confidently differentiated on EUS [20–22].

9.9 Diseases of the Pleura and Pericardium

Effusions arising medially or in the interlobar fissure can be clearly seen by EUS (Fig. 9.24). Pleural nodules may be seen in patients with malignant pleural involvement. Small pericardial effusions can be identified on EUS.

References

1. Vassallo P, Wernecke K, Roos N et al (1992) Differentiation of benign from malignant superficial lymphadenopathy: the role of high-resolution US. Radiology 183(1):215–220
2. Vassallo P, Edel G, Roos N et al (1993) In-vitro high-resolution ultrasonography of benign and malignant lymph nodes. A sonographic-pathologic correlation. Invest Radiol 28(8):698–705
3. Bhutani MS, Hawes RH, Hoffman BJ (1997) A comparison of the accuracy of echo features during endoscopic ultrasound (EUS) and EUS-guided fine-needle aspiration for diagnosis of malignant lymph node invasion. Gastrointest Endosc 45(6):474–479. doi:S0016510797001314 [pii]
4. Catalano MF, Sivak MV Jr, Rice T et al (1994) Endosonographic features predictive of lymph node metastasis. Gastrointest Endosc 40(4):442–446. doi:S0016510794000696 [pii]

5. Toloza EM, Harpole L, McCrory DC (2003) Noninvasive staging of non-small cell lung cancer: a review of the current evidence. Chest 123(1 Suppl):137S–146S
6. Varadarajulu S, Hoffman BJ, Hawes RH et al (2004) EUS-guided FNA of lung masses adjacent to or abutting the esophagus after unrevealing CT-guided biopsy or bronchoscopy. Gastrointest Endosc 60(2):293–297. doi:S0016510704016803 [pii]
7. Macchiarini P, Ostertag H (2004) Uncommon primary mediastinal tumours. Lancet Oncol 5(2):107–118. doi:10.1016/S1470-2045(04)01385-3 S1470204504013853 [pii]
8. McGrath KM, Ballo MS, Jowell PS (2001) Schwannoma of the mediastinum diagnosed by EUS-guided fine needle aspiration. Gastrointest Endosc 53(3):362–365. doi:S0016510701794588 [pii]
9. Annema JT, Veselic M, Rabe KF (2005) EUS-guided FNA of centrally located lung tumours following a non-diagnostic bronchoscopy. Lung Cancer 48(3):357–361. doi:S0169-5002(04)00610-5 [pii] 10.1016/j.lungcan.2004.11.017; discussion 363–354
10. Varadarajulu S, Schmulewitz N, Wildi SM et al (2004) Accuracy of EUS in staging of T4 lung cancer. Gastrointest Endosc 59(3):345–348. doi:S0016510703025410 [pii]
11. Mountain CF, Dresler CM (1997) Regional lymph node classification for lung cancer staging. Chest 111(6):1718–1723. doi:10.1378/chest.111.6.1718
12. Eloubeidi MA, Seewald S, Tamhane A et al (2004) EUS-guided FNA of the left adrenal gland in patients with thoracic or GI malignancies. Gastrointest Endosc 59(6):627–633. doi:S0016510704002962 [pii]
13. Ringbaek TJ, Krasnik M, Clementsen P et al (2005) Transesophageal endoscopic ultrasound/fine-needle aspiration diagnosis of a malignant adrenal gland in a patient with non-small cell lung cancer and a negative CT scan. Lung Cancer 48(2):247–249. doi:S0169-5002(04)00547-1 [pii] 10.1016/j.lungcan.2004.10.019
14. Siemsen M, Svendsen LB, Knigge U et al (2003) A prospective randomized comparison of curved array and radial echoendoscopy in patients with esophageal cancer. Gastrointest Endosc 58(5):671–676. doi:S0016510703021345 [pii]
15. Singh P, Mukhopadhyay P, Bhatt B et al (2009) Endoscopic ultrasound versus CT scan for detection of the metastases to the liver: results of a prospective comparative study. J Clin Gastroenterol 43(4):367–373. doi:10.1097/MCG.0b013e318167b8cc00004836-200904000-00014 [pii]
16. Nguyen P, Feng JC, Chang KJ (1999) Endoscopic ultrasound (EUS) and EUS-guided fine-needle aspiration (FNA) of liver lesions. Gastrointest Endosc 50(3):357–361. doi:S0016-5107(99)00424-1 [pii]10.1053/ge.1999.v50.97208
17. Wallace MB, Hawes RH, Sahai AV et al (2000) Dilation of malignant esophageal stenosis to allow EUS guided fine-needle aspiration: safety and effect on patient management. Gastrointest Endosc 51(3):309–313. doi:S0016510700440678 [pii]
18. Van Dam J, Rice TW, Catalano MF et al (1993) High-grade malignant stricture is predictive of esophageal tumor stage. Risks of endosonographic evaluation. Cancer 71(10):2910–2917
19. Pfau PR, Ginsberg GG, Lew RJ et al (2000) Esophageal dilation for endosonographic evaluation of malignant esophageal strictures is safe and effective. Am J Gastroenterol 95(10):2813–2815. doi:S0002-9270(00)01101-1 [pii] 10.1111/j.1572-0241.2000.02309.x
20. Chak A, Canto MI, Cooper GS et al (2000) Endosonographic assessment of multimodality therapy predicts survival of esophageal carcinoma patients. Cancer 88(8):1788–1795. doi:10.1002/(SICI)1097-0142(20000415)88:8<1788::AID-CNCR5>3.0.CO;2-6 [pii]
21. Isenberg G, Chak A, Canto MI et al (1998) Endoscopic ultrasound in restaging of esophageal cancer after neoadjuvant chemoradiation. Gastrointest Endosc 48(2):158–163. doi:S0016510798002168 [pii]
22. Agarwal B, Swisher S, Ajani J et al (2004) Endoscopic ultrasound after preoperative chemoradiation can help identify patients who benefit maximally after surgical esophageal resection. Am J Gastroenterol 99(7):1258–1266. doi:10.1111/j.1572-0241.2004.30692.x AJG30692 [pii]

Linear EUS of the Stomach

10

Amol Bapaye and Advay Aher

10.1 Introduction

EUS is effective in evaluation of lesions of the gastric wall and the perigastric area. Although radial EUS or catheter probe is often preferred for assessment of gastric lesions, linear EUS provides optimum scanning of this region and also permits FNA at the same time.

10.2 Indications

- Staging of gastric cancer
- Evaluation and staging of gastric lymphoma
- Evaluation of sub mucosal lesions including FNA
- To perform FNA of perigastric lesions or lymph nodes

A. Bapaye, M.D. (M.S.) (✉)
Department of Digestive Diseases and Endoscopy,
Deenanath Mangeshkar Hospital and Research Center,
Erandwane, Pune 411004, Maharashtra, India
e-mail: amolbapaye@gmail.com

A. Aher,
Clinical Research Fellow, Department of Digestive Diseases and Endoscopy,
Deenanath Mangeshkar Hospital and Research Center,
Erandwane, Pune 411004, Maharashtra, India

K. Akahoshi, A. Bapaye (eds.), *Practical Handbook of Endoscopic Ultrasonography*,
DOI 10.1007/978-4-431-54014-4_10, © Springer 2012

10.3 Technique of Linear EUS in the Stomach

10.3.1 Basic EUS Scanning Technique

There are two techniques generally used to scan the gastric wall –

- Water immersion – This technique is used to scan the wall layers. Advance the endoscope up to the pylorus and aspirate air to decompress the stomach. Instill 200–400 mL of lukewarm, de-aerated water to distend the lumen. Turn off air and perform scanning in this submerged position.
- Balloon inflation – This technique is often used to evaluate small submucosal lesions. Localize the lesion on endoscopic vision and position the transducer over it. Inflate the balloon over the lesion, decompress the stomach and scan the lesion.

10.3.2 Salient Points of Technique

1. Commence scanning in antrum and withdraw endoscope slowly, rotating CW and CCW every few centimeters to see the entire circumference. Three hundred and sixty degree rotation is mandatory for complete examination.
2. Scanning perpendicular to the wall prevents overlap of layers.
3. Limiting peristalsis using anti-cholinergic agents provides a steady image.
4. Lower frequency 5 or 7.5 MHz is used to scan the perigastric area; higher frequency 10 or 12 MHz to scan the gastric wall layers.
5. Adjust ultrasound focal length to get the area of interest in focus.
6. Turning the patient supine may sometimes provide improved perpendicular scanning. In such a case, ensure airway protection as the patient may regurgitate the water instilled in the stomach causing laryngeal aspiration.

10.4 Linear EUS Anatomy of the Stomach

Linear EUS shows the standard five layer anatomy with alternating hyper and hypoechoic wall layers (Fig. 10.1). Layer thickness differs in various regions of the stomach; muscularis propria is thicker in the antrum than in the fundus or body.

The perigastric area must be searched for enlarged lymph nodes, especially in patients with gastric cancer or lymphoma. Celiac nodes are examined from the gastro-esophageal junction (Fig. 10.2). Other perigastric lymph nodes of significance are those in the region of the left gastric artery, right gastro-epiploic vessels, perigastric, periduodenal or peripancreatic and in the liver hilum.

Fig. 10.1 Linear EUS showing five layered structure of the gastric wall

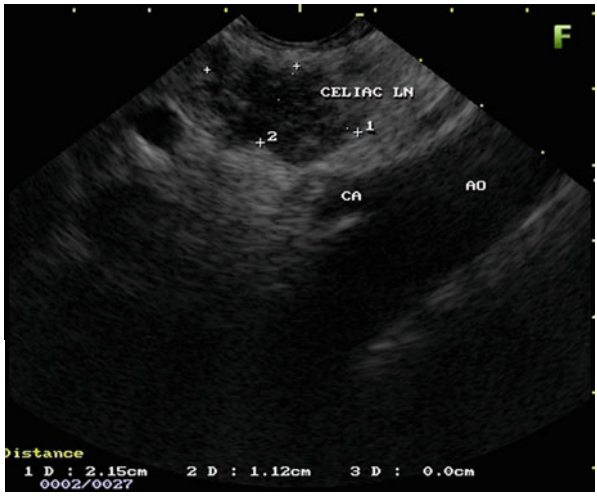

Fig. 10.2 Enlarged hypoechoic celiac lymph node seen from the gastro esophageal junction in a patient with esophageal cancer

10.5 EUS Evaluation of Gastric Lesions

10.5.1 Gastric Cancer

Gastric cancer is seen on EUS as a hypoechoic lesion originating in the mucosal layer and infiltrating into the deeper layers for a variable extent.

EUS is exceptionally effective in evaluating the T and N stage of gastric cancer [1]. Its role is to identify and differentiate lesions that can be treated by EMR or ESD (T1 lesions); and to differentiate T2 and T3 tumors (which primarily require surgery) from T4 lesions (requiring neoadjuvant chemotherapy and /or radiotherapy or palliative therapy). Radial EUS may provide greater detail about the exact depth of invasion in T1 and T2 lesions. On the other hand, a linear instrument can provide all the information required to take appropriate therapeutic decisions [2]. EUS is exceptionally useful in diagnosis of diffuse infiltrating gastric carcinoma (Linitis plastica). Enlarged perigastric lymph nodes indicate nodal metastasis and FNA can confirm malignant involvement.

10.5.1.1 Early T1 Gastric Cancer

Typical Gastroscopy and EUS Findings (Figs. 10.3 and 10.4)

1. Nodular or polypoid mucosal lesion
2. EUS shows involvement of first layer
3. SM (third) layer is free
4. Lymph node enlargement rare

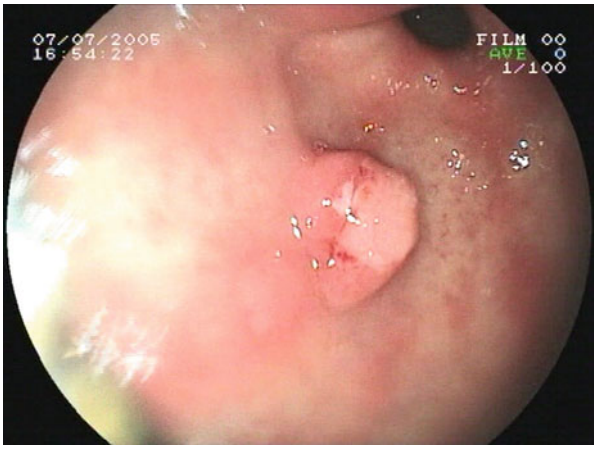

Fig. 10.3 Endoscopic image of T1 gastric cancer

Fig. 10.4 Linear EUS showing involvement of mucosal layer and free SM layer

10.5.1.2 T4 Gastric Cancer

Typical Gastroscopy and EUS Findings (Figs. 10.5 and 10.6)

1. Hypoechoic mass lesion involving all layers of stomach
2. Infiltration beyond serosa
3. Layer structure is not preserved in the area of tumor
4. Enlarged perigastric or celiac lymph nodes may be seen

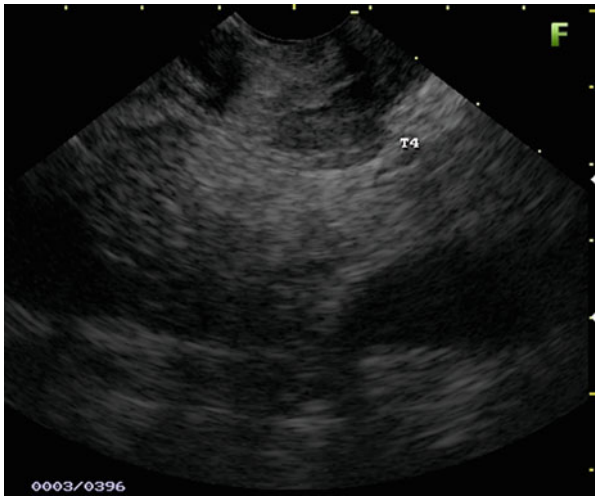

Fig. 10.5 Linear EUS showing T4 gastric cancer with breach of serosa

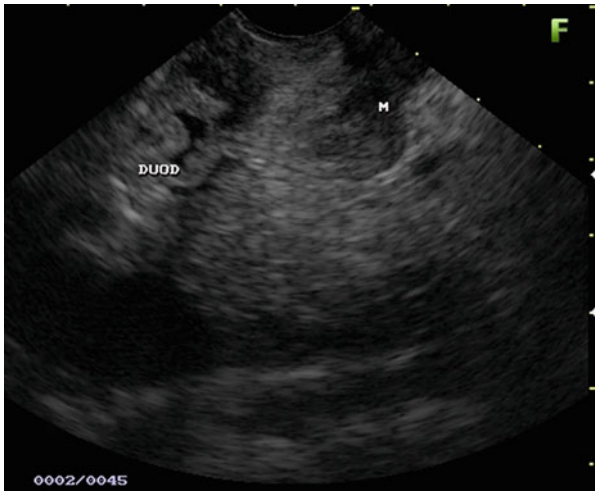

Fig. 10.6 Large T4 pyloric tumor with involvement of all layers. The duodenum is seen on the left of the screen and is free from the tumor

10.5.1.3 Diffuse Infiltrating Gastric Cancer (Linitis Plastica)

Typical Gastroscopy and EUS Findings (Figs. 10.7 and 10.8)

1. Diffuse mucosal thickening, breach or ulceration rarely seen
2. EUS shows diffuse thickening of the first and second layers
3. All five layers involved and loss of layer architecture in advanced disease
4. Perigastric lymph nodes may be present
5. Differential diagnosis is gastric lymphoma

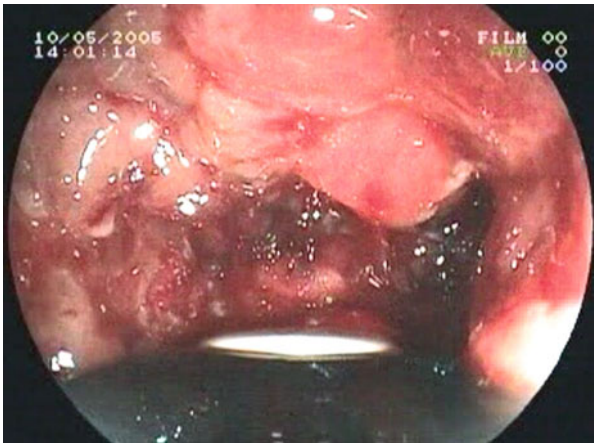

Fig. 10.7 Gastric mucosal nodularity and non distensibility seen on endoscopy

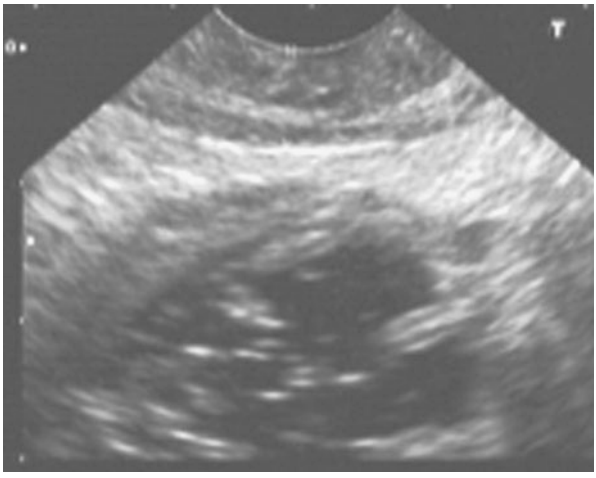

Fig. 10.8 Linear EUS showing diffuse thickening of the first and second layers of gastric wall in linitis plastic

10.5.2 Gastric Lymphoma

The gastrointestinal tract is the commonest extra nodal site for development of non Hodgkin's lymphoma (NHL). Mucosa associated lymphoid tissue (MALT) is a concept introduced to describe and differentiate these NHL's from other forms of the disease [3]. The stomach is the commonest organ to be affected by MALT lymphomas, although non MALT varieties are also known to occur.

Typical Gastroscopy and EUS Findings (Figs. 10.9 and 10.10)

1. Hypertrophic or edematous mucosal folds or diffuse thickening
2. EUS shows thickening of the second and third layers
3. Involvement of fourth and fifth layers or fusion of all layers with disease progression
4. Infiltration into adjacent organs in advanced disease
5. Perigastric enlarged lymph nodes?
6. Differential diagnosis is diffuse infiltrating gastric cancer

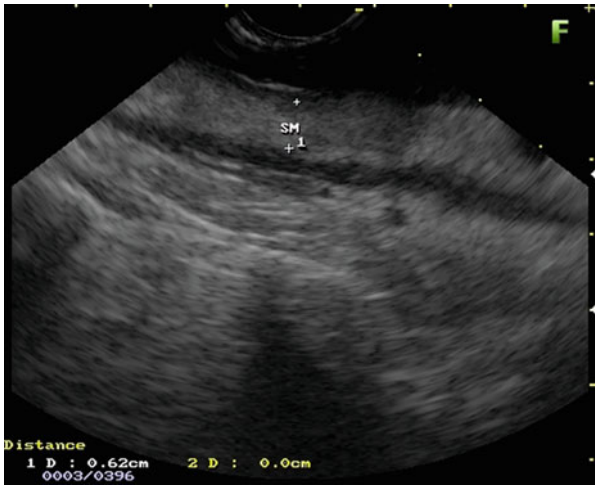

Fig. 10.9 Linear EUS showing thickening of the second and third layers of stomach in a case of gastric lymphoma

Fig. 10.10 Linear EUS showing a large gastric mass with obliteration of all layers. FNA revealed non Hodgkin's lymphoma

It is often difficult to differentiate between gastric lymphoma and diffuse infiltrating gastric cancer (Linitis plastica). In both conditions, overlying mucosa is often normal or only edematous. Ulceration is uncommon in early disease. Mucosal biopsies are positive in only 50% cases [4]. Gastric carcinoma produces more vertical growth through all the layers whereas lymphoma primarily shows horizontal extension in the second and third layers [5]. EUS guided FNA from the area of wall thickening can provide tissue diagnosis [6].

10.5.3 Submucosal Tumors (SMT)

SMT's in the stomach occur as in other areas of the gastrointestinal tract. EUS helps to characterize the lesion, identify the layer of origin, perform FNA and assess feasibility for endoscopic submucosal dissection. Commonest tumors in the stomach are leiomyoma, gastrointestinal stromal tumor (GIST), lipoma, carcinoid and ectopic pancreatic rest.

Salient Points for Linear EUS Examination of SMT's

- Identify layer of origin and/or involved layers
- Scan initially with 7.5 MHz and later using 10 or 12 MHz frequency
- Examine the lesion at three locations – proximal border, distal border and surface

10.5.3.1 Gastrointestinal Stromal Tumor (GIST)

Typical EUS Findings (Fig. 10.11)

1. Hypoechoic mass lesion in layer 4
2. Heterogeneous appearance with hyper and hypoechoic areas
3. Calcification may be seen
4. Layer structure may be disturbed in case of infiltration

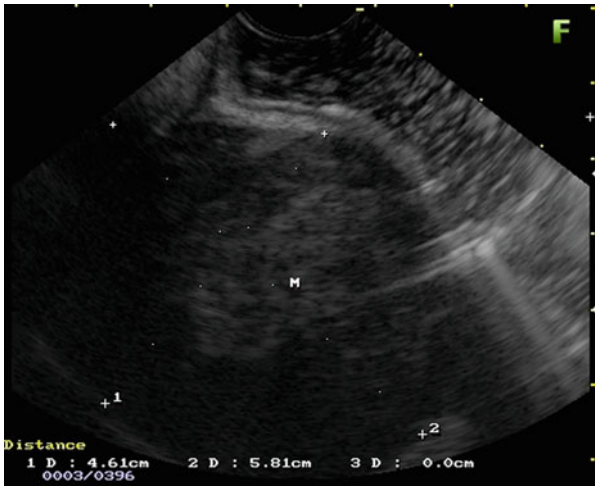

Fig. 10.11 Linear EUS showing large encapsulated tumor arising from fourth muscle layer – GIST

10.5.3.2 Leiomyoma

Typical EUS Findings

1. Well circumscribed hypoechoic mass in layers 2 or 4
2. Layer structure is well preserved

10.5.3.3 Ectopic Pancreas

Typical Gastroscopy and EUS Findings

1. Located in gastric antrum
2. Punctum usually seen on the mucosal surface
3. Heterogeneous hypoechoic lesion in submucosal layer

References

1. Sobin LH, Wittekind C (eds) (2002) TNM classification of malignant tumours. UICC (International Union against Cancer), 6th edn. Wiley, New York
2. Shimoyama S, Yasuda H, Hashimoto M et al (2004) Accuracy of linear-array EUS for preoperative staging of gastric cardia cancer. Gastrointest Endosc 60(1):50–55. doi:S0016510704013124 [pii]
3. Isaacson PG, Spencer J (1987) Malignant lymphoma of mucosa-associated lymphoid tissue. Histopathology 11(5):445–462
4. Andriulli A, Recchia S, De Angelis C et al (1990) Endoscopic ultrasonographic evaluation of patients with biopsy negative gastric linitis plastica. Gastrointest Endosc 36(6):611–615
5. Bolondi L, Casanova P, Caletti GC et al (1987) Primary gastric lymphoma versus gastric carcinoma: endoscopic US evaluation. Radiology 165(3):821–826
6. Vander Noot MR 3rd, Eloubeidi MA, Chen VK et al (2004) Diagnosis of gastrointestinal tract lesions by endoscopic ultrasound-guided fine-needle aspiration biopsy. Cancer 102(3):157–163. doi:10.1002/cncr.20360

Linear EUS of the Anorectum

11

Amol Bapaye and Advay Aher

11.1 Introduction

The utility of endorectal and endoanal ultrasound has evolved in the last few years [1]. Both radial and linear EUS are used for evaluation of anorectal diseases. Radial EUS is preferred for examination of anal canal whereas linear is preferred for rectal and para rectal examination and to perform interventions.

11.2 Indications for Anorectal Linear EUS

- T and N staging of rectal cancer
- To evaluate recurrence of rectal cancer during follow up
- To perform EUS-FNA of pararectal and pelvic tumors
- Evaluation of anal incontinence and other sphincter abnormalities
- Evaluation and treatment of perianal and pararectal disorders like abscess and fistula

A. Bapaye, M.D. (M.S.) (✉)
Department of Digestive Diseases and Endoscopy,
Deenanath Mangeshkar Hospital and Research Center,
Erandwane, Pune 411004, Maharashtra, India
e-mail: amolbapaye@gmail.com

A. Aher
Clinical Research Fellow, Department of Digestive Diseases and Endoscopy,
Deenanath Mangeshkar Hospital and Research Center,
Erandwane, Pune 411004, Maharashtra, India

K. Akahoshi, A. Bapaye (eds.), *Practical Handbook of Endoscopic Ultrasonography*,
DOI 10.1007/978-4-431-54014-4_11, © Springer 2012

11.3 Technique of Linear EUS in the Rectum

11.3.1 Patient Preparation and Sedation

1. We prefer to administer standard bowel preparation as for colonoscopy, although enema cleansing is considered adequate by some workers.
2. Sedation is rarely required as the echoendoscope is advanced only up to the recto sigmoid junction.
3. It is preferable to have a distended urinary bladder during anorectal EUS.
4. Antibiotic prophylaxis may be considered for patients undergoing trans-rectal EUS-FNA or other interventions.

11.3.2 Technique

1. Perform anorectal EUS usually in left lateral position. Some authors prefer prone position for female patients to prevent lateral displacement of anterior pelvic organs.
2. Digital examination is mandatory prior to endoscope insertion.
3. If you need to perform colonoscopy during the same session, defer it until EUS is completed so that insufflated air during colonoscopy does not interfere with the EUS examination.
4. Introduce the linear echoendoscope inside the rectum for about 10 cm. Turn the transducer anteriorly towards the pubic symphysis and record this as the reference 12 o'clock position. Gradually withdraw the endoscope while inspecting the layers of the rectum and the surrounding organs. As in other linear EUS procedures, CW and CCW rotation is important to ensure complete 360° examination.
5. The rectum shows a standard five layered wall architecture.
6. The inner circular muscle layer extends into the anal canal as the internal sphincter. This can be seen as a thick hypoechoic layer. Proximally, the internal sphincter is contiguous with the levator ani (Fig. 11.1). Outside the layer of the internal sphincter, the external anal sphincter can be seen as a bright hyperechoic layer just below the skin.
7. The urinary bladder (UB) is seen as an anechoic distended muscular bag anterior to the rectum. The bladder wall shows a three layered architecture (Fig. 11.2).
8. In males, follow the UB from cranial to caudal direction. The prostate is located at the lowermost tip of the UB and is seen as a globular hypoechoic encapsulated structure (Fig. 11.3). Seminal vesicles are seen as moustache shaped symmetrical organs at the lower border of the prostate on both sides of midline, and can be examined by CW and CCW rotation (Fig. 11.4).
9. In females, the vagina is seen as a three layered muscular organ between the rectum and the UB. Air in the lumen of the vagina is often seen as a bright streak (Fig. 11.5).

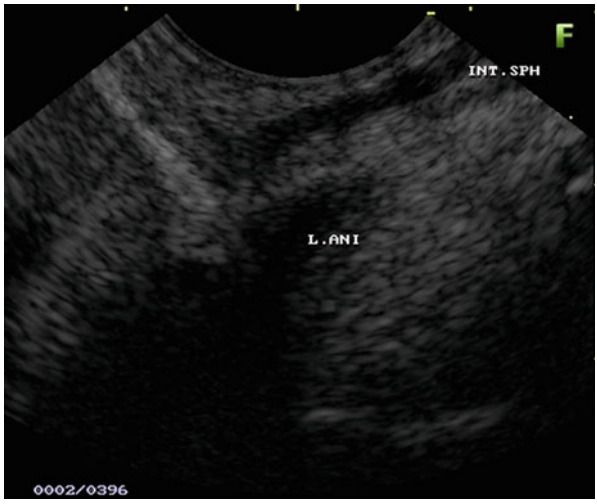

Fig. 11.1 Linear EUS showing internal sphincter being continued as levator ani

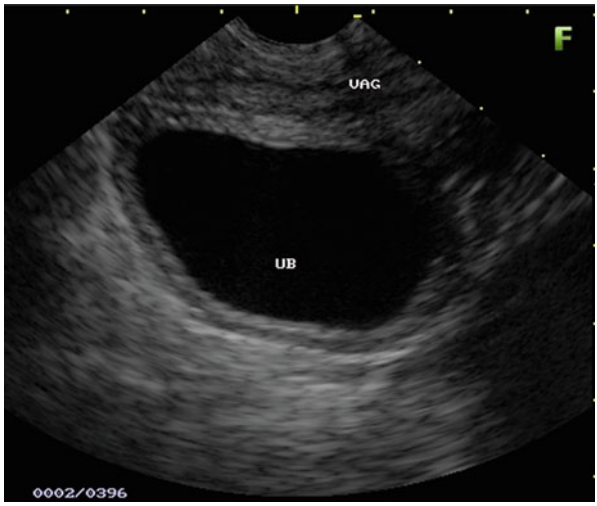

Fig. 11.2 Linear EUS showing urinary bladder with its three layered wall structure

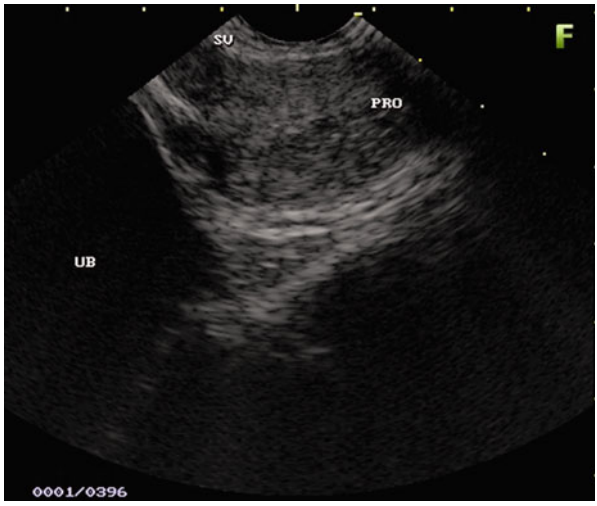

Fig. 11.3 Linear EUS showing prostate as a hypoechoic encapsulated structure

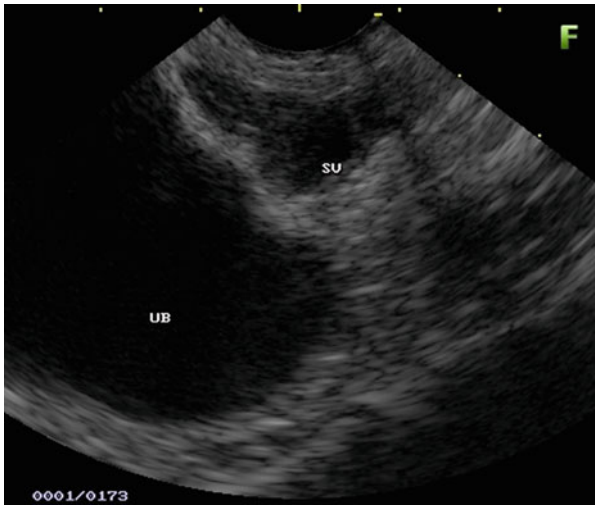

Fig. 11.4 Linear EUS showing seminal vesicle as a moustache shaped symmetrical structure on one side of midline

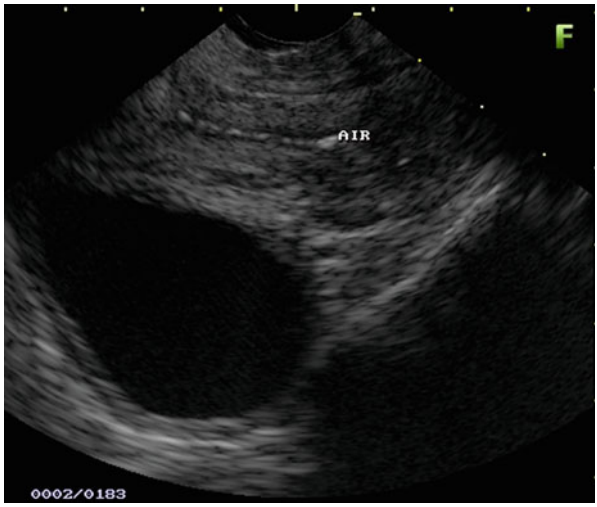

Fig. 11.5 Linear EUS showing vagina as a three layered muscular organ. A thin streak of air is seen in the lumen

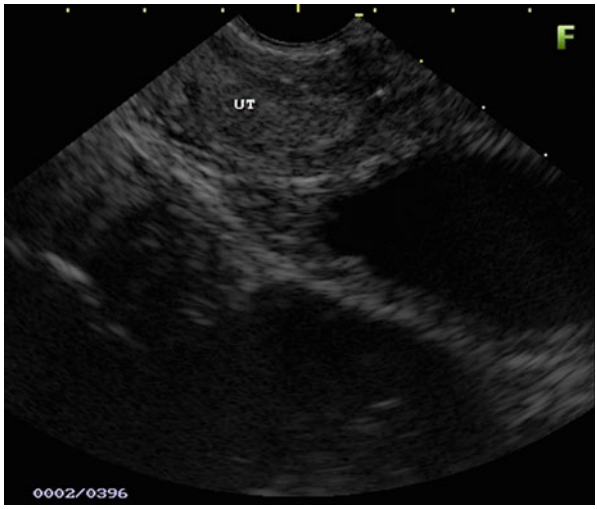

Fig. 11.6 Linear EUS showing pear shaped anteverted uterus

10. Proximal to the vagina (and just superior to the fundus of the UB), the pear shaped uterus is seen in anteverted or retroverted position (Fig. 11.6). The cervix is seen as a muscular structure between the vagina and uterus.
11. Rotate the endoscope CW or CCW to demonstrate the pararectal or ischiorectal space containing the hyperechoic perirectal fat tissue.
12. Rotate posteriorly to see the sacrum; further evaluation is rarely required.

11.4 EUS Staging of Rectal Cancer

Rectal carcinoma is seen as a hypoechoic mass lesion arising from the mucosal layer and infiltrating into the deeper layers for a variable extent.

EUS is effective in T and N staging of rectal cancer. It is used for preoperative staging as well as for follow up after neo-adjuvant chemotherapy and radiotherapy to assess response. When staging tumors using EUS, the stage is labeled with a prefix 'u' for ultrasound.

T Staging of Rectal Cancer (Figs. 11.7a, b and 11.8)

- uT_1 – extension up to layer III, layer IV intact, layer III intact
- uT_2 – extension up to layer III and IV, layer V intact
- uT_3 – All wall layers including layer V involved
- uT_4 – infiltration into surrounding organs – prostate, vagina, bladder or peritoneum

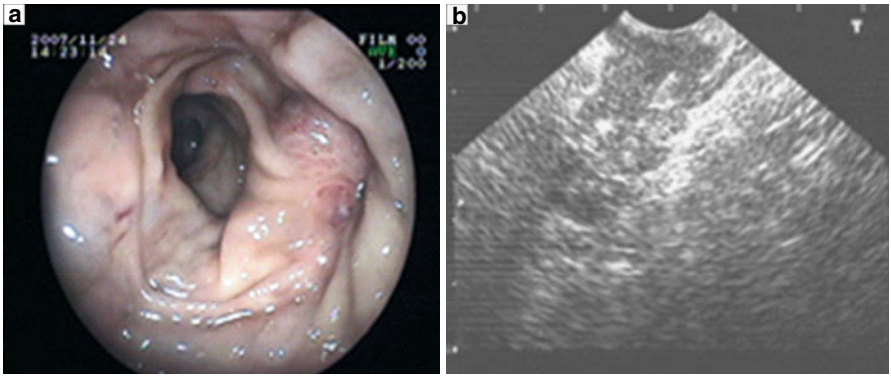

Fig. 11.7 Extraluminal recurrence of rectal cancer – (**a**) Endoscopic view showing mucosal nodularity, (**b**) Linear EUS shows a mass in the rectal wall

Fig. 11.8 T4 Ca rectum showing tumor extending in the para rectal space on linear EUS

EUS has 80–90% sensitivity for T staging of rectal cancer [2–5]. Perpendicular alignment to the rectal wall prevents overstaging. Prior biopsy may cause blurring of layers with resultant overstaging [6]. Pararectal lymph nodes seen on EUS usually denote N+ stage of disease as they are rarely inflammatory in nature. Lymph node characteristics on EUS aids differentiation and FNA can confirm the diagnosis [7]. Preoperative EUS staging can identify patients likely to benefit by neoadjuvant chemo-radiotherapy [8, 9]. EUS is reliable in diagnosis of post operative or post chemo-radiotherapy submucosal or pararectal recurrence.

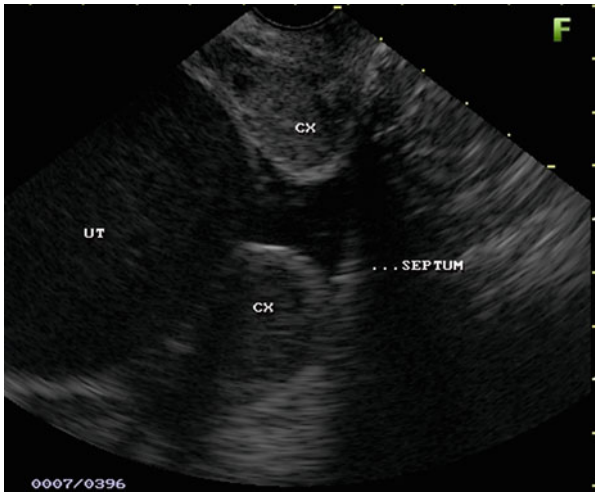

Fig. 11.9 Distended uterine cavity (hematometra) with a vaginal septum in a patient with congenital vaginal agenesis

11.5 Lesions of Pelvic Organs

EUS can evaluate tumors, anomalies and other lesions affecting pelvic organs – prostate, vagina, uterus and adnexa. Tumors appear as hypoechoic masses on EUS. Uterine conditions like hematometra can be diagnosed on EUS (Fig. 11.9).

11.6 Anal Sphincter Abnormalities

EUS is useful to detect anal sphincter abnormalities. Radial EUS is preferred as it provides circumferential imaging, but on occasions, linear EUS can also be used. During linear EUS, it is important to scan the anal sphincter anatomy with full 360° rotation by gently rotating the echoendoscope in small increments. Sphincter dehiscence is seen as a breach in continuity of the respective muscle layers.

References

1. Brugge WR (1998) Endoscopic ultrasonography: the current status. Gastroenterology 115(6):1577–1583. doi:S0016508598006222 [pii]
2. Akahoshi K, Kondoh A, Nagaie T et al (2000) Preoperative staging of rectal cancer using a 7.5 MHz front-loading US probe. Gastrointest Endosc 52(4):529–534. doi:doi:S0016510700116700 [pii]
3. Akasu T, Sugihara K, Moriya Y et al (1997) Limitations and pitfalls of transrectal ultrasonography for staging of rectal cancer. Dis Colon Rectum 40(10 Suppl):S10–S15

4. Sailer M, Leppert R, Bussen D et al (1997) Influence of tumor position on accuracy of endorectal ultrasound staging. Dis Colon Rectum 40(10):1180–1186
5. Kwok H, Bissett IP, Hill GL (2000) Preoperative staging of rectal cancer. Int J Colorectal Dis 15(1):9–20
6. Sailer M, Allgayer H, Dietrich CF (2006) Endoanal and endorectal sonography. In: Dietrich CF (ed) Endoscopic ultrasound an introductory manual and atlas, vol 1, 1st edn. Thieme, Stuttgart, pp 291–312
7. Giovannini M (1995) Endoscopic ultrasonography with a curved array transducer: normal echoanatomy of retroperitoneum. Gastrointest Endosc Clin N Am 5(3):523–528
8. Harewood GC, Wiersema MJ, Nelson H et al (2002) A prospective, blinded assessment of the impact of preoperative staging on the management of rectal cancer. Gastroenterology 123(1):24–32. doi:S0016508502000604 [pii]
9. Harewood GC, Wiersema MJ (2002) Cost-effectiveness of endoscopic ultrasonography in the evaluation of proximal rectal cancer. Am J Gastroenterol 97(4):874–882. doi:10.1111/j.1572-0241.2002.05603.x

Linear EUS of the Pancreas, Biliary Tract and Liver

12

Amol Bapaye and Advay Aher

12.1 Introduction

EUS offers excellent scanning views of the biliary-pancreatic region. Linear EUS can evaluate the biliary-pancreatic area with similar precision as that by radial EUS and in addition, allows FNA or other interventional procedures to be performed at the same time [1].

12.2 Indications

- Diagnosis and staging of mass lesions of the pancreas
- Diagnosis, evaluation and staging of tumors of the bile ducts, gall bladder and liver
- Evaluation of retroperitoneal masses and lymphadenopathy
- Diagnosis of biliary calculi and other causes of biliary obstruction
- Diagnosis and evaluation of chronic pancreatitis
- Evaluation of chronic intractable upper abdominal pain of suspected biliary-pancreatic etiology

A. Bapaye, M.D. (M.S.) (✉)
Department of Digestive Diseases and Endoscopy, Deenanath Mangeshkar Hospital and Research Center,
Erandwane, Pune 411004, Maharashtra, India
e-mail: amolbapaye@gmail.com

A. Aher
Clinical Research Fellow, Department of Digestive Diseases and Endoscopy, Deenanath Mangeshkar Hospital and Research Center,
Erandwane, Pune 411004, Maharashtra, India

K. Akahoshi, A. Bapaye (eds.), *Practical Handbook of Endoscopic Ultrasonography*,
DOI 10.1007/978-4-431-54014-4_12, © Springer 2012

12.3 Technique

12.3.1 Station Concept of EUS Examination

Biliary-pancreatic EUS is performed according to the station concept. There are four primary stations –

- Station 1 – Gastro-esophageal junction
- Station 2 – Duodenal bulb, pylorus and gastric antrum
- Station 3 – Descending duodenum adjacent to the papilla
- Station 4 – Horizontal duodenum beyond the papilla

Some operators label the deep duodenal station as station 1 and the gastro-esophageal junction as station 4.

12.3.2 Imaging from Station 1

Station 1 imaging begins with the echoendoscope positioned at 40 cm from the incisors at the gastro-esophageal junction. This may be confirmed by identification of the Z-line on the endoscopy view. Suction is applied to decompress the stomach. The balloon is inflated slightly if required to obtain good acoustic coupling with the mucosa. All important structures are seen at a distance of 40–45 cm.

A systematic EUS examination starts with the echoendoscope in the neutral position facing anteriorly. From this reference point, CW torque is applied in small increments with sequential visualization of the following structures –

1. Left lobe of liver – This is the first structure visualized and is seen close to the transducer. Familiarize yourself with the characteristic appearance of the liver parenchyma. Various tubular structures are seen within the parenchyma (Fig. 12.1).
2. The left hepatic vein (LHV) is seen as a tubular anechoic structure traversing from the left to right on the screen (Fig. 12.1). Doppler confirms blood flow within the vessel. By turning the endoscope CW, an elongated view of the LHV is seen. Advance the endoscope 2–3 cm to see the tip of the left lobe of liver.
3. Porta hepatis with portal vein (PV) and common bile duct (CBD) – on applying further CW torque, two parallel tubular anechoic structures come into view at the edge of the liver parenchyma. The structure nearer the transducer is the PV and the deeper is the CBD (confirm by applying Doppler) (Fig. 12.2). PV divides into right and left branches. The CBD is traced up to its bifurcation and the LHD is followed inside the left lobe for a considerable length. The right hepatic duct (RHD) goes deep inside the parenchyma and cannot be seen beyond the initial 2–3 cm. The left branch of the PV is seen deeper than the

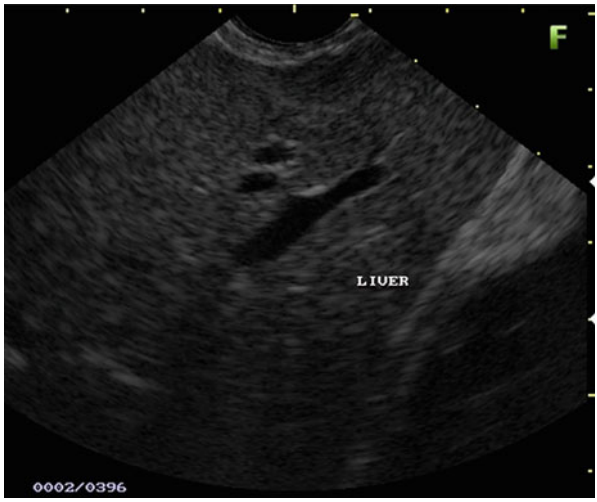

Fig. 12.1 Left lobe of liver seen at station 1 in neutral position. The LHV is seen within the liver parenchyma. Note the portal tracts with hyperechoic walls and the hepatic vein without hyperechoic walls

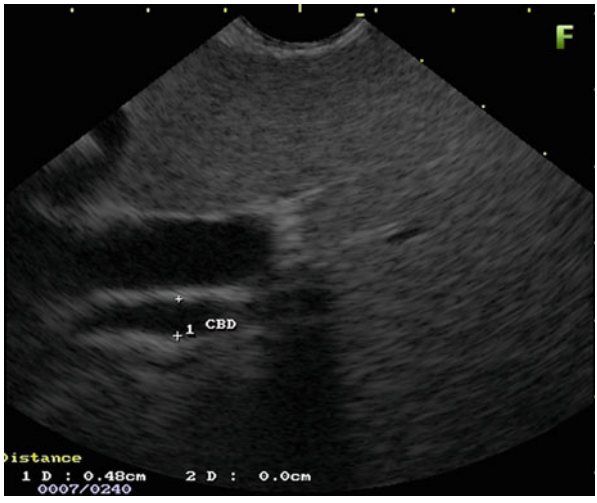

Fig. 12.2 Porta hepatis seen from station 1 on linear EUS. The PV is anterior to the CBD in this location

LHD inside the left lobe. The PV and CBD cross at the inferior border of the liver, the LHD crossing anterior to the right branch of the PV.

4. Inferior vena cava (IVC) and middle hepatic vein (MHV) – on further CW rotation, this large blood vessel can be seen traversing the entire length of the liver. The IVC is pulsatile due to transmitted pulsations from the right atrium. The LHV joins the IVC. The MHV is seen as a short vessel without bright walls on the right side of the screen joining the IVC (Fig. 12.3).
5. Abdominal aorta (AA) – On further rotation (we are 180° from our starting position), the AA comes into view as a large tubular vascular structure with bright hyperechoic walls. It traverses from the right to left, angling away from

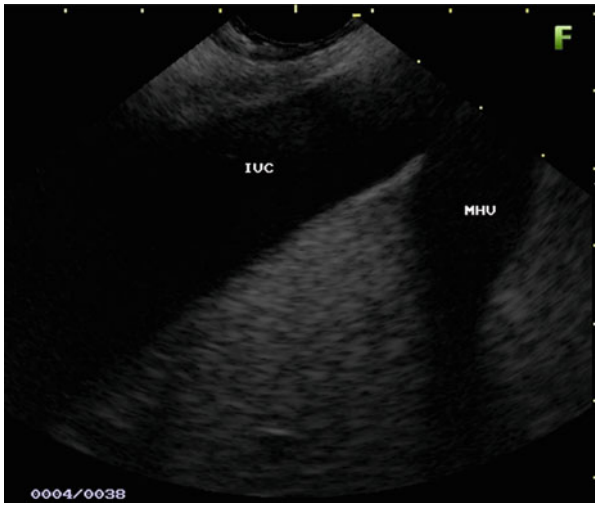

Fig. 12.3 Intra Hepatic IVC and MHV seen on Linear EUS from station 1 (GE junction)

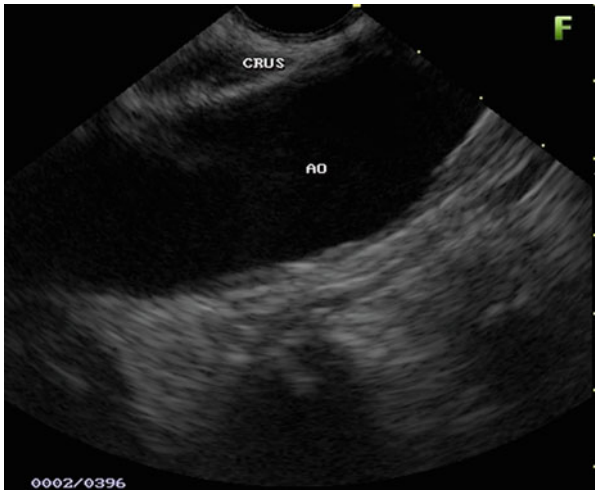

Fig. 12.4 Descending abdominal aorta seen by linear EUS. The left crus of the diaphragm is seen as hypoechoic crescent wrapped around the AA

the transducer (Fig. 12.4). AA is often seen as a double barreled structure due to reflection artifacts from the aorta onto the spine.

6. Celiac artery (CA) – The left diaphragmatic crus is seen as a hypoechoic crescent partly encircling the AA. The CA is the first branch of the AA caudal to this landmark and is located within a centimeter from the crus (Fig. 12.5). The CA immediately bifurcates into the splenic artery (SA) and the common hepatic artery (CHA). The SA runs to the left of the screen, whereas the CHA is seen for a short distance before it disappears from view.
7. Superior mesenteric artery (SMA) – The SMA arises within a centimeter of the origin of the CA. It runs downwards to the left of the screen (Fig. 12.5).

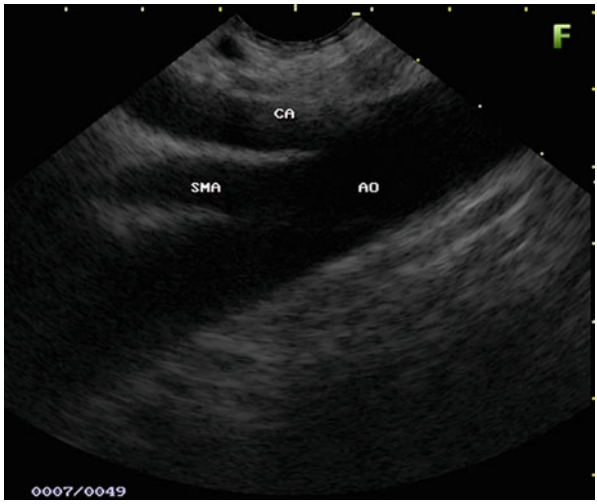

Fig. 12.5 Linear EUS from station 1 shows the take off of the CA and SMA from AA. The transducer faces dorsally in this position

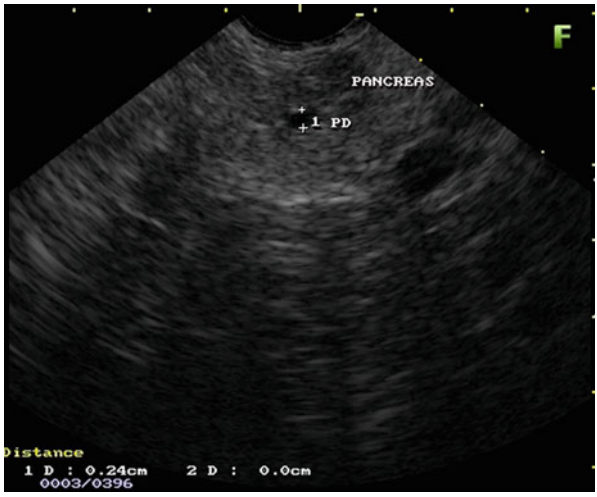

Fig. 12.6 Cross section of pancreatic body with MPD seen centrally within the parenchyma (Linear EUS image from station 1). The normal pancreas has a salt and pepper appearance on EUS

To see the other structures at station 1, a combination of torque, tip deflection and endoscope advancement/withdrawal are necessary.

8. Pancreatic body – The structure between the CA and the SMA is the pancreas. At the level of the CA, angle the endoscope slightly upwards with CW or CCW rotation to see the body of pancreas in cross section.
   On EUS, the pancreas has a salt and pepper echotexture (Fig. 12.6). The main pancreatic duct (MPD) is seen in cross section as a small hypoechoic structure within the parenchyma. The splenic vessels are seen at the left border of the pancreatic body on the screen in cross section. The SA is nearer the transducer than the SV (Fig. 12.7). Trace the tortuous course of the SA along the superior

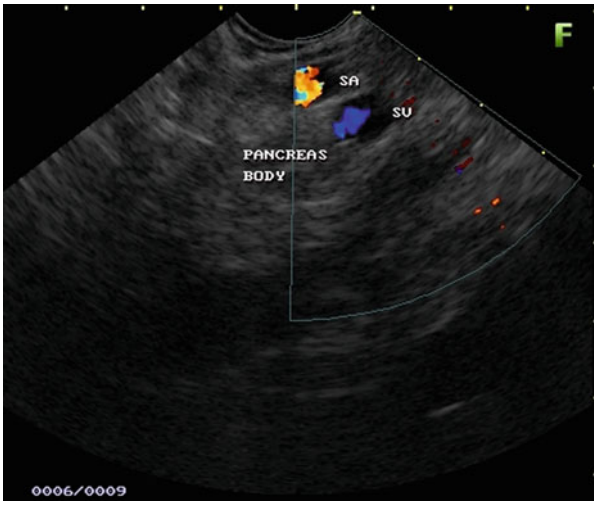

Fig. 12.7 EUS image from station 1 showing pancreatic body in cross section. The SA and SV are seen at the left border of pancreatic body. The SA is closer to the transducer than the SV

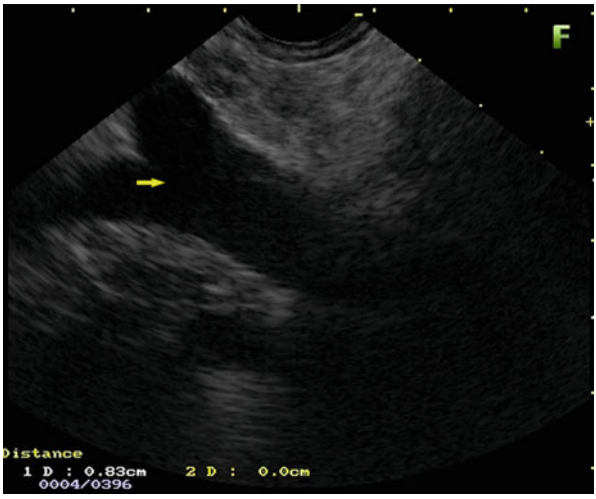

Fig. 12.8 SPC (*arrow*) seen from station 1 on linear EUS. The neck of pancreas lies anterior to the SPC

border of the pancreas. Look for the left renal vein (LRV) deep to the SV in longitudinal section.

From this position, withdrawal with CW rotation scans the body and tail, pushing in with CCW rotation shows the genu and head area.

9. Spleno-portal confluence (SPC) – Keeping the pancreatic body in view advance the endoscope slightly further, rotate CW and angle the tip upwards to see the SPC. The SV joins the superior mesenteric vein (SMV) to form the PV. The part of the pancreas between the transducer and the SMV is the neck of pancreas (Fig. 12.8).
10. Left kidney (LK) – On further rotating the endoscope CW at this level, the LK comes into view. Identify the renal hilum with the vessels (Fig. 12.9).

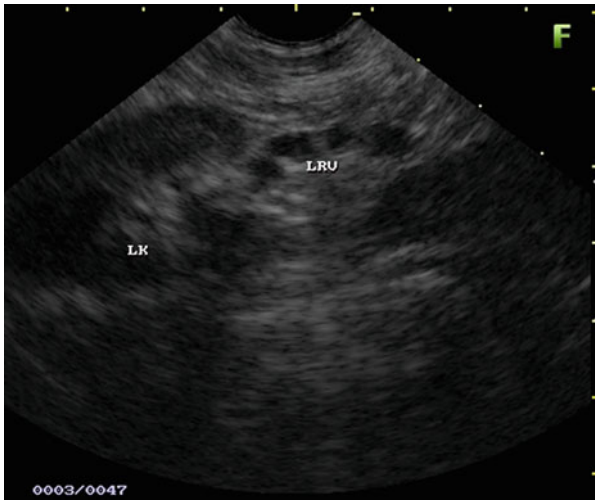

Fig. 12.9 The LK with the LRV at the hilum seen from station 1. The endoscope is upturned with CW rotation

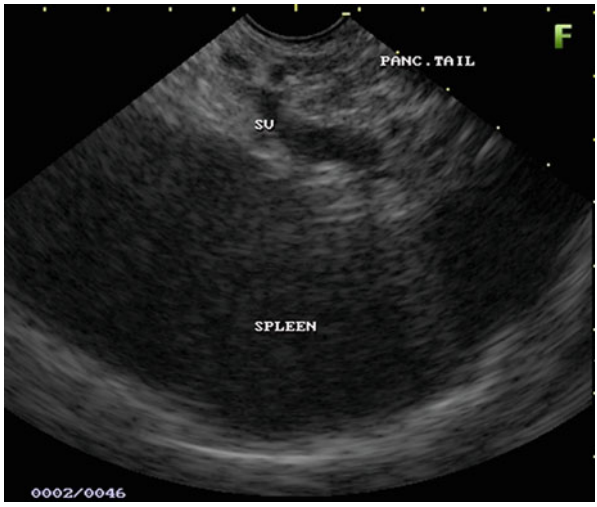

Fig. 12.10 Linear EUS at station 1 showing the spleen, splenic hilum and pancreatic tail

11. Spleen – Angle the tip upwards and pull back the endoscope to see the spleen. Visualize the splenic hilum with the splenic vessels and the pancreatic tail (Fig. 12.10). Minor scope tip deflections along with rotation are necessary to obtain good quality views.
12. Left adrenal gland – Slight CCW rotation from this point brings the AA partly in view on the right of the screen, with the upper pole of the LK on the left. The left adrenal gland is seen in this position, closer to the gastric wall and the AA than to the LK. It is seen as a characteristic sea gull shaped hypoechoic structure (Fig. 12.11).

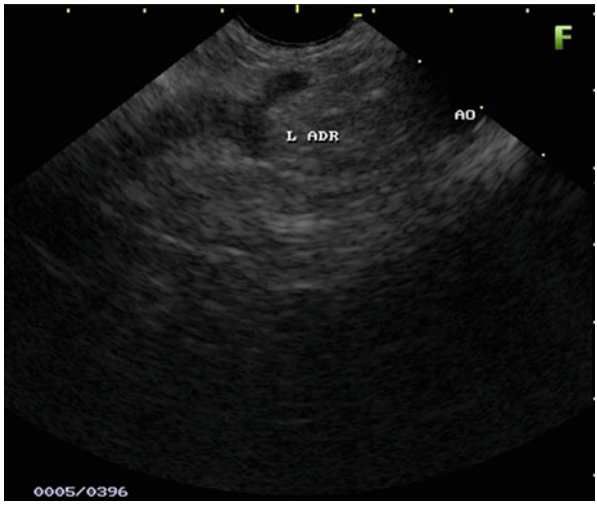

Fig. 12.11 Left adrenal gland (LAG) seen on linear EUS from station 1. LAG lies closer to the stomach and AA than the LK. The best views of the LAG are seen when the AA is partly in view and the LK disappearing from the screen

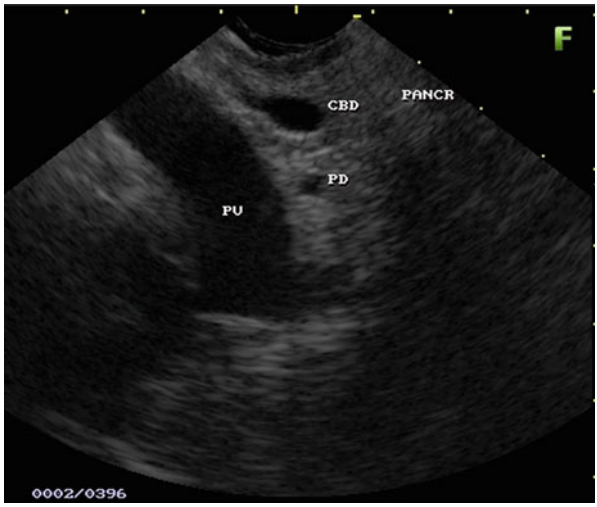

Fig. 12.12 EUS image from station 2 showing head of pancreas in cross section with central MPD, supra-pancreatic CBD on the left of the screen close to the transducer and PV angling downwards

Straighten the endoscope tip and rotate the scope back to the neutral position. This completes station 1 examination.

12.3.3 Imaging from Station 2

Advance the endoscope into the duodenal bulb in long loop position. Apply suction and wedge the endoscope tip against the duodenal wall at the inferior duodenal angle. Inflate the balloon to achieve good acoustic coupling. Identify the following structures – (Fig. 12.12).

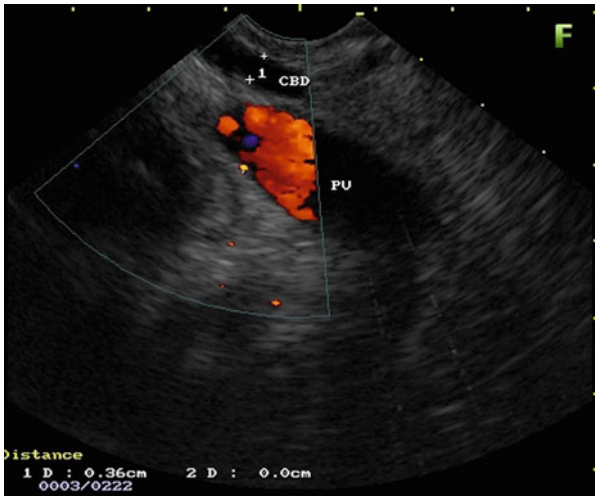

Fig. 12.13 On clockwise rotation, the CBD is seen to enter the pancreatic head and the PV is seen to traverse behind the pancreas

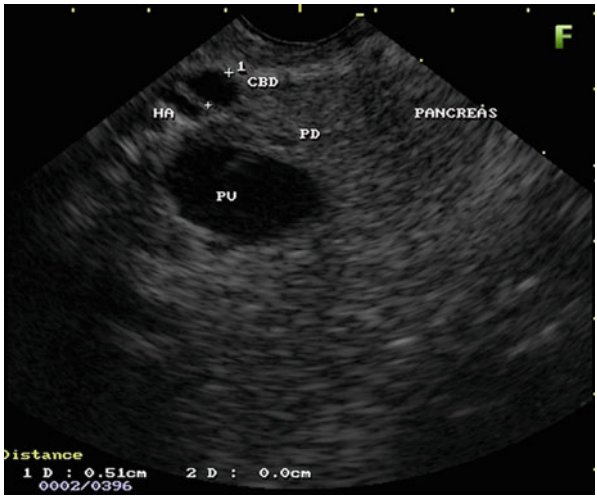

Fig. 12.14 Station 2 EUS imaging of the pancreatic head in cross section with surrounding structures. The MPD is seen within the pancreatic parenchyma. HA runs between the CBD and the PV towards the left of the screen

1. Pancreatic head in cross section and MPD within the parenchyma.
2. Supra-pancreatic CBD in longitudinal section to left of the screen near the duodenal wall (Seen as an anechoic structure without color flow on Doppler).
3. PV in oblique longitudinal section deep to the CBD, traversing behind the pancreas from right to left and angling downwards.
4. The IVC deep to the PV at the bottom of the screen.
   On CW rotation from this position
5. Gradually elongating views of the CBD are seen as it enters the pancreas. The CBD can be traced almost up to the ampulla (Fig. 12.13).
6. The CHA is seen adjacent to the CBD and close to the transducer. It bifurcates into the hepatic artery (HA) and the gastro-duodenal artery (GDA) (Fig. 12.14).

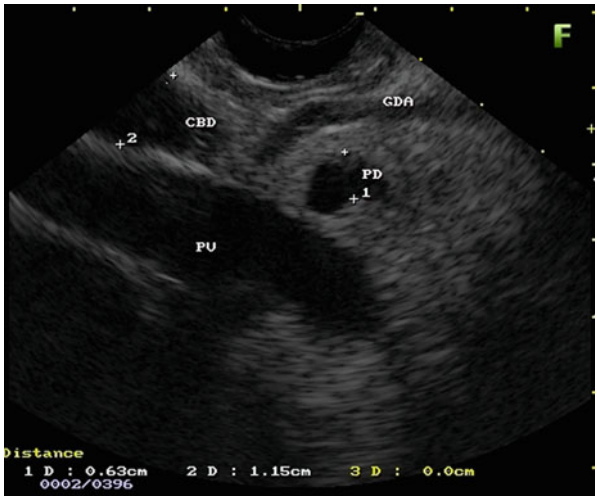

Fig. 12.15 EUS image from station 2 shows the pancreas head in cross section. The GDA runs between the pancreas and the duodenum towards the right of the screen. The pancreatic duct (MPD) appears dilated

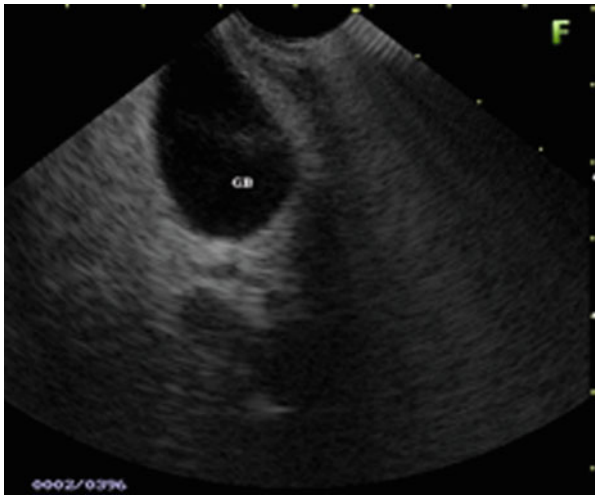

Fig. 12.16 Linear EUS showing GB from station 2

The GDA traverses to the right of the screen between the CBD and the pancreas (Fig. 12.15).

On CCW rotation from the base position –

7. The right lobe of liver is partially visualized.
8. The CBD and PV can be seen up to the porta hepatis.
9. The gall bladder (GB) is seen along the inferior border of liver. The position of the GB is variable; it may be visualized from the duodenal bulb or from the gastric antrum. It appears as a large balloon shaped anechoic structure (Fig. 12.16).

Important Tip
During Station 2 examination, the endoscope is in a long loop during duodenal intubation, but is in short loop while withdrawing from the ampulla. Different views may be available with either position, and it is necessary to perform both maneuvers to complete the examination.

12.3.4 Imaging from Stations 3 and 4

From station 2 position, withdraw and shorten the echoendoscope as when performing side viewing duodenoscopy to advance it beyond the papilla to the inferior duodenal angle. Angle the endoscope tip slightly upwards for good acoustic coupling. Gentle rotational movements in CW and CCW direction are required to scan the entire pancreatic head and uncinate process. Identify the following structures –

1. AA in longitudinal section. It is seen as a longitudinal vascular structure angling downwards from the left to right of the screen (Fig. 12.17).
2. On rotating the endoscope slightly CW, the IVC is seen parallel to the AA. The right renal vein (RRV) and upper pole of the right kidney (RK) is seen adjacent to the IVC. By following the IVC cranially the right adrenal gland can be located.
3. Uncinate process (UP) of pancreas – Keeping the AA in view, withdraw the endoscope, maintaining upward deflection of the tip. The aorta is seen to fall

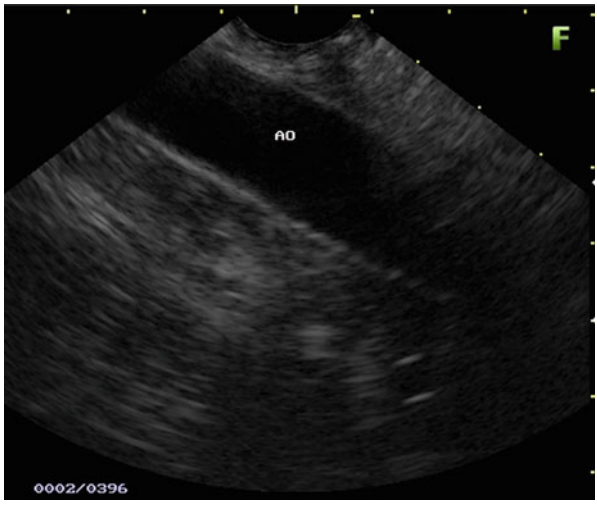

Fig. 12.17 The abdominal aorta seen from station 4 in the horizontal duodenum. AA is the first structure identified from this location

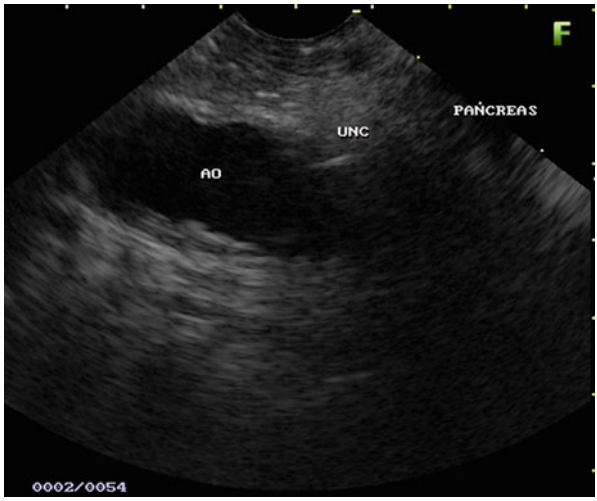

Fig. 12.18 Linear EUS showing normal uncinate process from station 4

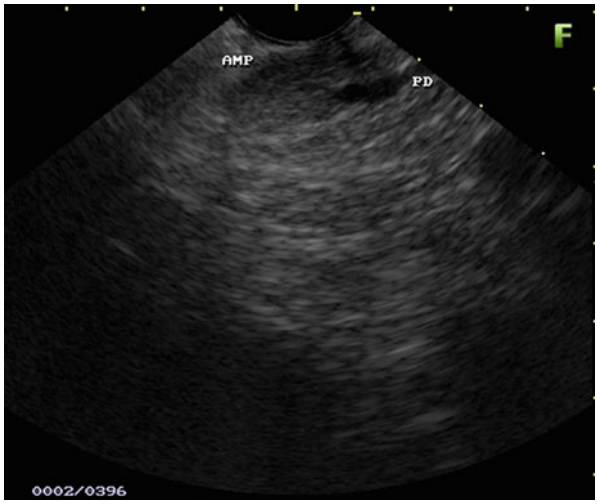

Fig. 12.19 Linear EUS image from station 3 showing normal hypoechoic ampulla with a short length of MPD

away from the transducer and the uncinate process is seen. The UP is hyperechoic as compared to the rest of the pancreas (Fig. 12.18).

4. Ampulla of Vater – Keep withdrawing the endoscope to reach the ampulla. This is seen as a small hypoechoic structure easily differentiated from pancreatic tissue (Fig. 12.19). Ampulla can also be identified endoscopically and then scanned by EUS. The normal ampullary size on EUS is 0.5–1 cm.
   To scan the layers of the ampulla, water must be instilled into the duodenum and peristalsis must be abolished. Never compress the ampulla with the endoscope tip or balloon; it tends to distort the images.

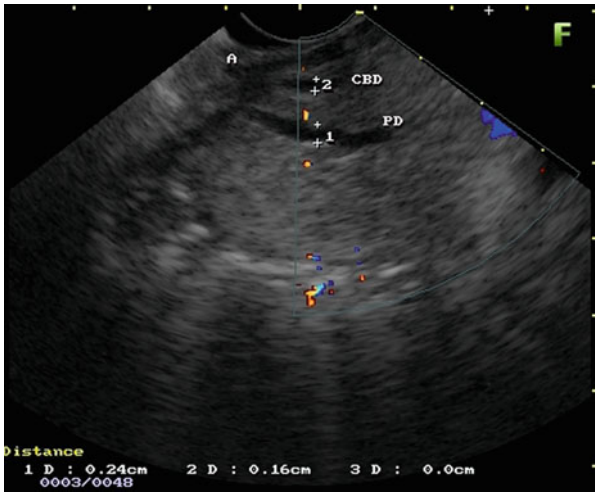

Fig. 12.20 The ampulla appears as a small hypoechoic structure on EUS. The CBD and MPD can be seen to converge on the ampulla

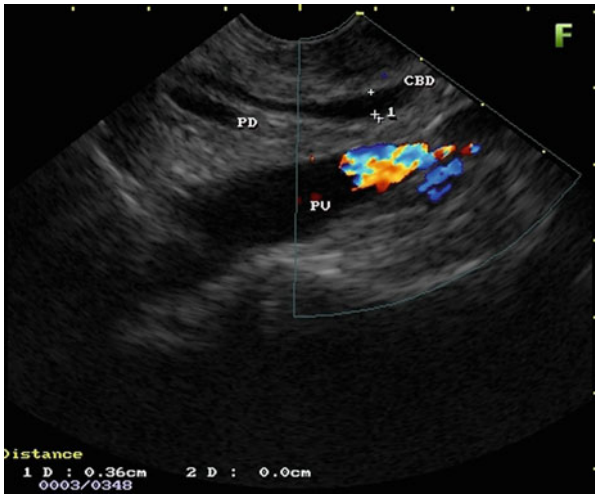

Fig. 12.21 Full length CBD seen from station 3. The transducer is positioned just proximal to the papilla. MPD runs parallel and in a deeper plane than CBD. The SMV and SPC are situated deep to the pancreas

5. CBD and MPD – Identify the CBD and MPD as they converge at the ampulla from right to left. The CBD is closer to the transducer and has well formed walls; the MPD is deeper and shows ramifications (Fig. 12.20). To visualize the CBD and PD, orient the endoscope parallel to the ampulla.
6. The pancreatic head is seen deep to the ampulla.
7. The SMV and SMA are seen deep to the pancreas. The SMV is closer to the transducer than the SMA (Fig. 12.21). Trace the SMV to locate the SPC and then follow the PV up to the porta hepatis.

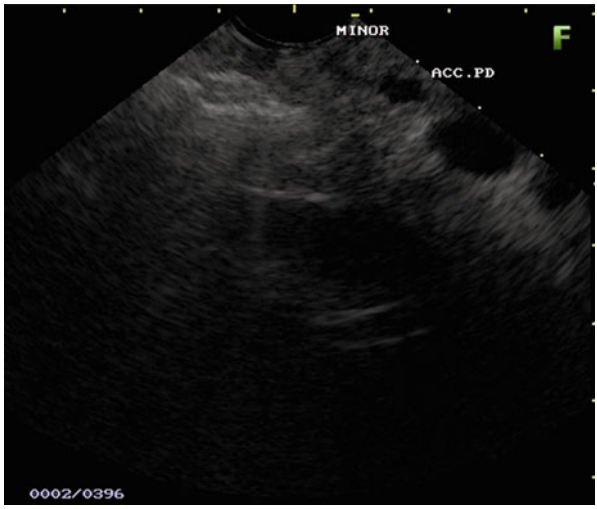

Fig. 12.22 Accessory pancreatic duct opening at the minor papilla seen on linear EUS. The duct shows irregular margins suggestive of early chronic pancreatitis. EUS image taken from a supra-ampullary position

8. Follow the CBD up to the porta hepatis. The cystic duct may be seen inserting into the CBD.
9. Trace the MPD into the pancreas. The accessory pancreatic duct and the minor papilla may be seen in patients with pancreas divisum (Fig. 12.22).
   This completes examination at Stations 3 and 4.

12.4 EUS Evaluation of Pancreatic Diseases

12.4.1 Chronic Pancreatitis (CP)

EUS is effective in evaluation of chronic pancreatitis including early parenchymal disease and may be superior to trans-abdominal ultrasound and CT scan. Secretin enhanced ERCP has been the conventional gold standard to diagnose CP [2], but is invasive and may induce pancreatitis. Secretin enhanced MRCP although non invasive, can identify duct abnormalities but lacks the ability to evaluate parenchymal changes seen in early disease.

12.4.1.1 Diagnosis

Effective diagnosis of early CP can be made using a scoring system of nine equally weighted EUS criteria [3] (Table 12.1, Figs. 12.23, 12.24, 12.25, and 12.26). The accuracy of this scoring system has been validated in multiple studies using ERCP [4–6] or histopathology [7, 8] as reference standards. CP is confirmed if >5 criteria are present and is ruled out if <2 are seen [4]. EUS has a tendency to over diagnose CP. A recent Rosemont classification [9] attempts to resolve this problem but yet awaits universal acceptance [10].

Table 12.1 EUS criteria for diagnosis of chronic pancreatitis

Parenchymal criteria	Ductal criteria
Hyperechoic foci	MPD calculi
Hyperechoic strands	Dilated MPD
Lobularity	Irregularity of MPD contour
Cyst formation	Dilated side branches
	Hyperechoic duct margins

Fig. 12.23 Hyperechoic foci in the pancreatic parenchyma

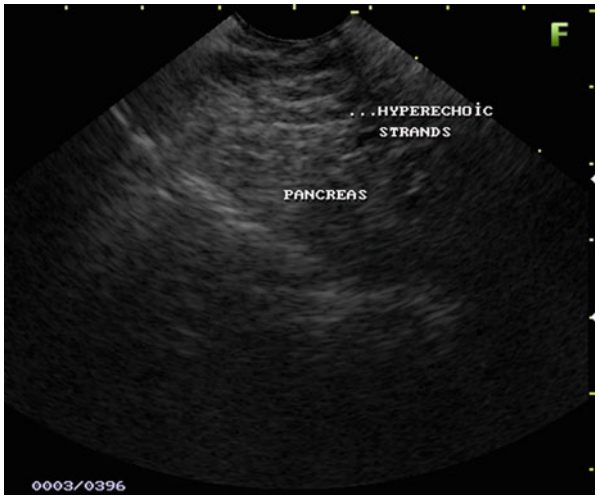

Fig. 12.24 Hyperechoic strands on EUS may signify early chronic pancreatitis

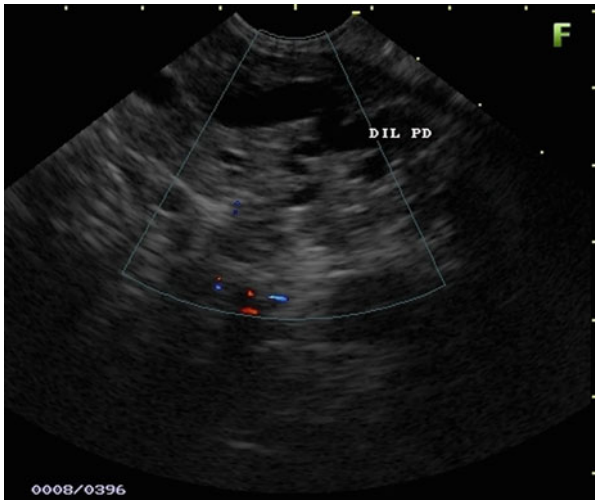

Fig. 12.25 Linear EUS showing dilated MPD with side branch dilatation

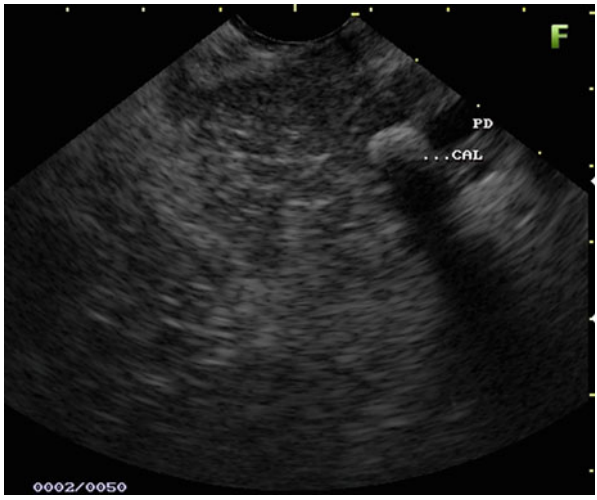

Fig. 12.26 Linear EUS showing an MPD calculus with posterior acoustic shadowing

12.4.1.2 Etiology

EUS can provide etiological information in patients with obstructive CP or idiopathic recurrent acute pancreatitis (RAP) [11]. Obstructive ductal calculi or calcification, pancreatic duct tumors, intraductal papillary mucinous neoplasms or ampullary tumors can be diagnosed by EUS [11–13] (Figs. 12.27 and 12.28).

Linear EUS can reliably exclude pancreas divisum [14]. The technique is to follow the MPD from the major papilla to the body of pancreas and/or note the duct

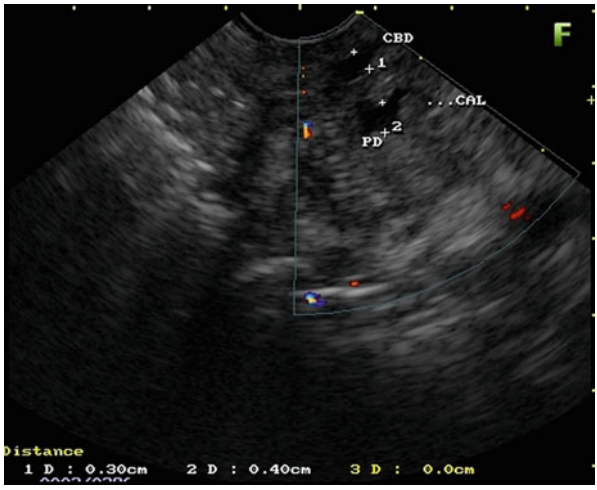

Fig. 12.27 Linear EUS showing pancreatic duct calculi

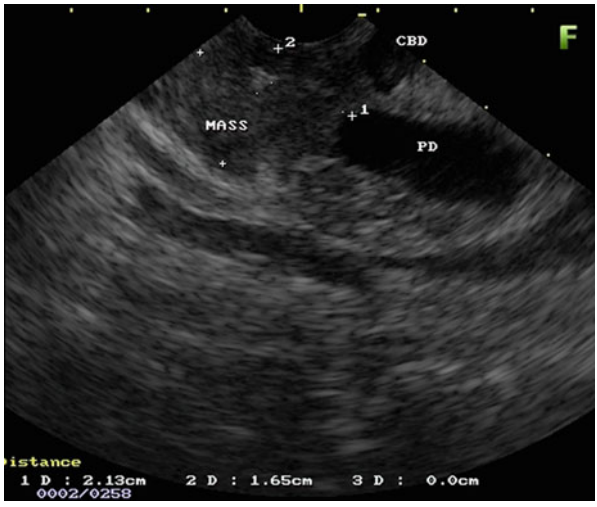

Fig. 12.28 Linear EUS showing an ampullary tumor

crossing over from the ventral to the dorsal pancreas (Fig. 12.22). Gall stones, CBD stones or gall bladder microlithiasis/sludge may be seen in patients with RAP [11–13] (Figs. 12.29 and 12.30).

12.4.1.3 Selection of Patients for Appropriate Therapy

EUS may avoid unnecessary diagnostic ERCP in patients with CP [15] and can identify patients who may benefit by pancreatic endotherapy – pancreas divisum, biliary or pancreatic duct calculi, strictures or cysts. EUS helps to differentiate

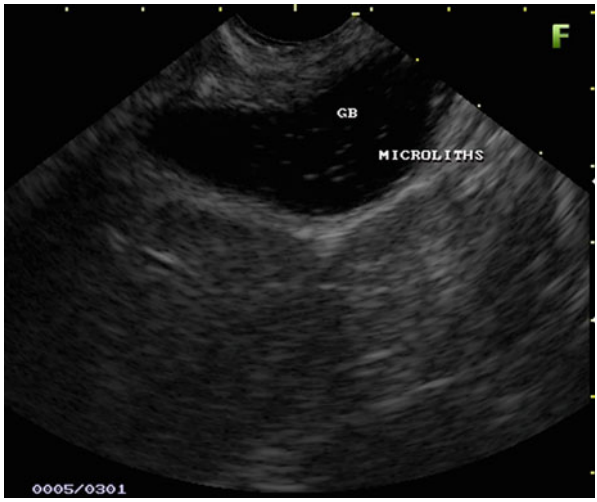

Fig. 12.29 Linear EUS showing gall bladder microliths. The gall bladder is typically well distended and has normal wall thickness

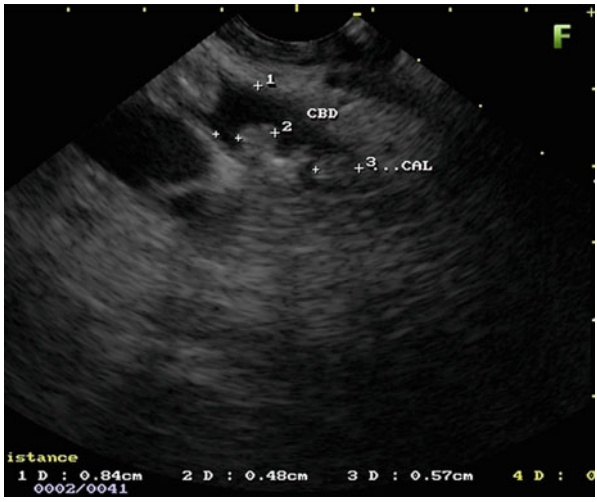

Fig. 12.30 Linear EUS showing soft stones/sludge balls in the CBD without posterior acoustic shadow

pseudocysts from cystic lesions of the pancreas and pseudoaneurysms (Discussed further in Sect. 12.4.4 and Chap. 16). EUS guided pancreatic endotherapy may be considered in patients when ERCP guided therapy fails (Chap. 19).

12.4.1.4 Diagnosis of Malignancy in CP

Inflammatory mass lesions may occur in patients with CP. These must be differentiated from adenocarcinoma. Although EUS has limited efficacy in this regard, accuracy can be improved by addition of contrast enhanced EUS and fine needle aspiration (FNA) (Refer to Chap. 16).

12.4.2 Autoimmune Pancreatitis (AIP)

AIP is a more recently recognized clinical entity of CP and often mimics a solid pancreatic mass lesion [16].

Typical EUS Findings [17, 18]

1. Diffuse hypoechoic pancreatic enlargement (sausage shaped gland) or a focal hypoechoic head mass
2. Irregular narrow MPD with hyperechoic walls
3. Distal CBD stricture with concentric wall thickening is common
4. Pseudocysts or fluid collections not common
5. Other biochemical parameters of autoimmune disease rarely diagnostic

Diagnosis can be confirmed by testing serum IgG4 levels (elevated in up to 85% patients) and may be confirmed by EUS guided trucut biopsies (using 19G Quickcore™, stain positive on IgG4 immuno-histochemistry) [19].

12.4.3 Pancreatic Tumors

12.4.3.1 Pancreatic Adenocarcinoma

Adenocarcinoma is the commonest occurring tumor in the pancreas. EUS has high sensitivity and specificity to diagnose pancreatic cancer, especially for lesions <2 cm in size [20, 21].

Typical EUS Findings (Figs. 12.31 and 12.32)

1. Focal hypoechoic mass in pancreas
2. Small lesions <2 cm – generally well circumscribed and homogeneous
3. Larger lesions are inhomogeneous, have poorly defined margins, and show areas of fibrosis. Anechoic areas within the tumor represent necrosis
4. Calcification within the tumor is rare unless the tumor has developed on the background of underlying chronic pancreatitis
5. The pancreatic duct often shows upstream dilatation. This dilatation is uniform (as against that in chronic pancreatitis, where an irregular duct wall is seen). Following a dilated pancreatic duct from the body to the head can often locate a small tumor
6. Surrounding pancreatic tissue is usually normal in appearance (unless there is underlying chronic pancreatitis)

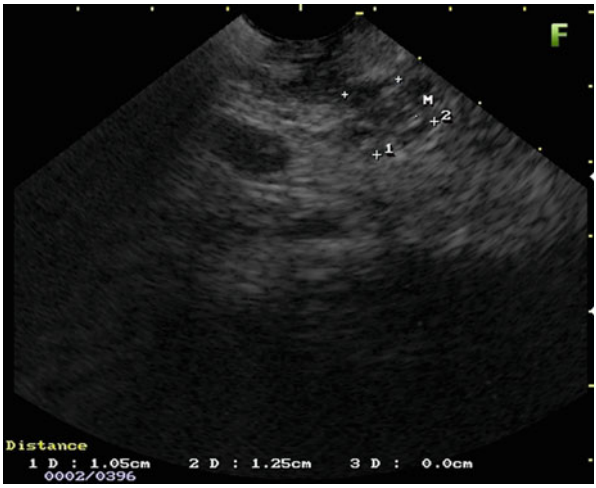

Fig. 12.31 Small mass in the pancreatic body diagnosed on linear EUS

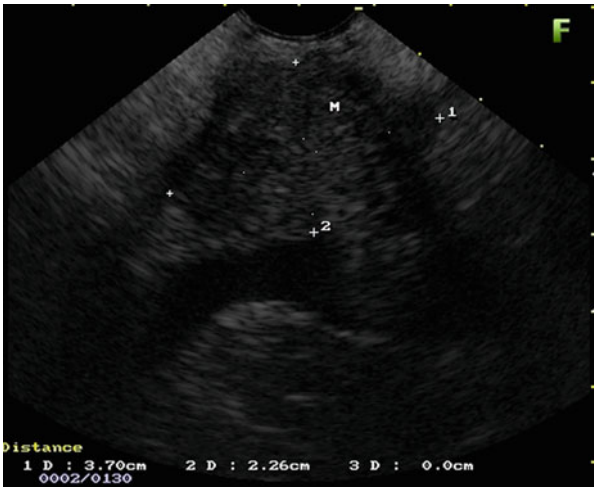

Fig. 12.32 Homogenous hypoechoic mass seen in the pancreas on linear EUS

12.4.3.2 Pancreatic Neuroendocrine Tumors (PNET's)

1. PNET's comprise about 10% of all pancreatic tumors. They are of two types – functional (fPNET) – 70–85% and non functional (nfPNET) – 15–30%, which depends upon whether the tumor does or does not secrete tumor hormones causing typical clinical syndromes. Insulinomas and gastrinomas are the two common fPNET's of clinical relevance. EUS is the most sensitive imaging modality for PNET's (Sensitivity 77–94%). EUS-FNA is accurate for diagnosis of tiny PNET's in up to 90% patients [22].

Typical EUS Findings (Fig. 12.33)

1. Tiny, discreet, encapsulated, hypoechoic mass lesions, often along the anterior or posterior surface of the pancreas
2. High vascularity on color Doppler
3. Large tumors show presence of cystic and necrotic areas within
4. Differentiation between benign or malignant tumors is difficult on EUS or surgical pathology. Presence of metastases or their absence on prolonged follow up is the only confirmation of its malignant potential

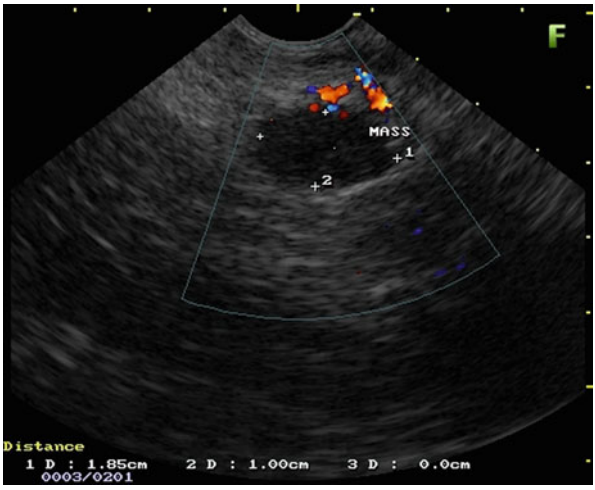

Fig. 12.33 Linear EUS showing discreet hypoechoic well circumscribed mass in the pancreatic body suggestive of pancreatic neuroendocrine tumor

12.4.3.3 Solid and Papillary Epithelial Neoplasm of Pancreas (SPEN)

SPEN are rare tumors predominantly seen in young females (15–45 years). Although often large at the time of diagnosis, these tumors have a very low malignant potential, are most commonly found in the body and tail and have an excellent prognosis if resected.

Typical EUS Findings (Fig. 12.34)

1. Mixed solid and cystic encapsulated tumor
2. Distinct margins seen on EUS
3. Differential diagnosis is a neuroendocrine tumor

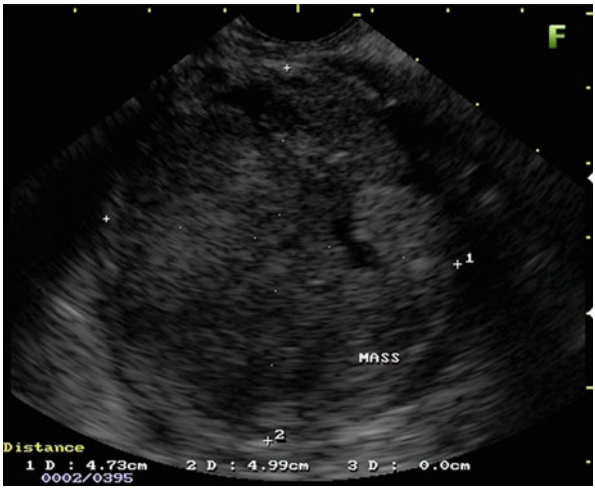

Fig. 12.34 Large heterogeneous well circumscribed mass in the pancreatic body with cystic component in a 19 years old girl – SPEN. FNA confirmed the diagnosis

12.4.3.4 Peripancreatic and Retroperitoneal Enlarged Lymph Nodes

Pancreatic head masses reported on CT scan may sometimes be enlarged peripancreatic lymph nodes due to tuberculosis, lymphoma or metastases.

Typical EUS Findings (Figs. 12.35 and 12.36)

1. Rounded or oval hypo or isoechoic lesions separate from pancreas
2. Matted appearance in tubercular lymphadenopathy
3. Situated at the periphery of the pancreas, never within the gland. To differentiate between an enlarged lymph node and a pancreatic tumor, trace the normal pancreas to the border of the tumor and then beyond. If the lesion is within the pancreas, it is a pancreatic tumor, if at the border, very likely a lymph node
4. Normal caliber pancreatic duct
5. Enlarged lymph nodes may be present at other locations

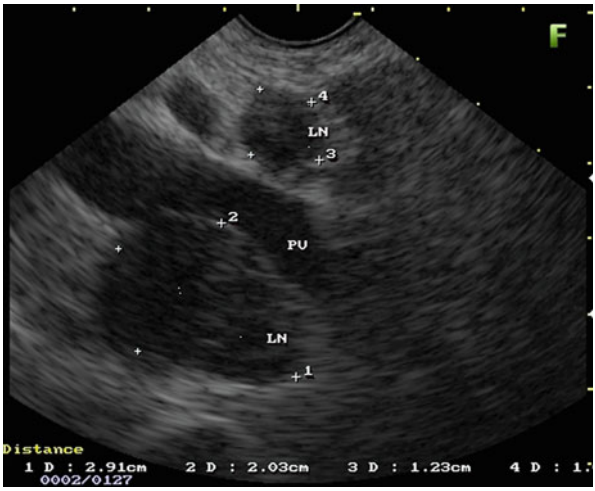

Fig. 12.35 Multiple enlarged hypoechoic discreet lymph nodes on both sides of PV in a patient with non-Hodgkin's lymphoma. The lymph nodes show a rounded appearance with hypoechoic centre. FNA confirmed the diagnosis

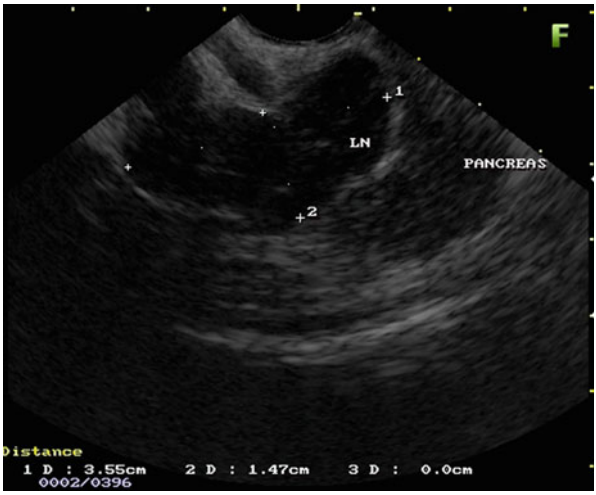

Fig. 12.36 Enlarged hypoechoic matted peri-pancreatic lymph nodes with necrotic centers seen in tuberculosis

12.4.3.5 Limitations of EUS in Diagnosis of Solid Pancreatic Tumors

EUS is the most accurate imaging modality for detection of pancreatic tumors (96% with a range 86–100%) [23]. However, some lesions may go undetected.

Common Causes of False Negative EUS

1. Presence of underlying chronic pancreatitis
2. Diffusely infiltrating carcinoma
3. Prominent ventral/dorsal anlage split
4. Recent episode (<4 weeks) of acute pancreatitis where edema can conceal a focal lesion [24]
5. Presence of a biliary or pancreatic duct stent, due to shadow cast by the stent and air artifacts [25]

It is important to follow up these patients after 2–3 months by repeat EUS in case of strong suspicion of cancer [24, 26]. Temporary removal of plastic biliary stents prior to EUS may prove helpful.

12.4.4 Pancreatic Cystic Lesions

12.4.4.1 Classification of Cystic Lesions of the Pancreas [27]

- Congenital and simple cysts – 5–10%
- Pseudocysts – 80–90%
- Cystic neoplasms – 5–10%
  - Serous cystadenoma (SCA)
  - Mucinous cystadenoma (MCA)
  - Mucinous cystadenocarcinoma (MCAC)
  - Intraductal papillary mucinous neoplasm (IPMN)

Congenital or simple cysts are found in patients with von Hippel Lindau disease, adult polycystic kidney disease or as coincidental findings. On EUS they appear as small, thin walled, uniformly anechoic lesions in an otherwise normal pancreas (Fig. 12.37).

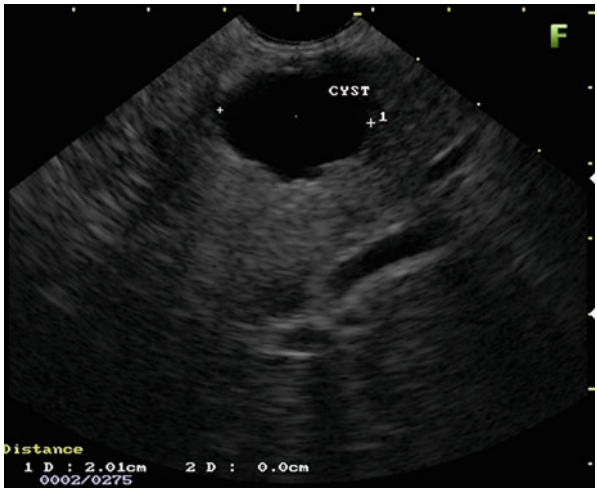

Fig. 12.37 Simple cyst in the pancreatic head on linear EUS

12.4.4.2 Pseudocysts of Pancreas

Pancreatic pseudocysts (PPC) may occur due to acute or chronic pancreatitis.

Typical EUS Findings (Fig. 12.38)

1. Uniloculated collection without septations
2. Necrotic debris may be seen in the floor; mural nodules are not seen

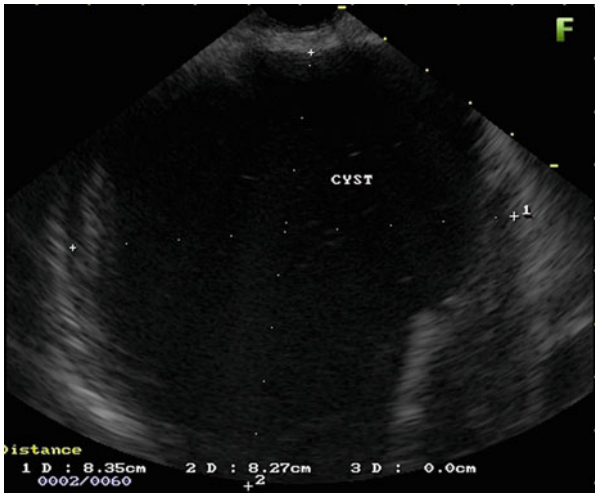

Fig. 12.38 Unilocular PPC in the lesser sac with sediments in the floor

Endoscopic management of pseudocysts is described in detail in Chap. 18.

12.4.4.3 Cystic Tumors of Pancreas

Serous cystadenomas are microcystic with a honeycomb appearance and multiple small cysts. Mucinous cystadenomas are large, show septations and mural nodules in the wall. Intraductal papillary mucinous neoplasms (IPMN) may be main duct (MD) or branch duct (BD), show ductal communication, a dilated MPD and mural nodules (Figs. 12.39, 12.40, 12.41, and 12.42) [28]. (A detailed comparative description of pancreatic cystic lesions is given in Table 16.1)

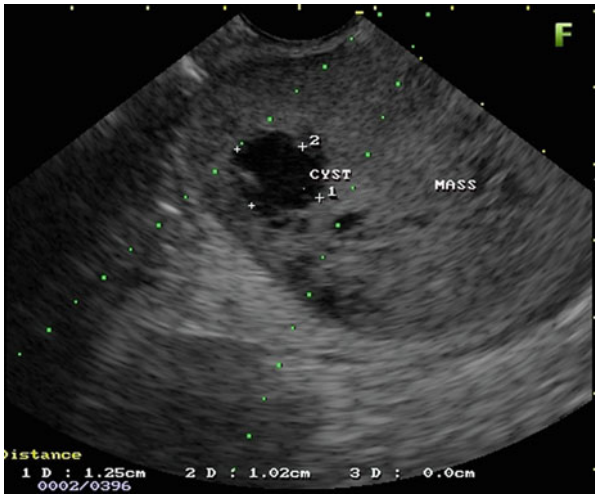

Fig. 12.39 Large well circumscribed mass seen in the pancreatic head with multiple small cystic lesions within – Serous Cyst Adenoma. Note the classical honeycomb appearance. One cyst is larger in size and can be targeted for EUS guided aspiration

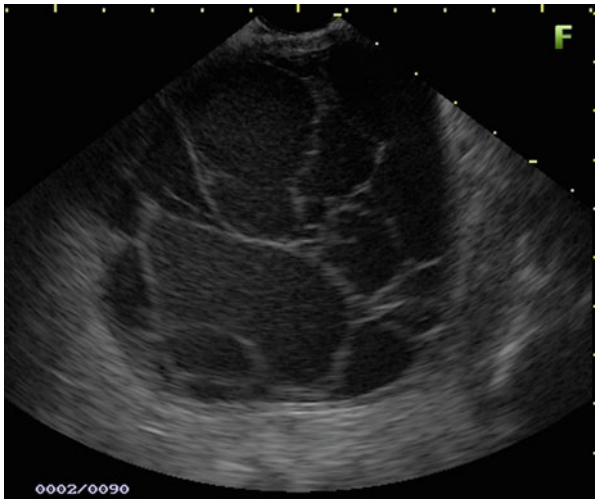

Fig. 12.40 A large cystic multiseptate lesion is characteristic of mucinous pancreatic neoplasm

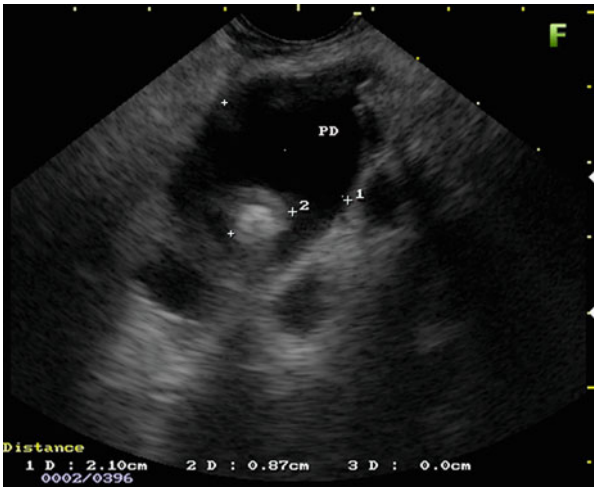

Fig. 12.41 Cystic dilatation of MPD with solid component in a patient with main duct IPMN

Fig. 12.42 Large cystic tumors with solid component are typically pancreatic mucinous cystadenocarcinomas. The CBD is dilated (seen on the *right* of the screen)

12.5 Evaluation of Common Bile Duct (CBD) Disorders

12.5.1 CBD Calculi

EUS has very high specificity, sensitivity and accuracy for diagnosis of stones in the CBD or ampullary region (93–99% accuracy) [29–34]. This has been proven to be significantly superior to MRCP (82–95%) [32, 33] or to helical CT scan (86–94%) [35] in multiple randomized comparative trials. It is especially useful to detect small stones in a normal sized duct and those near the ampulla, where MRCP has limited sensitivity.

Typical EUS Findings (Figs. 12.43 and 12.44)
1. Bright hyperechoic intraductal foci
2. Wedge shaped posterior acoustic shadowing
3. CBD is usually dilated
4. Shadowing may not be evident with small stones or sludge balls

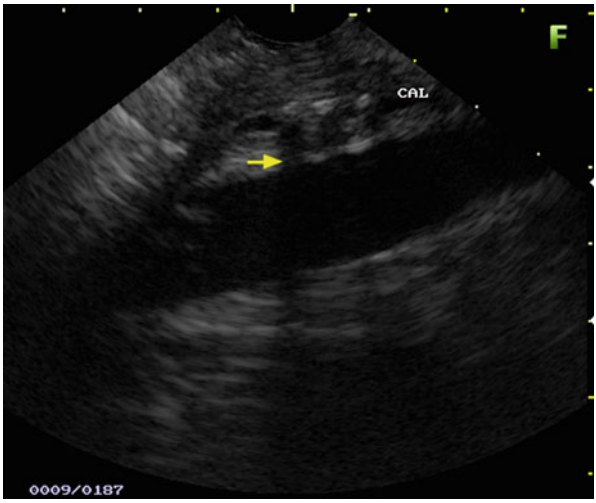

Fig. 12.43 Linear EUS showing normal caliber CBD with calculi casting posterior acoustic shadow (*arrow*)

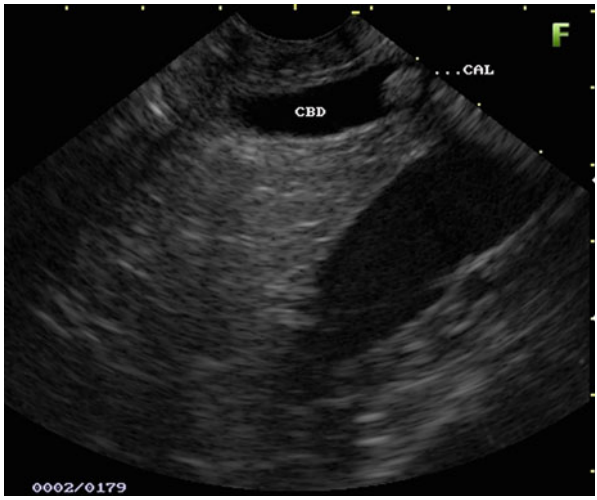

Fig. 12.44 Linear EUS showing dilated CBD with calculus. Note posterior acoustic shadow cast by the stone

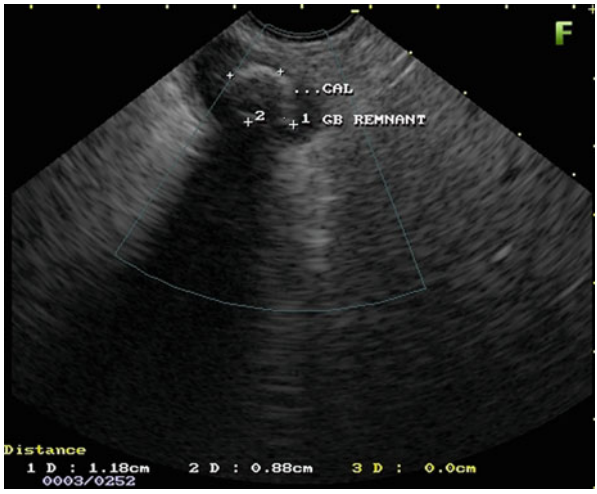

Fig. 12.45 Linear EUS showing a large calculus in the cystic duct stump remnant

Stones at the ampulla can be effectively diagnosed by EUS. For ampullary examination, it often helps to instill water in the duodenum and abolish peristalsis to get high quality images of the ampulla. EUS evaluation of symptomatic post cholecystectomy patients may detect stones in the post cholecystectomy cystic duct stump (Fig. 12.45).

12.5.2 Anatomical and Developmental Anomalies

Choledochal cysts may be suspected or diagnosed by linear EUS. Type II choledochal cysts must be differentiated from duodenal duplication cysts in the juxtaampullary location (Fig. 12.46).

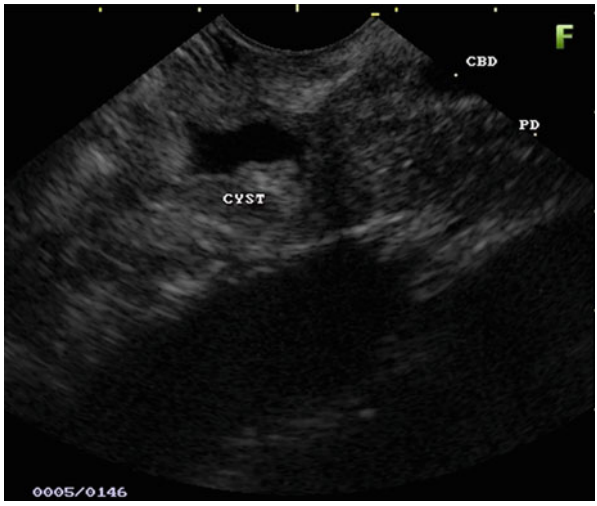

Fig. 12.46 Linear EUS showing type II choledochal cyst

12.5.3 Intraductal Tumors of the Common Bile Duct (CBD)

Bile duct tumors may present as a proliferative intraductal mass or as a fibrotic stricture.

Typical EUS Findings (Figs. 12.47 and 12.48)
1. Soft tissue mass lesion in CBD with proximal dilatation
2. Absence of acoustic shadowing differentiates it from a CBD calculus
3. Fibrotic lesions are difficult to diagnose by extra ductal EUS

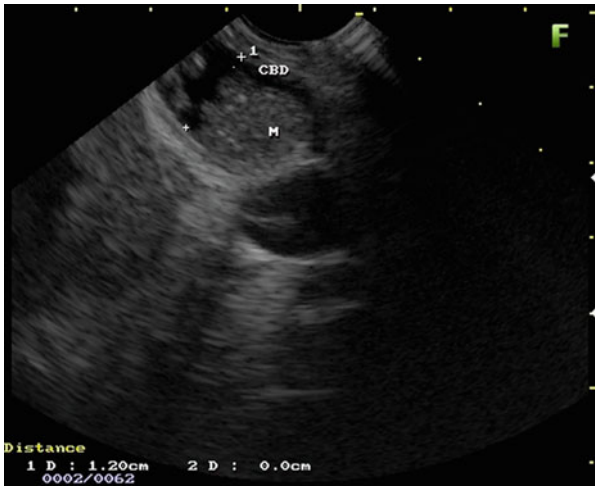

Fig. 12.47 Dilated CBD with soft tissue mass lesion without acoustic shadowing – Intraductal cholangiocarcinoma

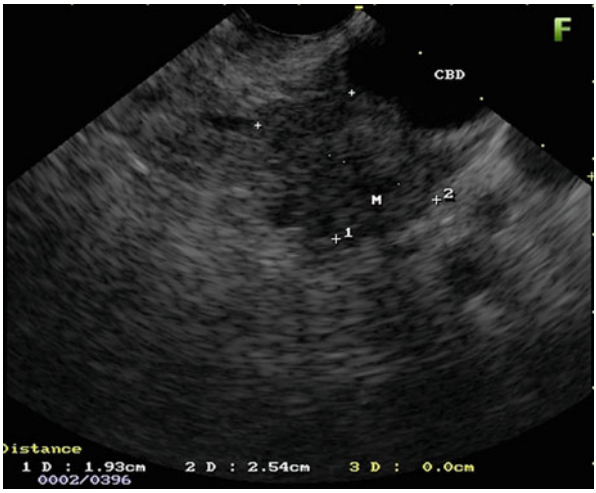

Fig. 12.48 Bile duct cancer infiltrating into the pancreatic head. The proximal CBD is dilated

Along with EUS and EUS-FNA, ERCP, cholangioscopy, intraductal biopsy and intraductal EUS using a catheter probe are important adjuncts for diagnosis of cholangiocarcinoma.

12.5.4 Ampullary Tumors

Adenomas, adenocarcinomas or other tumors can occur at the ampulla. Adenomas are premalignant. Tumors may be polypoid or ulcerative. The polypoid variety may be visible or intramural within the ampulla.

Typical EUS and Duodenoscopy Findings (Fig. 12.49)
1. Hypoechoic mass at the ampulla
2. CBD and pancreatic duct will often show dilatation
3. Tumor may show infiltration into the deeper layers indicating malignancy

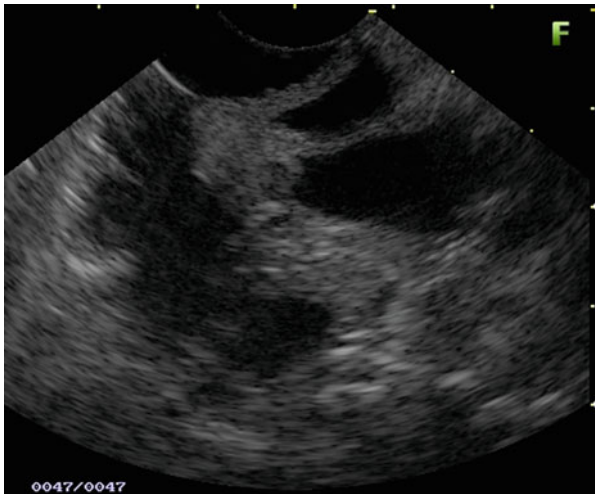

Fig. 12.49 Ampullary adenocarcinoma – irregular hypoechoic tumor involving the ampulla. The dilated CBD and MPD are seen converging on the tumor. The tumor is localized to the ampulla

12.6 Evaluation of Gall Bladder Diseases

12.6.1 Gall Bladder Microlithiasis

EUS detects gall bladder (GB) microcalculi or sludge missed by other imaging techniques [11, 13, 15]. It is important to note that layered sludge in the GB is often found in patients not on oral feeds; this usually disappears once feeds are resumed. This is physiological and must not be mistakenly considered as an abnormality. GB microcalculi must be evaluated after the acute attack settles, oral feeding is restored and with a standard 6 h fasting state.

Typical EUS Findings (Refer Sect. 12.4.1.2, Fig. 12.29)
1. Multiple tiny bright spots on an anechoic background – starry sky appearance
2. Gall bladder is distended and shows normal walls

12.6.2 Gall Bladder Stones and Cholecystitis

Typical EUS Findings
1. Hyperechoic focus with posterior acoustic shadow
2. Thick walled, contracted gall bladder in chronic cholecystitis

12.6.3 Gall Bladder Cancer

Typical EUS Findings (Fig. 12.50)
1. Soft tissue mass arising from the wall of the gall bladder
2. Invasion of the layers indicates malignant etiology

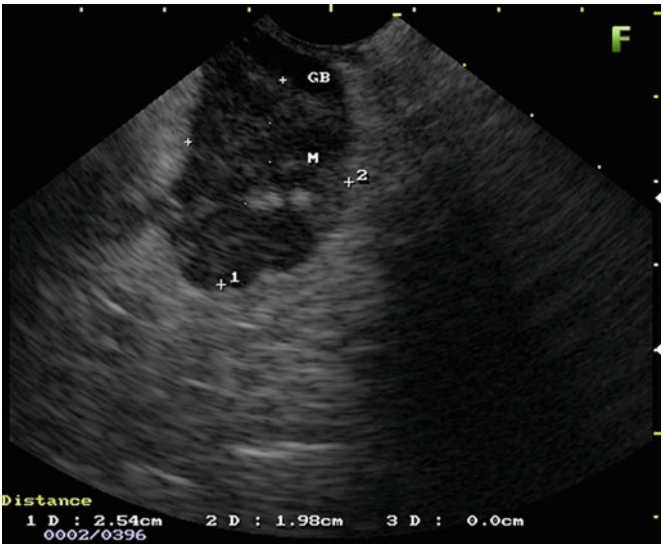

Fig. 12.50 Soft tissue mass in the gall bladder lumen – gall bladder carcinoma

12.7 EUS Staging of Biliary-Pancreatic Cancers

EUS is useful for T and N staging of biliary-pancreatic cancers. It has high sensitivity and specificity for diagnosis of biliary-pancreatic tumors, especially those <2 cm in size. It is excellent in detecting portal vein (PV) and splenic vein (SV) invasion [20, 21] (Fig. 12.51). Helical CT scan is superior to EUS for detecting involvement of the superior mesenteric artery [36, 37].

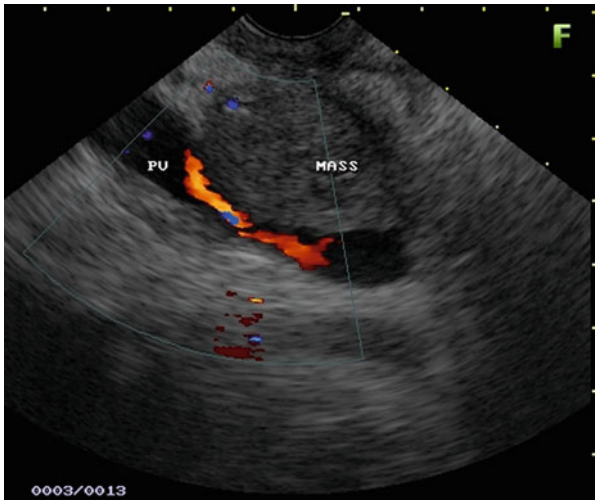

Fig. 12.51 Pancreatic head cancer involving the PV seen on linear EUS from station 2

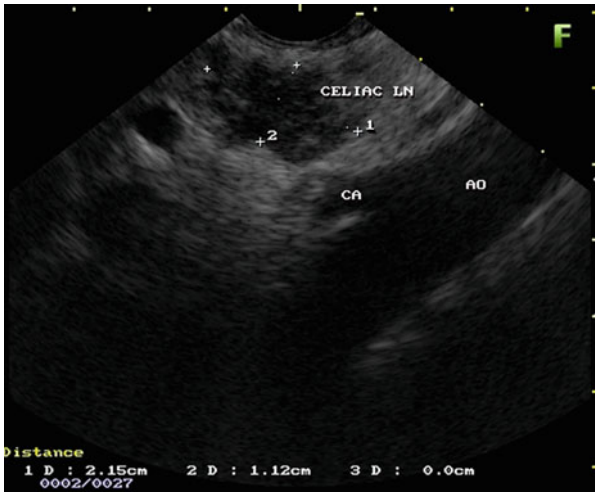

Fig. 12.52 Linear EUS showing enlarged hypoechoic celiac node in a patient with pancreatic cancer – metastatic lymphadenopathy

EUS has good accuracy in detecting enlarged regional lymph nodes [38], although FNA may be necessary to confirm metastases. Important nodal stations examined are perigastric, peripancreatic, retroperitoneum, hepatic hilum, celiac area and mediastinum (Fig. 12.52).

EUS has limited application for M-staging, but can incidentally detect small ascites or metastases in the left lobe of liver missed on other imaging (Figs. 12.53 and 12.54).

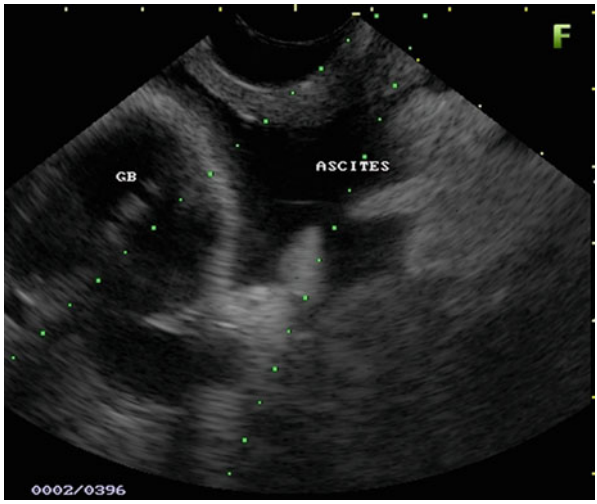

Fig. 12.53 Small ascites seen as fluid in the Morrison's pouch in a patient of pancreatic cancer. Fluid cytology revealed malignant cells indicating Stage 4 disease

Fig. 12.54 Linear EUS showing a small metastasis in the left lobe of the liver

EUS Criteria for Predicting Vascular Invasion

1. Loss of interface with vessel wall
2. Irregular vessel wall
3. Cross-sectional vascular encasement
4. Luminal narrowing
5. Presence of intravascular filling defects
6. Vascular occlusion
7. Venous collaterals

12.8 Vascular Abnormalities

Portal or splenic vein thrombosis can occur due to tumor invasion or due to acute or chronic pancreatitis [39] (Fig. 12.55). Collateral vessels (varices) in the esophagus, stomach, duodenum, around the bile duct and in the retroperitoneum can be identified on EUS. Portal biliopathy as a cause of biliary obstruction can be diagnosed on EUS (Fig. 12.56).

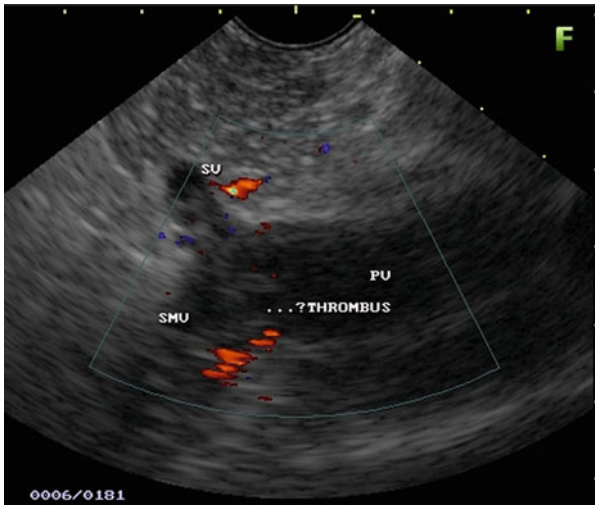

Fig. 12.55 Linear EUS showing portal vein thrombosis

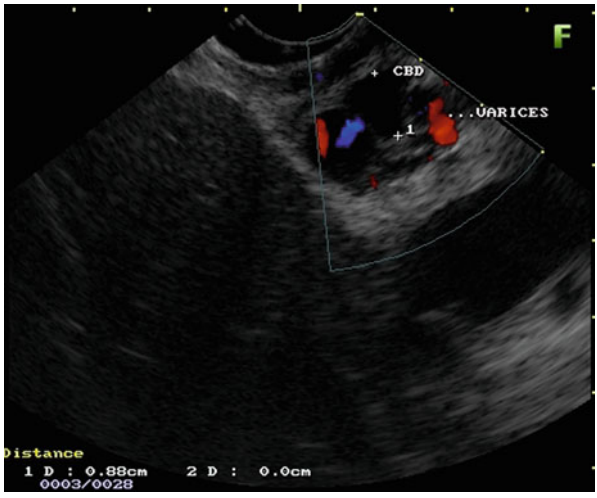

Fig. 12.56 Linear EUS showing peri-choledochal varices

References

1. Gress F, Savides T, Cummings O et al (1997) Radial scanning and linear array endosonography for staging pancreatic cancer: a prospective randomized comparison. Gastrointest Endosc 45(2):138–142. doi:S0016-5107(97)70236-0 [pii]
2. Lankisch PG, Seidensticker F, Otto J et al (1996) Secretin-pancreozymin test (SPT) and endoscopic retrograde cholangiopancreatography (ERCP): both are necessary for diagnosing or excluding chronic pancreatitis. Pancreas 12(2):149–152
3. Lees WR (1986) Endoscopic ultrasonography of chronic pancreatitis and pancreatic pseudocysts. Scand J Gastroenterol Suppl 123:123–129
4. Catalano MF, Lahoti S, Geenen JE et al (1998) Prospective evaluation of endoscopic ultrasonography, endoscopic retrograde pancreatography, and secretin test in the diagnosis of chronic pancreatitis. Gastrointest Endosc 48(1):11–17. doi:S0016510798001679 [pii]
5. Sahai AV, Zimmerman M, Aabakken L et al (1998) Prospective assessment of the ability of endoscopic ultrasound to diagnose, exclude, or establish the severity of chronic pancreatitis found by endoscopic retrograde cholangiopancreatography. Gastrointest Endosc 48(1):18–25. doi:S0016510798001849 [pii]
6. Wiersema MJ, Hawes RH, Lehman GA et al (1993) Prospective evaluation of endoscopic ultrasonography and endoscopic retrograde cholangiopancreatography in patients with chronic abdominal pain of suspected pancreatic origin. Endoscopy 25(9):555–564. doi:10.1055/s-2007-1010405
7. Varadarajulu S, Eltoum I, Tamhane A et al (2007) Histopathologic correlates of noncalcific chronic pancreatitis by EUS: a prospective tissue characterization study. Gastrointest Endosc 66(3):501–509. doi:S0016-5107(06)03557-7 [pii] 10.1016/j.gie.2006.12.043
8. Chong AK, Hawes RH, Hoffman BJ et al (2007) Diagnostic performance of EUS for chronic pancreatitis: a comparison with histopathology. Gastrointest Endosc 65(6):808–814. doi:S0016-5107(06)02951-8 [pii] 10.1016/j.gie.2006.09.026
9. Catalano MF, Sahai A, Levy M et al (2009) EUS-based criteria for the diagnosis of chronic pancreatitis: the Rosemont classification. Gastrointest Endosc 69(7):1251–1261. doi:S0016-5107(08)02339-0 [pii] 10.1016/j.gie.2008.07.043
10. Stevens T, Lopez R, Adler DG et al (2010) Multicenter comparison of the interobserver agreement of standard EUS scoring and Rosemont classification scoring for diagnosis of chronic pancreatitis. Gastrointest Endosc 71(3):519–526. doi:S0016-5107(09)02697-2 [pii] 10.1016/j.gie.2009.10.043
11. Yusoff IF, Raymond G, Sahai AV (2004) A prospective comparison of the yield of EUS in primary vs. recurrent idiopathic acute pancreatitis. Gastrointest Endosc 60(5):673–678. doi:doi:S0016510704020188 [pii]
12. Chen RY, Hawes RH (2002) Idopathic acute pancreatitis: is EUS worth doing? Am J Gastroenterol 97(5):1244–1246. doi:10.1111/j.1572-0241.2002.05674.x
13. Liu CL, Lo CM, Chan JK et al (2000) EUS for detection of occult cholelithiasis in patients with idiopathic pancreatitis. Gastrointest Endosc 51(1):28–32. doi:S0016510700784318 [pii]
14. Lai R, Freeman ML, Cass OW et al (2004) Accurate diagnosis of pancreas divisum by linear-array endoscopic ultrasonography. Endoscopy 36(8):705–709. doi:10.1055/s-2004-825663
15. Frossard JL, Sosa-Valencia L, Amouyal G et al (2000) Usefulness of endoscopic ultrasonography in patients with "idiopathic" acute pancreatitis. Am J Med 109(3):196–200. doi:S0002-9343(00)00478-2 [pii]
16. Robison LS, Canon CL, Varadarajulu S et al (2010) Autoimmune pancreatitis mimicking pancreatic cancer. J Hepatobiliary Pancreat Sci. doi:10.1007/s00534-010-0321-1
17. Farrell JJ, Garber J, Sahani D et al (2004) EUS findings in patients with autoimmune pancreatitis. Gastrointest Endosc 60(6):927–936. doi:S0016510704022308 [pii]
18. Kubota K, Kato S, Akiyama T et al (2009) A proposal for differentiation between early- and advanced-stage autoimmune pancreatitis by endoscopic ultrasonography. Dig Endosc 21(3):162–169. doi:DEN879 [pii] 10.1111/j.1443-1661.2009.00879.x

19. Levy MJ, Reddy RP, Wiersema MJ et al (2005) EUS-guided trucut biopsy in establishing autoimmune pancreatitis as the cause of obstructive jaundice. Gastrointest Endosc 61(3): 467–472. doi:S0016510704028020 [pii]
20. Varadarajulu S, Wallace MB (2004) Applications of endoscopic ultrasonography in pancreatic cancer. Cancer Control 11(1):15–22
21. Brugge WR (1995) Pancreatic cancer staging. Endoscopic ultrasonography criteria for vascular invasion. Gastrointest Endosc Clin N Am 5(4):741–753
22. Anderson MA, Carpenter S, Thompson NW et al (2000) Endoscopic ultrasound is highly accurate and directs management in patients with neuroendocrine tumors of the pancreas. Am J Gastroenterol 95(9):2271–2277. doi:S0002-9270(00)01272-7 [pii] 10.1111/j.1572-0241.2000.02480.x
23. Akahoshi K, Chijiiwa Y, Nakano I et al (1998) Diagnosis and staging of pancreatic cancer by endoscopic ultrasound. Br J Radiol 71(845):492–496
24. Bhutani MS, Gress FG, Giovannini M et al (2004) The No Endosonographic Detection of Tumor (NEST) study: a case series of pancreatic cancers missed on endoscopic ultrasonography. Endoscopy 36(5):385–389. doi:10.1055/s-2004-814320
25. Agarwal B, Abu-Hamda E, Molke KL et al (2004) Endoscopic ultrasound-guided fine needle aspiration and multidetector spiral CT in the diagnosis of pancreatic cancer. Am J Gastroenterol 99(5):844–850. doi:10.1111/j.1572-0241.2004.04177.x AJG4177 [pii]
26. Catanzaro A, Richardson S, Veloso H et al (2003) Long-term follow-up of patients with clinically indeterminate suspicion of pancreatic cancer and normal EUS. Gastrointest Endosc 58(6):836–840. doi:S0016510703023010 [pii]
27. Balthazar EJ, Chacko AC (1990) Computed tomography of pancreatic masses. Am J Gastroenterol 85:343–349
28. Lennon AM, Penman ID (2006) EUS in evaluation of pancreatic cysts. In: Hawes RH, Fockens P (eds) Endosonography, 1st edn. Saunders/Elsevier, Philadelphia, pp 205–216
29. Kohut M, Nowakowska-Dulawa E, Marek T et al (2002) Accuracy of linear endoscopic ultrasonography in the evaluation of patients with suspected common bile duct stones. Endoscopy 34(4):299–303. doi:10.1055/s-2002-23641
30. Prat F, Amouyal G, Amouyal P et al (1996) Prospective controlled study of endoscopic ultrasonography and endoscopic retrograde cholangiography in patients with suspected commonbileduct lithiasis. Lancet 347(8994):75–79
31. Canto MI, Chak A, Stellato T et al (1998) Endoscopic ultrasonography versus cholangiography for the diagnosis of choledocholithiasis. Gastrointest Endosc 47(6):439–448. doi:S0016510798001394 [pii]
32. Scheiman JM, Carlos RC, Barnett JL et al (2001) Can endoscopic ultrasound or magnetic resonance cholangiopancreatography replace ERCP in patients with suspected biliary disease? A prospective trial and cost analysis. Am J Gastroenterol 96(10):2900–2904. doi:S0002-9270(01)02807-6 [pii] 10.1111/j.1572-0241.2001.04245.x
33. de Ledinghen V, Lecesne R, Raymond JM et al (1999) Diagnosis of choledocholithiasis: EUS or magnetic resonance cholangiography? A prospective controlled study. Gastrointest Endosc 49(1):26–31. doi:S0016510799000073 [pii]
34. Palazzo L, Girollet PP, Salmeron M et al (1995) Value of endoscopic ultrasonography in the diagnosis of common bile duct stones: comparison with surgical exploration and ERCP. Gastrointest Endosc 42(3):225–231. doi:S0016510795001374 [pii]
35. Sugiyama M, Atomi Y (1997) Endoscopic ultrasonography for diagnosing choledocholithiasis: a prospective comparative study with ultrasonography and computed tomography. Gastrointest Endosc 45(2):143–146. doi:S0016-5107(97)70237-2 [pii]
36. Gress FG, Hawes RH, Savides TJ et al (1999) Role of EUS in the preoperative staging of pancreatic cancer: a large single-center experience. Gastrointest Endosc 50(6):786–791. doi:S0016510799005854 [pii]
37. Soriano A, Castells A, Ayuso C et al (2004) Preoperative staging and tumor resectability assessment of pancreatic cancer: prospective study comparing endoscopic ultrasonography,

helical computed tomography, magnetic resonance imaging, and angiography. Am J Gastroenterol 99(3):492–501. doi:10.1111/j.1572-0241.2004.04087.x AJG4087 [pii]
38. Yasuda K, Mukai H, Nakajima M et al (1993) Staging of pancreatic carcinoma by endoscopic ultrasonography. Endoscopy 25(2):151–155. doi:10.1055/s-2007-1010274
39. Lai L, Brugge WR (2004) Endoscopic ultrasound is a sensitive and specific test to diagnose portal venous system thrombosis (PVST). Am J Gastroenterol 99(1):40–44

Part V

Endoscopic Ultrasonography-Guided Fine Needle Aspiration (EUS-FNA)

Techniques of EUS-FNA

13

Amol Bapaye and Advay Aher

13.1 Introduction

EUS-FNA is the commonest intervention performed through the EUS endoscope. Mass lesions or enlarged lymph nodes in the mediastinum, retroperitoneum and pancreas or in the gut wall require tissue diagnosis to plan optimum treatment strategies. EUS-FNA was first described by Vilmann et al. in 1992 [1].

13.2 Indications

To obtain tissue diagnosis from various lesions in the gastrointestinal tract.

13.3 Equipment

13.3.1 Endoscope

The linear convex array echoendoscope (EG-530UT, Fujifilm Inc., Japan or other linear echoendoscope from other manufacturers) is used to perform EUS-FNA.

A. Bapaye, M.D. (M.S.) (✉)
Department of Digestive Diseases and Endoscopy,
Deenanath Mangeshkar Hospital and Research Center,
Erandwane, Pune 411004, Maharashtra, India
e-mail: amolbapaye@gmail.com

A. Aher
Clinical Research Fellow, Department of Digestive Diseases and Endoscopy,
Deenanath Mangeshkar Hospital and Research Center,
Erandwane, Pune 411004, Maharashtra, India

K. Akahoshi, A. Bapaye (eds.), *Practical Handbook of Endoscopic Ultrasonography*,
DOI 10.1007/978-4-431-54014-4_13, © Springer 2012

13.3.2 Needles

Standard EUS-FNA needles are available from many manufacturers and come in various sizes – 19G, 22G and 25G (Echotip and Echotip Ultra™, Cook Endoscopy, Winston-Salem, USA; Sonotip™ I and II, Mediglobe GmBH, Germany; Expect™, Boston Scientific Corporation, Natick, Massachusetts, USA). The QuickCore™ and Procore™ (19G, 19 and 22G respectively; Cook) are available for core biopsies. The 22G needle is commonly used to perform FNA.

Needles come in a range of options for the stylet – ball tipped or sharp, and protruding or flush with the tip.

13.3.3 Other Material

Pathology glass slides, fixative, containers for transport of clot, tissue and other material in appropriate preservative solutions.

Presence of an onsite cytopathologist is a desirable but not mandatory requirement. If present, the endoscopy suite should be equipped with the required instrumentation – microscopes, staining materials, etc.

13.4 Technique

The technique of EUS-FNA has been standardized over the last two decades. Variations may exist between operators and when FNA is performed in different anatomical locations. We describe here the standard FNA technique applicable in most situations. Specific variations are dealt with in the respective chapters.

13.4.1 Salient Points of Patient Preparation

1. Confirm normal coagulation profile and patient is advised to withhold anticoagulation medication.
2. Antibiotics are not routinely recommended but should be administered to patients with high risk of post procedure infection – those with cystic lesions for FNA, valvular heart defects or cardiac implants.

13.4.2 Locating the Lesion for FNA and Positioning the Endoscope

1. Locate the lesion on linear EUS.
2. Activate the on-screen guide of the needle track of the FG-530UT and SU-7000 on the ultrasound screen (seen as two diverging green dotted lines). The needle path follows the upper dotted line during the FNA. The lower dotted line marks the maximum vertical movement that may be achieved by using the elevator.

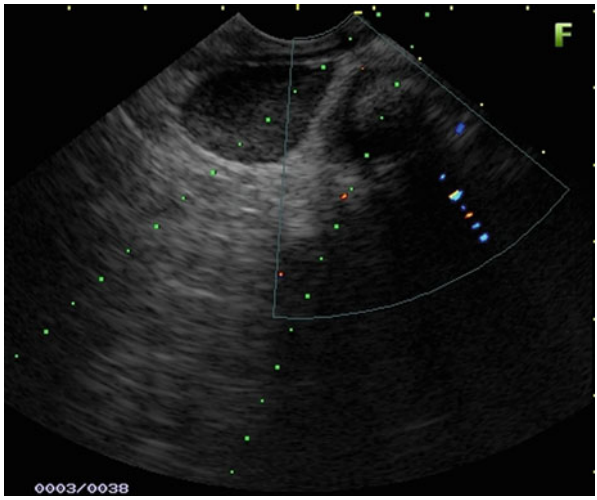

Fig. 13.1 Position the lesion along the upper marker line to perform FNA

3. Position the lesion in the natural path of this track, preferably along the upper dotted line or between the two lines (Fig. 13.1). It is advisable to use the elevator as infrequently as possible during FNA.
4. Position the lesion close to the transducer (preferably 1–2 cm).
5. Confirm absence of intervening vasculature in the needle track by applying color Doppler (Fig. 13.1).
6. As a general rule, maintain the endoscope in straight position.
7. Sometimes it is beneficial to keep the endoscope wedged against the bowel wall, providing mechanical advantage to advance the needle into the lesion (e.g. long loop in the duodenal bulb for pancreatic head FNA) (See Fig. 16.1).

13.4.3 Insert the Needle into the Echoendoscope

1. Check if all the parts of the needle are functioning properly and that the stylet is not stuck within the needle.
2. Keeping the echendoscope as straight as possible, insert the needle into the endoscope. If there is resistance to needle passage, withdraw the scope until it becomes straight before advancing the needle further. Do not force the needle through the endoscope as it may damage the channel.
3. Position the needle sheath so that the tip exits the endoscope tip by 1–1.5 cm and rests on the transducer. Adjust the length of the sheath and fix it in this position. Lock the needle to the biopsy channel using the Luer-lock.
4. Reposition the echoendoscope to locate the lesion at the desired position. The sheath of the needle may retract into the endoscope tip if the endoscope is in loop position. In such a case, push the sheath out by another centimeter to compensate for this retraction.
5. Keep elevator open at all times during the above maneuvers.

13.4.4 Prepare the Needle

1. Lock the needle sheath in the desired position.
2. Measure the distance from the center of the lesion to the point of entry of the needle (1 o'clock on the ultrasound screen).
3. Set the limit of the stopping device on the needle to this distance.
4. Withdraw the stylet into the needle by about 5 mm to expose the sharp beveled tip for puncture. When using a 19G needle through the endoscope in long loop, it may be impossible to withdraw the stylet once the needle is within the lesion. FNA can be performed without stylet in such a case.
5. Hold the needle in the recommended position (Fig. 13.2). The fixed shaft of the needle should be grasped between the palm of the hand and the last three fingers of the right hand. The movable portion should be held between the thumb and the index finger. This permits fine control of the needle movement.

Fig. 13.2 Photograph showing position of the hands while holding the FNA needle

13.4.5 **Puncture the Lesion** (Fig. 13.3)

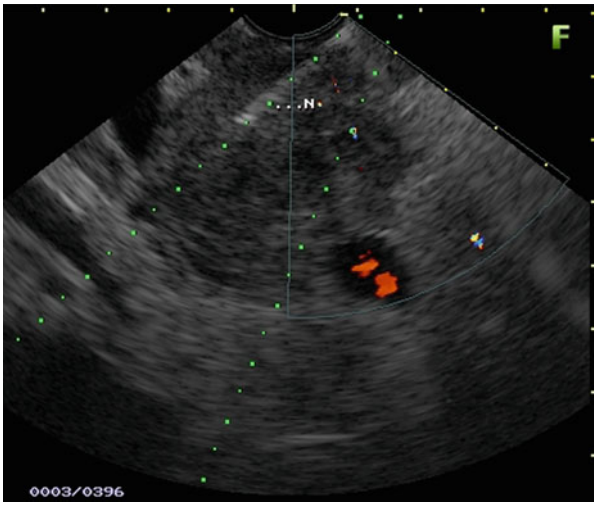

Fig. 13.3 Linear EUS showing needle path following the upper dotted line

1. Reapply color Doppler to confirm absence of intervening vessels.
2. Apply firm upward tip deflection to the endoscope tip using the up/down wheel. This fixes the endoscope and prevents the needle from pushing the endoscope tip away from the bowel wall.
3. Open the elevator fully.
4. Advance the needle by a few millimeters to locate it on ultrasound.
5. Advance it further into the lesion under ultrasound guidance. If the needle tip disappears from ultrasound view after entry into the lesion, do not attempt to advance the needle further unless view is regained. Minor lateral rotational movements will usually bring the needle back in view. If this fails, withdraw the needle slowly to identify the tip. Once located, re-advance the needle into the lesion under vision. If this too fails, withdraw the needle completely, reposition the endoscope and repeat the puncture.
6. It may be necessary to direct the needle into the lesion using the elevator. As a rule, make minimal use of the elevator as it increases the resistance to needle passage.
7. In hard lesions and when the endoscope is in a long loop, the needle may not enter the lesion. In such situations, plant the needle in the wall of the bowel and then advance the endoscope to push it into the lesion (Fig. 13.4).
8. To target small, mobile lesions, it is helpful to pass the needle first through the bowel wall and then into the lesion – a two step approach.

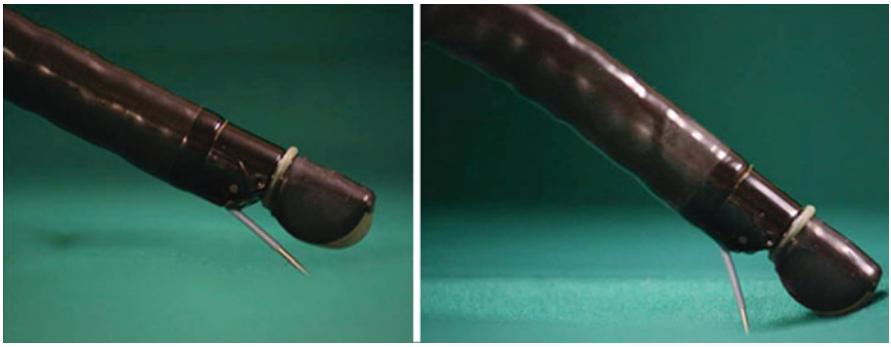

Fig. 13.4 Photograph showing the plant and push technique

9. Once the needle is in position and clearly visualized, remove the stylet. Before removing the stylet, push it back in completely and then withdraw to dislodge any mucosal tissue that may have clogged the needle tip.
10. Apply a 5 or 10 ml suction syringe (usually supplied with the needle by the manufacturer) over a three way stop-cock and activate suction. Some endosonographers prefer not to use suction as a bloody aspirates are considered suboptimal in quality for pathological examination [2].
11. Move the needle back and forth in the lesion several (10–12) times with a thrusting force to shear off the cells. Push the needle sharply in to shear off cells and pull back slowly so that they enter the needle. Take care to always remain within the lesion at all times. Do not withdraw the needle out of the lesion in the bowel lumen, otherwise the sample will be sucked into the syringe and cannot be processed.
12. Maintain upward deflection with the endoscope tip to remain close to the bowel wall at all times.
13. Once a pass has been completed, deactivate suction and withdraw the needle completely into the sheath.
14. Slide the locking device to its highest position and lock it and withdraw the needle from the endoscope.

13.4.6 Sample Collection

Expel the aspirate from the needle into an appropriate container containing preservative and/or onto glass slides. This can be performed either by injecting about 10 ml of air through the needle with a syringe, or by slowly advancing the stylet into the needle while collecting droplets of tissue onto slides. We prefer to use the stylet technique since is better controls the expulsion of tissue and its subsequent collection.

Hand over the slides to the onsite cytopathologist if available, alternatively, label slides and containers and submit to the laboratory as per standard hospital policy. The detailed procedure of preparation of smears is described in Chap. 14.

13.4.7 Preparation for Subsequent Passes

If an onsite cytopathologist is present, he or she would guide the necessity to perform subsequent passes. If not, current data suggests that at least 5 passes should be performed for diagnosis of cancer [2, 3].

The same needle can be used for subsequent passes provided it is not damaged and the tip has not become too blunt. Rinse the lumen of the needle with water and then air and reinsert the stylet. Straighten the needle if the tip is bent.

13.5 Complications

13.5.1 Potential Complications of EUS-FNA

1. **Bleeding** – Torrential hemorrhage requiring surgery or radiological intervention, although has been reported, is exceedingly rare [4]. Bleeding may occur if a blood vessel is punctured during needle passage. If the puncture site shows bleeding after needle withdrawal, leave the balloon inflated for about 5 min. This will tamponade and stop the bleed.
2. **Infection** – Cystic lesions have a higher risk of developing infection post FNA [5]. Intravenous antibiotics should be prescribed while draining or performing FNA of cystic lesions.
3. **Perforation** – is almost unknown after FNA using a 22G needle. It has been described with use of the 19G QuickCore™ needle.
4. **Tumor seedling** – Tumor seedling in the needle track can occur after EUS-FNA although it is less common than CT guided FNA [6]. Care should be taken to perform FNA from a site which will be included in the subsequent surgical resection, e.g. from the duodenum for a pancreatic head mass. In other situations, the risk of seedling must be weighed against the risk of not performing FNA for preoperative diagnosis.
5. **Pancreatitis** – Pancreatitis may occur after EUS-FNA of pancreatic mass lesions in about 1% cases [7].

References

1. Vilmann PJG, Henriksen FW, Hancke S (1992) Endoscopic ultrasonography with guided fine needle aspiration biopsy in pancreatic disease: a new diagnostic procedure. Gastrointest Endosc 38:172–173
2. Wallace MB, Kennedy T, Durkalski V et al (2001) Randomized controlled trial of EUS-guided fine needle aspiration techniques for the detection of malignant lymphadenopathy. Gastrointest Endosc 54(4):441–447. doi:S0016510701559982 [pii]
3. LeBlanc JK, Ciaccia D, Al-Assi MT et al (2004) Optimal number of EUS-guided fine needle passes needed to obtain a correct diagnosis. Gastrointest Endosc 59(4):475–481. doi:S0016510703028633 [pii]

4. Affi A, Vazquez-Sequeiros E, Norton ID et al (2001) Acute extraluminal hemorrhage associated with EUS-guided fine needle aspiration: frequency and clinical significance. Gastrointest Endosc 53(2):221–225. doi:S0016510701370335 [pii]
5. Diehl DL, Cheruvattath R, Facktor MA et al (2010) Infection after endoscopic ultrasound-guided aspiration of mediastinal cysts. Interact Cardiovasc Thorac Surg 10(2):338–340. doi:icvts.2009.217067 [pii] 10.1510/icvts.2009.217067
6. Micames C, Jowell PS, White R et al (2003) Lower frequency of peritoneal carcinomatosis in patients with pancreatic cancer diagnosed by EUS-guided FNA vs. percutaneous FNA. Gastrointest Endosc 58(5):690–695. doi:S0016510703020091 [pii]
7. Eloubeidi MA, Tamhane A, Varadarajulu S et al (2006) Frequency of major complications after EUS-guided FNA of solid pancreatic masses: a prospective evaluation. Gastrointest Endosc 63(4):622–629. doi:S0016-5107(05)02108-5 [pii] 10.1016/j.gie.2005.05.024

Cytopathological Aspects of EUS-FNA

14

Vijayshri Pethe-Bhide and Amol Bapaye

14.1 Introduction

Fine needle aspiration cytology (FNAC) is a procedure wherein cells are aspirated from a lesion/tumor using a needle and syringe by applying negative pressure [1]. The aspirated material contains cells, either isolated or in clusters. Cell morphology, nuclear characteristics and cytological features of malignancy can be studied in these smears. The B in FNAB stands for biopsy; here, a core of tissue is examined for architectural characteristics or patterns. Pathological diagnosis of malignancy is made by using a combination of cytological and architectural disturbances. Despite advances in imaging modalities, histopathology and cytology still remain the gold standard for diagnostic confirmation of a disease.

14.2 Methods of Sample Collection

It is preferable to perform EUS – FNA in presence of an onsite cytopathologist who can confirm the adequacy of the sample. In absence of an onsite pathologist, multiple passes (more than five) should be made to improve the diagnostic yield [2, 3].

V. Pethe-Bhide (✉)
Department of Pathology, Deenanath Mangeshkar Hospital and Research Center,
Erandwane, Pune 411004, Maharashtra, India
e-mail: drvijayshrimb@yahoo.com

A. Bapaye, M.D. (M.S.)
Department of Digestive Diseases and Endoscopy,
Deenanath Mangeshkar Hospital and Research Center,
Erandwane, Pune 411004, Maharashtra, India

K. Akahoshi, A. Bapaye (eds.), *Practical Handbook of Endoscopic Ultrasonography*,
DOI 10.1007/978-4-431-54014-4_14, © Springer 2012

There are two methods of collecting the aspirated material on slides:

1. **Controlled technique –** Reintroduce the stylet into the needle and move it forward slowly to expel the material carefully and in a controlled manner. It can be collected as droplets on separate slides.
2. **Air expulsion technique –** In this method, air is injected into the needle using a syringe to expel the material which is collected onto slides. This technique can cause uncontrolled expulsion leading to loss of specimen.

At our centre, the controlled technique is used. One to five cytology smears are prepared by the onsite pathologist depending upon the obtained material. Remaining material (and blood clot, if any) is collected in 10% formalin for histopathology.

14.3 Preparation of Cytology Smears

Place a drop of aspirated material at one end of the slide. Spread using another slide placed vertically over the drop to prepare a thin smear. Too thick a smear cannot be interpreted. Use light pressure. If heavy pressure is used, all cells appear falsely elongated making identification difficult [4].

14.3.1 Fixation of Smears

Maintaining a good binocular light microscope in the endoscopy suite is advisable. The onsite cytopathologist air dries one of the smears and stains it with Toluidene Blue (Flood smear with Toluidene Blue solution for 60 s and then wash under tap water). He wet mounts it in tap water and immediately examines it under the microscope to report sample adequacy.

The remaining smears are placed in a Coplin jar containing liquid fixative (1:1 mixture of absolute alcohol and ether). These smears are later sent to the pathology department for staining with Papanicolaou (PAP) stain [4]. Alternatively, spray fixation of the smears can be performed.

14.3.2 Role of Onsite Cytopathologist

Presence of an onsite cytopathologist improves the diagnostic yield of EUS-FNA. The rate of non-diagnostic or inadequate samples in absence of a pathologist is 13–19%; this drops to 1.6–20.4% in presence of a pathologist. Immediate on-site evaluation of specimen adequacy reduces unsatisfactory samples, increases sensitivity and thus the overall accuracy of EUS-FNA. Time, money and expertise are the primary reasons for non availability of rapid onsite assessment [5–7].

The utility of onsite cytopathology was studied at our center. Using a retrospective – prospective comparative study, the pathological yield of 116 retrospective samples without onsite pathologist was compared to 44 prospective samples collected in presence of a pathologist. Conclusive reports were obtained in 82.8% patients in the 'pathologist absent' group as against 100% in the 'pathologist present' group ($p < 0.05$) [8]. The minimum number of slides to be examined to ensure adequacy varies; Jhala et al. reviewed an average 15 Diff-Quick stained slides (Range: 4–34) to report sample adequacy in pancreatic EUS-FNA [9].

14.3.3 Staining of Cytology Smears

The pathologist chooses the stain to be used. Papanicolaou stain is the commonest used to stain cytology smears as both the nucleus and cytoplasm are stained well [4]. The Giemsa, Diff-Quik [10], Hematoxylin – Eosin (H & E) [11], May-Grunwald-Giemsa (MGG) stain and others can also be used.

Ziehl-Neelsen stain must be used for examination of caseous material to identify Acid Fast Bacilli (AFB) and diagnose tuberculosis.

Liquid preservation of aspirated material (Preserv Cyt) followed by thin prep slides has also been performed; however the accuracy of this technique is inferior to that of conventional cytology.

14.4 Clot Biopsy in 10% Formalin

The aspirated material contains clot and material. After preparing cytology smears, the clot and remaining material is placed in 10% formalin. This material is later processed like a histopathology specimen and sections and slides can be prepared. EUS guided core biopsies (using Tru-Cut or Pro-Core needles) must also be processed in this manner [12]. Clot and core biopsies are especially important when immunohistochemistry (IHC) staining is required, e.g. samples from lymph nodes suspected to harbor lymphoma or metastatic carcinoma, neuroendocrine tumors (NET) and gastrointestinal stromal tumors (GIST).

14.5 Fluid Analysis and Cytology

Analysis of fluid aspirated by EUS-FNA is an integral part of the pathological examination. Fluid may be aspirated from serous or cystic mucinous pancreatic neoplasms, pancreatic pseudocysts or other benign cysts or cystic degeneration in malignant tumors. Thick, caseous material may be aspirated from tubercular lymph nodes. Small pleural or peritoneal fluid collections can be aspirated by EUS [11, 13].

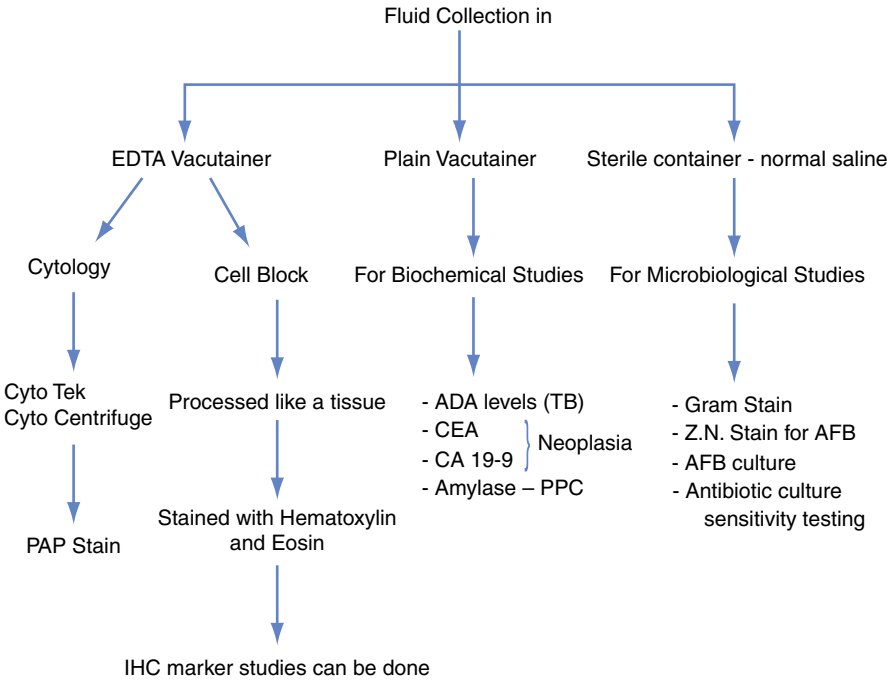

Fig. 14.1 Algorithm for fluid analysis (*ADA* adenosine deaminase, *TB* tuberculosis, *CEA* Carcinoembryonic antigen, *CA* 19–9 Carbohydrate antigen, *PPC* pancreatic pseudocyst, *ZN* Ziehl-Neelsen, *AFB* Acid fast bacilli, *PAP* Papanicolaou, *IHC* immunohistochemistry)

An algorithm for fluid analysis is shown in Fig. 14.1. Fluid must be used judiciously so that all relevant tests can be performed and if necessary, it should be refrigerated for preservation for further tests required at a later date.

References

1. Hajdu SI (1977) Cytology from antiquity to Papanicolaou. Acta Cytol 21(5):668–676
2. Wallace MB, Kennedy T, Durkalski V et al (2001) Randomized controlled trial of EUS-guided fine needle aspiration techniques for the detection of malignant lymphadenopathy. Gastrointest Endosc 54(4):441–447. doi:S0016510701559982 [pii]
3. LeBlanc JK, Ciaccia D, Al-Assi MT et al (2004) Optimal number of EUS-guided fine needle passes needed to obtain a correct diagnosis. Gastrointest Endosc 59(4):475–481. doi:S0016510703028633 [pii]
4. Morse A (2002) Diagnostic cytopathology: specimen collection and preparation. In: Bancroft JD, Gamble M (eds.) Theory and practice of histological techniques, 5th edn. Churchill Livingstone, London, pp 621–636
5. Alsohaibani F, Girgis S, Sandha GS (2009) Does onsite cytotechnology evaluation improve the accuracy of endoscopic ultrasound-guided fine-needle aspiration biopsy? Can J Gastroenterol 23(1):26–30

6. Klapman JB, Logrono R, Dye CE et al (2003) Clinical impact of on-site cytopathology interpretation on endoscopic ultrasound-guided fine needle aspiration. Am J Gastroenterol 98(6):1289–1294. doi:S0002927003002466 [pii] 10.1111/j.1572-0241.2003.07472.x
7. Nasuti JF, Gupta PK, Baloch ZW (2002) Diagnostic value and cost-effectiveness of on-site evaluation of fine-needle aspiration specimens: review of 5,688 cases. Diagn Cytopathol 27(1):1–4. doi:10.1002/dc.10065
8. Bapaye A, Aher A, Bhide V et al (2010) A single center experience of EUS guided fine needle aspiration cytology (FNAC) in pancreatic mass lesions. J Gastroenterol Hepatol 25(suppl 2):A151
9. Jhala NC, Jhala D, Eltoum I et al (2004) Endoscopic ultrasound-guided fine-needle aspiration biopsy: a powerful tool to obtain samples from small lesions. Cancer 102(4):239–246. doi:10.1002/cncr.20451
10. Chhieng DC, Jhala D, Jhala N et al (2002) Endoscopic ultrasound-guided fine-needle aspiration biopsy: a study of 103 cases. Cancer 96(4):232–239. doi:10.1002/cncr.10714
11. Wilson I, Gamble M (2002) The hematoxylins and eosin. In: Bancroft JD, Gamble M (eds.) Theory and practice of histological techniques, 5th edn. Churchill Livingstone, London, pp 125–138
12. Anderson G, Bancroft J (2002) Tissue processing and microtomy. In: Bancroft JD, Gamble M (eds.) Theory and practice of histological techniques, 5th edn. Churchill Livingstone, London, pp 85–107
13. Dabbs DJ (2006) Immunohistology of metastatic carcinoma of unknown primary. In: Dabbs D (ed.) Diagnostic immunohistochemistry, 2nd edn. Churchill Livingstone Elsevier, pp 180-226

EUS-FNA of the Esophagus and Mediastinum

15

Amol Bapaye and Advay Aher

15.1 Introduction

EUS is accurate in identification and evaluation of mediastinal mass lesions. Tissue acquisition of these lesions has always been a challenging task. FNA can be performed under EUS guidance under real-time vision with precise needle control and accurate needle placement inside the tumor. Doppler further improves safety of the procedure. A majority of mediastinal lesions do not require surgery as primary treatment, and therefore EUS helps to prevent an unnecessary thoracotomy in these patients [1, 2].

The detailed technique of EUS-FNA has been described in Chap. 13. In this chapter, we shall discuss specific tips regarding mediastinal FNA. The diagnostic criteria of mediastinal lesions on EUS and cytopathology are also discussed.

A. Bapaye, M.D. (M.S.) (✉)
Department of Digestive Diseases and Endoscopy,
Deenanath Mangeshkar Hospital and Research Center,
Erandwane, Pune 411004, Maharashtra, India
e-mail: amolbapaye@gmail.com

A. Aher
Clinical Research Fellow, Department of Digestive Diseases and Endoscopy,
Deenanath Mangeshkar Hospital and Research Center,
Erandwane, Pune 411004, Maharashtra, India

K. Akahoshi, A. Bapaye (eds.), *Practical Handbook of Endoscopic Ultrasonography*,
DOI 10.1007/978-4-431-54014-4_15, © Springer 2012

15.2 Indications for Trans-esophageal (TE) EUS-FNA

- Submucosal tumors of the esophagus
- FNA of contralateral enlarged lymph nodes for staging of lung cancer
- Unexplained mediastinal lymphadenopathy
- Suspected lung cancer with negative bronchoscopy and presence of a paraesophageal mass
- Restaging after induction chemotherapy
- Evaluation of unknown mediastinal mass lesions
- Evaluation of cystic mediastinal mass lesions (high risk of infection must be anticipated)

15.3 Specific Technique, Tricks and Tips for TE EUS-FNA

Lesions in the mediastinum or esophageal wall must be targeted for FNA through the esophageal wall.

1. The esophagus is a tubular organ, and the FNA needle tends to exit parallel to the wall. It may sometimes be difficult to puncture the esophageal wall or the lesion as the needle tends to push the endoscope tip away from the wall, thereby obscuring EUS vision. Constant upward tip deflection must be maintained during FNA to prevent this occurrence.
2. Mediastinal organs are surrounded by major vascular structures. While performing FNA, care must be taken to prevent injury to these structures. Although a trans-aortic approach for EUS-FNA has been described, it is not recommended as routine practice [3].
3. The needle should never traverse the primary tumor to reach a lymph node while performing FNA (especially in patients of esophageal cancer).
4. EUS-FNA of cystic mediastinal lesions is associated with high risk of post procedure mediastinitis [4–6]. FNA in these cases should be performed only for a strong indication. If aspiration is performed, the entire cyst should be aspirated and antibiotics must be prescribed to prevent infection.
5. While performing FNA of mediastinal lymph nodes, it is preferable to select the largest node. Avoid necrotic lymph nodes as only necrotic cells may be aspirated and no diagnosis will be possible.
6. The retroperitoneum must always be scanned prior to FNA; it is possible that the disease process extends beyond the diaphragm. Mediastinal lymph nodes may often be reactive or inflammatory, especially those found in patients with chronic obstructive lung disease. In these patients, FNA of the retroperitoneal lymph nodes may provide better diagnostic accuracy.

7. EUS-FNA of lymph nodes is often characterized by an unacceptably bloody sample on aspiration and can limit interpretation by the cytopathologist. Performing FNA without applying suction has been suggested as an option to minimize a bloody aspirate.

15.4 Differential Diagnosis of Esophageal and Mediastinal Mass Lesions

Submucosal tumors (SMT) of the esophagus are leiomyoma, gastrointestinal stromal tumor (GIST), lipoma, fibroma etc. FNA of SMT's is discussed separately in Chap. 17.

Masses in the posterior mediastinum may be as follows –

1. Lymph node mass or enlarged lymph nodes
2. Solid tumors arising from the bronchus or esophagus
3. Metastatic cancers
4. Neurogenic tumors
5. Cystic mediastinal masses
6. Infective (mediastinal abscess)

A majority of mediastinal mass lesions arise from lymph nodes. Although no standard guideline to differentiate between enlarged discreet lymph nodes and a lymph node mass exists, a nodal mass is usually larger in size than a single enlarged node and is formed by conglomeration (matting) of several lymph nodes.

15.4.1 Mediastinal Lymphadenopathy May Occur Due to –

- Malignancy – lymphoma or metastases from thoracic or extra thoracic malignancy
- Benign or inflammatory – reactive lymph nodes, tuberculosis, sarcoidosis or histoplasmosis

15.4.1.1 Malignant Lymphadenopathy

Although largely dependent on local demographics and referral patterns, the rate of diagnosis of malignancy in unclassified mediastinal lymphadenopathy may be up to 50%, with majority of tumors being pulmonary in origin [1, 7, 8]. Sensitivity, specificity and accuracy of EUS-FNA for diagnosis of malignant mediastinal lymphadenopathy is >90% [1, 8, 9].

EUS-FNA further improves the diagnostic accuracy (Fig. 15.1b).

EUS Appearance of Malignant Lymphadenopathy – [10, 11] (Fig. 15.1a)

1. Round shape
2. Hypoechoic echo pattern
3. Well demarcated border
4. Short axis diameter of more than 10 mm

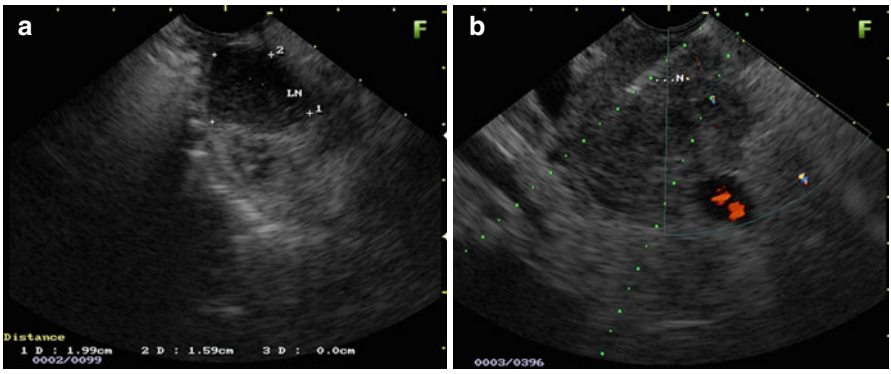

Fig. 15.1 (**a**) EUS shows rounded hypoechoic enlarged lymph node with well demarcated borders classical of malignant involvement, (**b**) EUS guided FNA from a lymph node mass

Fig. 15.3 (**a**) Linear EUS showing large, multiple, rounded lymph nodes in the AP window, (**b**) cytopathology showing atypical lymphoid cells showing irregular nuclear membranes with large hyperchromatic nuclei classical of lymphoma (PAP 40×)

Metastatic Cancer

Metastatic lymphadenopathy commonly occurs from bronchial tumors, or less frequently from an extra thoracic malignancy. Metastases from cancers of the breast, kidney, colon, pancreas, testicular and esophagus have been reported (Fig. 15.2a, b).

Non-Hodgkin's Lymphoma (NHL)

NHL presenting as mediastinal lymphadenopathy can be diagnosed by EUS-FNA (Fig. 15.3a, b). For diagnosis of NHL, the sample should be subjected to cytology, immuno-cytochemistry and flow cytometry. Addition of flow cytometry to cytology has shown to improve accuracy from 44% to 86% [12]. It is therefore important to collect adequate samples from the node for all these tests. Granulomas may be present in lymphomatous nodes; adequate samples must therefore be collected even if a granulomatous pathology is suspected on initial cytological examination. For low grade lymphomas, a Trucut needle biopsy may be necessary to assess architectural evaluation of the node [13].

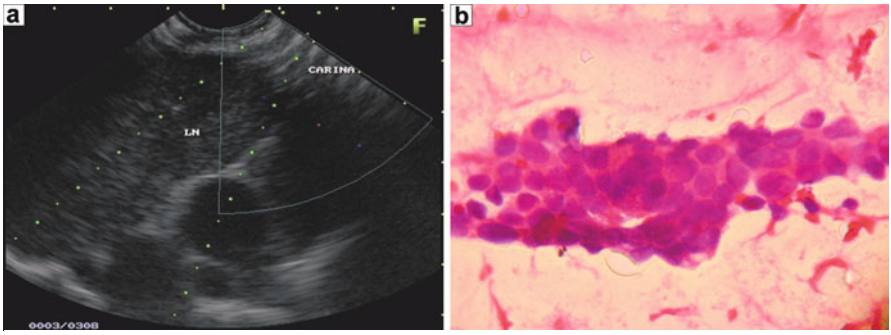

Fig. 15.2 (**a**) Linear EUS showing a large hypoechoic sub carinal lymph node, (**b**) cytopathology showing cluster of malignant epithelial cells: metastatic adenocarcinoma in a known case of previously treated rectal cancer (PAP 10×)

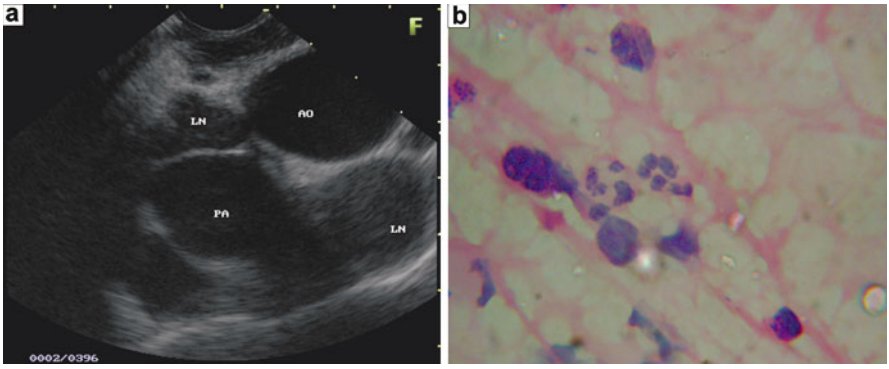

15.4.1.2 Benign or Inflammatory Lymphadenopathy

Reactive Lymph Nodes

Reactive lymph nodes may be seen when there is history of past infection.

EUS and Cytopathological Appearance [10, 11] (Fig. 15.4)

1. Oval shape
2. Isoechoic
3. Short axis diameter less than 10 mm
4. Preservation of hilar architecture seen as a bright hyperechoic area
5. Cytopathology shows reactive and hyperplastic lymphoid elements

Fig. 15.4 Linear EUS showing oval isoechoic lymph node with preservation of hilar architecture suggestive of reactive lymph node

Tuberculosis

Lymph nodal tuberculosis is commonly seen in endemic geographical regions with high incidence of this disease, but should also be considered in immuno-compromised patients [14, 15].

EUS and Cytopathological Appearance (Fig. 15.5a–c)

1. Tubercular lymph nodes may appear as enlarged, multiple, discreet nodes or may be seen as a necrotic matted nodal mass
2. FNA will often aspirate cheesy, caseous material, especially while aspirating large matted necrotic masses
3. Cytology shows epitheloid granulomas and presence of Langhan's giant cells
4. Acid fast bacilli may be seen on Ziehl-Nielsen stain

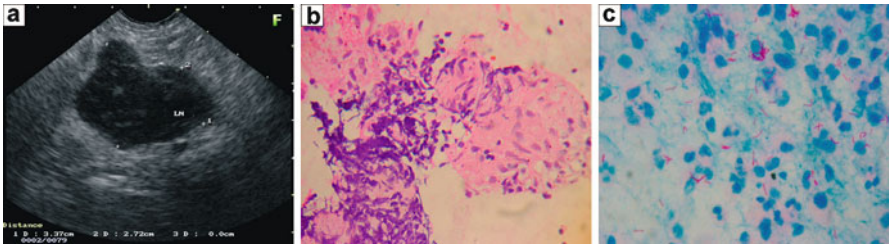

Fig. 15.5 (**a**) Linear EUS showing matted enlarged lymph nodes, (**b**) cytology showing an epithelial cell cluster with ill defined cytoplasmic borders and vesicular slipper shaped nuclei consistent with tubercular inflammation (PAP 40×), (**c**) cytology showing bright red staining beeded long slender acid-fast bacilli against a blue background in a case of tubercular lymphadenitis

When the suspected diagnosis is tuberculosis, it is advisable to collect additional material for polymerase chain reaction (PCR) testing of Mycobacterium tuberculosis and for culture [16].

Sarcoidosis

Sarcoidosis is a systemic granulomatous disease that typically affects the mediastinal lymph nodes. EUS shows multiple discreet enlarged hypoechoic lymph nodes. FNA usually reveals non caseating granulomas. (Fig. 15.6a, b) Final diagnosis is often by exclusion of other granulomatous disease since there are no pathognomonic laboratory tests. Serum angiotensin converting enzyme (ACE) levels may be elevated in patients with sarcoidosis.

EUS-FNA has high accuracy in diagnosis of sarcoidosis (90% sensitivity, 95% specificity) [17–19].

Histoplasmosis

Histoplasmosis is caused by Histoplasma capsulatum and is found worldwide. It must be suspected in areas endemic for Histoplasma infection. The lymph nodes in this condition are often necrotic, matted and may form a mass. The esophageal wall may show focal thickening. Calcification may be seen within the lymph nodes. FNA shows granulomas [20].

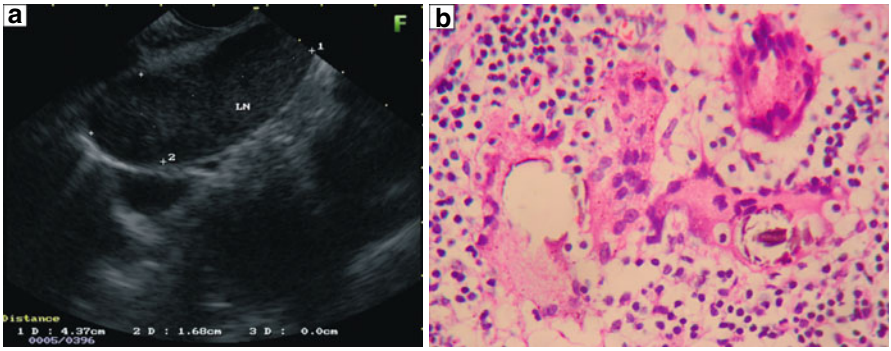

Fig. 15.6 (**a**) Linear EUS showing enlarged hypoechoic lymph nodes, (**b**) section from clot in formalin showing giant cell with calcification: Schaumann bodies, suggestive of sarcoidosis (H&E, 40×)

15.4.2 Solid Mediastinal Masses

Solid mediastinal mass lesions are most often pulmonary tumors extending into the mediastinum or metastases from extra thoracic malignancies. EUS-FNA can be performed for tumors adjacent to the esophagus [21].

Neurogenic tumors are of various types (schwannoma, neurilemoma, neurofibroma, ganglioneuroma, ganglioneuroblastoma, neuroblastoma or paraganglionoma). They are the commonest primary posterior mediastinal tumors and account for 75% of all the primary posterior mediastinal tumors [22]. Malignancy may be seen in 10–20% tumors. EUS-FNA can diagnose schwannoma (Fig. 15.7a, b) [23].

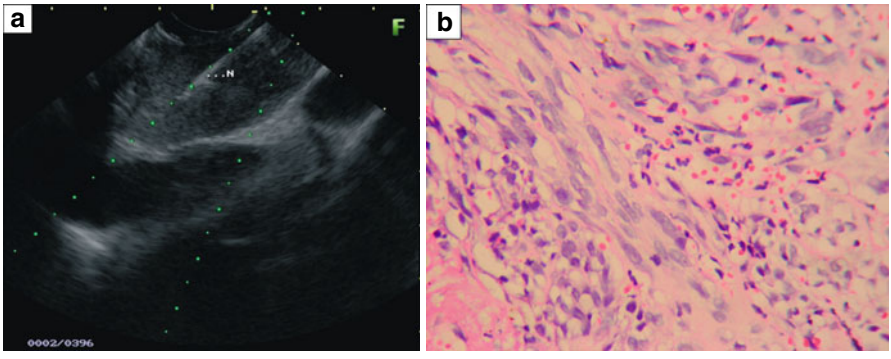

Fig. 15.7 (**a**) Linear EUS showing hypoechoic mediastinal mass, (**b**) section from clot in formalin showing spindle shaped cells with elongated nuclei suggestive of shwannoma (H&E, 40×)

15.4.3 Cystic Mediastinal Masses

Mediastinal cysts are most often congenital foregut cysts and account for 10–15% of all mediastinal mass lesions [24, 25]. Based on their location, they are classified as either esophageal duplication cysts when they are adherent to the wall of the esophagus or bronchogenic cysts when situated at a distance from the esophagus.

EUS Appearance (Fig. 15.8a–c)

1. Round, oval or tubular anechoic structure with wall enhancement
2. Usually it is difficult to differentiate between bronchogenic and esophageal origin of the cyst
3. Wall enhancement and sometimes a multilayered wall structure are seen
4. The contents may be fluid with a layer of dead epithelial cells, or often may be thick, gelatinous material which is hypo rather than anechoic. This may lead to confusion as to whether the lesion is a cyst or a mass

Fig. 15.8 Linear EUS showing (**a**) esophageal duplication cyst, (**b**) bronchogenic cyst, (**c**) mediastinal cyst

EUS-FNA is usually avoided in mediastinal cysts as this may cause infection and mediastinitis [4–6]. The commonest reason for performing FNA is misdiagnosis of the cyst as a solid mass lesion [26, 27]. If aspiration is performed, the cyst must be completely aspirated and antibiotics must be prescribed. Surgery may be required if mediastinitis develops.

15.4.4 Mediastinal Abscess or Mediastinitis

Acute mediastinitis and abscess can occur after thoracic surgery or esophageal perforation. The abscess on EUS usually appears as a well demarcated fluid collection with heterogeneous contents. Mediastinal abscess can be subjected to EUS-FNA to aspirate the pus and to subject material for microbiological examination and culture [28]. A mediastinal abscess has also been drained into the esophagus under EUS guidance using a pigtail stent [29].

15.5 Mediastinal EUS-FNA Compared to Other Methods of Tissue Diagnosis

Apart from EUS-FNA, the other methods for tissue diagnosis in the mediastinum include trans-bronchial FNA (TB-FNA), percutaneous CT guided FNA, Mediastinoscopy, VATS and exploratory thoracotomy.

TB-FNA is a blind procedure and therefore has applicability limited to the sub carinal area [30, 31]. Percutaneous CT guided FNA is not recommended for posterior mediastinal lesions due to the risk of bleeding or pneumothorax [20]. Mediastinoscopy is highly effective in evaluation and performing biopsy in the superior mediastinum, and can provide solid tissue rather than a cytological aspirate for diagnosis. However, it cannot be used for lesions situated below the great vessels and aortic arch. It is invasive, requires general anesthesia and has a 2% morbidity rate [32]. VATS and thoracotomy are invasive procedures best reserved for therapeutic intervention. EUS-FNA has been proven to significantly reduce the need for thoracic surgery [1].

References

1. Savides TJ, Perricone A (2004) Impact of EUS-guided FNA of enlarged mediastinal lymph nodes on subsequent thoracic surgery rates. Gastrointest Endosc 60(3):340–346. doi:S0016510704017092 [pii]
2. Larsen SS, Krasnik M, Vilmann P et al (2002) Endoscopic ultrasound guided biopsy of mediastinal lesions has a major impact on patient management. Thorax 57(2):98–103
3. von Bartheld MB, Rabe KF, Annema JT (2009) Transaortic EUS-guided FNA in the diagnosis of lung tumors and lymph nodes. Gastrointest Endosc 69(2):345–349. doi:S0016-5107(08)02091-9 [pii] 10.1016/j.gie.2008.06.021
4. Wildi SM, Hoda RS, Fickling W et al (2003) Diagnosis of benign cysts of the mediastinum: the role and risks of EUS and FNA. Gastrointest Endosc 58(3):362–368. doi:S0016510703017358 [pii]
5. Ryan AG, Zamvar V, Roberts SA (2002) Iatrogenic candidal infection of a mediastinal foregut cyst following endoscopic ultrasound-guided fine-needle aspiration. Endoscopy 34(10): 838–839. doi:10.1055/s-2002-34262
6. Wiersema MJ, Vilmann P, Giovannini M et al (1997) Endosonography-guided fine-needle aspiration biopsy: diagnostic accuracy and complication assessment. Gastroenterology 112(4): 1087–1095. doi:S0016508597001546 [pii]

7. Catalano MF, Nayar R, Gress F et al (2002) EUS-guided fine needle aspiration in mediastinal lymphadenopathy of unknown etiology. Gastrointest Endosc 55(7):863–869. doi:S0016510702574836 [pii]
8. Fritscher-Ravens A, Sriram PV, Bobrowski C et al (2000) Mediastinal lymphadenopathy in patients with or without previous malignancy: EUS-FNA-based differential cytodiagnosis in 153 patients. Am J Gastroenterol 95(9):2278–2284. doi:S0002-9270(00)01035-2 [pii] 10.1111/j.1572-0241.2000.02243.x
9. Eloubeidi MA, Cerfolio RJ, Chen VK et al (2005) Endoscopic ultrasound-guided fine needle aspiration of mediastinal lymph node in patients with suspected lung cancer after positron emission tomography and computed tomography scans. Ann Thorac Surg 79(1):263–268. doi:S0003-4975(04)01425-0 [pii] 10.1016/j.athoracsur.2004.06.089
10. Vassallo P, Wernecke K, Roos N et al (1992) Differentiation of benign from malignant superficial lymphadenopathy: the role of high-resolution US. Radiology 183(1):215–220
11. Vassallo P, Edel G, Roos N et al (1993) In-vitro high-resolution ultrasonography of benign and malignant lymph nodes. A sonographic-pathologic correlation. Invest Radiol 28(8): 698–705
12. Ribeiro A, Vazquez-Sequeiros E, Wiersema LM et al (2001) EUS-guided fine-needle aspiration combined with flow cytometry and immunocytochemistry in the diagnosis of lymphoma. Gastrointest Endosc 53(4):485–491. doi:S0016-5107(01)24438-1 [pii] 10.1067/mge.2001.112841
13. Levy MJ, Jondal ML, Clain J et al (2003) Preliminary experience with an EUS-guided trucut biopsy needle compared with EUS-guided FNA. Gastrointest Endosc 57(1):101–106. doi:10.1067/mge.2003.49 S0016510703500256 [pii]
14. Song HJ, Park YS, Seo DW et al (2010) Diagnosis of mediastinal tuberculosis by using EUS-guided needle sampling in a geographic region with an intermediate tuberculosis burden. Gastrointest Endosc 71(7):1307–1313. doi:S0016-5107(10)00132-X [pii] 10.1016/j.gie.2010.01.059
15. Puri R, Vilmann P, Sud R et al (2010) Endoscopic ultrasound-guided fine-needle aspiration cytology in the evaluation of suspected tuberculosis in patients with isolated mediastinal lymphadenopathy. Endoscopy 42(6):462–467. doi:10.1055/s-0029-1244133
16. Sriram PVJ, Kaffes AJ, Rajasekhar P et al (2004) EUS features of mediastinal tuberculosis: a PCR based cytodiagnosis by transesophageal EUS-FNA. Gastrointest Endosc 59:AB216
17. Wildi SM, Judson MA, Fraig M et al (2004) Is endosonography guided fine needle aspiration (EUS-FNA) for sarcoidosis as good as we think? Thorax 59(9):794–799. doi:10.1136/thx.2003.009472 59/9/794 [pii]
18. Fritscher-Ravens A, Sriram PV, Topalidis T et al (2000) Diagnosing sarcoidosis using endosonography-guided fine-needle aspiration. Chest 118(4):928–935
19. Annema JT, Veselic M, Rabe KF (2005) Endoscopic ultrasound-guided fine-needle aspiration for the diagnosis of sarcoidosis. Eur Respir J 25(3):405–409. doi:25/3/405 [pii] 10.1183/09031936.05.00098404
20. Savides TJ (2006) EUS diagnosis of posterior mediastinal masses, lymph nodes, and cysts. In: Hawes R, Fockens P (eds) Endosonography, 1st edn. Elsevier, Philadelphia, pp 85–94
21. Varadarajulu S, Hoffman BJ, Hawes RH et al (2004) EUS-guided FNA of lung masses adjacent to or abutting the esophagus after unrevealing CT-guided biopsy or bronchoscopy. Gastrointest Endosc 60(2):293–297. doi:S0016510704016803 [pii]
22. Macchiarini P, Ostertag H (2004) Uncommon primary mediastinal tumours. Lancet Oncol 5(2):107–118. doi:10.1016/S1470-2045(04)01385-3 S1470204504013853 [pii]
23. McGrath KM, Ballo MS, Jowell PS (2001) Schwannoma of the mediastinum diagnosed by EUS-guided fine needle aspiration. Gastrointest Endosc 53(3):362–365. doi:S0016510701794588 [pii]
24. Ribet ME, Copin MC, Gosselin B (1995) Bronchogenic cysts of the mediastinum. J Thorac Cardiovasc Surg 109(5):1003–1010. doi:S0022-5223(95)70327-6 [pii]
25. Snyder ME, Luck SR, Hernandez R et al (1985) Diagnostic dilemmas of mediastinal cysts. J Pediatr Surg 20(6):810–815. doi:S0022346885001671 [pii]

26. Westerterp M, van den Berg JG, van Lanschot JJ et al (2004) Intramural bronchogenic cysts mimicking solid tumors. Endoscopy 36(12):1119–1122. doi:10.1055/s-2004-826042
27. Eloubeidi MA, Cohn M, Cerfolio RJ et al (2004) Endoscopic ultrasound-guided fine-needle aspiration in the diagnosis of foregut duplication cysts: the value of demonstrating detached ciliary tufts in cyst fluid. Cancer 102(4):253–258. doi:10.1002/cncr.20369
28. Fritscher-Ravens A, Schirrow L, Pothmann W et al (2003) Critical care transesophageal endosonography and guided fine-needle aspiration for diagnosis and management of posterior mediastinitis. Crit Care Med 31(1):126–132. doi:10.1097/01.CCM.0000045024.16388.96
29. Kahaleh M, Yoshida C, Kane L et al (2004) EUS drainage of a mediastinal abscess. Gastrointest Endosc 60(1):158–160. doi:S0016510704013100 [pii]
30. Toloza EM, Harpole L, Detterbeck F et al (2003) Invasive staging of non-small cell lung cancer: a review of the current evidence. Chest 123(1 Suppl):157S–166S
31. Annema JT, Veselic M, Rabe KF (2004) Analysis of subcarinal lymph nodes in (suspected) non-small-cell lung cancer after a negative transbronchial needle aspiration – what's next? A preliminary report. Respiration 71(6):630–634. doi:RES2004071006630 [pii] 10.1159/000081765
32. Hammoud ZT, Anderson RC, Meyers BF et al (1999) The current role of mediastinoscopy in the evaluation of thoracic disease. J Thorac Cardiovasc Surg 118(5):894–899. doi:S002252239900481X [pii]

EUS-FNA of Lesions of the Pancreas, Biliary Tract, and Liver

16

Amol Bapaye and Advay Aher

16.1 Introduction

Preoperative tissue diagnosis of mass lesions in the biliary pancreatic region has always been a challenging task. EUS guided fine needle aspiration (FNA) provides an impressive solution to this preoperative dilemma. EUS permits real-time imaging from close quarters which allows precise control and accurate needle placement and permits accurate biopsy to be performed.

The detailed technique of EUS-FNA is discussed in Chap. 13. We present here the technical tips to perform EUS-FNA in the biliary pancreatic region and discuss the differential diagnosis based upon EUS appearance and cytopathology.

16.2 Indications

- Mass lesions detected or suspected on other imaging modalities – Ultrasonography, CT scan, MRI or previous EUS examination
- Cystic lesions in the pancreas or peripancreatic area
- Enlarged lymph nodes or masses in the peripancreatic, periportal or retroperitoneal region
- Histological staging of biliary-pancreatic cancer
- Paracentesis of ascites for diagnosis of peritoneal disease

A. Bapaye, M.D. (M.S.) (✉)
Department of Digestive Diseases and Endoscopy, Deenanath Mangeshkar Hospital and Research Center, Erandwane, Pune 411004, Maharashtra, India
e-mail: amolbapaye@gmail.com

A. Aher
Clinical Research Fellow, Department of Digestive Diseases and Endoscopy, Deenanath Mangeshkar Hospital and Research Center, Erandwane, Pune 411004, Maharashtra, India

K. Akahoshi, A. Bapaye (eds.), *Practical Handbook of Endoscopic Ultrasonography*,
DOI 10.1007/978-4-431-54014-4_16, © Springer 2012

16.3 Specific Technique, Tips and Tricks to Perform FNA

16.3.1 FNA of Pancreatic Lesions

Pancreatic tumors are typically hard in consistency and difficult to FNA. The tumors are fibrotic and FNA yield is typically pauci-cellular. Multiple passes may be necessary to obtain adequate samples for cytopathology [1]. Specific tricks are often necessary to obtain satisfactory FNA samples from these tumors.

16.3.1.1 Pancreatic Head Lesions and Peripancreatic Lymph Nodes

1. FNA is performed from the duodenal bulb.
2. Position the echoendoscope in the long loop wedged against the apex of the duodenal bulb (Fig. 16.1a).
3. Perform FNA using a 22G needle. For very hard fibrotic lesions, 25G may be used. 19G needle is difficult to manipulate in this location and is seldom used.
4. Take precaution to ensure that the needle sheath does not retract into the endoscope during loop formation (Fig. 16.1b, c).
5. Maintain the endoscope close to the duodenal wall at all times using the up/down wheel to prevent it from being deflected away from the wall by the needle pushing into the tissue. Lock the wheels if necessary.
6. Make minimal use of the endoscope elevator during passage of the needle.
7. Use the "plant and push maneuver" (Fig. 13.4) to puncture hard tumors.
8. Make multiple passes; it is helpful to have an onsite cytopathologist to ascertain sample adequacy [2–6].
9. Lymph nodes are often situated posterior to the pancreatic head, and the echoendoscope must be maintained in an awkward position to obtain the correct needle trajectory.

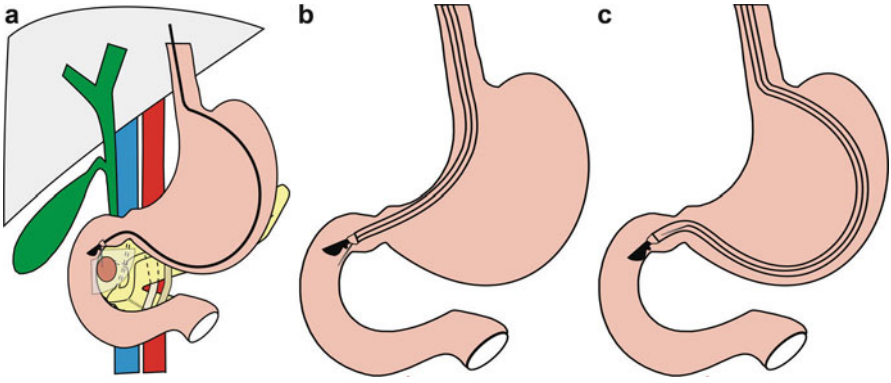

Fig. 16.1 Diagrammatic representation of (**a**) Endoscope position for pancreatic head scanning; (**b**, **c**) showing retraction of the needle within the scope while loop formation

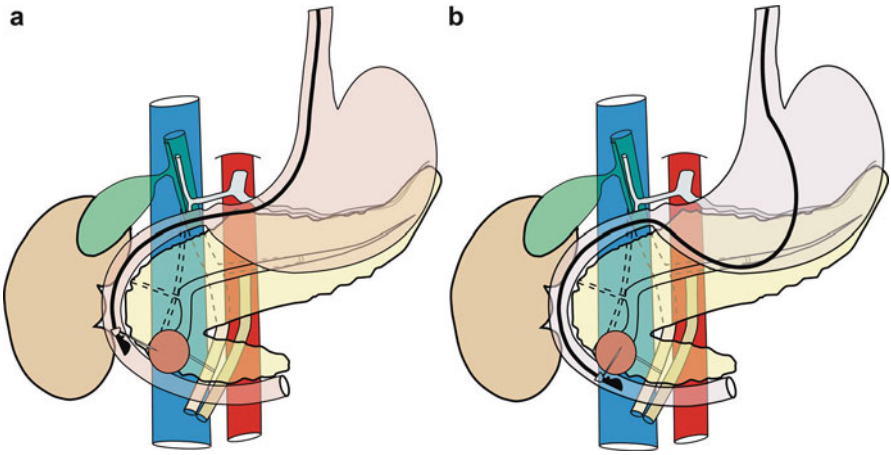

Fig. 16.2 FNA of uncinate lesions – (**a**) Diagrammatic representation showing endoscope tip deflection away from the duodenal wall thereby preventing effective puncture and (**b**) showing corrected position of endoscope

16.3.1.2 Uncinate Process Lesions

1. FNA is performed from the third part of duodenum.
2. The endoscope is in short loop position and needle exits easily. However the endoscope tip lies free in the duodenum and is difficult to fix against the wall. During puncture, the needle tends to push the free endoscope tip away from the wall (Fig. 16.2a).
3. Correct the position by pushing the endoscope deeper into the third part and angling the tip upwards. This wedges the endoscope tip against the wall and permits the needle to pass into the tumor (Fig. 16.2b).

16.3.1.3 Pancreatic Body

1. Perform FNA through the stomach. Exercise appropriate judgment to ascertain the benefits of preoperative FNA of a potentially malignant tumor against the risk of tumor seedling in the gastric wall.
2. Maintain the endoscope in straight position.
3. Maintain endoscope tip in close opposition to the gastric wall to prevent it from swinging away during puncture.
4. Small lesions are often sampled using the two step technique. (Refer Chap. 13)

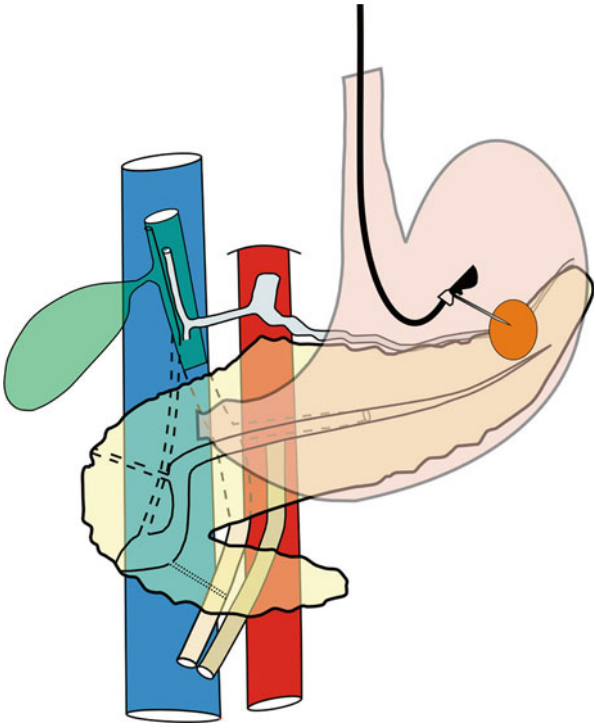

Fig. 16.3 EUS-FNA of pancreatic tail lesions – diagrammatic representation

16.3.1.4 Pancreatic Tail, Lesions at the Splenic Hilum and Left Adrenal Gland (Fig. 16.3)

1. Trans-gastric route for FNA, endoscope is in partly retroflexed position.
2. Due to the acute angle, advancing the needle and puncture is difficult. Push the endoscope further inside to form a longer loop; this may provide adequate leverage for puncture.

16.3.2 FNA at Other Locations

16.3.2.1 Lymph Nodes at Porta Hepatis

1. Perform FNA from the duodenal bulb with the transducer turned upwards facing the liver hilum. To achieve this position, insert the endoscope into the descending duodenum using the standard maneuver, and withdraw slowly with a clockwise torque up to the duodenal bulb. The structures at the porta hepatis can be seen.
2. Maintaining a stable position during FNA is challenging as the endoscope tends to slip back into the antrum. Inflate the balloon and/or request an assistant to hold the endoscope at the patient's mouth.

16.3.2.2 Intraductal Tumors of the Common Bile Duct (CBD)

1. Use a 25G needle
2. Position needle deep within tumor prior to suction to prevent sample contamination by bile
3. Use short to and fro movements of the needle to avoid aspiration of bile
4. If bile is aspirated, collect in a separate container to be processed as a centrifuged sample and repeat FNA from the solid area

16.3.2.3 Lesions of the Gall Bladder

1. Tumors of the gall bladder or focal areas of wall thickening may be subjected to EUS-FNA [7].
2. Take care – FNA of an over distended gall bladder in presence of biliary obstruction may cause biliary leak

16.3.2.4 Ampullary Lesions

1. FNA is necessary only for intramural lesions within the ampulla; lesions at the orifice or ulcerated lesions should be biopsied by duodenoscopy
2. Fill the duodenum with water and abolish peristalsis for clear views of the ampulla
3. Lesions are typically small, soft but discreet. They tend to slip from the needle during puncture
4. Use a 25G needle for FNA

16.4 Diagnosis of Solid Pancreatic Tumors

16.4.1 Pancreatic Adenocarcinoma

This is the commonest tumor occurring in the pancreas. EUS-FNA has high sensitivity and specificity for diagnosis of pancreatic adenocarcinoma [8, 9].

Typical EUS and Cytopathology Findings (Fig. 16.4a, b)

1. Focal hypoechoic mass in pancreas
2. Small lesions <2 cm are generally well circumscribed and homogeneous
3. Larger lesions are inhomogeneous, have poorly defined margins, and show areas of fibrosis. Anechoic areas within the tumor represent necrosis
4. Calcification within the tumor is rare, unless tumor has developed in underlying chronic pancreatitis
5. Pancreatic duct (MPD) often shows upstream uniform dilatation (as against chronic pancreatitis which shows irregular duct walls). Follow a dilated MPD from the body to the head to locate a small pancreatic tumor
6. Surrounding pancreatic tissue is usually normal in appearance (unless there is underlying chronic pancreatitis)
7. FNA is typically pauci-cellular. Cytology shows pleomorphic cells with large hyperchromatic nuclei, nucleoli and mitotic figures arranged in a vague adenoid pattern

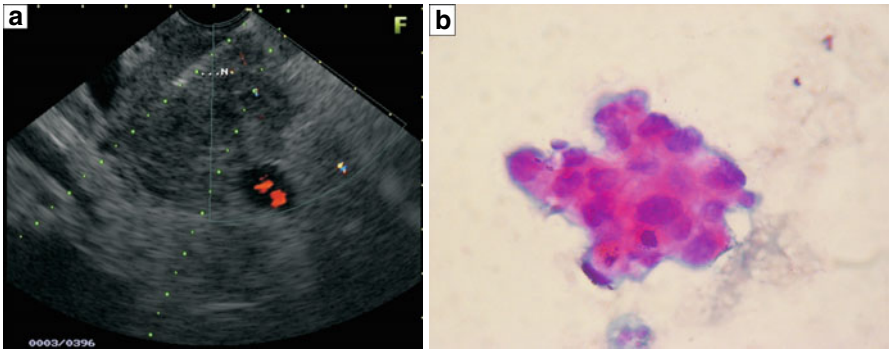

Fig. 16.4 (**a**) EUS-FNA of a large pancreatic mass, (**b**) cytology smear shows a cluster of malignant cells with large hyperchromatic nuclei arranged in vague adenoid pattern – pancreatic adenocarcinoma (PAP, 40×)

16.4.2 Neuroendocrine Tumors of the Pancreas (PNET's)

PNET's comprise about 10% of all tumors of the pancreas. They are of two types – functional (fPNET) – 70% to 85% and non functional (nfPNET) – 15% to 30%, depending upon whether the tumor does or does not secrete tumor hormones causing typical clinical syndromes. Insulinomas and gastrinomas are two common fPNET's of clinical relevance. EUS is the most sensitive imaging modality for PNET's (Sensitivity 77–94%). EUS-FNA is accurate in diagnosis of even tiny PNET's in up to 90% patients [10].

Typical EUS and Cytopathology Findings (Fig. 16.5a–c)

1. Tiny, discreet, encapsulated, hypoechoic mass lesions, often along anterior or posterior surface of pancreas
2. High vascularity on color Doppler
3. Large tumors show cystic and necrotic areas
4. It is difficult to differentiate between benign or malignant on the basis of EUS or surgical pathology. Presence of metastases on long term follow up is the only confirmation of malignant potential of the tumor
5. Immunohistochemistry (IHC) aids in cytopathological diagnosis – cells stain positive for chromogranin

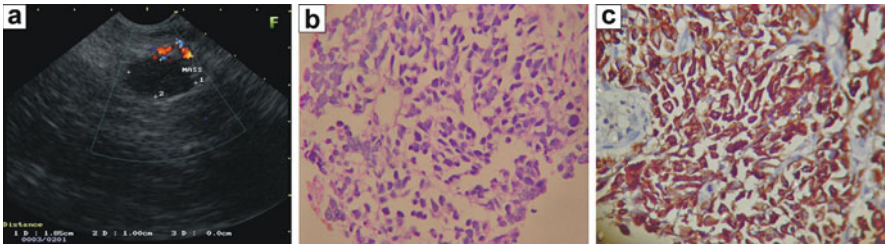

Fig. 16.5 (**a**) Linear EUS showing discreet hypoechoic well circumscribed mass in the pancreatic body suggestive of pancreatic NET, (**b**) section of clot fixed in formalin showing large cells with large hyperchromatic nuclei arranged in sheets suggestive of neuro endocrine carcinoma (H&E, 40×), (**c**) immunohistochemistry on section of clot fixed in formalin showing strong cytoplasmic positivity to chromogranin confirms neuroendocrine cells (Chromogranin, 40×)

16.4.3 Solid and Papillary Epithelial Neoplasm (SPEN)

SPEN are rare tumors predominantly seen in young females (15–45 years). Often large at diagnosis, these tumors are usually found in the body and tail, have a very low malignant potential and have an excellent prognosis if resected. Differential diagnosis is a neuroendocrine tumor.

Typical EUS and Cytopathology Findings (Fig. 16.6a, b)

1. Mixed solid and cystic encapsulated tumor
2. Distinct margins seen on EUS
3. Cytopathology shows a characteristic appearance of branching papillae with myxoid and fibro-vascular stroma. Tumor cells are monomorphic, have round nuclei and show an eosinophilic, foamy cytoplasm
4. Cyst contents are often bloody and contain necrotic debris

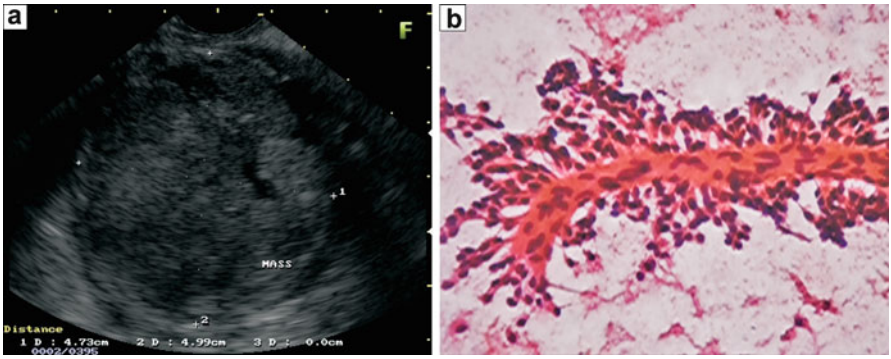

Fig. 16.6 (**a**) Large heterogeneous pancreatic mass seen on linear EUS. Hypoechoic areas within the mass represent areas of necrosis. FNA should be directed toward the hyperechoic areas to improve tissue yield, (**b**) cytology showing a well formed papillary frond with central fibro-vascular core surrounded by uniform cells – classical of SPEN (PAP, 40×)

16.4.4 Metastases to Pancreas from Surrounding Organs

Metastases to the pancreas are rare (2–3% of pancreatic resections) and are important to identify as the treatment modality differs from that of primary adenocarcinoma. Metastases have been reported from various sites – kidney, breast, skin, lung, colon, esophagus, NSCLC, non-Hodgkin lymphoma and ovary.

Typical EUS and Cytopathology Findings (Fig. 16.7a, b)
1. Round, homogeneous and well circumscribed lesions within the pancreas
2. Cytology confirms the primary pathology

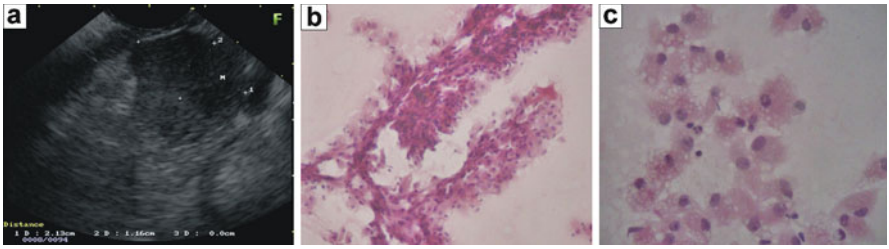

Fig. 16.7 (**a**) Hypoechoic well circumscribed mass lesion in the pancreatic body, (**b**) Cytology showing cellular smears with tumor cells arranged in papillary fashion (low-power). (**c**) High-power showing dissociated round cells with vacuolated eosinophilic cytoplasm with large nuclei and conspicuous nucleoli

16.4.5 Results of EUS-FNA for Diagnosis of Solid Pancreatic Tumors

The overall sensitivity, specificity and accuracy rates of EUS-FNA for diagnosis of pancreatic tumors in multiple studies are 78–95%, 75–100% and 78–95% respectively [8, 11, 12].

Common Pitfalls Leading to a Failed Diagnosis After EUS-FNA
1. Hard fibrotic tumor with a pauci-cellular sample
2. FNA from necrotic area of tumor
3. Presence of underlying chronic pancreatitis

Methods to improve accuracy of EUS-FNA –
1. Presence of an onsite cytopathologist may improve accuracy [2–6].
2. Contrast enhanced EUS helps to choose the right location for FNA [13]. NET's and inflammatory masses show marked hyperperfusion, adenocarcinoma shows hypoperfusion.

16.5 Diagnosis of Pancreatic Cystic Lesions

16.5.1 Classification of Cystic Lesions of the Pancreas [14]

- Congenital and simple cysts – 5% to 10%
- Pseudocysts – 80% to 90%
- Cystic neoplasms – 5% to 10%
  - Serous cystadenoma (SCA)
  - Mucinous cystadenoma (MCA)
  - Mucinous cystadenocarcinoma (MCAC)
  - Intraductal papillary mucinous neoplasm (IPMN)

Pancreatic cystic lesions are differentiated using the following parameters –
- Clinical history
- Appearance on EUS
- Cyst fluid analysis

The typical EUS appearances, fluid analysis and cytopathology characteristics of various cystic lesions of the pancreas are described in Table 16.1 and Figs. 16.8, 16.9, 16.10, and 16.11 [15]. The management of pseudocysts is described in detail in Chap. 18.

Table 16.1 EUS and pathological characteristics of cystic lesions of the pancreas

Characteristics	Serous cystadenoma	Mucinous cystadenoma	IPMN	SPEN	Pseudocyst
Location	Body/tail >head	Body/tail >head	Arise from main branch or side branch, head >body/tail	Anywhere	Anywhere
Age in years		40–50	60–70	20–40	
History of pancreatitis/pain	No	Occasional dull ache in large lesions	±, occasional dull ache in large lesions	Occasional	Almost always
Malignant potential	Very low	High	Variable, high	Low	Nil
EUS features	Multiple small cysts; often microcystic honeycomb; central fibrosis or calcification	Macrocystic (1–3+); can be large, septations; nodularity or papillary projections	Mural nodule or mass arising in dilated main or side branch of PD	Mixed solid-cystic, hemorrhagic center	Unilocular, variable size and wall thickness; echogenic material; features of acute/chronic pancreatitis
Communication with PD	Rare	Rare	Yes, often PD dilated ++	Rare	Sometimes
Vascularity	++	++	±	±	±
Cytology	Bland glycogen +ve cuboidal cells	Columnar/cuboidal, mucin positive cells; may show atypia, dysplasia or malignant features	Columnar/cuboidal, mucin positive cells; may show atypia, dysplasia or malignant features	Heterogeneous; eosinophillic papillary cells, PAS +ve deposits, vimentin +ve	Macrophages, inflammatory cells, debris
Cyst fluid	Small volume, low viscosity	Often large volume, high viscosity	Small volume, high viscosity	Low viscosity, bloody and necrotic	Large volume, low viscosity, may be bloody or turbid
Amylase	Low	Low	Variable, often high	Low	High
CEA	Low	High	Variable	Unknown	Low

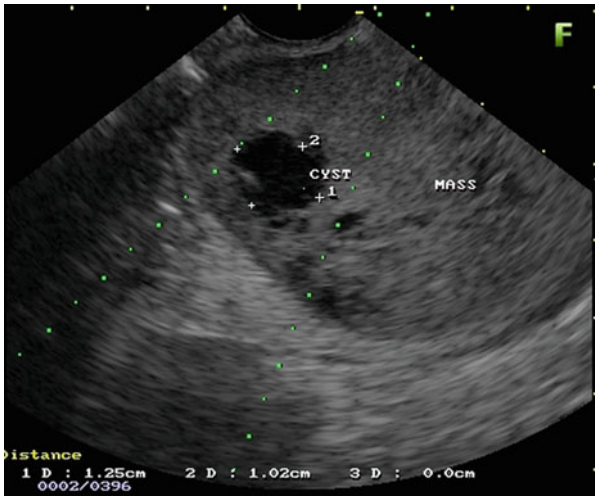

Fig. 16.8 Large well circumscribed mass seen in the pancreatic head with multiple small cystic lesions within – Serous cystadenoma. Note the classical honeycomb appearance. One of the cyst is larger and can be targeted for EUS-FNA

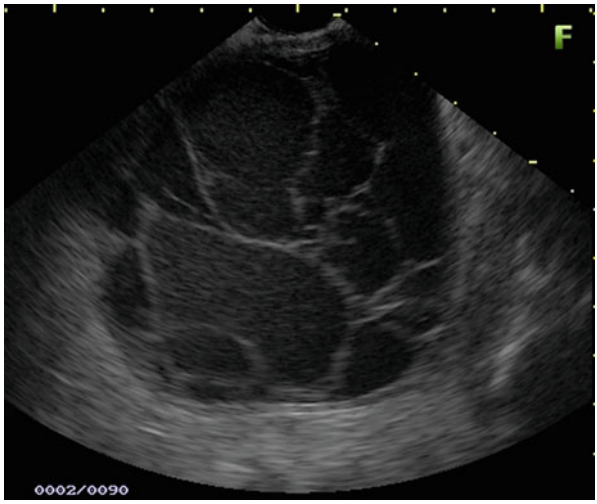

Fig. 16.9 Large cystic tumor in pancreatic body with septations. Aspirated fluid showed high mucin content – mucinous cystic tumor of the pancreas

16.5.2 Technical Aspects of FNA/Aspiration of Cystic Lesions –

1. Use a 19 G needle to aspirate cysts with viscid, mucinous or turbid contents.
2. Always confirm an avascular window prior to cyst puncture. Bleeding after FNA of cystic lesions often occurs inside the cyst [16].
3. Always aspirate the cyst completely to prevent infection.
4. Always send fluid for all biochemical, microbiological and cytological testing. It is embarrassing to realize that fluid initially sent for limited tests based on

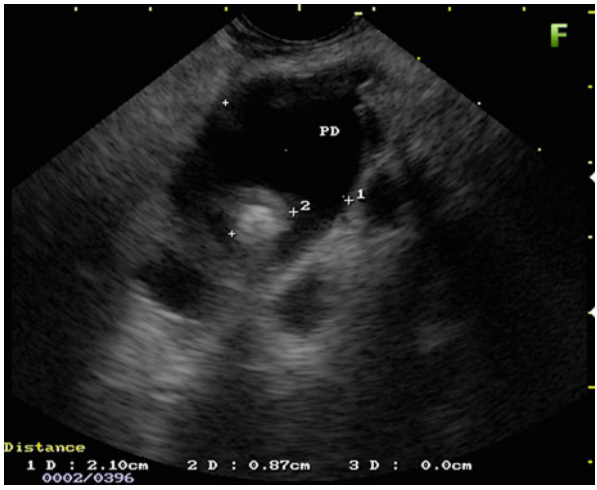

Fig. 16.10 Cystic dilatation of main pancreatic duct with solid component within. Aspirated fluid showed high mucin content and cells with atypical mitosis – Main duct IPMN

Fig. 16.11 Large cystic tumor of the pancreas with solid component. Aspirated fluid showed high CEA levels, FNA from solid component revealed malignant cells – Mucinous Cyst Adenocarcinoma of the pancreas

clinical impression was insufficient for further testing and additional fluid cannot be obtained. Collect and store additional fluid in separate containers under refrigeration if additional tests are necessary

5. Never perform cyst-enterostomy unless you are sure that you are dealing with a pseudocyst. It is disastrous to realize that the cyst treated by endoscopic cyst-enterostomy later turns out to be an MCA or MCAC.
6. Broad spectrum antibiotics are always administered to patients undergoing FNA for cystic lesions. Infection within a potentially resectable cystic mass can lead to significant perioperative morbidity.

16.5.3 Accuracy of EUS-FNA in Diagnosis of Pancreatic Cystic Lesions

The overall accuracy of diagnosis of pancreatic cystic lesions is in the range of 77–94% [17–22]. All studies have shown a high specificity (up to 100%), but a low sensitivity 55–89% [22–25]. Cyst fluid CEA is the only tumor marker that has shown predictive value, with a level >192 ng/ml showing 79% accuracy in diagnosis of mucinous tumors [22]. Other tumor markers – Ca 19–9, Ca 125 and molecular markers – Ki-*ras* mutations in DNA samples of aspirated fluid have not shown consistent results [22].

References

1. LeBlanc JK, Ciaccia D, Al-Assi MT et al (2004) Optimal number of EUS-guided fine needle passes needed to obtain a correct diagnosis. Gastrointest Endosc 59(4):475–481. doi:S0016510703028633 [pii]
2. Cleveland P, Gill KR, Coe SG et al (2010) An evaluation of risk factors for inadequate cytology in EUS-guided FNA of pancreatic tumors and lymph nodes. Gastrointest Endosc 71(7):1194–1199. doi:S0016-5107(10)00043-X [pii] 10.1016/j.gie.2010.01.029
3. Alsohaibani F, Girgis S, Sandha GS (2009) Does onsite cytotechnology evaluation improve the accuracy of endoscopic ultrasound-guided fine-needle aspiration biopsy? Can J Gastroenterol 23(1):26–30
4. Eloubeidi MA, Tamhane A, Jhala N et al (2006) Agreement between rapid onsite and final cytologic interpretations of EUS-guided FNA specimens: implications for the endosonographer and patient management. Am J Gastroenterol 101(12):2841–2847. doi:AJG852 [pii] 10.1111/j.1572-0241.2006.00852.x
5. Klapman JB, Logrono R, Dye CE et al (2003) Clinical impact of on-site cytopathology interpretation on endoscopic ultrasound-guided fine needle aspiration. Am J Gastroenterol 98(6):1289–1294. doi:S0002927003002466 [pii] 10.1111/j.1572-0241.2003.07472.x
6. Bapaye A, Aher A, Bhide V et al (2010) A single center experience of EUS guided fine needle aspiration cytology (FNAC) in pancreatic mass lesions. J Gastroenterol Hepatol 25(Suppl 2): A151
7. Varadarajulu S, Eloubeidi MA (2005) Endoscopic ultrasound-guided fine-needle aspiration in the evaluation of gallbladder masses. Endoscopy 37(8):751–754. doi:10.1055/s-2005-870161
8. Varadarajulu S, Wallace MB (2004) Applications of endoscopic ultrasonography in pancreatic cancer. Cancer Control 11(1):15–22
9. Brugge WR (1995) Pancreatic cancer staging. Endoscopic ultrasonography criteria for vascular invasion. Gastrointest Endosc Clin N Am 5(4):741–753
10. Anderson MA, Carpenter S, Thompson NW et al (2000) Endoscopic ultrasound is highly accurate and directs management in patients with neuroendocrine tumors of the pancreas. Am J Gastroenterol 95(9):2271–2277. doi:S0002-9270(00)01272-7 [pii] 10.1111/j.1572-0241.2000.02480.x
11. Akahoshi K, Chijiiwa Y, Nakano I et al (1998) Diagnosis and staging of pancreatic cancer by endoscopic ultrasound. Br J Radiol 71(845):492–496
12. Yoshinaga S, Suzuki H, Oda I et al (2011) Role of endoscopic ultrasound-guided fine needle aspiration (EUS-FNA) for diagnosis of solid pancreatic masses. Dig Endosc 23(Suppl 1): 29–33. doi:10.1111/j.1443-1661.2011.01112.x
13. Rickes S, Malfertheiner P (2004) Echo-enhanced sonography – an increasingly used procedure for the differentiation of pancreatic tumors. Dig Dis 22(1):32–38. doi:10.1159/000078733 DDI2004022001032 [pii]

14. Balthazar EJCA (1990) Computed tomography of pancreatic masses. Am J Gastroenterol 85:343–349
15. Lennon AM, Penman ID (2006) EUS in evaluation of pancreatic cysts. In: Hawes RH, Fockens P (eds) Endosonography, 1st edn. Saunders/Elsevier, Philadelphia, pp 205–216
16. Varadarajulu S, Eloubeidi MA (2004) Frequency and significance of acute intracystic hemorrhage during EUS-FNA of cystic lesions of the pancreas. Gastrointest Endosc 60(4):631–635. doi:S0016510704018917 [pii]
17. Moparty B, Brugge WR (2007) Approach to pancreatic cystic lesions. Curr Gastroenterol Rep 9(2):130–135
18. Brugge WR (2006) Cystic pancreatic lesions: can we diagnose them accurately what to look for? FNA marker molecular analysis resection, surveillance, or endoscopic treatment? Endoscopy 38(Suppl 1):S40–S47. doi:10.1055/s-2006-946650
19. Brugge WR (2005) Should all pancreatic cystic lesions be resected? Cyst-fluid analysis in the differential diagnosis of pancreatic cystic lesions: a meta-analysis. Gastrointest Endosc 62(3):390–391. doi:S0016-5107(05)01899-7 [pii] 10.1016/j.gie.2005.04.036
20. Sahani DV, Kadavigere R, Saokar A et al (2005) Cystic pancreatic lesions: a simple imaging-based classification system for guiding management. Radiographics 25(6):1471–1484. doi:25/6/1471 [pii] 10.1148/rg.256045161
21. Brugge WR (2004) Evaluation of pancreatic cystic lesions with EUS. Gastrointest Endosc 59(6):698–707. doi:S0016510704001750 [pii]
22. Brugge WR, Lewandrowski K, Lee-Lewandrowski E et al (2004) Diagnosis of pancreatic cystic neoplasms: a report of the cooperative pancreatic cyst study. Gastroenterology 126(5):1330–1336. doi:S0016508504001933 [pii]
23. Hernandez LV, Mishra G, Forsmark C et al (2002) Role of endoscopic ultrasound (EUS) and EUS-guided fine needle aspiration in the diagnosis and treatment of cystic lesions of the pancreas. Pancreas 25(3):222–228. doi:00006676-200210000-00002 [pii]
24. Frossard JL, Amouyal P, Amouyal G et al (2003) Performance of endosonography-guided fine needle aspiration and biopsy in the diagnosis of pancreatic cystic lesions. Am J Gastroenterol 98(7):1516–1524. doi:S0002927003003599 [pii] 10.1111/j.1572-0241.2003.07530.x
25. Brandwein SL, Farrell JJ, Centeno BA et al (2001) Detection and tumor staging of malignancy in cystic, intraductal, and solid tumors of the pancreas by EUS. Gastrointest Endosc 53(7): 722–727. doi:S0016-5107(01)80988-3 [pii] 10.1067/mge.2001.114783

EUS-FNA for Submucosal Tumor

17

Kazuya Akahoshi and Masafumi Oya

17.1 Indication

At present, EUS-FNA is a reliable technique for obtaining tissue samples of the submucosal tumor with minimal risks. A large group of submucosal lesions such as lipomas (hyperechoic mass), cysts (anechoic mass), and submucosal varices has typical features that allow accurate diagnosis based solely on the data gathered from endoscopy and EUS imaging [1–4]. However, an important subset of submucosal lesions such as GISTs, leiomyoma, neurinoma, carcinoid tumors, ectopic pancreas, lymphoid mass tissues, SMT-like cancers, and metastases may have overlapping echo (hypoechoic solid mass) and endoscopic features and cannot be accurately determined without a biopsy sample. Therefore, EUS-FNA should be performed for all hypoechoic solid tumors imaged by EUS (Fig. 17.1) [2].

17.2 Technique

EUS-FNA is performed on a 1 day inpatient basis, with conscious sedation, using the convex array echoendoscope in our institute [4]. Color flow and Doppler sonography are performed to exclude intervening vascular structures and to select a vessel-free needle track. The needle is inserted into the working channel of the echoendoscope. Once the tip of the catheter is visualized, the needle was advanced from the catheter sheath through the GI tract wall and into the target lesion under

K. Akahoshi (✉)
Department of Gastroenterology, Aso Iizuka Hospital,
Yoshiomachi 3-83, Iizuka city, Fukuoka 820-8505, Japan
e-mail: kakahoshi2@aol.com

M. Oya
Department of Pathology, Aso Iizuka Hospital,
Yoshiomachi 3-83, Iizuka city, Fukuoka 820-8505, Japan
e-mail: moyah1@aih-net.com

K. Akahoshi, A. Bapaye (eds.), *Practical Handbook of Endoscopic Ultrasonography*,
DOI 10.1007/978-4-431-54014-4_17, © Springer 2012

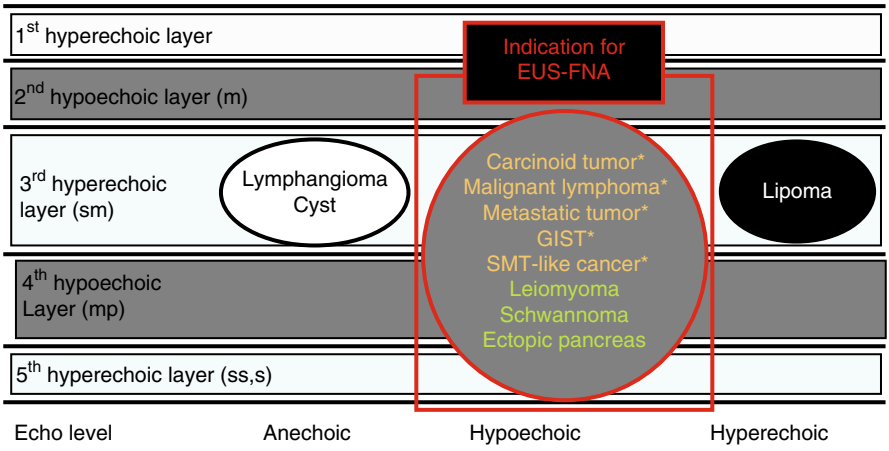

Fig. 17.1 Differential diagnosis of gastrointestinal submucosal tumor by EUS. * malignant tumor, *m* mucosa, *sm* submucosa, *mp* muscularis propria, *ss,s* subserosa, serosa (Quoted and modified from Akahoshi et al. [2])

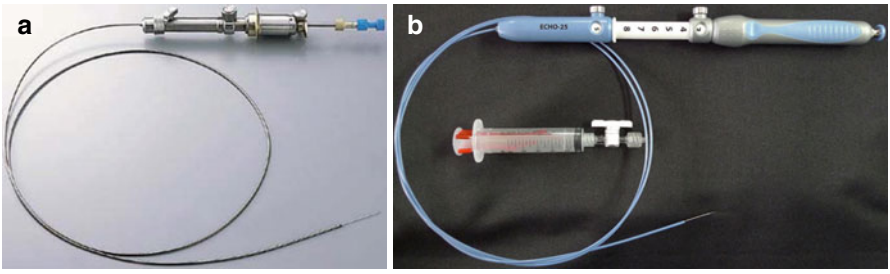

Fig. 17.2 Needles of EUS-FNA for GI tract SMT. (**a**) Olympus power shot type 22 gauge metallic needle NA-11J-KB. (**b**) Wilson-Cook 25 gauge needle Echo tip

ultrasonographic guidance. The stylet is removed and continuous suction applied with a 20-mL syringe. The needle is moved back and forth within the lesion under ultrasonographic guidance. The suction is then released and the needle removed from the working channel. My recommended FNA needles (Fig. 17.2) are the Olympus 22-gauge power-shot style needle (NA-11J-KB) or the Cook 25-gauge needle. Key steps for obtaining good specimens are shown in Fig. 17.3.

The aspirates are placed on glass slides, and both air-dried and alcohol-fixed smears are prepared. Air dried smears are stained with a modified Giemsa stain and assessed immediately by a cytopathologist on site to ensure specimen adequacy. The remaining prepared histologic specimens are processed at a later time in the pathology laboratory for hematoxylin and eosin staining and additional ancillary studies such as immunohistochemistry (c-kit, CD34, desmin, muscle actin, S-100, CD20, etc.). The diagnosis of EUS-FNA is based on histology using the cell block method [4].

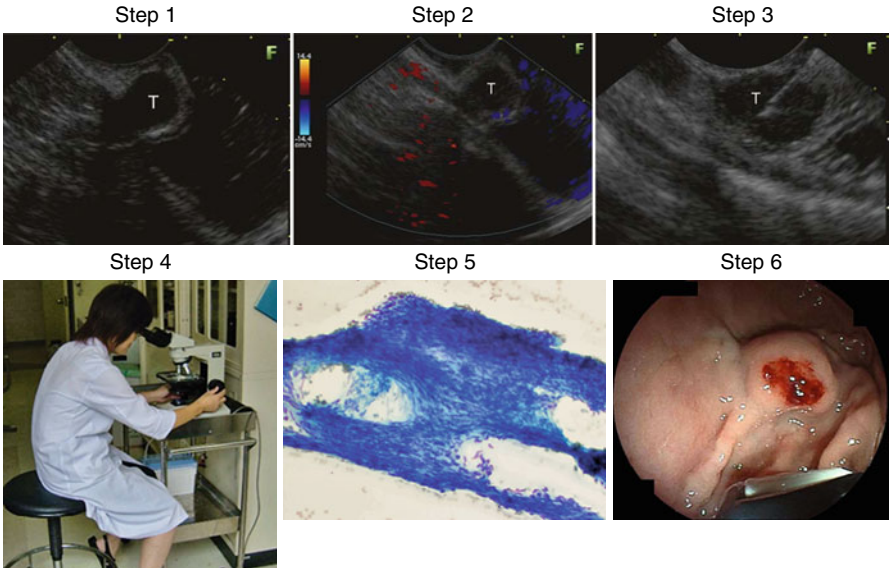

Fig. 17.3 Key steps of EUS-FNA for GI tract SMT
Step 1: Detecting the target SMT (T) under EUS image
Step 2: Ruling out blood vessels between EUS and the target lesion using color Doppler flow mapping
Step 3: Puncturing the target lesion (T). Then, after withdrawing the stylet and attaching a negative-pressure syringe (usually 20 mL), the needle is moved back and forth in the tumor 20 strokes or more
Step 4, 5: Checking the adequacy of obtained tissue samples by on-site cytoscreener
Step 6: Checking the puncture point endoscopically (ruling out bleeding related to EUS-FNA)

17.3 Clinical Impact

Observations to date indicate that EUS-FNA is a safe and accurate procedure [2–9]. The reported accuracy of preoperative diagnosis of EUS-FNA using immunohistochemical analysis for surgically resected GIST cases ranges from 91% to 100% [4–8]. A precise preoperative histologic diagnosis has the potential to directly affect clinical management. Operative planning including type of surgery conducted varies dramatically in relation to the histologic results [3, 4]. For example, a patient with localized GIST can be cured with a wedge resection, or if the patient has inoperable-SMT-like anastomotic cancer recurrence, can receive chemotherapy; however, a patient with SMT-like GI tract cancer would undergo surgical resection with lymph-node dissection. A patient with benign SMT could avoid surgery reliably because of confirmation of histologic benignancy such as ectopic pancreas. In addition, EUS-FNA can provide a conclusive histological diagnosis, which is routinely requested by oncologists before starting any

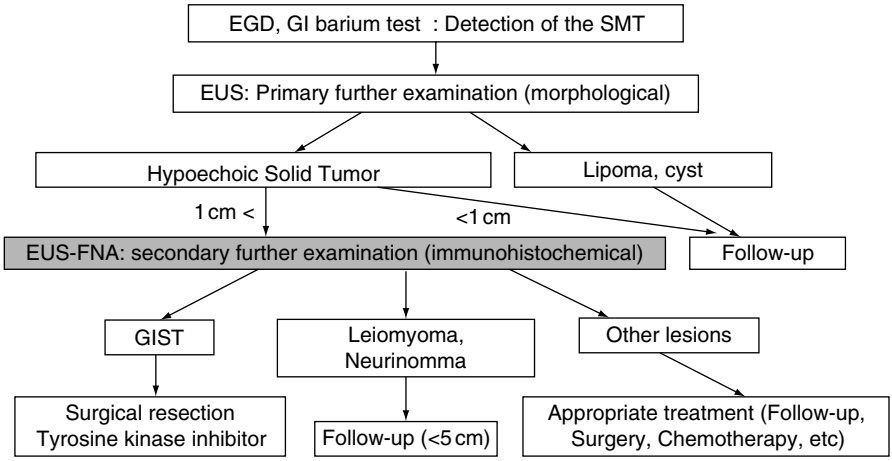

Fig. 17.4 Diagnostic and therapeutic algorithm of GI tract submucosal tumor using EUS-FNA (Quoted and modified from Akahoshi [11])

chemotherapy, radiotherapy, or palliative treatment [10]. Figure 17.4 shows our institutional management algorithm of SMT using EUS-FNA [11]. Thus EUS-FNA has a high clinical impact for determining the appropriate therapeutic option of GI tract SMT.

17.4 Typical Case Presentations

17.4.1 A Case of GIST

Representative patient management in a case of small gastric GIST (1.5 cm) according to our institutional algorithm of SMT using EUS-FNA is shown in Fig. 17.5. The results of immunohistochemical analysis of the tumor were positive reaction for c-kit and CD34, and negative reaction for muscle actin and S-100. The tumor was diagnosed as GIST conclusively, and the patient underwent local resection. The immunohistochemical staining pattern in the surgically resected lesion had similar results (diagnosed as GIST).

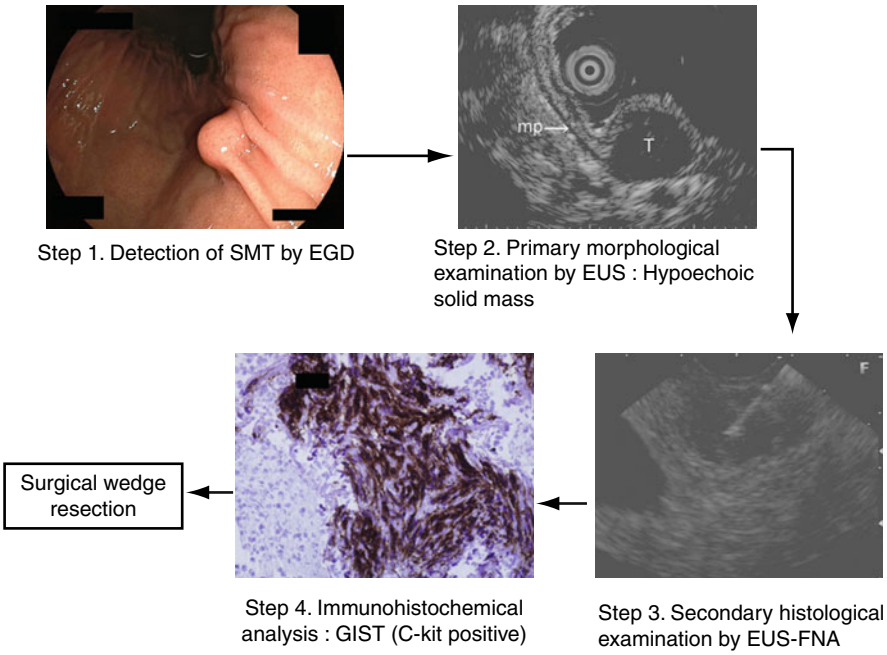

Fig. 17.5 Management process of gastric submucosal tumor (in a case of gastrointestinal stromal tumor) according to our institutional algorithm (Fig. 17.4)
Step 1: EGD shows submucosal tumor in the middle portion of the body of the stomach
Step 2: EUS reveals 1.2 cm subepithelial hypoechoic solid tumor (T) with continuity to proper muscle layer (arrow-mp)
Step 3: Puncture of the small GIST under EUS guidance
Step 4: The immunohistochemical finding of EUS-FNA specimen of GIST. The tumor is diffusely positive for c-kit

17.4.2 A Case of Ectopic Pancreas

Figure 17.6 shows representative patient management in a case of small gastric ectopic pancreas according to our institutional algorithm of SMT using EUS-FNA. EUS revealed a small hypoechoic tumor within the submucosal layer suspected as lymphoma, carcinoid tumor, or metastatic tumor, etc. The tumor was diagnosed as ectopic pancreas by the following EUS-FNA, and then follow-up was performed on the patient.

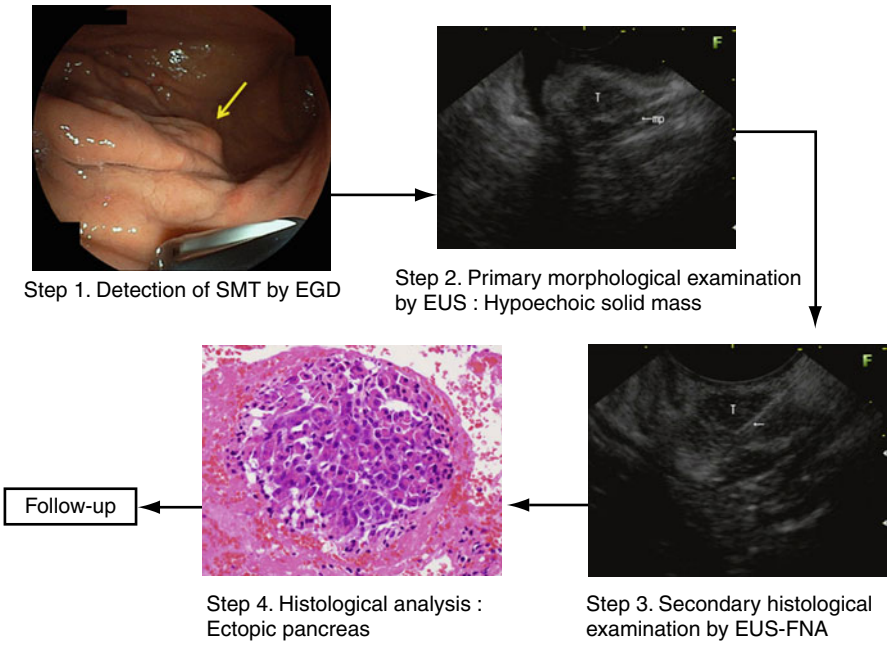

Fig. 17.6 Management process of gastric submucosal tumor (in a case of ectopic pancreas) according to our institutional algorithm (Fig. 17.4)
Step 1: EGD showing submucosal tumor in the middle body of the stomach
Step 2: EUS revealing 1.3 cm subepithelial hypoechoic solid tumor within submucosal layer. arrow-mp muscularis propria
Step 3: Puncture of the small submucosal tumor (T) under EUS guidance. Arrow: tip of needle
Step 4 Histology of EUS-FNA specimen reveals pancreatic acinar cells

17.4.3 A Case of MALT Lymphoma

Figure 17.7 shows representative patient management in a case of gastric MALT lymphoma according to our institutional algorithm of SMT using EUS-FNA. EUS revealed a hypoechoic solid tumor with continuity with muscularis propria suspected as GIST, carcinoid tumor, lymphoma, or metastatic tumor, etc. The tumor was diagnosed as MALT lymphoma by the following EUS-FNA (CD20 positive, CD5 negative, CD10 negative). In this patient, Helicobacter pyrori was negative and radiation therapy was performed.

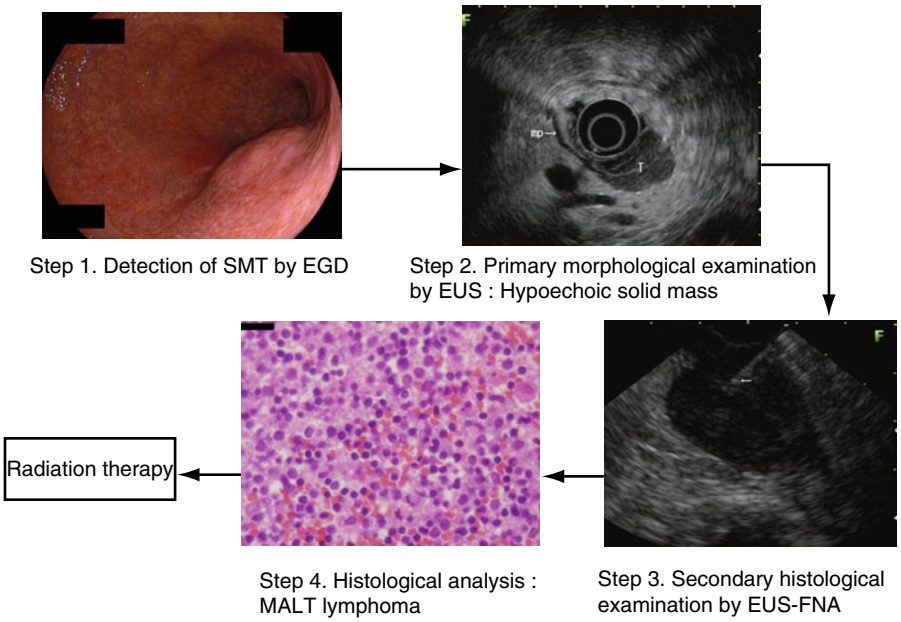

Fig. 17.7 Management process of gastric submucosal tumor (in a case of MALT lymphoma) according to our institutional algorithm (Fig. 17.4)
Step 1: EGD showing submucosal tumor in the middle body of the stomach
Step 2: EUS reveals 3 cm subepithelial hypoechoic solid tumor (T) with continuity to muscularis propia (arrow-mp)
Step 3: Puncture of the gastric submucosal tumor under EUS guidance. Arrow tip of needle
Step 4: The EUS-FNA specimen revealing MALT lymphoma

17.5 Complication

The reported complication rate of EUS-FNA for SMT is 0% [2–9]. In our experience, we encountered only one arterial bleeding (0.3%:1/145 cases) after EUS-FNA (Fig. 17.8). This case was successfully treated by endoscopic clipping. If bleeding from the needle punctured hole occurs immediately after EUS-FNA, compression of the bleeding point by the probe is recommended, because it is easy and effective. The second hemostatic options are conventional endoscopic hemostatic treatment such as clipping, injection of hypertonic saline epinephrine solution, etc.

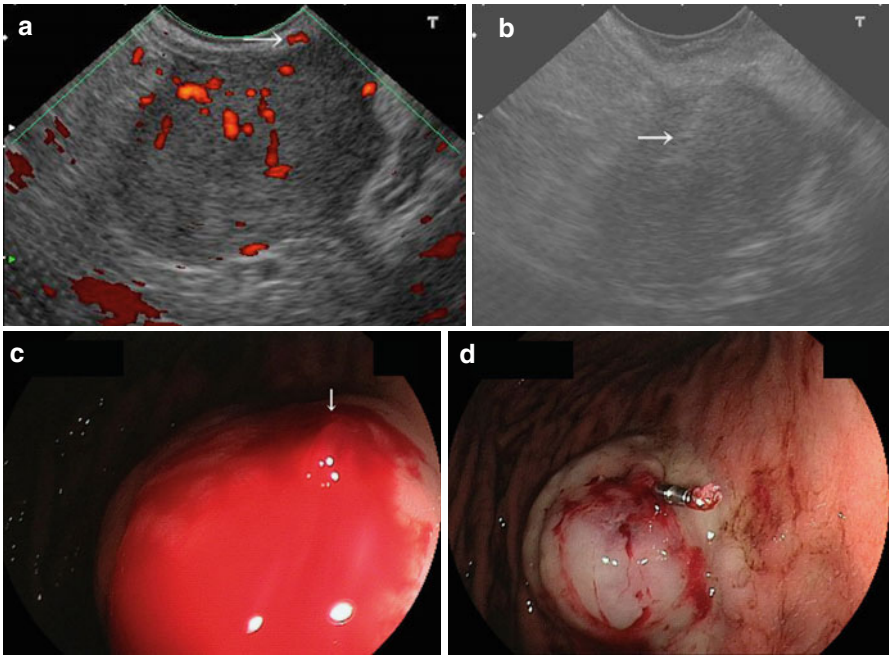

Fig. 17.8 EUS and endoscopic images in a patient of arterial bleeding after EUS-FNA. (**a**) EUS showing blood vessel (*arrow*) in submucosal layer and in the tumor. (**b**) EUS image during EUS-FNA. *Arrow* tip of the needle. (**c**) Endoscopic image revealing a arterial bleeding (*arrow*) from the puncture point. (**d**) Endoscopic picture showing a successful hemostasis by injection of hypertonic saline epinephrine solution plus endoscopic clipping

References

1. Akahoshi K, Harada N, Nawata H (2003) The current state of endoscopic ultrasonography. In: Pandalai SG (ed) Recent research developments in radiology. Transworld Research Network, Trivandrum, pp 1–37
2. Akahoshi K, Matsui N, Sumida Y et al (2009) Diagnosis of the gastric submucosal tumors by endoscopic ultrasonography-guided fine needle aspiration. Endoscopia Digestiva 21:1709–1717 (in Japanese)
3. Akahoshi K, Oya M (2010) Gastrointestinal stromal tumor of the stomach: how to manage? World J Gastrointest Endosc 2:271–277
4. Akahoshi K, Sumida Y, Matsui N et al (2007) Preoperative diagnosis of gastrointestinal stromal tumor by endoscopic ultrasound-guided fine needle aspiration. World J Gastroenterol 14:2077–2082
5. Sawaki A, Mizuno N, Takahashi K et al (2006) Long-term follow up of patients with small gastrointestinal stromal tumors in the stomach using endoscopic ultrasonography-guided fine-needle aspiration biopsy. Dig Endosc 18:40–44
6. Ando N, Goto H, Niwa Y et al (2002) The diagnosis of GI stromal tumors with EUS-guided fine needle aspiration with immunohistochemical diagnosis. Gastrointest Endosc 55:37–43

7. Okubo K, Yamao K, Nakamura T et al (2004) Endoscopic ultrasound-guided fine-needle aspiration biopsy for the diagnosis of gastrointestinal stromal tumors in the stomach. J Gastroenterol 39:747–753
8. Chatzipantelis P, Salla C, Karoumpalis I et al (2008) Endoscopic ultrasound-guided fine needle aspiration biopsy in the diagnosis of gastrointestinal stromal tumors of the stomach. A study of 17 cases. J Gastrointest Liver Dis 17:15–20
9. Matsui N, Akahoshi K, Motomura Y et al (2010) Successful endoscopic ultrasound-guided fine-needle aspiration of the pelvic lesion through the sigmoid colon. Dig Endosc 22:337–340
10. Wu PC, Langerman A, Ryan CW et al (2003) Surgical treatment of gastrointestinal stromal tumors in the imatinib (STI-571) era. Surgery 134:656–665
11. Akahoshi K (2009) Endoscopic ultrasonography in the stomach. In: Tajiri H, Oyama T (eds) Knack and pitfall of gastrointestinal endoscopy in diagnosis of esophageal, gastricand duodenal diseases. Yodosya, Tokyo, pp 149–156

Part VI

Interventional EUS

EUS Guided Drainage of Pancreatic Pseudocysts (PPC's), Abscesses and Fluid Collections (PFC's)

18

Amol Bapaye and Advay Aher

18.1 Introduction

Fluid collections around the pancreas occur as a sequel to an attack of acute pancreatitis, or less often secondary to ductal obstruction in chronic pancreatitis. Not all fluid collections around the pancreas are called pseudocysts (PPC's). A PPC is a well demarcated collection of fluid rich in pancreatic enzymes and having a well defined wall of fibrous or granulation tissue [1]. Formation of a PPC requires at least 4 weeks from the onset of pancreatitis. Before 4 weeks, it is called a pancreatic fluid collection (PFC). PPC's are usually sterile. In presence of pus, they are called pancreatic abscess. Some amount of solid debris is often found in the floor of a PPC, even without active infection [1].

PPC's in chronic pancreatitis occur due to extravasation of enzyme rich pancreatic fluid into peripancreatic tissues secondary to ductal obstruction.

PPC's can be drained by surgical cystoenterostomy; percutaneously aspirated or drained by an indwelling catheter; or drained endoscopically by a transpapillary or transmural approach. Endoscopic transmural drainage (ETMD) of PPC's is an established treatment modality [2–4], either with or without application of EUS. The EUS guided approach has gained favor in the last decade. EUS enhances safety of this procedure and improves the applicability of ETMD in a majority of PPC's [5–9].

A. Bapaye, M.D. (M.S.) (✉)
Department of Digestive Diseases and Endoscopy, Deenanath Mangeshkar Hospital and Research Center, Erandwane, Pune 411004, Maharashtra, India
e-mail: amolbapaye@gmail.com

A. Aher
Clinical Research Fellow, Department of Digestive Diseases and Endoscopy, Deenanath Mangeshkar Hospital and Research Center, Erandwane, Pune 411004, Maharashtra, India

K. Akahoshi, A. Bapaye (eds.), *Practical Handbook of Endoscopic Ultrasonography*,
DOI 10.1007/978-4-431-54014-4_18, © Springer 2012

18.2 Indications

Not all post pancreatitis fluid collections require drainage. Up to 30–60% may resolve spontaneously if adequate time is permitted for resolution [2].

18.2.1 Indications for PPC Drainage

- Symptomatic PPC's >6 cm in size, >6 weeks old
- PPC's causing compression symptoms
- Complicated PPC's – hemorrhage, infection
- PPC's communicating with pancreatic duct on ERP/MRCP

Softer indications may include abdominal fullness, early satiety, mild pain or symptomatic cysts smaller than 6 cm.

Prerequisites for Endoscopic Drainage of PPC's (Figs. 18.1 and 18.2)

- Cyst >4 weeks old
- Liquefied contents
- Well formed fibrous wall
- Cyst accessible through the stomach or duodenum on EUS

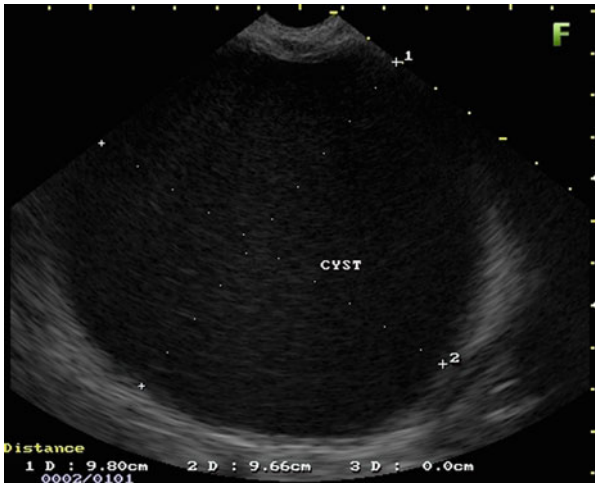

Fig. 18.1 Large PPC with clear contents seen on linear EUS

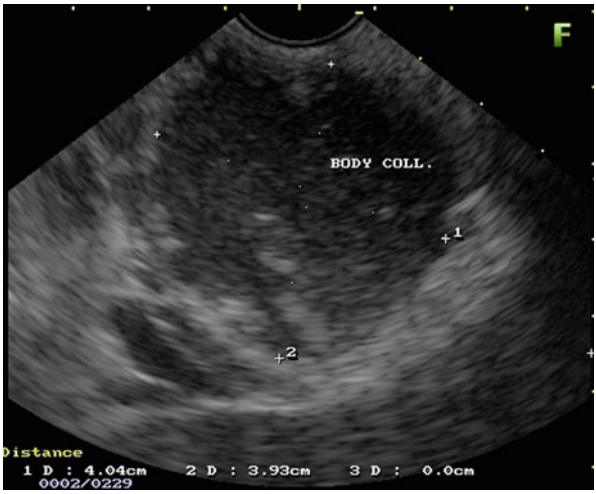

Fig. 18.2 Linear EUS showing large pseudocyst with turbid fluid

PPC's with solid component are no longer a contraindication for endoscopic drainage [2, 10, 11]. They can be treated by necrosectomy after puncture and dilatation of the tract.

18.2.2 Contraindications for ETMD (Fig. 18.3a–d)

- >1 cm wall thickness between cyst and stomach/duodenum, or cyst in a remote location (mesentery, paracolic space) [12]
- Pseudo-aneurysm in wall of PPC
- Inability to find avascular window for puncture
- Organized collections with solid necrosis and minimal fluid (relative contraindication)

PFC's may occasionally be drained before 4 weeks if contents are infected or drainage is expected to provide significant clinical benefit. Dilatation of the tract should be avoided in such situations for fear of bowel perforation.

18.3 EUS Anatomy

The optimum site for ETMD is the point of the maximal bulge in the stomach or duodenum. Here, the wall is thinnest and the risk of encountering a major blood vessel in the wall is the least. Although a non EUS guided approach to ETMD is feasible, only the EUS guided approach will be discussed in this chapter.

PPC's are generally drained from three locations–

1. Proximal stomach – PPC's in the body or tail are amenable for this approach. They are usually located high in the lesser sac and may sometimes reach up to the diaphragmatic hiatus. The left gastric, splenic and the dorsal pancreatic arteries

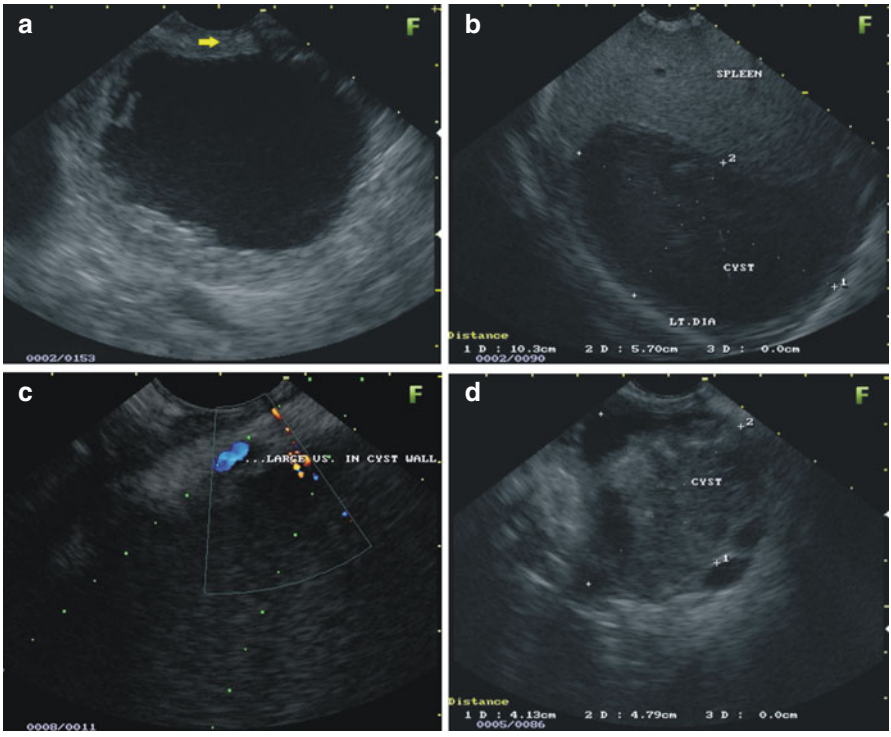

Fig. 18.3 Linear EUS showing (**a**) thick walled PPC, wall thickness (*arrow*) >10 mm, (**b**) PPC behind the spleen, (**c**) large blood vessel in cyst wall in the puncture tract, (**d**) PPC showing significant solid debris and minimal fluid. These PPC's cannot be drained by ETMD

are the major vascular structures to be protected during the procedure. The usual puncture site is high on the lesser curve 2–3 cm below the gastro-esophageal junction (Fig. 18.4).

2. Distal stomach – PPC's in the pancreatic body can be drained from this location. The puncture site is in the gastric body close to the incisura.
3. Duodenal bulb or descending duodenum – pancreatic head or uncinate process cysts are drained from this location (Fig. 18.5). The puncture site is at the duodenal genu or just beyond. The gastro-duodenal artery and the pancreatico-duodenal arcade must be avoided during puncture.

The locations described above are only illustrative; the actual location may differ in the individual patient. Rarely, PPC's may extend into the mediastinum and may require drainage through the esophagus [13].

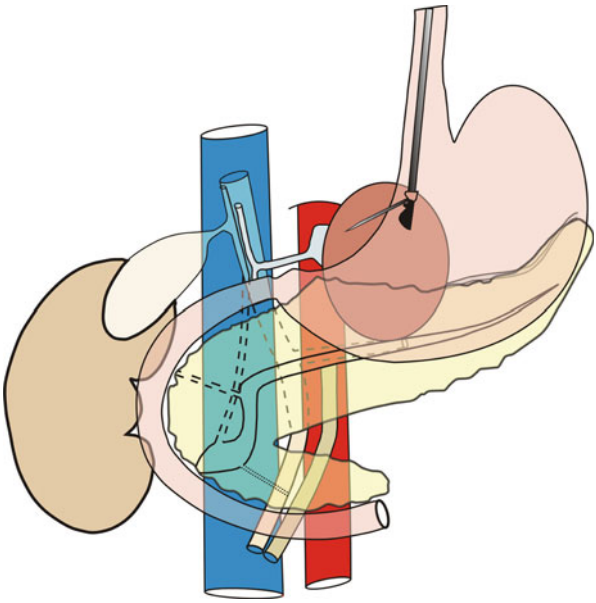

Fig. 18.4 Diagrammatic representation of the puncture site of a PPC in the lesser sac

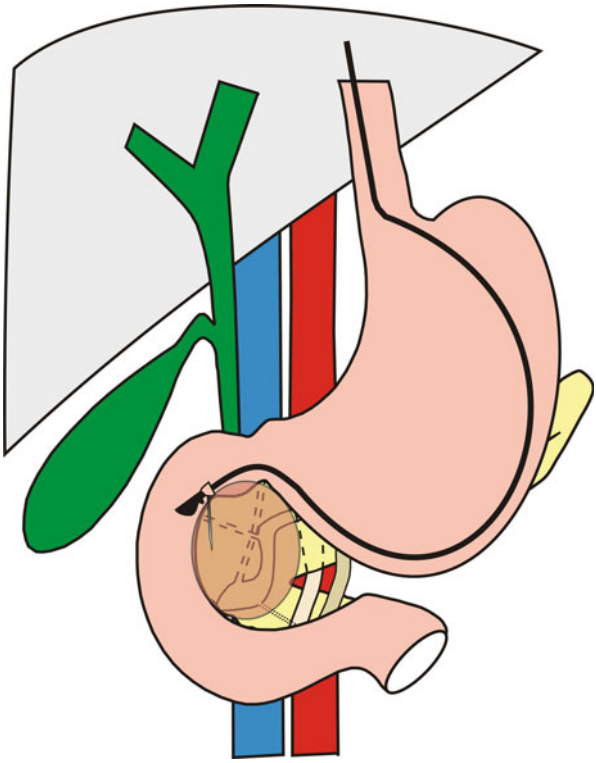

Fig. 18.5 Diagrammatic representation of position of the endoscope for drainage of a PPC in relation to the head of pancreas

18.4 Technique

18.4.1 Salient Points About Patient Preparation

1. High quality multi slice CT scan [14]
2. Administer intravenous broad spectrum antibiotics
3. Insert a large bore nasogastric tube in patients with large cysts (to permit rapid suction of the fluid from the stomach to avoid airway aspiration)

18.4.2 Instrumentation

EUS guided ETMD is performed using a therapeutic large channel (3.7 mm) echoendoscope (FG-530UT or equivalent).

Two variations of EUS guided ETMD are described –

1. Puncture with a sharp needle and subsequent dilatation – using a 19G FNA needle followed by balloon or diathermy dilatation
2. Puncture using diathermy – using a needle knife, cystotome or Giovannini Needle Wire system (Cook Endoscopy, Winston-Salem, USA).

Other material to be kept ready –

1. Guide wires – 0.018″, 0.032″ and 0.035″
2. Over the wire balloon dilators – 8, 12, 15 and 18 mm
3. Double pigtail stents – 7Fr, 8.5Fr and 10Fr
4. Nasocystic catheter/s – 7Fr
5. Hemoclips
6. Polypectomy snare or Roth basket to perform necrosectomy
7. Appropriate containers for collecting fluid for pathological examination – culture tubes, serum containers for amylase, CEA, and for cytological examination

18.4.3 Procedure

The technique of ETMD follows the same principles for both the EUS or non EUS guided approach. EUS helps to locate and assess the cyst, its wall and contents; and provides an avascular window for puncture. The further steps are performed under endoscopic and if necessary, under fluoroscopic guidance.

1. Select the optimum puncture site – locate the cyst, measure the size and wall thickness and inspect the contents. Note solid debris and apply Doppler to identify vascular structures in the wall. Large tortuous vessels may be seen in patients with left sided portal hypertension. Ideally, puncture should be performed where the wall is <10 mm thick and where there are no intervening blood vessels.

   When planning necrosectomy, position the puncture site just below the gastroesophageal junction on the posterior gastric wall in a straight line (Fig. 18.6).

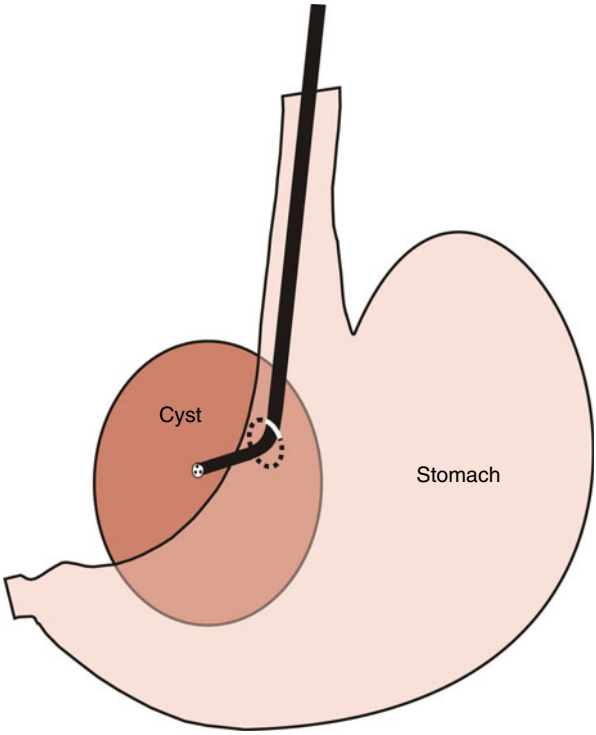

Fig. 18.6 Diagrammatic representation showing passage of the endoscope into the cyst cavity after dilatation of the tract

This aids subsequent passage of an endoscope into the cyst cavity for debridement and necrosectomy. A low or angular puncture in the stomach may make subsequent entry into the cyst difficult or impossible.

2. Puncture – puncture the PPC using either a needle or diathermy. Our personal preference is to use a 19G EUS-FNA needle for puncture as the needle is stiff, maintains a straight path during puncture and no diathermy is required. Using the 19G needle in the duodenal bulb may be difficult due to long loop.

   Puncture perpendicular to the bowel wall. The needle exits the endoscope at an angle due to the obliquity of the channel. Maintain the endoscope tip close to the wall to correct the angle and use a combination of elevator and upward angulation of the scope (Figs. 18.7 and 18.8).

3. After puncture, aspirate 10–20 ml of fluid for biochemical, cytological and microbiological examination. Standard tests on cyst fluid are amylase, CEA, cytology, Gram stain and culture. Introduce a 0.035″ guide wire (or thinner for some brands of needles) through the needle into the cyst cavity. This step may be monitored on an X-ray image intensifier though the guide wire can often be

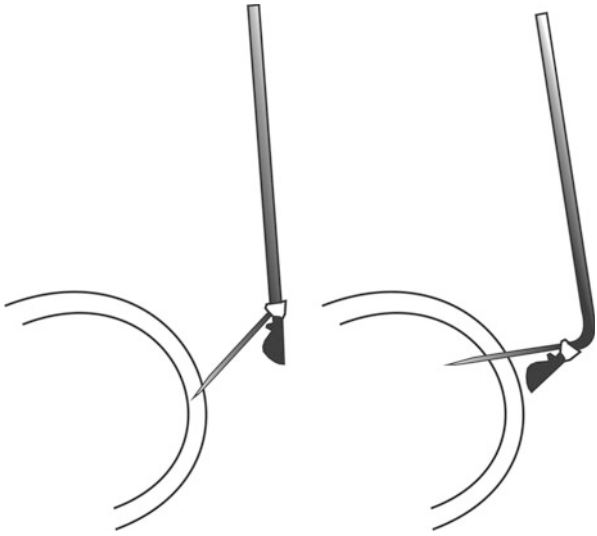

Fig. 18.7 Diagrammatic representation showing corrected position of scope tip for perpendicular puncture of cyst

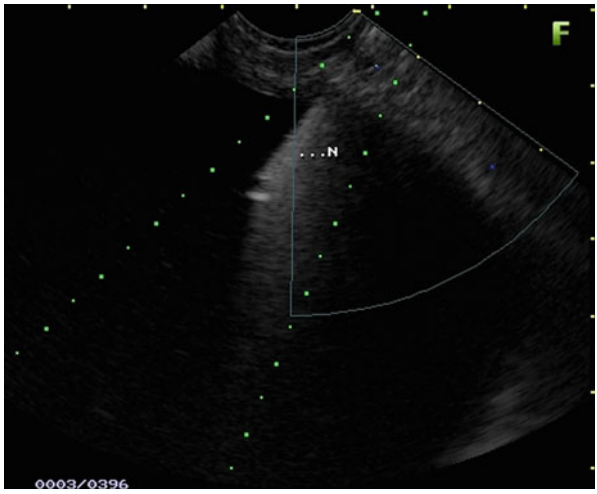

Fig. 18.8 PPC punctured using a 19G needle under linear EUS guidance

easily seen on EUS. Maintain adequate wire inside the cyst to avoid slipping out accidentally (Fig. 18.9a, b).

Never pull back a coated guide wire through the needle; the coating may shear and can break off within the cyst. The recently launched Echotip Ultra – 19A needle (Cook Endoscopy, Winston-Salem, USA) has an atraumatic tip specially designed for guide wire passage and may prevent this occurrence.

4. Dilate the tract over the guide wire to the desired size using either a diathermy current (cystotome), biliary dilatation balloon or both. Extent of dilatation depends upon the further intervention planned. Cysts with clear contents can be

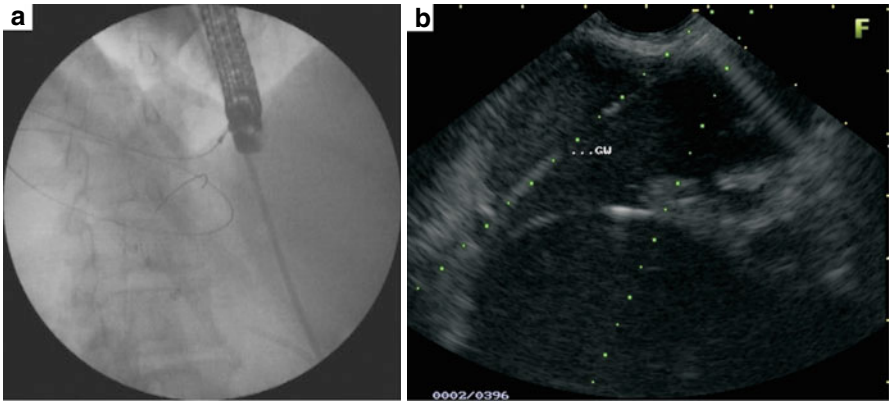

Fig. 18.9 (**a**) X-ray image intensifier showing guide wire loop in the cavity, (**b**) guide wire well seen in linear EUS

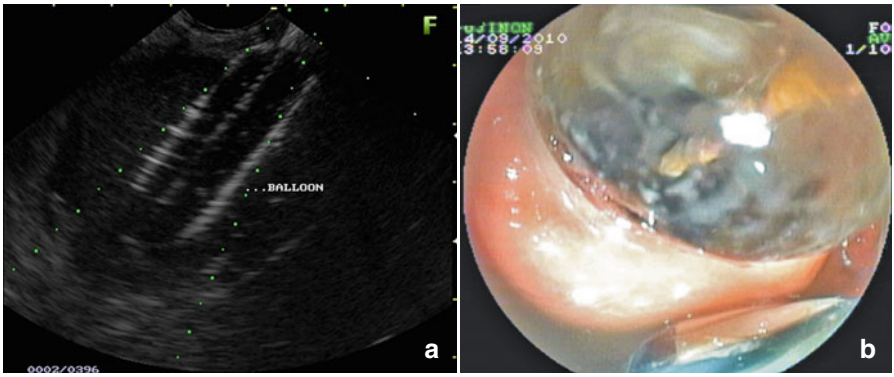

Fig. 18.10 (**a**) Linear EUS showing dilatation of the tract with 15 mm balloon, (**b**) endoscopic view showing dilatation of the tract using a 15 mm balloon

dilated up to 10 or 12Fr – adequate for stent placement. Thick fluid, debris or pus necessitates dilatation up to 24Fr or more (Fig. 18.10a, b).

Necrosectomy for cysts with solid contents requires dilatation up to 15–18 mm using esophageal balloon dilators (CRE, Microvasive, Natick, Massachusetts, USA), so that an endoscope can be introduced into the cavity. Dilatation may be performed in a stepwise manner over two sessions or may be completed as a single step (Authors' preference) [15].

5. Multiple double pigtail stents are placed from the stomach into the cyst cavity (Fig. 18.11). Stents can be placed one after another over a single wire (cumbersome, risk of losing access); or multiple guide wires can be placed within the cyst through the outer sheath of a 10Fr cystotome and then stents can be placed over the wires [15, 16].

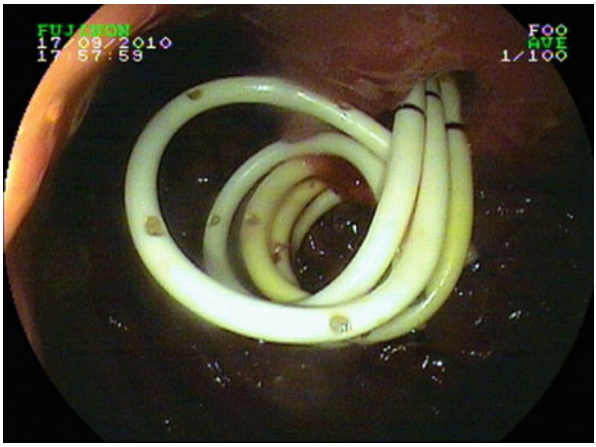

Fig. 18.11 Multiple stents endoscopic view

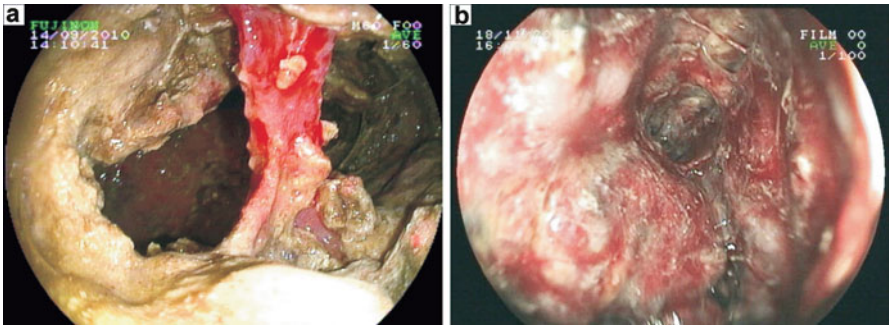

Fig. 18.12 (**a**) Endoscopic view from inside the collection in a patient undergoing endoscopic necrosectomy. A large blood vessel is seen traversing the lumen of the cavity. Caution must be exercised to avoid damage to such blood vessels during necrosectomy, (**b**) endoscopic view showing healthy granulation in the cyst wall after multiple sessions of necrosectomy and irrigation through a naso-cystic catheter

6. Necrosectomy is recommended if the cyst contains solid debris. After dilatation up to at least 15 mm, a gastroscope or duodenoscope is passed into the cyst cavity and loose necrotic debris lying within the cyst is removed (Fig. 18.12a). A nasocystic catheter is kept in the cyst cavity and the cavity is irrigated with saline to loosen the debris. Multiple sessions of cyst-endoscopy and necrosectomy are required at 2–3 days interval until all solid debris is loosened and removed and the cyst wall shows healthy granulation (Fig. 18.12b). Interim drainage by multiple stents and nasocystic catheter between sessions of necrosectomy is mandatory. Tract dilatation can be repeated if necessary at subsequent sessions [2, 12].

18.5 Complications

18.5.1 Bleeding

Bleeding during ETMD can be torrential and life threatening. It may occur during puncture due to damage to intervening blood vessels in the puncture tract, during necrosectomy due to avulsion of a vessel in the wall or from the bed of the PPC cavity due to a pseudo aneurysm in the cyst wall.

Tricks to Minimize Risk of Bleeding

1. Use color Doppler during puncture
2. Avoid oblique tract of puncture
3. Gradual stepwise dilatation
4. Remove only loose debris from cyst bed during necrosectomy and leave adherent debris behind for subsequent sessions

Bleeding from the puncture site is usually evident and can be controlled by endoclips. Intracavitatory bleeding can rarely be controlled endoscopically.

Management of a patient with suspected internal bleed –

Blood can accumulate in the PPC cavity and may not appear in the gastric lumen. Increasing tachycardia, persistent hypotension or serial drop in hematocrit are indicators of continued bleeding within the cyst cavity, even though the patient may not present with hematemesis or hemorrhagic nasogastric tube aspirate.

The treatment for ongoing bleeding is early radiological or surgical intervention. Angio-embolization or ligation of the splenic artery or its branches is necessary. Intravenous broad spectrum antibiotics are administered, as blood in the cavity can lead to secondary infection.

18.5.2 Perforation

Perforation during PPC drainage is due to poor case selection or inadvertent rapid overzealous dilation of the tract. It can occur when the cyst has a poorly formed wall or when the cyst wall has not adhered sufficiently to the stomach. Perforations invariably require immediate surgical intervention.

18.5.3 Infection

Infection of a PPC following drainage always indicates incomplete drainage. Even a PPC with clear contents may get infected if inadequately drained and can form an abscess. Maintaining adequate drainage throughout the entire duration

of treatment is mandatory. A combination of dilatation, stents, nasocystic catheters, irrigation and necrosectomy may be utilized. Broad spectrum antibiotics must be routinely administered to all patients scheduled for PPC drainage. Microbiological examination of the cyst fluid may indicate sensitivity patterns to antibiotics. Infection in PPC's requires early recognition and aggressive management.

18.5.4 Other

Pulmonary complications due to aspirated fluid can be prevented by placing a large diameter nasogastric tube alongside the scope prior to drainage, aspirating the gastric contents judiciously after puncture and dilation, and by maintaining the patient in the left lateral decubitus position.

The diaphragmatic crus may be traversed when draining PPC's in a high, sub diaphragmatic location. This can cause respiratory pain and may be controlled by analgesics. The pain will subside once stents are removed.

A pancreatico-pleural fistula may result if the pleural space is traversed by the puncturing needle resulting in a left sided pleural effusion. Pleural drainage and pancreatic duct stent placement is recommended.

18.6 Role of Endoscopic Retrograde Pancreatography

This chapter is a technical guide for performing EUS guided PPC drainage and is not intended to be an elaborate treatise on endoscopic management of PPC's. It is however necessary to state here in short the role of ERP in these patients.

PPC's develop due to extravasation of pancreatic juice from pancreatic ductal leak (Fig. 18.13). Although the leak may spontaneously heal over time, it is the primary cause of PPC recurrence despite optimum drainage. Associated obstructive ductal pathology may be found in up to 20% patients (stricture, pancreas divisum, calculus). Pancreatic sphincterotomy and stent placement is recommended in these patients to facilitate closure of the leak [10, 17]. Many authors have recommended a pre drainage pilot ERP to demonstrate the leak and placement of stents [2, 14]. This approach may prove technically difficult due to pressure by the cyst on the stomach or duodenum or associated duodenal mucosal edema. We prefer to first drain the cyst as it simplifies the subsequent ERP.

As a rule, PPC's should always be drained by multiple stent placements and not by only aspiration [2, 10, 12]. Aspiration is reserved for small PPC's with clear contents and those which demonstrate a clear communication with the pancreatic duct on ERP. In these patients, cyst aspiration followed by pancreatic duct stent is the optimum treatment. Complete aspiration is mandatory; residual collections may develop secondary infection.

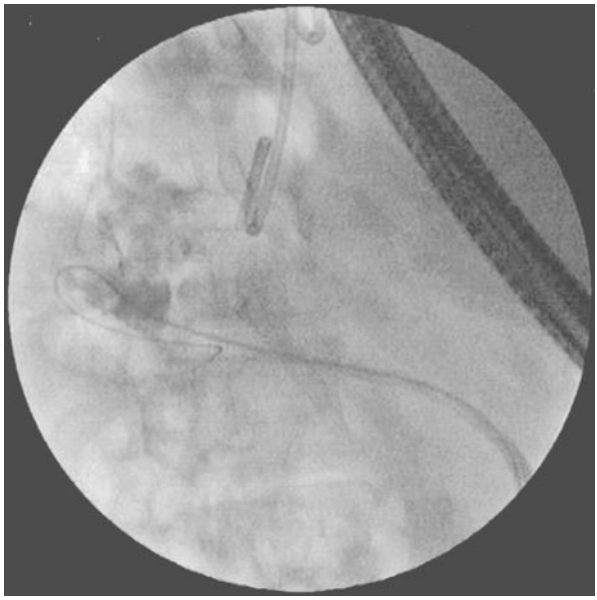

Fig. 18.13 ERP showing extravasation of contrast into the PPC cavity

18.7 Results of EUS Guided ETMD

EUS guided ETMD is as effective as surgical cystogastrostomy [18]. EUS guided drainage is superior to conventional drainage without EUS, with initial success rates of 94–100% for EUS guided drainage as compared to 72–85% for the non EUS technique [7, 9]. Inadequate drainage can be prevented by using an aggressive approach in patients with complicated PPC's and abscess [2, 10, 12]. The overall incidence of complications is 5–10% [9].

References

1. Bradley EL III, Clements JL (1993) A clinically based classification system for acute pancreatitis. Arch Surg 128:586–590
2. Baron TH, Harewood GC, Morgan DE, Yates MR (2002) Outcome differences after endoscopic drainage of pancreatic necrosis, acute pancreatic pseudocysts, and chronic pancreatic pseudocysts. Gastrointest Endosc 56:7–17. doi:10.1067/mge.2002.125106
3. Kozarek RA, Brayko CM, Harlan J et al (1985) Endoscopic drainage of pancreatic pseudocysts. Gastrointest Endosc 31(5):322–327
4. Hershfield NB (1984) Drainage of a pancreatic pseudocyst at ERCP. Gastrointest Endosc 30(4):269–270
5. Park DH, Lee SS, Moon SH et al (2009) Endoscopic ultrasound-guided versus conventional transmural drainage for pancreatic pseudocysts: a prospective randomized trial. Endoscopy 41(10):842–848. doi:10.1055/s-0029-1215133

6. Galasso D, Voermans RP, Fockens P (2009) Role of endosonography in drainage of fluid collections and other NOTES procedures. Best Pract Res Clin Gastroenterol 23(5):781–789. doi:S1521-6918(09)00099-7 [pii] 10.1016/j.bpg.2009.06.009
7. Varadarajulu S, Christein JD, Tamhane A et al (2008) Prospective randomized trial comparing EUS and EGD for transmural drainage of pancreatic pseudocysts (with videos). Gastrointest Endosc 68(6):1102–1111. doi:S0016-5107(08)01773-2 [pii] 10.1016/j.gie.2008.04.028
8. Barthet M, Lamblin G, Gasmi M et al (2008) Clinical usefulness of a treatment algorithm for pancreatic pseudocysts. Gastrointest Endosc 67(2):245–252. doi:S0016-5107(07)02114-1 [pii] 10.1016/j.gie.2007.06.014
9. Catalano MF, George S, Thomas M et al (2004) EUS-guided pancreatic pseudocyst drainage: comparison with standard endoscopic cystenterostomy. Gastrointest Endosc 59:AB202
10. Seewald S, Groth S, Omar S et al (2005) Aggressive endoscopic therapy for pancreatic necrosis and pancreatic abscess: a new safe and effective treatment algorithm (videos). Gastrointest Endosc 62(1):92–100. doi:S0016510705005419 [pii]
11. Seifert H, Wehrmann T, Schmitt T et al (2000) Retroperitoneal endoscopic debridement for infected peripancreatic necrosis. Lancet 356(9230):653–655. doi:S0140-6736(00)02611-8 [pii] 10.1016/S0140-6736(00)02611-8
12. Seewald S, Ang TL, Teng KC et al (2009) EUS-guided drainage of pancreatic pseudocysts, abscesses and infected necrosis. Dig Endosc 21(Suppl 1):S61–S65. doi:DEN860 [pii] 10.1111/j.1443-1661.2009.00860.x
13. Trevino JM, Christein JD, Varadarajulu S (2009) EUS-guided transesophageal drainage of peripancreatic fluid collections. Gastrointest Endosc 70(4):793–797. doi:S0016-5107(09)01925-7 [pii] 10.1016/j.gie.2009.05.023
14. Hawes RH (2003) Endoscopic management of pseudocysts. Rev Gastroenterol Disord 3(3):135–141
15. Seifert H, Dietrich CF (2006) Pancreatic interventions. In: Dietrich CF (ed) Endoscopic ultrasound an introductory manual and atlas, vol 1, 1st edn. Thieme, Stuttgart, pp 230–250
16. Seewald S, Thonke F, Ang TL et al (2006) One-step, simultaneous double-wire technique facilitates pancreatic pseudocyst and abscess drainage (with videos). Gastrointest Endosc 64(5):805–808. doi:S0016-5107(06)02554-5 [pii] 10.1016/j.gie.2006.07.049
17. Trevino JM, Tamhane A, Varadarajulu S (2010) Successful stenting in ductal disruption favorably impacts treatment outcomes in patients undergoing transmural drainage of peripancreatic fluid collections. J Gastroenterol Hepatol 25(3):526–531. doi:JGH6109 [pii] 10.1111/j.1440-1746.2009.06109.x
18. Varadarajulu S, Lopes TL, Wilcox CM et al (2008) EUS versus surgical cyst-gastrostomy for management of pancreatic pseudocysts. Gastrointest Endosc 68(4):649–655. doi:S0016-5107(08)00289-7 [pii] 10.1016/j.gie.2008.02.057

EUS Guided Biliary and Pancreatic Duct Interventions

19

Amol Bapaye and Advay Aher

19.1 Introduction

Endoscopic retrograde cholangio-pancreatography (ERCP) is the standard treatment modality for decompression of the obstructed biliary tree [1]. ERCP may fail to achieve deep biliary cannulation in about 5–10% patients due to anatomical or technical causes. Traditionally, percutaneous biliary drainage (PTBD) has been employed to achieve biliary decompression in such situations. PTBD has been reported to have complication rates up to 15% [2–6]. EUS guided intervention is an attractive alternative in these patients. Under EUS guidance, one can puncture the biliary tract, obtain a cholangiogram and achieve biliary drainage.

The pancreatic duct can be punctured under EUS guidance from the posterior gastric wall. In situations when ERP fails in deep cannulation of the main pancreatic duct (MPD), this approach may be utilized for pancreatic endotherapy.

A. Bapaye, M.D. (M.S.) (✉)
Department of Digestive Diseases and Endoscopy,
Deenanath Mangeshkar Hospital and Research Center,
Erandwane, Pune 411004, Maharashtra, India
e-mail: amolbapaye@gmail.com

A. Aher
Clinical Research Fellow, Department of Digestive Diseases and Endoscopy,
Deenanath Mangeshkar Hospital and Research Center,
Erandwane, Pune 411004, Maharashtra, India

K. Akahoshi, A. Bapaye (eds.), *Practical Handbook of Endoscopic Ultrasonography*,
DOI 10.1007/978-4-431-54014-4_19, © Springer 2012

19.2 Indications

- Inability to reach the ampulla
  - Post operative status – Billroth II gastrectomy, Whipple's procedure, gastrectomy with Roux-en-Y anastomosis
  - Pyloric stenosis or duodenal stenosis due to tumor infiltration
  - Anatomical variants like upside down stomach
- Inability to locate the ampulla
  - Post duodenal stent placement
  - Extensive ampullary/duodenal tumor infiltration
- Failed cannulation at ERCP after multiple attempts at the hands of an experienced endoscopist

19.3 EUS Anatomy

The biliary tree is accessible to the echoendoscope from two locations –

1. The left hepatic duct (LHD) is seen in longitudinal section from the lesser curve of the stomach. At this location, the duct is superficial (1–1.5 cm of intervening liver parenchyma) and the tract is avascular (Fig. 19.1a, b).
2. The common bile duct (CBD) is seen in cross section from the apex of the duodenal bulb. It lies posteriorly adjacent to the duodenum (Fig. 19.2a, b). There are usually no intervening blood vessels in the tract.

The MPD can be seen from the posterior wall of the body of the stomach (Fig. 19.3a, b).

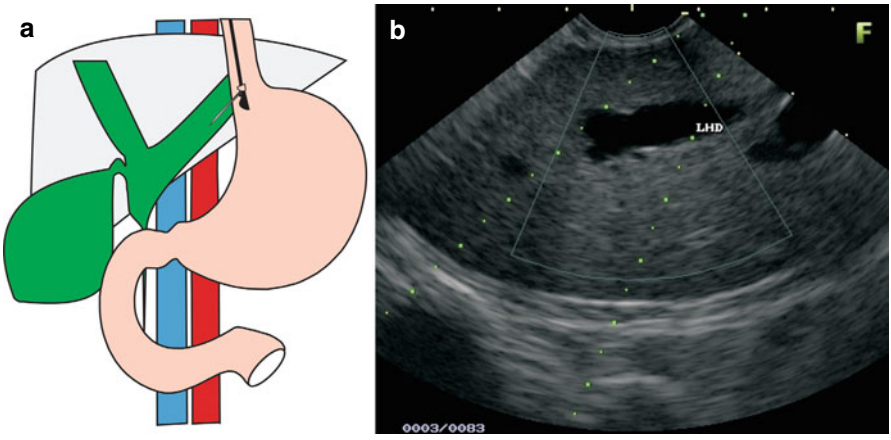

Fig. 19.1 (**a**) Diagrammatic representation showing puncture of the left hepatic duct from the lesser curvature of stomach, (**b**) EUS – dilated left hepatic duct seen from lesser curvature

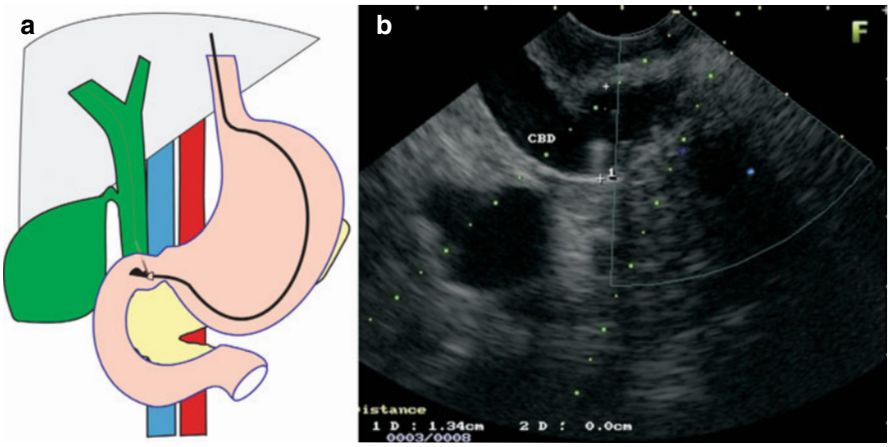

Fig. 19.2 (**a**) Diagrammatic representation showing puncture of CBD from duodenal bulb, (**b**) EUS image showing supra pancreatic CBD from duodenal bulb

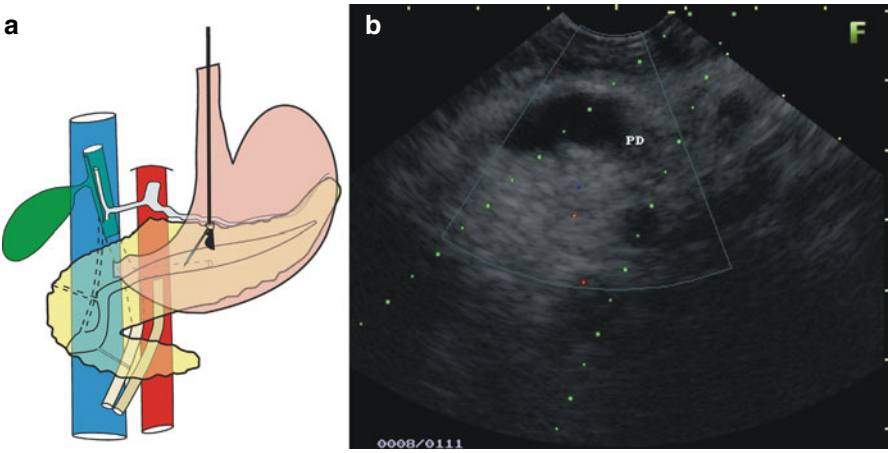

Fig. 19.3 (**a**) Diagrammatic representation showing puncture of MPD through gastric body, (**b**) linear EUS showing dilated MPD from posterior wall of stomach

19.4 Technique

19.4.1 EUS Guided Biliary Interventions

EUS guided cholangiography was first described by Wiersema et al. in 1996 [7]. Later, Sahai et al. described feasibility of performing EUS guided hepatico-gastrostomy in pigs [8]. Giovannini et al. described EUS guided choledocho-duodenostomy in humans in 2001 [9]. Since then, a number of case reports have appeared in literature describing the utility of this technique [10, 11].

Two approaches for EUS guided access to the biliary tract –

- Through the duodenal bulb into the common bile duct (also called extrahepatic approach, EUS guided choledocho-duodenostomy)
- Through the stomach into the left hepatic duct (also called intrahepatic approach, EUS guided hepatico-gastrostomy)

19.4.1.1 The Extrahepatic Approach (EUS Guided Choledocho-Duodenostomy)

1. Position the echoendoscope at the duodenal bulb apex in long loop position (Fig. 19.2a).
2. Locate the extrahepatic CBD at the upper border of the pancreas (Fig. 19.2b).
3. Puncture the CBD using a 19G FNA needle as for EUS-FNA (Authors' preference) (Fig. 19.4). Use of a needleknife has also been described.
4. After puncture, remove the stylet and confirm position by aspiration of bile. Pass a 0.018″, 0.032″ or 0.035″ guide wire through the needle into the CBD to form an adequate loop within the CBD. Monitor guide wire movement on fluoroscopy (Fig. 19.5). Although contrast may be injected at this stage to obtain a cholangiogram, we prefer to reserve injection until the guide wire is further secured within the duct.
5. Remove the needle maintaining the guide wire in position. Dilate the tract using diathermy or balloon to create a fistula. We prefer 6Fr. cystotome (Endoflex GmBH, Germany) and coagulating current (Fig. 19.6). Balloon dilatation using 4 or 6 mm biliary dilator balloons has also been described.
6. Cannulate the CBD through the fistula using a catheter and inject contrast to obtain a cholangiogram (Fig. 19.7).
7. Place a stent over the guide wire across this fistulous tract (Figs. 19.8 and 19.9)

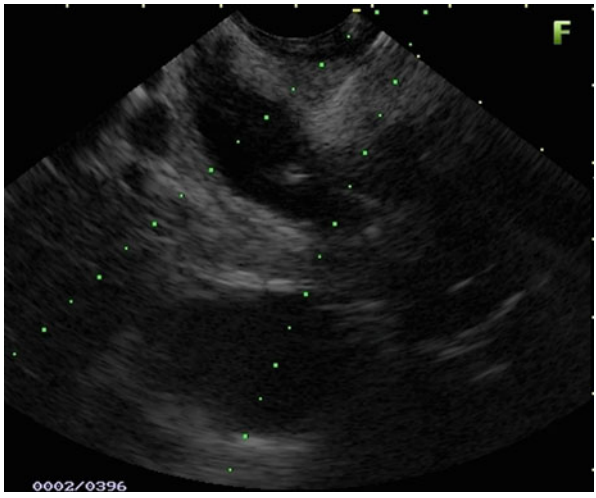

Fig. 19.4 CBD punctured through duodenal bulb with a 19G FNA needle

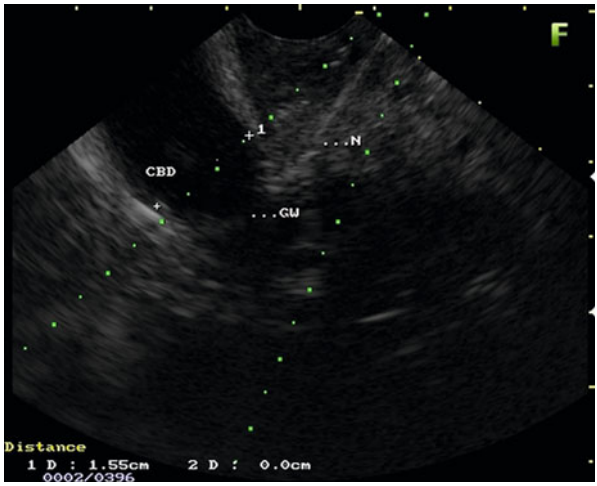

Fig. 19.5 Guide wire passed into CBD through the 19G needle

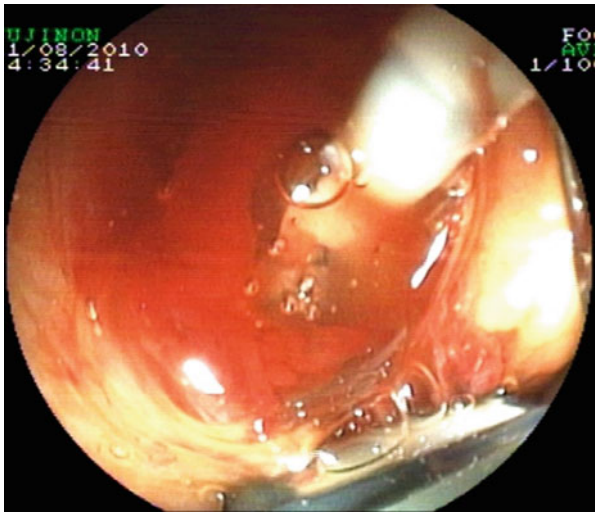

Fig. 19.6 Endoscopic view showing dilatation of the tract using a 6Fr. cystotome

8. Alternatively, once the catheter is inside the CBD, manipulate the guide wire across the stricture out from the papilla. Grasp it with a polypectomy snare and draw it out of the endoscope. Exchange the echoendoscope for a duodenoscope over the guide wire, perform retrograde cannulation over the guide wire through the ampulla and place the stent by ERCP. This is the EUS – ERCP rendezvous technique.
9. Once the guide wire has crossed the stricture, stent can also be placed through the fistula across the stricture (ante grade placement).

Fig. 19.7 Cholangiogram showing lower CBD stricture

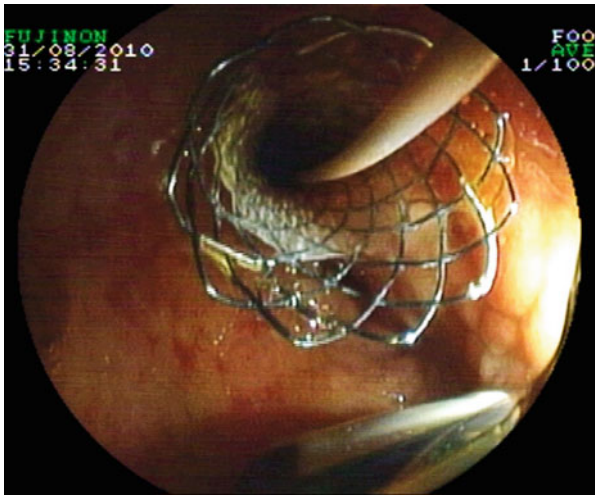

Fig. 19.8 Endoscopic view showing placement of a covered expandable metal stent

19.4.1.2 The Intrahepatic Approach (EUS Guided Hepatico-Gastrostomy)

Technique is similar to the extrahepatic approach. Following differences exist –

1. Position the echoendoscope beyond the gastric cardia approximated against the lesser curvature (Figs. 19.1 and 19.10).
2. The gastric wall thickness and thickness of intervening liver parenchyma make puncture and dilatation considerably more difficult. The endoscope tip tends to swing away from the wall during puncture. Strong upward pressure using the up-wheel along with use of the elevator is necessary.

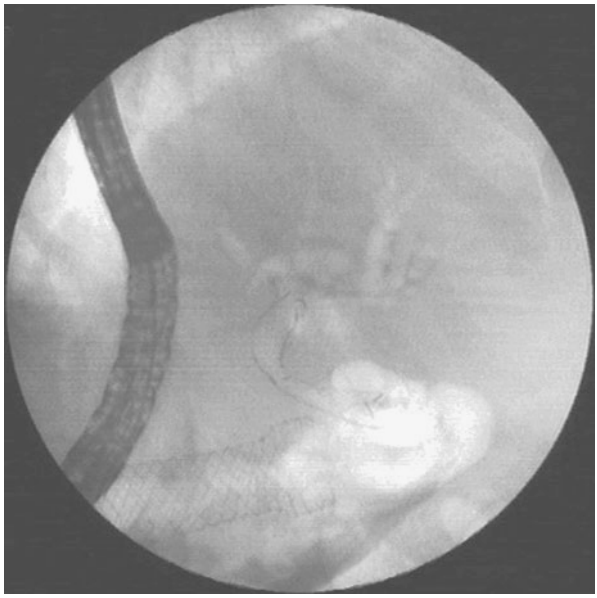

Fig. 19.9 Air cholangiogram after completion of choledocho-duodenostomy

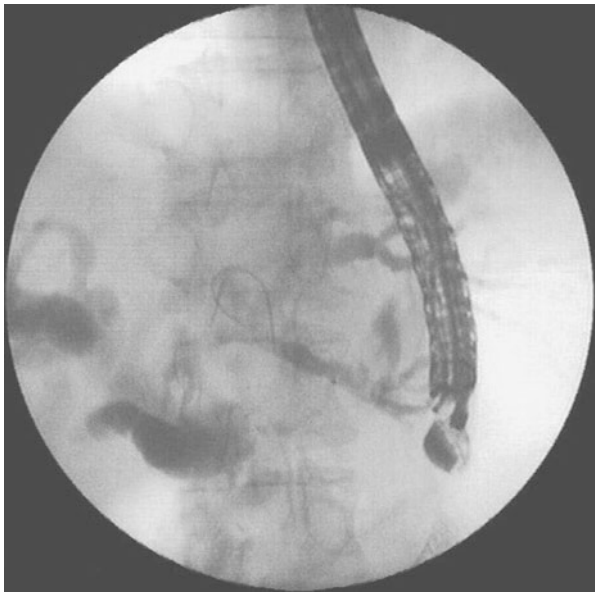

Fig. 19.10 Cholangiogram after left hepatic duct puncture

3. Rendezvous approach or ante grade stent placement is more difficult from this location as the guide wire has to traverse a longer distance through the biliary tract.

The intrahepatic approach is therefore best reserved when the duodenal bulb is inaccessible, e.g. post Billroth II gastrectomy, post Whipple's surgery, etc., or when the biliary obstruction is at the porta hepatis.

19.4.2 EUS Guided Pancreatic Duct Interventions

EUS guided pancreatography was first described in 1995 [12]. Subsequent reports have confirmed the utility of this approach for MPD drainage when ERCP fails.

Locate the MPD near the posterior gastric wall on linear EUS (Fig. 19.3a, b). Puncture and subsequent procedure is similar to that for biliary interventions. Stents can be placed through the stomach (antegrade stent placement) or over a guide wire retrieved from the papilla (rendezvous approach).

19.5 Outcomes

Various reports of EUS guided biliary drainage have appeared in literature during the last decade. Most are case reports or case series. Overall success rates are about 90% [13]. The largest series is of 23 patients and has reported 91% success rate [11]. A single step approach for fully covered metallic stent placement has been described recently [14, 15]. Long term patency rates of these stents are acceptable [16]. There are no randomized clinical trials comparing this approach to PTBD to date. A recent report describes the use of this approach for further interventions inside the bile duct following placement of a fully covered metal stent [17]. The utility of this approach has still not been validated in randomized clinical trials.

EUS guided pancreatic duct interventions has been reported less frequently. Francois et al. reported successful procedures in four patients [18]. A recent review has discussed the utility and efficacy of this technique [19].

19.6 Complications

EUS guided biliary drainage is a relatively new procedure. It is potentially dangerous and must be performed by endoscopists with considerable experience in biliary – pancreatic endotherapy. Potential complications include [20] –

1. Biliary peritonitis – due to loss of guide wire access during the procedure, stent migration [21] or biliary leak by the side of the stent.
2. Bleeding can occur during puncture or tract dilatation.
3. Pneumoperitoneum has been reported, often asymptomatic but rarely associated with bowel perforation.

EUS guided pancreatic duct drainage may lead to hemorrhage or pancreatic duct leak with resultant pancreatic ascites [19].

References

1. Fogel EL, Sherman S, Devereaux BM et al (2001) Therapeutic biliary endoscopy. Endoscopy 33(1):31–38. doi:10.1055/s-2001-11186
2. Joseph PK, Bizer LS, Sprayregen SS et al (1986) Percutaneous transhepatic biliary drainage. Results and complications in 81 patients. JAMA 255(20):2763–2767

3. Yee AC, Ho CS (1987) Complications of percutaneous biliary drainage: benign vs malignant diseases. AJR Am J Roentgenol 148(6):1207–1209
4. Cozzi G, Ostinelli C, Bellomi M et al (1989) Percutaneous transhepatic biliary drainage. Complications and their treatment. Radiol Med 77(4):399–404
5. Gu YK, Fan WJ, Wei HW et al (2008) Interventional management of severe complications after percutaneous transhepatic cholangic drainage and percutaneous implantation of biliary stents. Zhonghua Yi Xue Za Zhi 88(41):2916–2919
6. Weber A, Gaa J, Rosca B et al (2009) Complications of percutaneous transhepatic biliary drainage in patients with dilated and nondilated intrahepatic bile ducts. Eur J Radiol 72(3):412–417. doi:S0720-048X(08)00469-5 [pii] 10.1016/j.ejrad.2008.08.012
7. Wiersema MJ, Sandusky D, Carr R et al (1996) Endosonography-guided cholangiopancreatography. Gastrointest Endosc 43(2 Pt 1):102–106. doi:S0016510796000430 [pii]
8. Sahai AV, Hoffman B, Hawes RH (1998) Endoscopic ultrasound guided hepatico-gastrostomy to palliate obstructive jaundice: preliminary results in pigs. Gastrointest Endosc 47:AB37 (Abstract)
9. Giovannini M, Moutardier V, Pesenti C et al (2001) Endoscopic ultrasound-guided bilioduodenal anastomosis: a new technique for biliary drainage. Endoscopy 33(10):898–900. doi:10.1055/s-2001-17324
10. Burmester E, Niehaus J, Lieneweber T et al (2003) EUS-cholangiodrainage of the bile duct: report of 4 cases. Gastrointest Endosc 57:246–250
11. Kahaleh M, Hernandez AJ, Tokar J et al (2006) Interventional EUS-guided cholangiography: evaluation of a technique in evolution. Gastrointest Endosc 64(1):52–59. doi:S0016-5107(06)00225-2 [pii] 10.1016/j.gie.2006.01.063
12. Gress F, Ikenberry S, Sherman S et al (1996) Endoscopic ultrasound-directed pancreatography. Gastrointest Endosc 44(6):736–739. doi:S0016510796003501 [pii]
13. Will U, Thieme A, Fueldner F et al (2007) Treatment of biliary obstruction in selected patients by endoscopic ultrasonography (EUS)-guided transluminal biliary drainage. Endoscopy 39(4):292–295. doi:10.1055/s-2007-966215
14. Ito K, Fujita N, Noda Y et al (2010) Endosonography-guided biliary drainage with one-step placement of a newly developed fully covered metal stent followed by duodenal stenting for pancreatic head cancer. Diagn Ther Endosc 2010:426534. doi:10.1155/2010/426534
15. Park do H, Koo JE, Oh J et al (2009) EUS-guided biliary drainage with one-step placement of a fully covered metal stent for malignant biliary obstruction: a prospective feasibility study. Am J Gastroenterol 104(9):2168–2174. doi:ajg2009254 [pii] 10.1038/ajg.2009.254
16. Yamao K, Bhatia V, Mizuno N et al (2008) EUS-guided choledochoduodenostomy for palliative biliary drainage in patients with malignant biliary obstruction: results of long-term follow-up. Endoscopy 40(4):340–342. doi:10.1055/s-2007-995485
17. Eum J, Park do H, Ryu CH et al (2010) EUS-guided biliary drainage with a fully covered metal stent as a novel route for natural orifice transluminal endoscopic biliary interventions: a pilot study (with videos). Gastrointest Endosc 72(6):1279–1284. doi:S0016-5107(10)01896-1 [pii] 10.1016/j.gie.2010.07.026
18. Francois E, Kahaleh M, Giovannini M et al (2002) EUS-guided pancreaticogastrostomy. Gastrointest Endosc 56(1):128–133. doi:S001651070200024X [pii]
19. Varadarajulu S, Trevino JM (2009) Review of EUS-guided pancreatic duct drainage (with video). Gastrointest Endosc 69(2 Suppl):S200–S202. doi:S0016-5107(08)03070-8 [pii] 10.1016/j.gie.2008.12.032
20. Shami VM, Kahaleh M (2007) Endoscopic ultrasonography (EUS)-guided access and therapy of pancreatico-biliary disorders: EUS-guided cholangio and pancreatic drainage. Gastrointest Endosc Clin N Am 17(3):581–593. doi:S1052-5157(07)00069-4 [pii] 10.1016/j.giec.2007.05.015, vii-viii
21. Martins FP, Rossini LG, Ferrari AP (2010) Migration of a covered metallic stent following endoscopic ultrasound-guided hepaticogastrostomy: fatal complication. Endoscopy 42(Suppl 2):E126–E127. doi:10.1055/s-0029-1243911

EUS Guided Celiac Plexus Interventions

20

Rajkumar Wadhwa and Amol Bapaye

20.1 Introduction

Pain associated with pancreatic cancer and chronic pancreatitis is usually severe and may not respond to commonly used analgesics either NSAID's or opiods [1, 2]. Effective control of pain in these situations often employs non-pharmacological therapies such as celiac plexus neurolysis (CPN) and block (CPB) using injection of absolute alcohol or steroids respectively. These procedures not only control the pain but reduce the risk of side effects of opiods and NSAID's.

20.2 Anatomy

The celiac plexus transmits the sensation of pain for the pancreas [3] and is located below and anterior to diaphragm surrounding the origin of celiac trunk. It comprises of a dense network of ganglia and interconnecting fibers. Celiac ganglia are located between T12 and L2 and are generally two to five in number [4].

20.3 Technique

CPN can be performed surgically, percutaneously or under EUS guidance. EUS guided CPN was described by Wiersema and Wiersema in 1996 [5].

R. Wadhwa (✉)
Department of Gastroenterology, Vikram Jyoth – Centre for Advanced GI and Hepato-biliary Sciences, 2909 Temple Road, V. V. Moholla, Mysore, Karnataka, India
e-mail: drrwadhwa@hotmail.com

A. Bapaye, M.D. (M.S.)
Department of Digestive Diseases and Endoscopy,
Deenanath Mangeshkar Hospital and Research Center,
Erandwane, Pune 411004, Maharashtra, India

K. Akahoshi, A. Bapaye (eds.), *Practical Handbook of Endoscopic Ultrasonography*,
DOI 10.1007/978-4-431-54014-4_20, © Springer 2012

20.3.1 Salient Points About Patient Preparation

1. Hydrate patient before procedure with 500–1,000 ml normal saline.
2. Administration of broad spectrum antibiotics in patients who are not likely to be injected with alcohol during CPB [6].

20.3.2 Selection of Needle

Any commercially available 22 gauge EUS-FNA needle may be used for the procedure. A special 20 gauge 'spray' needle (EUS-20-CPN, Cook Endoscopy, Winston Salem, NC, USA) with multiple side holes is available and is believed to facilitate spread of the injectate.

20.3.3 Injectate Selection

Combination of bupivacaine (10 ml 0.5%) and absolute alcohol (10 ml) is used for CPN whereas combination of bupivacaine and steroids (triamcinolone 40–80 mg) or bupivacaine alone is used for CPB [6–8].

20.3.4 Methods

On linear EUS imaging from the posterior gastric lesser curve, identify the aorta (appears in a longitudinal plane). Trace the aorta distally till the origin of the celiac trunk – the first major branch of aorta below the diaphragm (Fig. 20.1a, b).

EUS – CPN can be performed by blind injection at the base of the origin of celiac trunk or by identification of celiac ganglia (can be identified in 79–86% patients) [9]. Celiac ganglia are oval, 2–20 mm in size and usually echo poor [10].

Advance a 22G or CPN needle through the biopsy channel and fix to the hub. Prime the needle with 3 ml of injectate and deliver the complete injectate either by using a single injection aimed 'centrally' or two injections aimed 'bilaterally'. Perform a check aspirate prior to injection to identify inadvertent vessel puncture.

Advantage of single injection is that it is safer and simpler as celiac trunk can be kept in view during the entire procedure (Fig. 20.2a). Bilateral injection gives theoretical advantage of injecting deeper and laterally where the plexus is actually located but carries a higher risk of injury to the celiac artery or aorta.

Injection of alcohol will temporarily cause an echogenic "blush" and will transiently cause discomfort and slight decrease in blood pressure (Fig. 20.2b). This is believed to be a good sign as it indicates delivery of injectate in the celiac plexus [11].

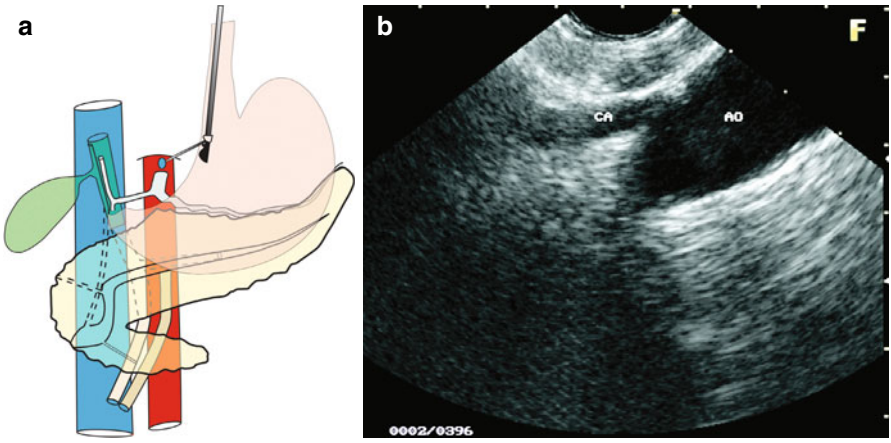

Fig. 20.1 (**a**) Diagrammatic representation showing position of the scope for celiac ganglion puncture, (**b**) linear EUS showing hypoechoic oval appearance of celiac ganglion

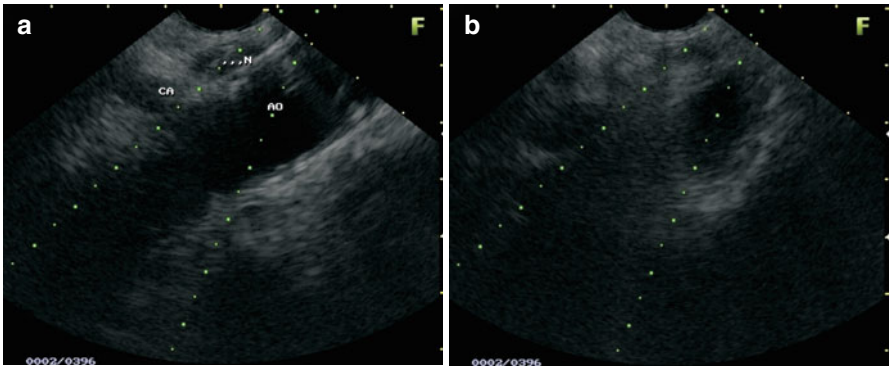

Fig. 20.2 (**a**) Linear EUS showing puncture of celiac ganglion with a 22G needle, (**b**) linear EUS showing echogenic cloud (*blush*) after injection of celiac ganglion

20.4 Complications

EUS guided CPN and CPB are safe and well tolerated procedures. Minor complications include transient increase in pain (9%). Self limiting diarrhea and orthostatic hypotension can occur in up to one-third of patients [6, 8, 12, 13]. Major complications (1–2%) include retroperitoneal bleeding and peripancreatic abscesses and are uncommon [12]. Paraplegia described using percutaneous posterior approach has not been reported using the EUS guided technique.

20.5 Outcomes

The efficacy of CPN for cancer related pain is well established and good to excellent response is seen in 70–90% patients [14]. The benefit declines over 8–12 weeks in patients not undergoing simultaneous chemotherapy; those receiving chemotherapy show a more sustained response up to 24 weeks [12]. CPN is generally reserved for patients with refractory pain but CPN used early in course of therapy has better efficacy [14].

Pain relief using CPB in patients with chronic pancreatitis is less effective (about 55%). Persistent benefit beyond 12 and 24 weeks is seen only in 26% and 10% patients [6]. Pain relief is more likely in older patients (>45 years) and those who have not undergone previous surgery for chronic pancreatitis.

A prospective randomized study comparing EUS versus CT guided CPN showed significant superiority of the EUS guided approach [15]. EUS guided approach has shown an efficacy of 78% pain relief in patients with pancreatic cancer [16]. This, along with the fewer complications and the added benefits of staging and obtaining tissue diagnosis using EUS makes the EUS guided approach a preferred choice.

References

1. Singh VV, Toskes PP (2003) Medical therapy for chronic pancreatitis pain. Curr Gastroenterol Rep 5(2):110–116
2. Lebovits AH, Lefkowitz M (1989) Pain management of pancreatic carcinoma: a review. Pain 36(1):1–11. doi:0304-3959(89)90106-1 [pii]
3. Plancarte R, Velazquez R, Patt RB (1993) Neurolytic blocks of the sympathetic axis. In: Patt RB (ed.) Cancer pain. JB Lippincott, Philadelphia, pp 377–425
4. Ward EM, Rorie DK, Nauss LA et al (1979) The celiac ganglia in man: normal anatomic variations. Anesth Analg 58(6):461–465
5. Wiersema MJ, Wiersema LM (1996) Endosonography-guided celiac plexus neurolysis. Gastrointest Endosc 44(6):656–662. doi:S0016510796003653 [pii]
6. Gress F, Schmitt C, Sherman S et al (2001) Endoscopic ultrasound-guided celiac plexus block for managing abdominal pain associated with chronic pancreatitis: a prospective single center experience. Am J Gastroenterol 96(2):409–416. doi:S0002-9270(00)02344-3 [pii] 10.1111/j.1572-0241.2001.03551.x
7. Levy MJ, Wiersema MJ (2003) EUS-guided celiac plexus neurolysis and celiac plexus block. Gastrointest Endosc 57(7):923–930. doi:10.1067/mge.2003.239 S0016510703003948 [pii]
8. Gunaratnam NT, Wong GY, Wiersema MJ (2000) EUS-guided celiac plexus block for the management of pancreatic pain. Gastrointest Endosc 52(6 Suppl):S28–S34. doi:a110718 [pii]
9. Gleeson FC, Levy MJ, Papachristou GI et al (2007) Frequency of visualization of presumed celiac ganglia by endoscopic ultrasound. Endoscopy 39(7):620–624. doi:10.1055/s-2007-966337
10. Levy M, Rajan E, Keeney G et al (2006) Neural ganglia visualized by endoscopic ultrasound. Am J Gastroenterol 101(8):1787–1791. doi:AJG685 [pii] 10.1111/j.1572-0241.2006.00685.x
11. Paquin S, Sahai AV (2007) EUS guided celiac plexus block and celiac plexus neurolysis. Tech Gastrointest Endosc 9:20
12. Hoffman BJ (2002) EUS-guided celiac plexus block/neurolysis. Gastrointest Endosc 56 (4 Suppl):S26–S28. doi:a127759 [pii]
13. Adler DG, Jacobson BC, Davila RE et al (2005) ASGE guideline: complications of EUS. Gastrointest Endosc 61(1):8–12. doi:S0016510704023934 [pii]

14. Ischia S, Ischia A, Polati E et al (1992) Three posterior percutaneous celiac plexus block techniques. A prospective, randomized study in 61 patients with pancreatic cancer pain. Anesthesiology 76(4):534–540
15. Gress F, Schmitt C, Sherman S et al (1999) A prospective randomized comparison of endoscopic ultrasound- and computed tomography-guided celiac plexus block for managing chronic pancreatitis pain. Am J Gastroenterol 94(4):900–905. doi:S0002927099000970 [pii] 10.1111/j.1572-0241.1999.01042.x
16. Gunaratnam NT, Sarma AV, Norton ID et al (2001) A prospective study of EUS-guided celiac plexus neurolysis for pancreatic cancer pain. Gastrointest Endosc 54(3):316–324. doi:S0016510701166393 [pii]

EUS Guided Anorectal Interventions

21

Amol Bapaye and Advay Aher

21.1 Introduction

EUS guided interventions in the anorectal region are a relatively new addition to the ever increasing indications for interventional EUS.

Types of EUS Guided Anorectal Interventions
EUS-FNA of pararectal or pelvic tumors
EUS guided aspiration or drainage of pelvic or pararectal fluid collections

21.2 EUS Guided FNA of Pararectal or Pelvic Tumors

Pelvic tumors may be seen in patients with previous history of pelvic malignancy from the rectum, prostate or cervix or de novo in patients without any prior history. Differentiation of tumor from scar tissue is often difficult on the basis of imaging alone. EUS-FNA provides tissue diagnosis in these situations.

A. Bapaye, M.D. (M.S.) (✉)
Department of Digestive Diseases and Endoscopy,
Deenanath Mangeshkar Hospital and Research Center,
Erandwane, Pune 411004, Maharashtra, India
e-mail: amolbapaye@gmail.com

A. Aher
Clinical Research Fellow, Department of Digestive Diseases and Endoscopy,
Deenanath Mangeshkar Hospital and Research Center,
Erandwane, Pune 411004, Maharashtra, India

K. Akahoshi, A. Bapaye (eds.), *Practical Handbook of Endoscopic Ultrasonography*,
DOI 10.1007/978-4-431-54014-4_21, © Springer 2012

21.2.1 Indications

- Extra luminal recurrence of rectal cancer
- Prostatic lesions
- Pelvic tumors – recurrent cervical cancer, masses in rectovaginal or rectovesical pouch
- Pararectal lymph nodes

21.2.2 Technique

Once the lesion has been identified on anorectal EUS, FNA is performed similar to that performed elsewhere in the gastrointestinal tract (Figs. 21.1a, b, 21.2, and 21.3).

21.2.3 Role of EUS-FNA in Pelvic Tumors

The sensitivity and specificity of EUS-FNA for pelvic mass lesions is 88% and 100% respectively [1]. Transrectal ultrasonography (TRUS) guided biopsy of the prostate gland is an established modality in urological practice. The procedure is safe and effective, with little patient discomfort and very low morbidity rates [2]. Infection is the most serious complication but is rare.

Recurrence of rectal cancer is often extra mucosal and therefore missed on mucosal biopsies. EUS-FNA can reliably demonstrate extra luminal recurrence during follow up of patients with rectal cancer [3, 4].

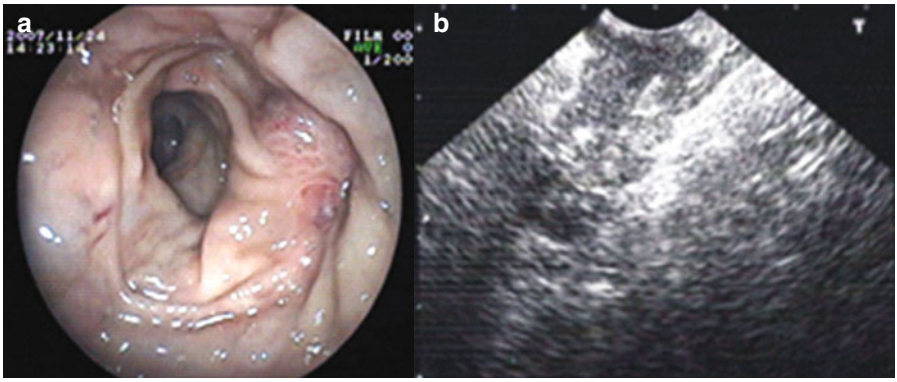

Fig. 21.1 (**a**) Endoscopic view showing recurrent rectal cancer, (**b**) linear EUS showing extra luminal extension of the tumor

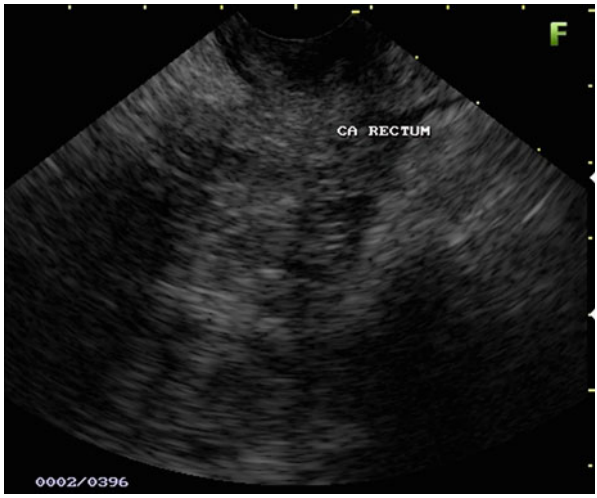

Fig. 21.2 T4 rectal cancer with infiltration into pararectal space

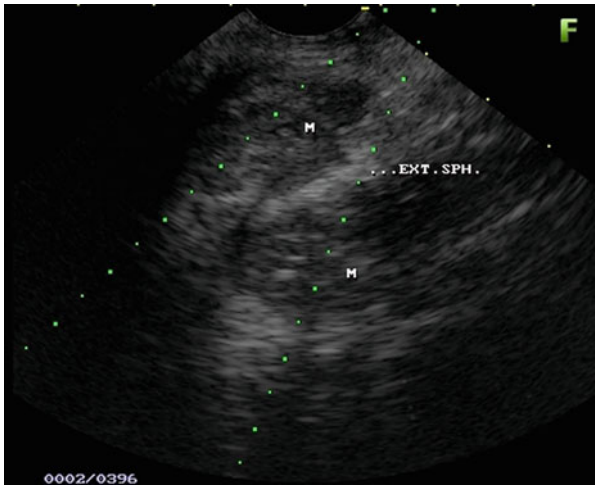

Fig. 21.3 Pararectal mass lesion on either sides of the external sphincter. FNA showed inflammation suggestive of organized inter sphincteric abscess

21.3 EUS Guided Aspiration or Drainage of Pelvic Fluid Collections

Fluid collections in the rectovaginal or rectovesical pouch may occur as a post operative complication following pelvic or abdominal surgery. EUS offers a minimally invasive approach for drainage of these fluid collections and may prevent reoperations [5–7].

21.3.1 Indications

- Localized fluid collections in the rectovesical or rectovaginal pouch
- Fluid collections or abscess in the pararectal space
- Prostatic abscess

21.3.2 Technique

The technique of EUS guided drainage of pelvic collections is similar to EUS guided drainage of pancreatic pseudocysts.

1. The collection is localized by the linear echoendoscope and wall thickness is measured (Fig. 21.4).
2. Using a 19G FNA needle, the collection is punctured and fluid/pus is collected for microbiological examination.
3. A guide wire is passed through the needle into the cavity.
4. Tract is dilated using a balloon or diathermy and one or more double pigtail stents are placed over the guide wire into the cavity (Fig. 21.5a, b).

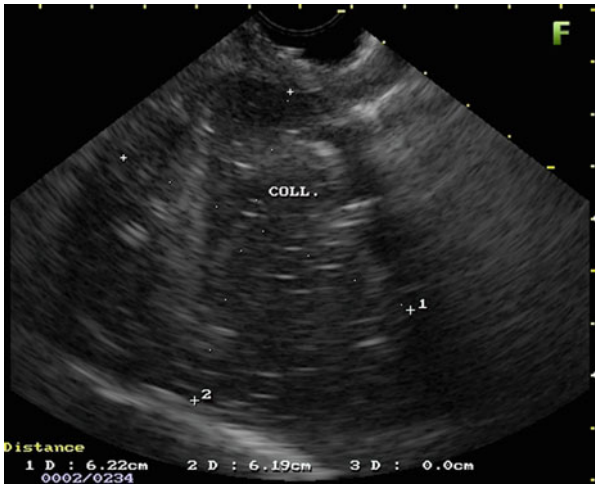

Fig. 21.4 Linear EUS showing pelvic collection in the rectovaginal pouch anterior to the rectum

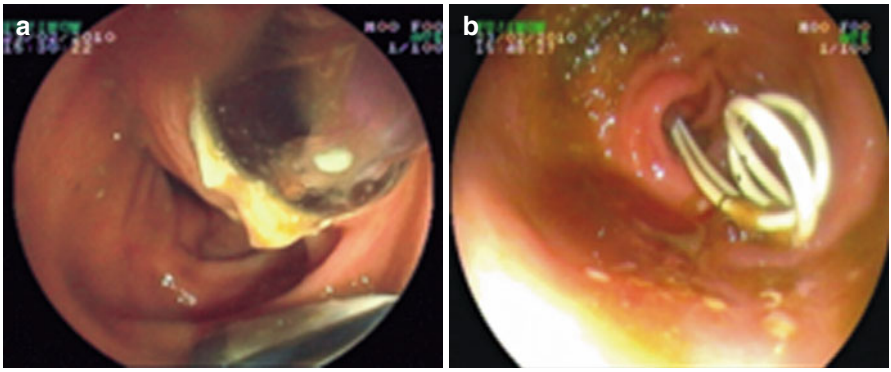

Fig. 21.5 (**a**) Endoscopic view showing balloon dilatation of the tract. (**b**) Endoscopic view showing multiple double pigtail stents inserted trans-rectally in the pelvic collection

21.3.3 Results of EUS Guided Drainage of Pelvic Fluid Collections

Successful drainage of pelvic collections under EUS guidance has been reported by many authors [5, 7, 8]. Complications are few and usually self limiting. Subsequent surgical intervention is seldom required. A case of tubercular prostatic abscess drained under EUS guidance has been reported [9].

References

1. Sailer M, Bussen D, Fein M et al (2002) Endoscopic ultrasound-guided transrectal biopsies of pelvic tumors. J Gastrointest Surg 6(3):342–346. doi:S1091255X01000129 [pii]
2. Rodriguez LV, Terris MK (1998) Risks and complications of transrectal ultrasound guided prostate needle biopsy: a prospective study and review of the literature. J Urol 160(6 Pt 1): 2115–2120
3. Lohnert MS, Doniec JM, Henne-Bruns D (2000) Effectiveness of endoluminal sonography in the identification of occult local rectal cancer recurrences. Dis Colon Rectum 43(4):483–491
4. Hunerbein M, Schlag PM (1997) Three-dimensional endosonography for staging of rectal cancer. Ann Surg 225(4):432–438
5. Sailer M, Bussen D, Fuchs KH et al (2004) Endoscopic ultrasound-guided transrectal aspiration of pelvic fluid collections. Surg Endosc 18(5):736–740. doi:10.1007/s00464-003-9206-6
6. Varadarajulu S, Drelichman ER (2007) EUS-guided drainage of pelvic abscess (with video). Gastrointest Endosc 66(2):372–376. doi:S0016-5107(07)00417-8 [pii]10.1016/j.gie.2007.02.054
7. Varadarajulu S, Lee YT (2009) EUS 2008 Working Group document: evaluation of EUS-guided drainage of pelvic-fluid collections (with video). Gastrointest Endosc 69(2 Suppl):S32–S36. doi:S0016-5107(08)02884-8 [pii] 10.1016/j.gie.2008.11.005
8. Varadarajulu S, Drelichman ER (2009) Effectiveness of EUS in drainage of pelvic abscesses in 25 consecutive patients (with video). Gastrointest Endosc 70(6):1121–1127. doi:S0016-5107(09)02434-1 [pii] 10.1016/j.gie.2009.08.034
9. Puri R, Jain P, Sud R et al (2010) EUS-guided drainage of an isolated primary tubercular prostatic abscess. Gastrointest Endosc 71(2):425–428. doi:S0016-5107(09)02274-3 [pii] 10.1016/j.gie.2009.07.032

Index

A
Abdominal aorta (AA), 40, 41, 56, 85, 94, 121, 167–169, 171, 172, 175
Accessory pancreatic duct, 178
Acute mediastinitis, 232
Adenomyomatosis of the GB, 114
Adrenal gland left (LAG), 88, 137, 138, 171, 172, 238
Adrenal gland, right , 175
Atrium, left(LA), 38, 40, 127–129
Ampulla of Vater, 176
Ampullary tumors, 180, 181, 198
Anal sphincter abnormalities, 162
Anechoic, 23, 121, 123, 127, 130, 135, 156, 166, 173, 174, 184, 190, 198, 231, 240, 251, 252
Antibiotic prophylaxis, 156
Aortic arch, 38, 42, 127, 128, 232
Aortic root, 127, 128
Aorto-pulmonary window (A-P window), 127, 137, 139, 226
Arch of aorta, 38, 42, 126, 127, 128, 232
Arterial bleeding after EUS-FNA, 257, 258
Ascending aorta, 40, 41
Ascites, 200, 201, 235, 284
Autoimmune pancreatitis (AIP)
  IgG4, 183
  immuno-histochemistry, 183
Azygos vein, 40, 127, 129

B
Balloon contact method, 33–34, 37, 83
Balloon contact plus water-filling method, 35
Basic scanning technique, EUS, 33–35, 83, 119–123
Bleeding, 16, 28, 215, 232, 246, 253, 257, 258, 273, 284, 289
Body of pancreas, 169, 180
Bowel preparation, 156
Branch duct (BD), 101–102, 191
Bronchogenic cysts, 134, 135, 231
  gelatinous, 231
Bronchus, left (LBr), 41
Bronchus, right , 41
Bulbourethral gland (BUG), 67, 69

C
Calcified stone, 107
Calculi, 121, 122, 161, 179–181
Carcinoembryonic antigen (CEA), 220, 245, 247, 248, 268, 269
CBD calculi, 194–195
  MRCP, 194
  posterior acoustic shadowing, 194
Celiac artery (CA), 168, 169, 288
Celiac ganglia, 287, 288
  echogenic “blush,” 299
Celiac plexus, 287–290
Celiac plexus block (CPB), 287–290
Celiac plexus neurolysis (CPN), 287–290
Celiac trunk, 85, 287, 288
Common hepatic artery (CHA)
Cholangiocarcinoma, 196, 197
Cholecystitis, 199
Choledochal cysts, 195, 196
Choledocholithiasis, 109
Cholelithiasis, 114
Chronic pancreatitis, 84, 104–108, 165, 178–184, 189, 191, 202, 240, 243, 245, 263, 287, 290
  endoscopic ultrasonography (EUS) criteria, 46, 105, 178, 179, 201
C-kit, 252, 254, 255
Clipping, 257, 258
Collateral veins, 25–27, 98
Color Doppler, power Doppler, 7
Colo-rectal cancer, 20

K. Akahoshi, A. Bapaye (eds.), *Practical Handbook of Endoscopic Ultrasonography*,
DOI 10.1007/978-4-431-54014-4, © Springer 2012

Common bile duct (CBD), 83–85, 90–93, 109, 110, 166, 167, 172–174, 177, 178, 181–183, 193–198, 239, 278–282
Common hepatic artery (CHA), 85, 110, 168, 173
Complications, 15, 27–29, 215, 257–258, 273–275, 277, 284, 289, 290, 294, 296, 297
Confluence, 86
Congenital foregut cysts, 134, 231
Congenital or simple cysts, 190, 244
Contrast enhanced EUS, 183, 243
Convex echoendoscope, 3
Cyst, 23, 59, 61, 100, 101, 103–105, 121, 123, 134, 135, 179, 181, 190–192, 195, 196, 219, 224, 231, 242, 245–248, 251, 264–266, 268–274
Cyst fluid analysis, 244
Cystic duct, 91, 178, 195
Cystic lesions of the pancreas, 100–104, 182, 190, 244–246
Cystic teratoma, 136

D
Dedicated echoendoscope, 3–7, 22
Descending aorta, 16, 17, 38–41, 47, 121, 126–129
Descending thoracic aorta, 126
Diaphragmatic crus, left, 168
Diffuse infiltrating gastric cancer (Linitis plastica), 149
Dressler, C.M., 137
Duodenal duplication cysts, 195
Duplication cysts, 134, 135, 195, 231

E
EASM. *See* External anal sphincter muscle (EASM)
Ectopic pancreas, 24, 60, 153, 251, 253, 255–256
Endoscopic resection
  intramural conditions, 28
  intramural vessels, 28
  submucosal blood vessel, 28
Endoscopic retrograde cholangio-pancreatography (ERCP), 109, 178, 181, 182, 197, 274–275, 277, 278, 281, 284
Endoscopic transmural drainage (ETMD)
  double pigtail stents, 268
  nasocystic catheter, 268
  necrosectomy, 268, 269, 273
ERCP. *See* Endoscopic retrograde cholangio-pancreatography (ERCP)
Esophageal cancer, 16, 17, 38, 44–46, 120, 125, 138–140, 145, 224
Esophageal cancer staging
  celiac lymph nodes, 139, 145
  TN staging, 44
Esophageal dilatation, 140
Esophageal duplication cysts, 134, 135, 231
Esophageal leiomyoma, 47, 134
Esophageal submucosal tumor, 46–47
Esophageal varices
  extramural collateral veins, 25
  paraesophageal collateral veins, 26
  perforating veins, 26, 27
  periesophageal collateral veins, 26, 27
  submucosal varices, 26, 27
  variceal recurrence, 25, 26
Esophageal wall, 37–38, 46, 47, 129, 133–135, 224, 230
Esophagus, 14–17, 25, 26, 33, 37–47, 125–140, 202, 223–232, 243, 266
EUS-ERCP rendezvous, 281
EUS-FNA, 6, 7, 47, 57, 59, 77, 80, 81, 95, 130, 136, 155, 156, 186, 197, 209–215, 217–220, 223–232, 235–248, 251–258, 269, 280, 288, 293–295
External anal sphincter muscle (EASM), 67, 70
Extra-esophageal compression, 38, 46, 47
Extra-gastric compression, 59, 61–62

F
Female, 66, 71–72, 156, 187, 242
Fine needle aspiration biopsy (FNAB), 217
Fine needle aspiration cytology (FNAC), 217
Five layer anatomy, 144
Five layered structure, 13, 37, 38, 49, 50, 65, 66, 145
Flow cytometry, 227
FNAB. *See* Fine needle aspiration biopsy (FNAB)
FNAC. *See* Fine needle aspiration cytology (FNAC)
Foregut cysts, 134, 231
Front loading ultrasound probe, 8–9

G
Gall bladder (GB), 83, 84, 90–92, 110–115, 121, 122, 165, 174, 181, 182, 198–199, 239
  cancer, 111

Ganglioneuroblastoma, 137, 230
Ganglioneuroma, 137, 230
Gastric, 59, 254
  Gastric cancer, 18–19, 50–57, 143, 144, 146–151
  Gastric cyst, 61
  Gastric ectopic pancreas, 24, 60, 152, 255
  Gastric lipoma, 23, 60
  Gastric lymphoma, 143, 149–151
  Gastric malignant lymphoma, 57–58
  Gastric MALT lymphoma, 21, 256
  Gastric peptic ulcer, 57
  Gastric submucosal tumor, 59–62, 255–257
  Gastric T1 intramucosal cancer, 53
  Gastric T1 submucosal cancer, 53
  Gastric T2 cancer, 54
  Gastric T3 cancer, 54
  Gastric T4 cancer, 55
Gastrinomas, 186, 241
Gastro-duodenal artery (GDA), 173, 174, 266
Gastro-esophageal junction, 144, 145, 166, 266, 268
Gastrointestinal mesenchymal tumor, 24, 47, 59, 77
Gastrointestinal stromal tumor (GIST), 133, 152, 219, 225, 255
Gastrointestinal wall layers, 22
GI tract cancer
  depth of invasion, 16
  early stage, 15, 27
  endoscopic mucosal resection, 15
  endoscopic submucosal dissection, 15

H
Hematometra, 162
Hepatic artery, 85, 110, 111, 168, 173
Hepatic vein, 166, 167
Hepatic duct, left (LHD), 166, 167, 278, 280, 283
Histoplasmosis, 130, 225, 230
Hyperechoic
  duct margins, 107, 179
  foci, 105, 179
  strands, 105, 106, 179

I
Immuno-cytochemistry, 227
Infection, 210, 215, 224, 228, 230, 231, 246, 247, 263, 264, 273–274, 294
Inferior duodenal angle, 172, 175
Inferior vena cava, 38, 39, 94, 167
Insertion, EUS, 33
Insulinomas, 186, 241
Internal anal sphincter muscle (IASM), 67, 70
Internal sphincter, 156, 157
Internal jugular vein, left (LJV), 43
Internal jugular vein, right , 43
Intraductal papillary mucinous neoplasia (IPMN), 100–102, 190, 191, 193, 244, 245, 247
Intramucosal cancer, 16–18, 20, 52–53, 73
Intramucosal gastric cancer, 18
Intramural evaluation, 27–29
Ischiorectal, 159

K
Kidney, left (LK), 85, 88, 89, 170–172
Kidney, right , 175

L
Liver, left lobe, 126, 137, 166, 167, 200
Liver, right lobe , 174
Leiomyoma, 47, 59, 77, 133, 134, 152, 153, 225, 251
Levator ani, 67, 156, 157
Lobular contour, 105, 106
Lymph node metastasis, 46, 55–56, 76, 95, 111, 113, 132
Lymph node stations
Lymphoepithelial cyst, 103

M
Main pancreatic duct (MPD), 51, 52, 85–94, 96, 101, 107, 108, 110, 169, 172–174, 176–180, 183, 191, 193, 198, 240, 247, 277–279, 284
Male anatomy, 66–70
MALT lymphomas, 150, 257
Management algorithm of SMT using EUS-FNA, 254
Mass forming type malignant lymphoma, 58
Matted appearance, 130, 188
Mediastinal abscess, 130, 188
Mediastinal disease, 38
Mediastinal lymphadenopathy
  granulomatous, 130, 227
  malignant, 130, 226, 227
  reactive, 130, 224, 225

Mediastinum, 37–47, 125–140, 200, 209, 223–232, 266
Metastases to pancreas, 243
Metastatic lymphadenopathy, 200, 227
Microlithiasis, 181, 198
Minor papilla, 178
Mitral valve, 127, 128
Mountain and Dressler classification
Mucinous cystadenocarcinoma (MCAC), 190, 193, 244, 247
Mucinous cystadenoma (MCA), 100, 191, 244, 245, 247
Mural nodules, 101, 102, 104, 191, 245
Muscularis propria, 7, 16, 19, 21–26, 28, 38, 44, 45, 47, 50, 53–54, 56–61, 66, 73, 74, 77, 79–81, 99, 113, 144, 252, 256

N
Necrosectomy, 265, 268, 269, 271–274
Needles of EUS-FNA, 252
Neurilemoma, 137, 230
Neuroblastoma, 137, 230
Neuroendocrine tumors
  gastrinomas, 186, 241
  insulinomas, 186, 241
Neurofibroma, 137, 230
Neurogenic tumors, 136, 225, 230
Non-Hodgkin's lymphoma (NHL), 150, 188, 227, 243
Non small cell lung cancer (NSCLC), 137, 138, 243
Normal esophageal wall, 37–38, 47
Normal gastric wall, 13, 14, 49, 50, 56, 61
Normal rectal wall, 65, 66

O
Onsite cytopathologist, 210, 214, 215, 217–219, 236, 243

P
Pancreas, 24, 50–52, 54, 55, 60, 83, 85–97, 99–104, 110, 111, 121, 153, 165–202, 209, 227, 235–248, 251, 253, 255–256, 263, 267, 274, 280, 287
Pancreatic
  Pancreas divisum, 178, 180, 181, 274
  Pancreatic abscess, 263
  Pancreatic adenocarcinoma, 184–185, 240
  Pancreatic body (PB), 55, 83, 84, 86, 87, 96, 99, 102, 103, 105–108, 114, 169, 170, 184, 186, 187, 237–238, 241, 243, 246, 266
  Pancreatic cancer, 184
  Pancreatic endotherapy, 181, 182, 277, 284
  Pancreatic head, 84, 85, 90–93, 97, 98, 100, 101, 107, 109, 110, 173, 175, 177, 188, 190, 192, 197, 200, 211, 215, 236–237, 246, 266
  Pancreatic neck, 86
  Pancreatic neuroendocrine tumors
  gastrinomas, 186
  insulinomas, 186
  Pancreatico-biliary system, 83–115
  Pancreatico-pleural fistula, 274
  Pancreatic tail, 85, 87, 89, 171, 238
Papilla of vater, 34, 35, 84, 93
Paraesophageal
  azygos vein, 127
  lower paratracheal, 127, 128
  lung, 127, 128, 224
  pleura, 127, 128, 139
Paraganglionoma, 137, 230
Pararectal EUS-FNA, 155, 293–295
Pelvic fluid collections, 296–297
Percutaneous biliary drainage (PTBD), 277, 284
Perforation, 28, 140, 215, 232, 265, 273, 284
Periesophageal lymph node metastasis, 46
Peripancreatic, 144, 188–189, 200, 235, 236, 263, 289
Peripancreatic lymph nodes, 188, 189, 236–237
Peri-rectal lymph node metastasis, 76
Plant and push maneuver, 236
Porta hepatis, 166, 167, 174, 177, 178, 238, 283
Portal biliopathy, 202
Portal invasion, 97, 98
Portal vein (PV), 51, 52, 85–94, 97, 98, 110, 111, 121, 166, 167, 170, 172–174, 177, 188, 199, 200, 202
Posterior mediastinal tumors, 136, 230
Preparation, EUS, 33, 156
Prostate, 66–70, 75, 78, 156, 158, 160, 162, 293, 294
Pseudocyst, 100, 104, 105, 136, 182, 183, 190, 191, 219, 220, 244, 245, 247, 263–275, 296
Pubococcygeus (PC), 67, 69
Puborectalis (PR), 67, 69
Pulmonary artery (PA), 38–43, 127
Pulmonary artery, left (LPA), 41
Pulmonary vein, left (LPV), 40
Puncture site, 215, 266–268, 273

R
Radial echoendoscope, 3, 125, 138
RAP. *See* Recurrent acute pancreatitis (RAP)
Rectal
  Rectal abscess, 78
  Rectal cancer, 20, 66, 73–76, 155, 160, 161, 163, 227, 294, 295
  Rectal endometriosis, 80, 81
  Rectal T1 intramucosal cancer, 73
  Rectal T2 cancer, 74
Recurrent acute pancreatitis (RAP), 180, 181
Renal vein, right , 175
Retroperitoneal, 165, 188, 224, 235
Rosemont classification, 178

S
Sacrum, 159
Salt and pepper echotexture, 169
Sarcoidosis, 130, 132, 135, 229, 230
Schwannoma, 137, 230
Secretin enhanced MRCP, 178
Sedation, EUS, 33, 156
Seminal vesicle (SV), 66, 67, 156, 158
Serous cystadenoma, 100, 101, 190, 191, 244–146
Small cell (SCLC), 137
SMT. *See* Submucosal tumor (SMT)
SMV. *See* Superior mesenteric vein (SMV)
Solid and papillary epithelial neoplasm (SPEN), 242, 245
Solid and papillary epithelial neoplasm (SPEN) of pancreas, 187
Sphincter dehiscence, 162
Sphincter urethrae muscle (SUM), 67, 69
Spine, 38–43, 47, 126, 168
Spleen, 85, 89, 171, 266
Splenic
  Splenic artery, 85, 113, 168, 273
  Splenic artery aneurysm, 61–62
  Splenic hilum, 171, 283
  Splenic vein, 62, 83, 85, 86, 89, 96, 98, 199, 202
Spleno-portal confluence (SPC), 170
Staging of biliary-pancreatic cancers, 199
Sub carinal space
  carina, 127, 129
  ring artifacts, 127
Submucosal
  cancer, 16, 19, 44, 53
Submucosal tumor (SMT), 14, 22, 34, 38, 46–47, 50, 59–62, 66, 77–81, 125, 152–153, 224, 225, 251–258
  leiomyoma, 47, 59, 77, 133, 152
  lipoma, 59, 60, 133, 152, 225
  varices, 26
SUM. *See* Sphincter urethrae muscle (SUM)
Superficial spreading type gastric malignant lymphoma, 58
Superficial spreading type gastric MALT lymphoma, 21
Superior mesenteric artery, 85, 95, 100, 168, 199
Superior mesenteric vein (SMV), 86, 94, 95, 98, 100, 170, 177
Supra-pancreatic CBD, 172, 173, 279

T
T1a cancer (lamina propria) of the gall bladder, 11
T1 pancreatic cancer, 96
T1-submucosal cancer, 44, 53
T3 cancer, 20, 21, 45, 54, 74, 110, 112, 113
  of the common bile duct, 110
T3 gallbladder cancer, 112, 113
T3 pancreatic cancer (infiltration to the portal vein), 97
T3 rectal cancer, 74
T4 pancreatic cancer, 100
T4 rectal cancer, 75, 295
Thyroid gland, 38, 43
Trachea, 38, 42, 43, 127, 128
Tuberculosis, 130, 131, 188, 189, 219, 220, 225, 229
Tumor seedling, 215, 237

U
UICC TNM staging of gall bladder cancer, 111
Ultrasound catheter probe (UCP)
  balloon-sheathed UCP method, 14
  complications, 15
  de-aerated water, 13, 14, 16
  five-layered structure, 13
  nine-layered structure, 13
  water-filled condom method, 15
  water-filling method, 15
Uncinate process (UP), 91, 94, 237, 266
Uncinate process (UP) of pancreas, 175–176
Urinary bladder (UB), 66, 67, 71, 72, 156, 157
Uterus, 71, 80, 159, 162

V
Vagina, 72, 80, 156, 159, 160, 162
Vascular invasion, 95, 97, 201
Ventricle, left (LV), 127

W
Water-filling method, 34, 35